ASPECTS OF LOW-GRADE METAMORPHISM IN NORTHERN SNOWDONIA, WALES

VOLUME II

David Cronshaw

A thesis submitted for the degree of Doctor of Philosophy,

University of Keele.

1984

IMAGING SERVICES NORTH
Boston Spa, Wetherby
West Yorkshire, LS23 7BQ
www.bl.uk

Volume 1

Figures 1.3, 1.4, 1.5, 2.1

Volume 2

Figures 5.1, 5.12, 6.6, 6.8, 7.9, 7.10, 8.1

Excluded at the request of the university

CHAPTER 5

ILLITE CRYSTALLINITY

5.1. Introduction

Illite is a non-specific term referring to the clay-size micaceous component of argillaceous sediment and differs from muscovite in containing more Si, Mg and OH and less interlayer K (Brindley and Brown, 1980). The general formula for illite is K_y, Al_4 $(Si_{8-y}$ $Al_y)$ O_{20} $(OH)_4$, (where $y < 2$ and is usually between 1 - 1.5), compared to the formula for muscovite which is KAl_2 (Si_3Al) O_{10} $(OH)_2$ (Deer et al.,1962). As sedimentary clays are progressively buried they undergo structural and chemical changes that ultimately lead to the development of a structurally well ordered, K-rich, white mica. These changes, along with an accompanying increase in the crystallite size through recrystallisation, are collectively termed "illite crystallinity" and can be quantified by measurement of the illite/muscovite (001) diffraction peak which has been shown to become progressively narrower and more intense as illite crystallinity increases (Weaver, 1960; Kubler, 1968; Dunoyer de Segonzac,1970; Kisch, 1980).

The study of the crystallinity of illite has developed in response to specific geological problems. For example, in the context of metamorphic petrology it allows a semi-quantitative examination of the lowest grades of metamorphism in rock types not usually suitable for conventional petrographic examination. Rocks most suited to this type of analysis are those rich in phyllosilicate minerals, for example, mudstones, shales, slates and schists which have undergone processes ranging from diagenetic change to low greenschist facies metamorphism. Often these rocks are very fine grained and the mineralogical reactions

in the transition from a diagenetic shale to a metamorphic schist involve transformation of the original clay minerals into white mica and chlorite with accompanying changes in mineral structure and a progressive increase in crystal size. None of these processes are particularly amenable to conventional petrographic examination.

The study of illite crystallinity by means of X-ray diffraction (XRD) particularly examines changes in the morphology of the first order basal reflection (001) of illite/muscovite. By quantifying the progressive change in peak morphology an estimate of the degree of ordering and chemical reconstitution can be obtained which is, in effect, a measurement of the amount of diagenetic change or grade of metamorphism. A survey of the literature quickly reveals the enormous influence of people such as Weaver (1960); Kubler (1968), Weber (1972) and more recently Kisch (1980) on the development and subsequent utilisation of techniques for the study of illite crystallinity.

The aims of the illite crystallinity work undertaken in northern Snowdonia were: i) to examine the regional and local illite crystallinity to see how it varies both on the large and small scale (between groups of samples from different geographical areas and between individual samples from the same small area) and attempt an explanation of any systematic variation, ii) to attempt a correlation between the variation in illite crystallinity and the secondary mineralogy of basic igneous rocks, fluid inclusion homogenisation temperatures and b_0 values obtained from white micas, and iii) to use the illite crystallinity results in conjunction with the other metamorphic indicators to formulate a model that accounts for the variation in metamorphism observed in northern Snowdonia.

5.2. The reaction of phyllosilicate minerals to progressive burial - a summary.

The basic premise inherent in illite crystallinity analysis is

that the morphology of the 10Å peak (the(001) reflection of illite/white mica) progressively changes throughout the course of diagenesis and low-grade metamorphism. Dunoyer de Segonzac (1970) outlined the chemical, mineralogical and structural responses of an original sedimentary montmorillonite-rich clay mineralogy to increases in pressure and temperature in the presence of alkali-rich solutions during progressive burial. The response of clay minerals to diagenesis are summarised in Figure 5.1. which is taken from Dunoyer de Segonzac (1970). During early anchizone metamorphism (Weaver, 1960) the illites become further ordered with the transformation of all the early 1Md illite into the 2M structural state (Maxwell and Hower, 1967). The crystallinity of illite increases progressively throughout the anchizone (Weaver, 1960; Kubler, 1968) initially as a reaction to the loss of mixed layers within the illite as K^+ ions are taken into the structure and later as a result of interlayer dehydration (Dunoyer de Segonzac, 1970). Above a concentration of 0.75 K^+ ions per half unit cell all mixed layers are lost and further contraction of the width of the 10Å peak is achieved by the loss of interlayer lenses of water and further K fixation as depth of burial increases.

The trends observed in the anchizone continue into the epizone with a continued reduction in width and increase in intensity of the illite/muscovite (001) peak. In the epizone illites are progressively converted into white mica with a continued increase in K^+ concentration per unit cell. The white mica produced usually contains a significant amount of Fe-Mg substituting for Al and often contain significant interlayer Na thus the white micas produced in the low epizone are phengitic (Fe-Mg) or paragonitic (Na) as distinct from the true muscovites produced at higher grades (Knipe, 1981).

Examples of reactions transforming illite into muscovite,phengite and paragonite during cleavage formation in slates from Rhosneigr

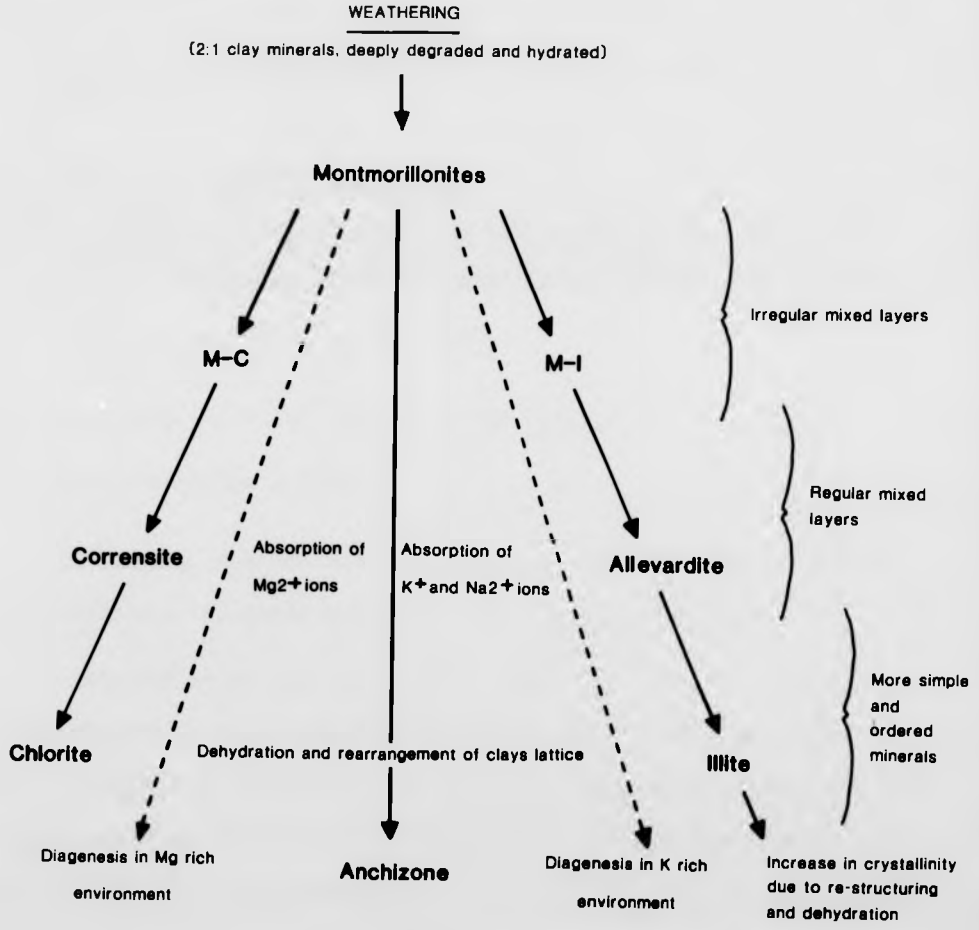
WEATHERING
(2:1 clay minerals, deeply degraded and hydrated)
Montmorillonites
M–C
M–I
Irregular mixed layers
Corrensite
Absorption of Mg2+ ions
Absorption of K+ and Na2+ ions
Allevardite
Regular mixed layers
Chlorite
Dehydration and rearrangement of clays lattice
Illite
More simple and ordered minerals
Diagenesis in Mg rich environment
Anchizone
Diagenesis in K rich environment
Increase in crystallinity due to re-structuring and dehydration

that the morphology of the 10Å peak (the(001) reflection of illite/white mica) progressively changes throughout the course of diagenesis and low-grade metamorphism. Dunoyer de Segonzac (1970) outlined the chemical, mineralogical and structural responses of an original sedimentary montmorillonite-rich clay mineralogy to increases in pressure and temperature in the presence of alkali-rich solutions during progressive burial. The response of clay minerals to diagenesis are summarised in Figure 5.1. which is taken from Dunoyer de Segonzac (1970). During early anchizone metamorphism (Weaver, 1960) the illites become further ordered with the transformation of all the early 1Md illite into the 2M structural state (Maxwell and Hower, 1967). The crystallinity of illite increases progressively throughout the anchizone (Weaver, 1960; Kubler, 1968) initially as a reaction to the loss of mixed layers within the illite as K^+ ions are taken into the structure and later as a result of interlayer dehydration (Dunoyer de Segonzac, 1970). Above a concentration of 0.75 K^+ ions per half unit cell all mixed layers are lost and further contraction of the width of the 10Å peak is achieved by the loss of interlayer lenses of water and further K fixation as depth of burial increases.

The trends observed in the anchizone continue into the epizone with a continued reduction in width and increase in intensity of the illite/muscovite (001) peak. In the epizone illites are progressively converted into white mica with a continued increase in K^+ concentration per unit cell. The white mica produced usually contains a significant amount of Fe-Mg substituting for Al and often contain significant interlayer Na thus the white micas produced in the low epizone are phengitic (Fe-Mg) or paragonitic (Na) as distinct from the true muscovites produced at higher grades (Knipe, 1981).

Examples of reactions transforming illite into muscovite,phengite and paragonite during cleavage formation in slates from Rhosneigr

FIGURE 5.1. The response of clay minerals to diagenesis, from Dunoyer de Segonzac (1970).

(Anglesey) include:

i) K + illite → muscovite + Si

$(K_{0.5})\ (Al_{1.87}Fe_{0.08}Mg_{0.05})\ (Si_{3.25}Al_{0.75})\ O_{10}\ (OH)_2 + 0.5K + 0.25Al$
$\rightarrow (K)\ (Al_{1.87}Fe_{0.08}Mg_{0.05})\ (Si_3Al)\ O_{10}\ (OH)_2 + 0.25Si$

ii) illite → phengite

$(K_{0.52})\ (Al_{1.81}Fe_{0.13}Mg_{0.23})\ (Si_{3.19}Al_{0.81})\ O_{10}\ (OH)_2 + 0.36K + 0.25Fe$
$\rightarrow (K_{0.88})\ (Al_{1.57}Fe_{0.38}Mg_{0.09})\ (Si_{3.15}Al_{0.85})\ O_{10}\ (OH)_2 + 0.2Al + 0.14Mg$
$+ 0.04Si$

iii) illite → paragonite + phengite

$2/\overline{\quad}\ (K_{0.5}Na_{0.3})\ (Al_{1.73}Fe_{0.27}Mg_{0.02})\ (Si_{3.14}Al_{0.86})\ O_{10}\ (OH_2)\ \overline{\quad}/ \rightarrow$
$(K_{0.12}Na_{0.6})\ (Al_{1.88}Fe_{0.16})\ (Si_{3.12}Al_{0.87})\ O_{10}\ (OH)_2 + (K_{0.88})\ (Al_{1.58}$
$Fe_{0.38}Mg_{0.04})\ (Si_{3.15}Al_{0.85})\ O_{10}\ (OH)_2$

(all reactions + any H_3O^+ released from illite).

Reactions from Knipe (1981).

In summary, the evolution of clay minerals to white mica during diagenesis and low-grade metamorphism is characterised by:

i) dehydration of the interlayer spaces.

ii) absorption of K^+ and Mg^{2+} ions from the circulating fluids

iii) progressive ordering of the lattice, increase of crystal size and large scale recrystallisation, originally of illite and chlorite but later of white mica as well.

These processes are thought to be related to pressure, temperature, chemistry of the fluid phase and, probably, local stress (Dunoyer de Segonzac, 1970). As a result of these trends illite crystallinity systematically increases from diagenesis, through anchizone metamorphism to low epizone metamorphism and can therefore be used to measure the grade of diagenesis/low-grade metamorphism. This correlation between

illite crystallinity and facies of low-grade metamorphism has been well established by many workers, for example, Weaver (1960) in the Quachita mountains where illite crystallinity was correlated with the degree of metamorphism through microscopic examination, and in the Alps by Frey (1970) where illite crystallinity was correlated to textural changes and low-grade metamorphic facies in pelitic rocks.

5.3. Sample collection and preparation

5.3.1. Sample collection

For the purpose of this survey 120 illite crystallinity determinations were undertaken. The samples were collected from as broad an area of northern Snowdonia as possible, primarily from argillaceous lithologies. Generally volcanic and coarse clastic sediment horizons were avoided, however, several of the Silurian samples from east of the river Conwy were of a distinctly silty nature. In the field as fresh a sample as possible of between 0.5 and 1.0 kg was taken. Samples were preferentially taken from several localities and stratigraphic horizons, in particular; i) the Cambrian slate belt around Llanberis and Bethesda (the Llanberis Slates Formation), ii) the middle and upper Cambrian slates of the western Llanberis and Nant Ffrancon passes (the Marchlyn Formation), iii) the Llanvirn slates from north and west of Snowdon (the Nant Ffrancon Formation), iv) the Caradocian slates from a wide area of northern Snowdonia, v) the upper Ordovician shales and slates sporadically exposed down the western side of the Conwy Valley, and vi) the lower Silurian(Llandovery and Wenlock) shales, siltstones and mudstones exposed around Conwy itself and down the eastern side of the Conwy Valley. The stratigraphic positions and distribution of samples can be seen in Figure 5.2.

The nature of the samples was quite variable although most showed the development of a cleavage ranging from a very good, closely spaced

FIGURE 5.2. The stratigraphic distribution of samples taken for the illite crystallinity determinations.

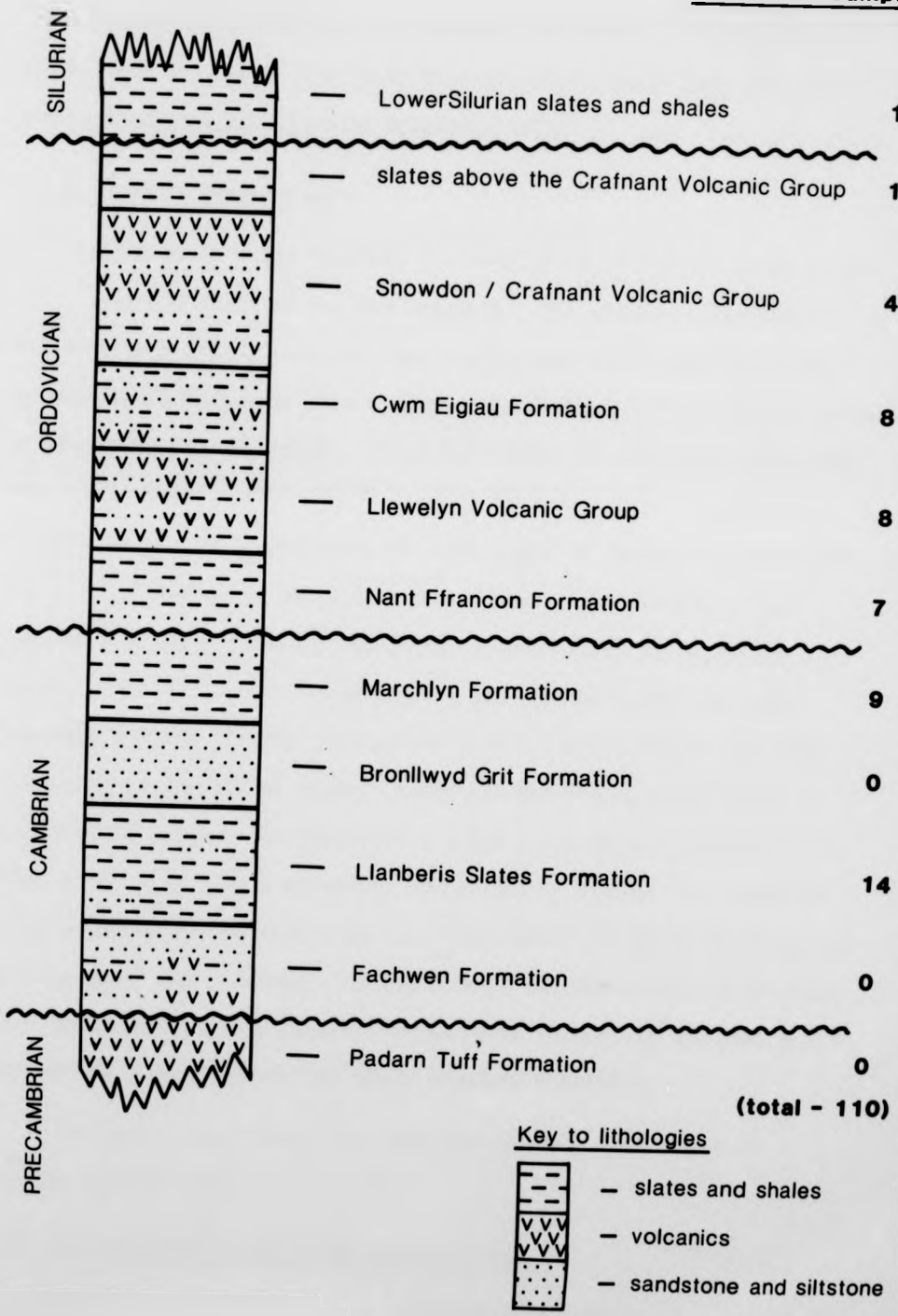

slaty cleavage, observed in many of the Cambrian and Ordovician slates, to a well spaced fracture cleavage observed in many of the upper Ordovician and lower Silurian siltstones and shales. Cleavage was not always seen in some of the upper Ordovician and lower Silurian samples. Sample locations are given in Appendix 2(ii).

5.3.2. Sample preparation

Sample preparation involved the production of a smear mount of the < 2 μ sediment fraction for XRD analysis. The procedure initially involved mechanically crushing the sample into small chips followed by ultrasonic treatment that caused surface disaggregation particularly of the finer clay material. After four hours of ultrasonic treatment the sample consisted of fine disaggregated material in suspension (mainly illite, mica and chlorite with traces of quartz and feldspar). The > 2 μ fraction is removed by centrifuge (after Hathaway, 1956) leaving the < 2 μ fraction suspended in about 300ml of distilled water. This is then filtered using a gas vacuum system and 0.45μ membrane filters thereby leaving the 0.45 - 2.0μ sediment fraction deposited on the filter paper. From this material a smear mount is prepared by pasting the sample onto a 3cm x 3cm glass slide which is then allowed to slowly air-dry. Occasionally because the amount of fine material in the sample was only very small an uneven distribution on the mount was obtained. In these cases another mount was produced and the amount of fine material enhanced by increasing the amount of mechanical crushing prior to the ultrasonic treatment.

The smear mounts were then used for the XRD measurement of illite crystallinity.

5.4. The measurement of illite crystallinity

Illite crystallinity can be measured in a variety of ways but all

quantify the degree of metamorphism as reflected by changes in the morphology of the illite (001) peak. In this study three indices were determined as a measure of crystallinity:

i) the Kubler index (Kubler, 1967, 1968) which is a simple measurement of the peak width at half peak height (expressed in mm). Kisch (1980) recommends that the half peak height width should be expressed in degrees 2θ in order to avoid problems caused by different scan and chart speeds. In the present study half peak height width is expressed as fractions of a degree 2θ

ii) the Weaver index (Weaver, 1960) which calculates a "sharpness ratio" by ratioing the counts corresponding to the top of the 10Å illite peak to the counts at a position on the peak 0.5Å towards the higher "d" spacing. This index is slightly modified in that a short scan (approximately 0.15^{o} 2θ) is undertaken across the expected position of the 10Å peak (8.84^{o} 2θ), to locate the maximum counts corresponding to the true position of the illite (001) peak. This was found to vary between 8.78 and 8.89^{o} 2θ. This variation is thought to possibly reflect small scale interlayering and/or chemical substitutions within the minerals. After the peak has been located the intensity is measured over an 80 second count time. The peak + 0.5Å position is then calculated and a similar reading taken, correction for the sloping background is achieved by similarly counting at fixed background positions (7.6 and 9.7^{o} 2θ). These values are then used to calculate a peak to peak +0.5Å ratio. A typical example of a Weaver index calculation would be:

	position	counts
intensity of the (001) peak	8.82^{o} 2_{θ}	9626
intensity of the (001) peak + 0.5Å	8.40^{o} 2_{θ}	2145
intensity of set background (1)	7.6^{o} 2_{θ}	1510
intensity of set background (2)	9.7^{o} 2_{θ}	1120

From these measurements the background intensity for the (001) peak and the (001) peak +0.5$\overset{o}{A}$ is calculated;

	counts
(001) peak (background intensity)	1283
(001) peak + 0.5$\overset{o}{A}$ (background intensity)	1361

The intensity of the (001) peak and the (001) peak + 0.5$\overset{o}{A}$ is then adjusted for background;

	counts
(001) peak (adjusted)	8343
(001) peak + 0.5$\overset{o}{A}$ (adjusted)	744

The Weaver index is then calculated using the formula;

$$\frac{\text{intensity of the (001) peak (counts)}}{\text{intensity of the (001) peak + 0.5}\overset{o}{A}\text{ (counts)}} = \frac{8343}{744} = 10.6$$

iii) the Weber index (Weber, 1972) is a modification of the Kubler index in that it ratios the half height peak width of the illite (001) peak to the half height peak width of a standard quartz (100) reflection. This is to minimise the effects of machine variation over a period of time or between different machines, in that any change in the half height peak width of the illite (001) should also be reflected by a proportional change in the quartz (100) half height peak width. Weber used polished rock slabs for this purpose, whereas, in this study the ratio of the illite (001) and quartz (100) half height peak widths are determined on the < 2 μ smear mounts. As such the results obtained are not directly comparable to those obtained by Weber. On the polished rock slabs the crystallinity determined is the mean crystallinity of all the phyllosilicate 10$\overset{o}{A}$ peaks. On the smear mounts the contribution of

finer grained phyllosilicates of lower crystallinity is enhanced at the expense of coarser grained phyllosilicates of higher crystallinity. As a result the mean crystallinity is correspondingly lower (Weber 1972). In order to express the results as whole numbers Weber multiplies the ratio of illite (001) to quartz (100) half height peak widths by 100.

The reasons why three crystallinity indices were measured are: i) that it allows direct comparison between results obtained using different techniques, ii) it allows investigation of large apparent differences in crystallinity when measured in different ways, and, iii) they allow some assessment of the relative reliability of the half height peak width and "sharpness ratio" measurements of illite crystallinity. By quantifying the relative reliability of the different indices the most suitable index for a given sample may be utilised. The question of the relative reliability of the different indices is discussed in Section 5.5.3.

A diagrammatic summary of the three measurements of illite crystallinity is shown in Figure 5.3. The machine conditions employed during the determination of illite crystallinity are listed in Appendix I (ii).

5.5. Results of the illite crystallinity determinations in northern Snowdonia.

5.5.1. Illite crystallinity data.

The results obtained from the measurement of illite crystallinity on 110 slates, shales and mudstones are contained in Appendix 6 (i), the results of repeat analyses on 24 samples are contained in Appendix 6 (ii). The illite crystallinity data is plotted on graphs and maps which are discussed in Sections 5.5.2. and 5.6.1. respectively.

FIGURE 5.3. A diagrammatic summary of the Kubler, Weaver and Weber illite crystallinity indices.

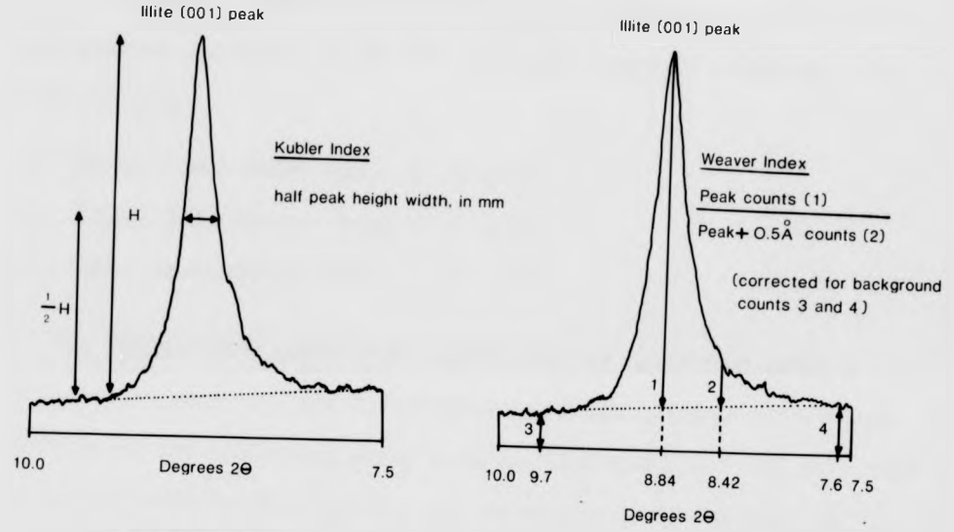

5.5.2. Correlation between the Kubler, Weaver and Weber indices

Figures 5.4 to 5.6 are graphical plots of the different crystallinity indices and demonstrate a good degree of correlation between different pairs of indices. Correlation coefficients (r) between indices are calculated on the basis of 146 illite crystallinity measurements. It was found that:

i) Kubler index/Weber index $r = +0.93$

ii) Kubler index/Weaver index $r = +0.88$

iii) Weber index/Weaver index $r = +0.84$

The Kubler/Weber correlation coefficient is calculated using a straight line equation, the Kubler/Weaver and Weber/Weaver correlation coefficients are calculated using a curved line equation. The fact that the indices relationships differ is a reflection of the methods of measurement employed for the calculation of each index. In the case of the Kubler and Weber indices slightly different measures of half height peak width are being used so that a good positive linear correlation is to be expected. In the case of the Kubler/Weaver and Weber/Weaver graphs measurements of half height peak width are plotted against a "sharpness ratio" measurement. Small changes in the crystallinity of illite at low-grade are reflected by only small relative differences in the Weaver index but large relative differences in the Kubler and Weber indices. Conversely, small changes in the crystallinity of illite at higher grade are reflected by only small relative differences in the Kubler and Weber indices but large relative differences in the Weaver index. This relationship reflects, in part, the relative reliability of the two types of measurement at higher and lower grades of metamorphism (section 5.5.3). As a result of the above observation it is evident that a curved line relationship must exist between the half height peak width

FIGURE 5.4. Kubler crystallinity index vs the Weber crystallinity index for samples from northern Snowdonia.

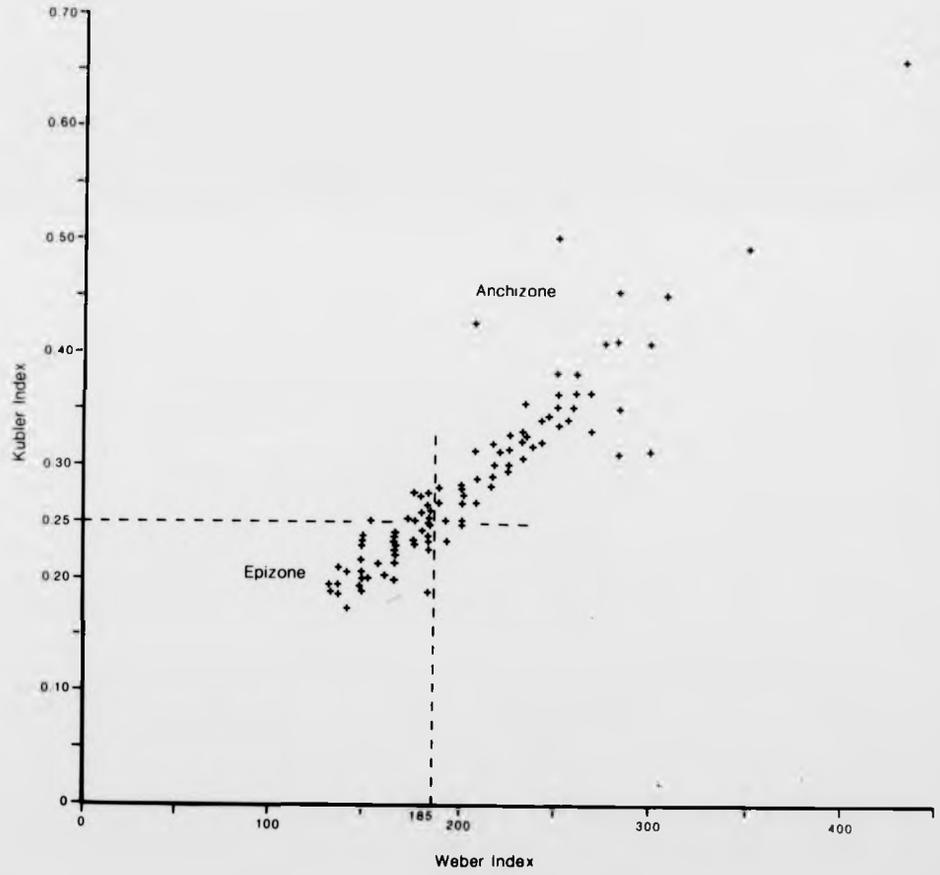

FIGURE 5.5. Kubler crystallinity index vs the Weaver crystallinity index for samples from northern Snowdonia.

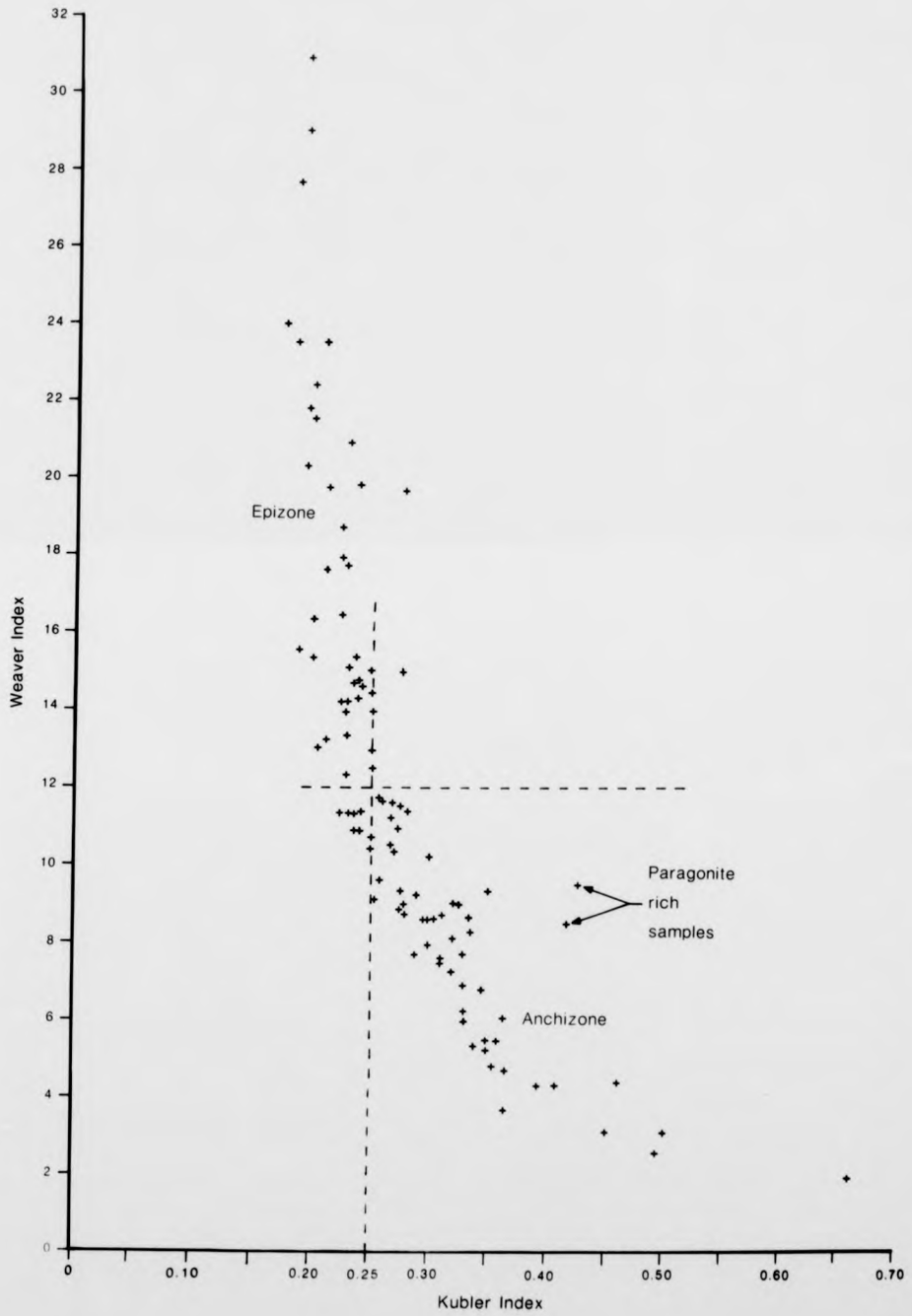

FIGURE 5.6. Weber crystallinity index vs the Weaver crystallinity index for samples from northern Snowdonia.

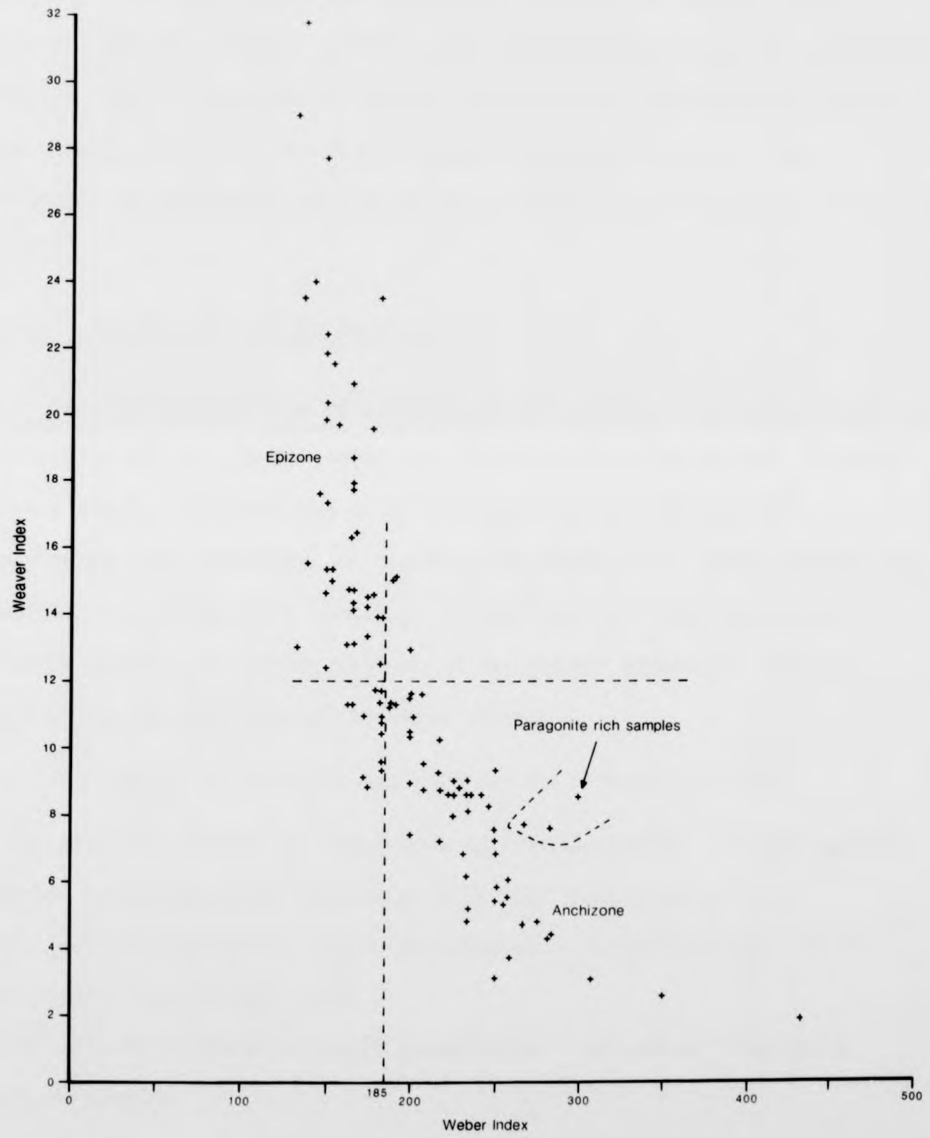

and"sharpness ratio" indices.

For the vast majority of samples (105) correlation between the different indices is generally good and the observed variation is within the limits of accuracy of the techniques outlined in Section 5.5.3. Several samples, however, exhibit poor correlation between the different indices, that is thought to reflect compositional inhomogeneity within the sample, in particular the presence of paragonite mica. The influence of paragonite on illite crystallinity is discussed in Section 5.10.1.

5.5.3. Reliability of the results

In order to test the reliability of the results obtained a large proportion of the samples (30%) had repeat analyses performed, ranging from a simple duplicate run with the sample rotated through 90^{o} (performed on 24 samples), to complete re-preparation, sedimentation and analysis (performed on 6 samples). In addition to these re-run and re-made samples all determinations of the Kubler index were measured without the sample orientation being changed.

The object of replicate analyses was to critically assess:

i) effects related to short term machine variation - determined from the two measurements of the Kubler index per sample run,

ii) effects related to sample orientation - determined from the 24 re-oriented sample runs, and

iii) effects related to sample preparation - determined from the 6 re-made samples.

In addition to these potential uncertainties it was necessary to determine the precision of actual measurement from the diffraction charts. In general measurements to within 0.5mm are possible.

and"sharpness ratio" indices.

For the vast majority of samples (105) correlation between the different indices is generally good and the observed variation is within the limits of accuracy of the techniques outlined in Section 5.5.3. Several samples, however, exhibit poor correlation between the different indices, that is thought to reflect compositional inhomogeneity within the sample, in particular the presence of paragonite mica. The influence of paragonite on illite crystallinity is discussed in Section 5.10.1.

5.5.3. Reliability of the results

In order to test the reliability of the results obtained a large proportion of the samples (30%) had repeat analyses performed, ranging from a simple duplicate run with the sample rotated through 90^{o} (performed on 24 samples), to complete re-preparation, sedimentation and analysis (performed on 6 samples). In addition to these re-run and re-made samples all determinations of the Kubler index were measured without the sample orientation being changed.

The object of replicate analyses was to critically assess:

i) effects related to short term machine variation - determined from the two measurements of the Kubler index per sample run,

ii) effects related to sample orientation - determined from the 24 re-oriented sample runs, and

iii) effects related to sample preparation - determined from the 6 re-made samples.

In addition to these potential uncertainties it was necessary to determine the precision of actual measurement from the diffraction charts. In general measurements to within 0.5mm are possible.

Index	variation related to measurement	variation related to short term machine factors	variation related to sample sedimentation	variation related to sample preparation
Kubler	$\pm 0.00625^{o}2\theta$ (1.5% of total range)	$\pm 0.0125^{o}2\theta$ (2.5% of total range)	$\pm 0.0226^{o}2\theta$ (5.5% of total range)	$\pm 0.0247^{o}2\theta$ (6.0% of total range)
Weaver	-	-	±0.96 (3.2% of total range)	±1.44 (4.8% of total range)
Weber	±4.2 (1.4% of total range)	-	±15.2 (5.1% of total range)	±14.4 (4.8% of total range)

TABLE 5.A. Calculated errors due to chart measurement, machine factors, sedimentation effects and sample preparation in the determination of illite crystallinity.

The results of the investigation into sources of potential error on the illite crystallinity results are summarized in Table 5.A. All the figures quoted are at the one standard deviation significance level and are mean errors calculated for the total range of results obtained for a particular index in northern Snowdonia.

The effects of short term machine variability on crystallinity measurement was assessed on the Kubler index and is based on two measurements per sample run. The reliability is assessed by calculating the variance for each pair of analyses and then producing a pooled variance for all the pairs of Kubler determinations.

Orientation effects are thought to reflect inhomogeneity in the sample cover on the glass mounts and were assessed by running duplicate analyses in different orientations on 24 samples for all three crystallinity indices. The pooled variance is again calculated, this time for each pair of analyses corresponding to runs in different orientations on the same sample.

Variation related to sample preparation was tested by complete re-preparation, sedimentation and analysis performed on 6 samples. The pooled variance is calculated for each group of analyses obtained from the different smear mounts of an individual sample.

The results contained in Table 5.A. demonstrate that the precision of the technique corresponds to a maximum of 6% of the observed range on any index at the one standard deviation significance level.

Kubler (1968) examined the reliability of crystallinity measurements on over 700 samples ranging from very low to very high crystallinity, and calculated errors related to measurement, machine variation and sample preparation. Kubler calculated relative errors of 3%; 6-8% and 15% for measurement, machine drift and sample preparation respectively. Figure

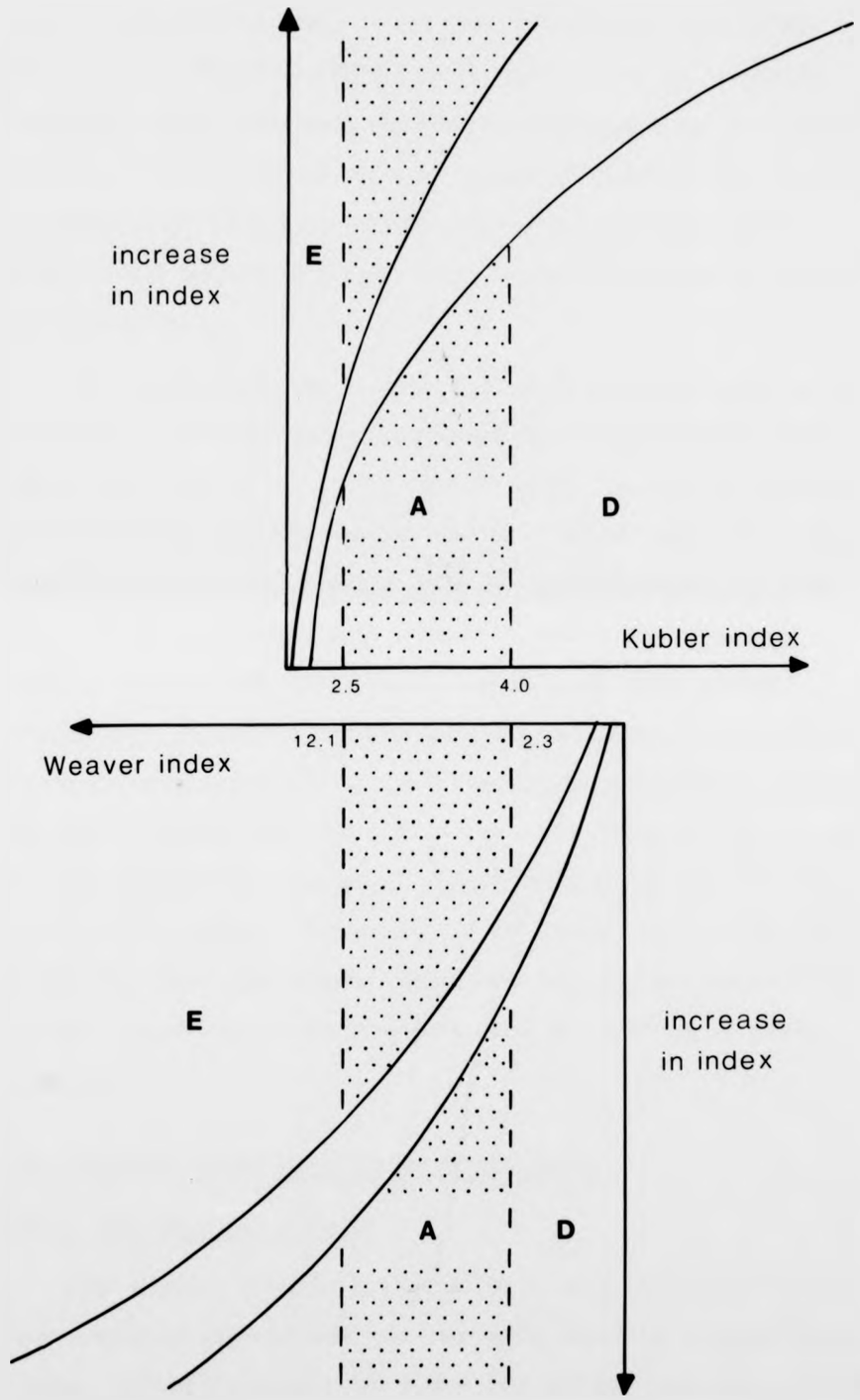

FIGURE 5.7. The relative reliability of the Kubler and Weaver crystallinity indices, from Kubler (1968). E = epizone, A = anchizone, D = diagenesis.

5.7. is from Kubler (1968) and shows the relative uncertainty in determining crystallinity utilising the half height peak width and "sharpness ratio" techniques at different metamorphic grades. Clearly the Kubler index is a more reliable measure of crystallinity in samples displaying relatively high crystallinity whilst the Weber index is a more reliable measure of crystallinity in samples displaying relatively low crystallinity.

The results contained in Table 5.A are only mean relative errors calculated on all re-made and re-run samples irrespective of whether they exhibit high or low illite crystallinity. In order to investigate the distribution of error between samples of higher and lower crystallinity the 24 re-oriented samples were divided into higher and lower crystallinity populations with critical crystallinity values of $0.25^{o}2\theta$, 12.0 and 185 for the Kubler, Weaver and Weber indices respectively, corresponding, approximately, to the anchizone/epizone boundary (see Section 5.6.1.). The results are presented in Table 5.B. and clearly demonstrate that variability on the Kubler and Weber indices for low crystallinity samples is significantly higher than for high crystallinity samples. Conversely, on the Weaver index variability is greater for high crystallinity samples and less for low crystallinity samples. These results are consistent with the findings of Kubler (1968).

5.6. Regional variation in illite crystallinity

5.6.1. The empirical evidence

From the maps (Figures 5.8. to 5.10) it is evident that there is a large amount of regional and local variation in illite crystallinity. In general it would appear that higher crystallinity values are obtained from samples taken from a belt approximately 8-10 km wide bounded to the

FIGURE 5.8. A map showing the distribution of anchizone and epizone Kubler crystallinity results in northern Snowdonia.

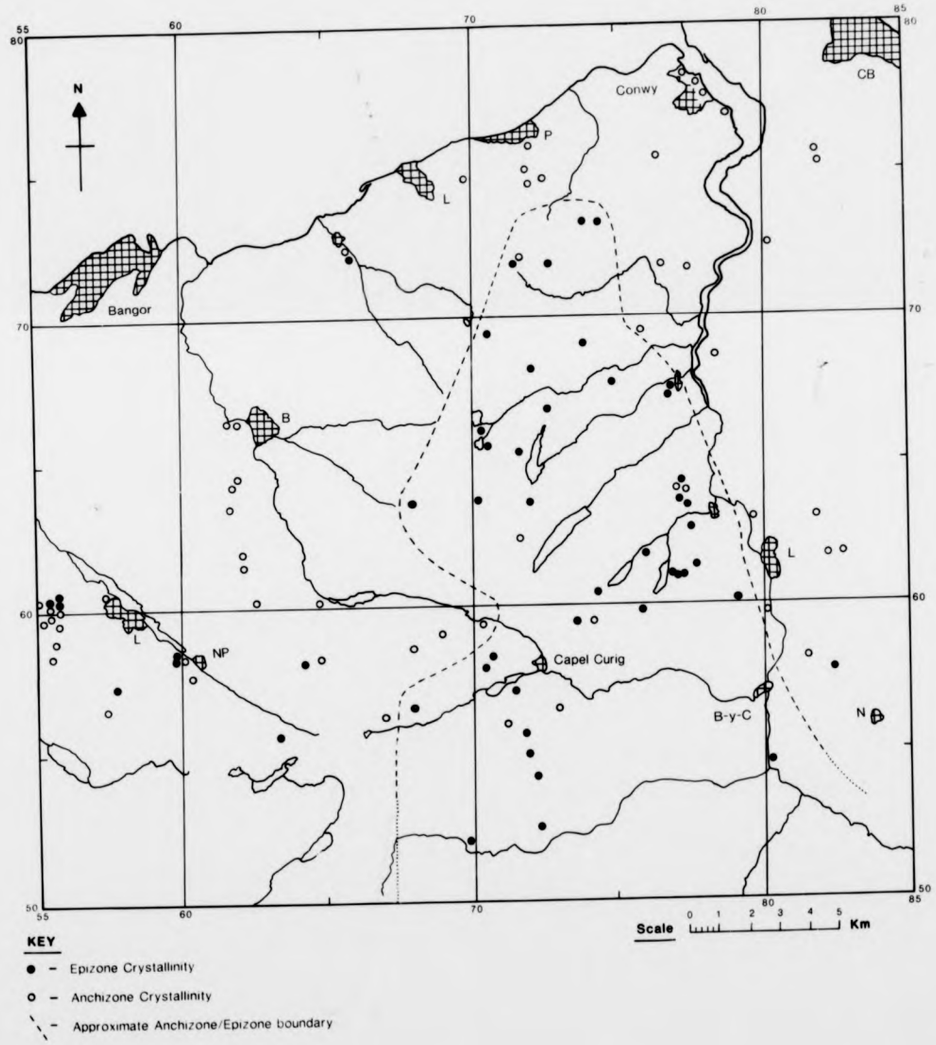

FIGURE 5.9. A map showing the distribution of anchizone and epizone Weaver crystallinity results in northern Snowdonia.

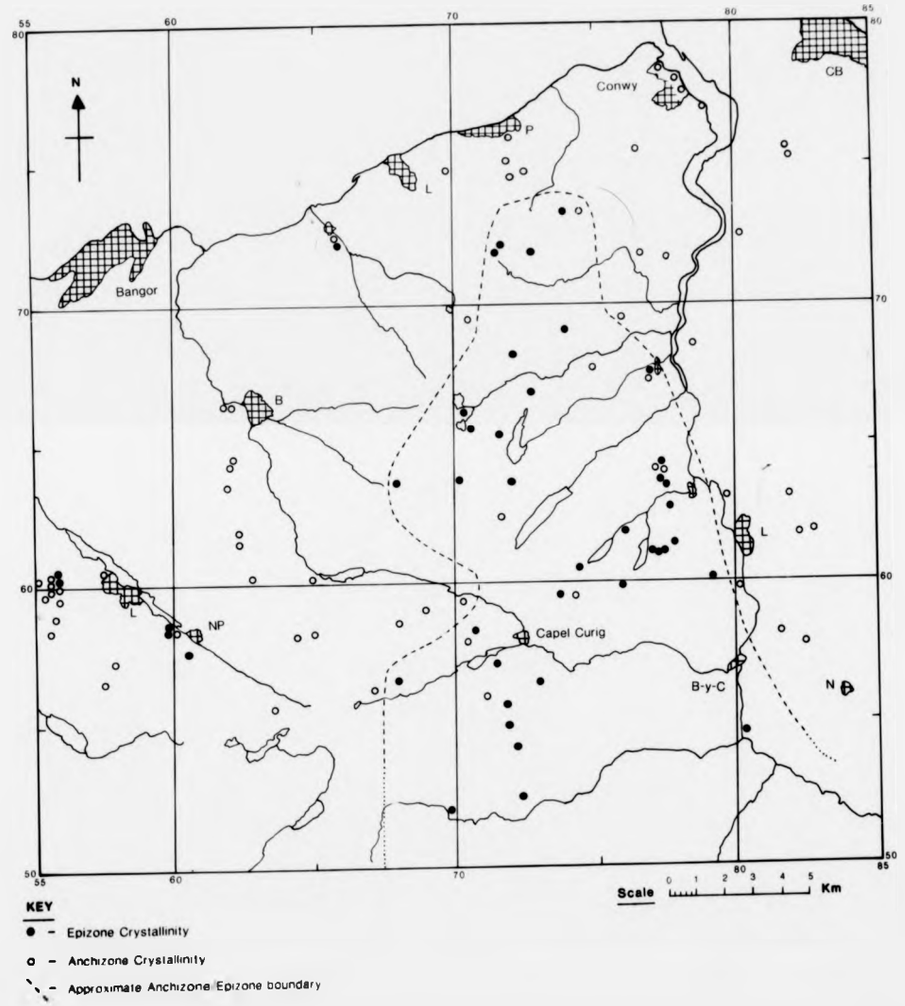

FIGURE 5.10. A map showing the distribution of anchizone and epizone Weber crystallinity results in northern Snowdonia.

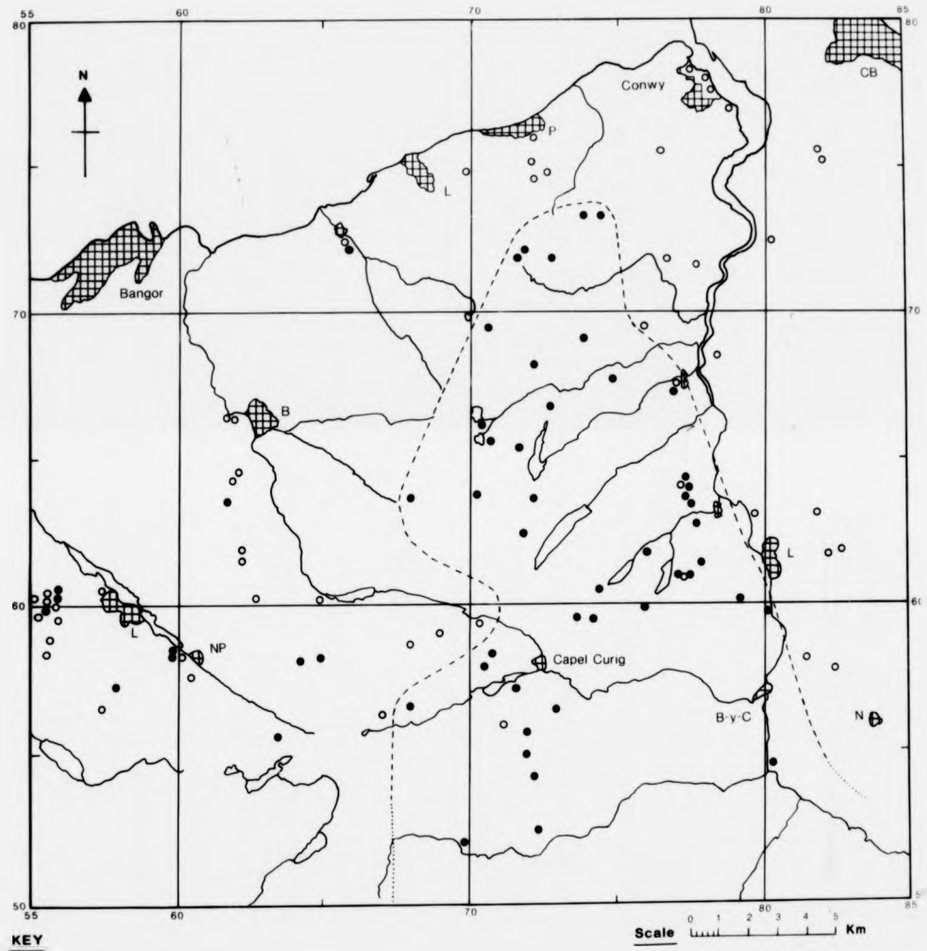

Index	mean error	error calculated for low crystallinity samples	error calculated for high crystallinity samples
Kubler	$\pm 0.0226^{o}2\theta$	$\pm 0.0268^{o}2\theta$	$\pm 0.0203^{o}2\theta$
Weaver	±0.96	±0.88	±1.13
Weber	±15.2	±18.3	±8.0

TABLE 5.B. Distribution of error between samples of relatively low and high crystallinity (calculated on the basis of 24 re-oriented sediment mounts).

	Area A		Area B	
	number of samples	% of total samples	number of samples	% of total samples
Kubler index subdivisions				
<0.225°2θ (high)	21	43%	1	1%
0.225-0.25°2θ (high/intermediate)	19	39%	6	11%
0.25-0.275°2θ (low/intermediate)	7	14%	6	11%
>0.275°2θ (low)	2	4%	43	77%
Weaver index subdivisions				
>13.44 (high)	30	61%	3	5%
13.44-12.0 (high/intermediate)	7	15%	0	0%
12.0-10.56 (low/intermediate)	6	12%	9	16%
<10.56 (low)	6	12%	44	79%
Weber index subdivisions				
<169.8 (high)	27	55%	4	7%
169.8-185 (high/intermediate)	17	35%	3	5%
185-200.2 (low/intermediate)	1	2%	2	4%
>200.2 (low)	4	8%	47	84%

TABLE 5.C. Distribution of samples with high, high/intermediate, low/intermediate and low crystallinity between area A (generally high crystallinity) and area B (generally low crystallinity).

east by the river Conwy, to the south west by the Glyders, to the north west by the Carneddau and to the north by Tal-y-Fan (for locations see Figure 1.1). On aggregate consistently lower crystallinity values are obtained from samples taken outside this belt. It would also appear that there is a relatively sharp break between the two areas. The critical values used in discriminating between a higher and a lower crystallinity area are $0.25^{o}2\theta$, 12.0 and 185 for the Kubler, Weaver and Weber indices respectively. The significance of these crystallinity values is discussed below. The presence of two populations of illite crystallinity can also be seen in the histograms of Figure 5.11. 1 - 3. In Table 5.C. the distribution of illite crystallinity results within the two proposed areas is clearly seen. Four categories of illite crystallinity are considered,these being "high" and "low", where the results fall either side of the critical values utilised to define the two areas by an amount that is greater than the calculated one standard deviation potential error (see Table 5.A); and "high/intermediate" and "low/intermediate", where the results fall either side of the critical values by an amount which is less than the calculated one standard deviation mean potential error. The tables are constructed in such a way that any tendency for results from either area to be over represented in any of the four crystallinity categories would be immediately apparent. The tables are produced from only 105 of the original 110 samples, 5 samples were not considered as they were taken from the cores of folds and it was felt that their illite crystallinity values had been significantly enhanced by folding (see Section 5.9.).

The boundary between the high and low crystallinity areas was estimated to occur at crystallinity values of $0.25^{o}2\theta$, 12.0 and 185 for the Kubler, Weaver and Weber indices respectively. Examples of the half height peak width and "sharpness ratio" values for the upper and lower boundaries of anchizone metamorphism are presented in Table 5.D. In

FIGURE 5.11.1. A histogram showing the distribution of epizone and anchizone Kubler crystallinity values between the western Conwy Valley (left) and the rest of northern Snowdonia (right).

FIGURE 5.11.2. A histogram showing the distribution of epizone and anchizone Weaver crystallinity values between the western Conwy Valley (right) and the rest of northern Snowdonia (left).

FIGURE 5.11.3. A histogram showing the distribution of epizone and anchizone Weber crystallinity values between the western Conwy Valley (left) and the rest of northern Snowdonia (right).

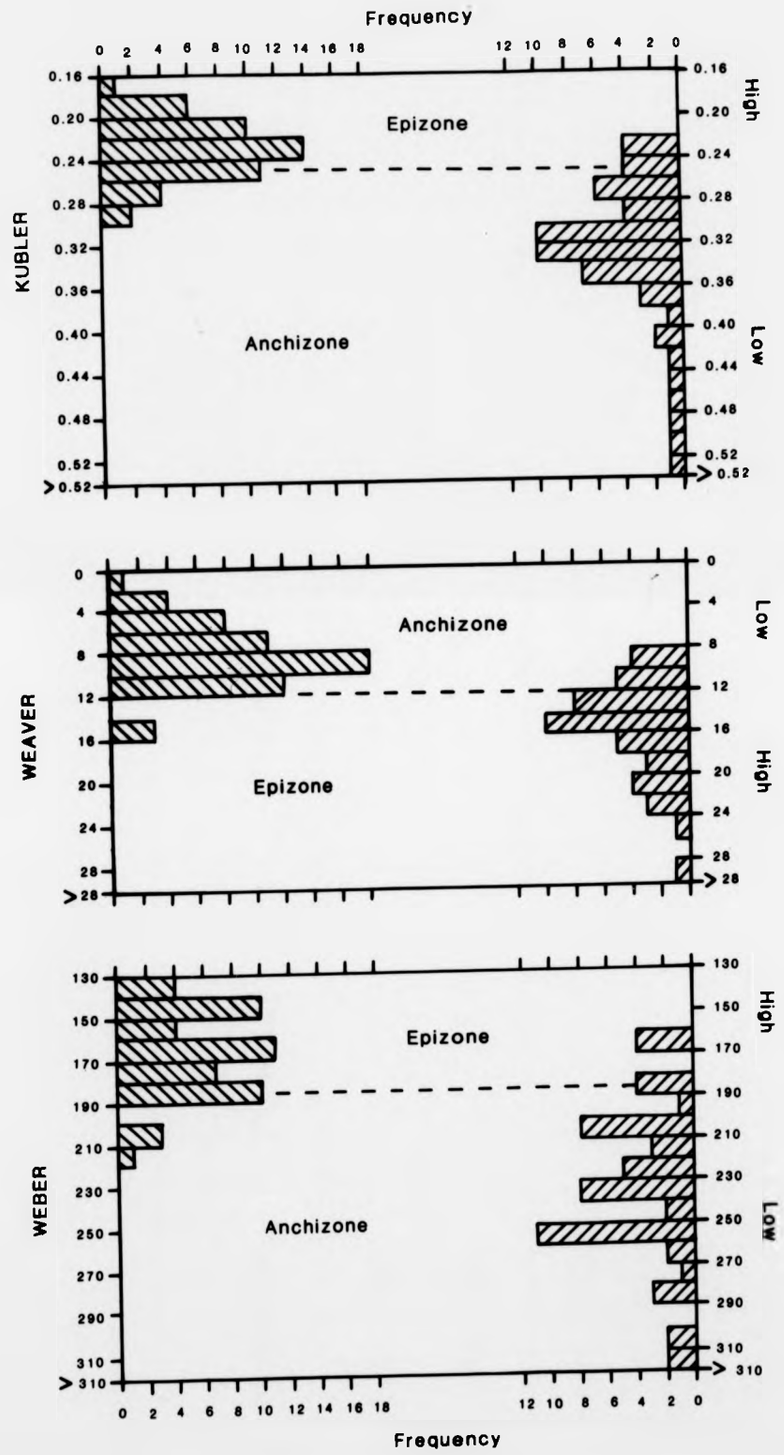

Source	Low-grade illite peak width of anchimetamorphic zone ($^{o}2\theta$)	High-grade illite peak width of anchimetamorphic zone ($^{o}2\theta$)	Minimum peak width of micas ($^{o}2\theta$)
Weaver (1960)	2.3 ("sharpness ratio")	12.1 ("sharpness ratio")	-
Kubler (1967)	$0.42^{o}2\theta$	$0.25^{o}2\theta$	$0.18^{o}2\theta$
Kubler (1968)	$0.56^{o}2\theta$	$0.30^{o}2\theta$	$0.21^{o}2\theta$
Weber (1972) (on polished rock slabs)	$0.25^{o}2\theta$	$0.17^{o}2\theta$	$0.15^{o}2\theta$
Kisch (1980)	$0.38^{o}2\theta$	$0.21^{o}2\theta$	$0.11^{o}2\theta$

TABLE 5.D. Critical values for the upper and lower boundary of the anchizone (from Kisch, 1980)

the case of the Weber index direct comparison between the data from northern Snowdonia and Weber's boundary values is not valid because of significant differences in sample preparation. By comparison to the Weaver and Kubler indices the anchizone/epizone boundary is given a value of approximately 185 on the Weber index which has been calculated on the < 2 μ fine clay sediment mounts.

From Table 5.D. it can be seen that the crystallinity values of 0.25^{o} 2θ, 12.0 and 185 are similar to the crystallinity values used to define the anchizone/epizone boundary in the literature. Most of the values of illite crystallinity obtained from samples taken from the area of high crystallinity (area A)are typical of epizone metamorphism (equivalent to low greenschist facies) whereas values in the low crystallinity area (area B) are typical of anchizone metamorphism.

The definition of the anchizone/epizone boundary in northern Snowdonia can only be tentative due to the lack of inter-laboratory standards necessary when ascribing absolute rather than relative values of illite crystallinity. However, bearing this limitation in mind,it is possible to distinguish groups of samples displaying crystallinities typical of the anchizone with > 85% of the lower crystallinity values in Table 5.C (area B) and crystallinities typical of the epizone with > 75% of the higher crystallinity values in Table 5.C (area A).

Weaver (1960) defined two subzones within the lower anchizone, "incipient to weak metamorphism" and "weak to very weak metamorphism", corresponding to mean Weaver values of 4.5 and 6.3 respectively. In the south and west of the area displaying typically anchizone crystallinity the mean Weaver value is 9.8, in the Silurian samples from east of the river Conwy the mean Weaver value is 8.2, both indicative of high-grade anchizone metamorphism. In contrast to this, samples taken from the northern coastal zone display mean Weaver values of 4.6 which is typical

FIGURE 5.12. Weaver vs Kubler crystallinity diagram showing the mean crystallinity values for samples from northern Snowdonia. Also shown is the range of crystallinity for: - low grade metamorphism (1), weak to very weak metamorphism (2), incipient to weak metamorphism (3), incipient metamorphism (4) and diagenesis (5). From Kubler (1968).

of low-grade anchizone metamorphism ("incipient to weak metamorphism", Weaver, 1960).

The empirical evidence, therefore, indicates that areas of typically epizone and anchizone illite crystallinity can be recognised. It would also appear that areas of typically high and low anchizone illite crystallinity can be distinguished within the anchizone area. The regional variation in illite crystallinity is summarised in Figure 5.12.

5.6.2. A statistical test for the significance of the variation in illite crystallinity in northern Snowdonia.

In this section the empirically derived hypothesis that two areas of contrasting illite crystallinity exist in northern Snowdonia is tested statistically. The most powerful parametric statistics for testing whether two groups of samples have been taken from the same background population is the T-test. The most serious constraints on its use are the assumptions that have to be made and subsequently tested before the statistic can be confidently employed. The two main assumptions are that the populations are normally or approximately normally distributed, and that there is no significant difference in the variance of the background populations (Hammond and McCullagh, 1974). The T-test is fairly tolerant of deviations from a normal sample distribution, especially if the sample numbers in each population are large; the critical assumption, therefore, is that the variance of the background populations are not significantly different. This is tested by calculating the "variance ratio"or F statistic where,

$$F = \frac{\text{greater estimate of population variance}^2}{\text{smaller estimate of population variance}^2}$$ (Hammond and McCullagh, 1978).

The null hypothesis (H_o) to be tested is.... "that there is no significant difference in the variance of samples taken from areas A and B". The calculated values of F are:

i) for the Kubler index $F = \frac{0.0262^2}{0.0756^2} = 8.15$

ii) for the Weaver index $F = \frac{2.9555^2}{4.2616^2} = 2.62$

iii) for the Weber index $F = \frac{18.3817^2}{45.5928^2} = 6.15$

These values for F are calculated on the basis of 49 samples from area A and 56 samples from area B. The 5 samples thought to have had their crystallinity enhanced by local folding (see Section 5.6.1.) are not included in the statistical analysis. The degrees of freedom are calculated as n_{1-1} and n_{2-1} where n_1 and n_2 are the numbers of samples taken from areas A and B, hence the degrees of freedom are 48 and 55. The critical values of F with 48 and 55 degrees of freedom at the 95% confidence level is 1.64 (Davies and Goldsmith, 1976, appendix Table D). The calculated values of F are all higher than the critical value of F, therefore H_o is rejected, hence significant differences between the variance of populations taken from areas A and B do exist.

The significance of these results is that they prove that the populations from the two crystallinity areas are significantly different in character, thus the assumptions inherent in parametric statistics are proved invalid thus making statistical examination dependent on non-parametric or distribution free statistics.

The most powerful non-parametric alternative to the T-test is the Mann-Whitney U-test (Siegel, 1956). This statistic makes no assumptions about the background populations. The H_o to be tested by the Mann-Whitney U-test is...."that there is no significant difference in the illite

crystallinity of samples taken from areas A and B". The alternative hypothesis (H_1) against which H_0 is tested is...."that samples taken from area A display significantly higher illite crystallinity than samples taken from area B". For large sample numbers the statistic Z is produced (Siegel, 1956). The determined Z values are:

i) for the Kubler index Z = 7.80

ii) for the Weaver index Z = 7.62

iii) for the Weber index Z = 7.78

The critical value of Z at the 95% confidence level is 1.60 (Siegel, 1956, Appendix Table A). All the calculated Z values are much higher than the critical value, therefore H_0 is rejected in favour of H_1 with the conclusion that illite crystallinity is significantly higher in area A than in area B.

In addition to testing the significance of differences in illite crystallinity between areas A and B, the population within area B was tested for homogeneity. Area B was divided into two subareas in Section 5.6.1. based on apparent differences in crystallinity between different parts of the area. Subarea B_1 consists of 40 samples taken from around Snowdon, the Glyders, the Carneddau, the southeastern part of the Conwy valley and around Llanberis and Bethesda. Subarea B_2 consists of 16 samples taken from the north of the area around Penmaenmawr, Conwy and north of Tal-y-Fan (see Figure 1.1. for locations). The H_0 that..."no significant difference in illite crystallinity exists between subareas $B_1$and B_2 was tested by the Mann-Whitney U-test. The determined Z values are:

i) for the Weaver index Z = 4.89

ii) for the Weber index Z = 3.83

The Z values are higher than the critical Z value of 1.60 and H_0

is, therefore, rejected leading to the conclusion that there is significant variation in illite crystallinity between different parts of area B.

By use of the Mann-Whitney U-test the empirically proposed hypothesis that areas of higher and lower illite crystallinity occur in northern Snowdonia has been substantiated. Further, it has also shown that significant variation occurs within the area of generally low (anchizone) crystallinity. Mann-Whitney U-tests between area A and subarea B_1 (the area of relatively higher illite crystallinity within area B) produced Z values of 6.04 for both the Weaver and Weber indices. This again supports the conclusion that areas of higher and lower crystallinity can be distinguished even after taking account of inhomogeneity within the populations concerned.

5.7. The boundary between the areas of typically anchizone and epizone crystallinity.

The regional crystallinity data can be divided into two distinct areas having significantly different illite crystallinity ranges (Figures 5.8. to 5.10). Area A is characterised by typically epizone crystallinity with mean Kubler, Weaver and Weber values of $0.229^{o}2\theta$ 15.6 and 168 respectively. The rest of northern Snowdonia (area B) is characterised by typically anchizone crystallinity with mean Kubler Weaver and Weber values of $0.332^{o}2\theta$, 8.0 and 234 respectively.

Figures 5.13.1 and 2 are cross-sections constructed from the Weaver crystallinity data and demonstrate the difference between the two crystallinity areas, especially the sharp nature of the boundary separating them. The boundary between the areas of typically epizone and anchizone crystallinity corresponds to the Ordovician/ Silurian unconformity from southeast of Betws-y-Coed (SH 795565) northwards towards Llanwrst (SH 800620). Between Llanwrst

FIGURE 5.13.1. Metamorphic cross-section between Dolwyddelan and Penmaenmawr, constructed from the Weaver illite crystallinity data.

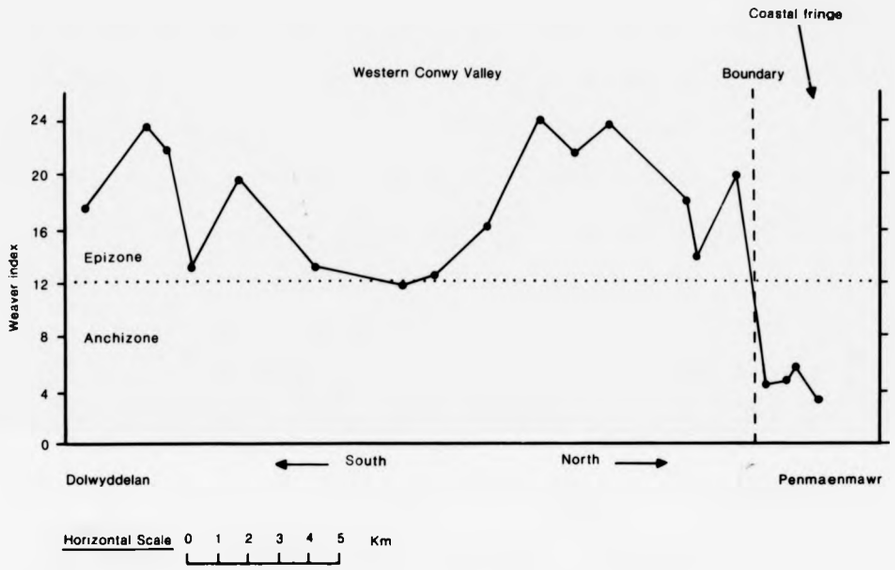

FIGURE 5.13.2. Metamorphic cross-section between Llanberis and Llanwrst, constructed from the Weaver crystallinity data.

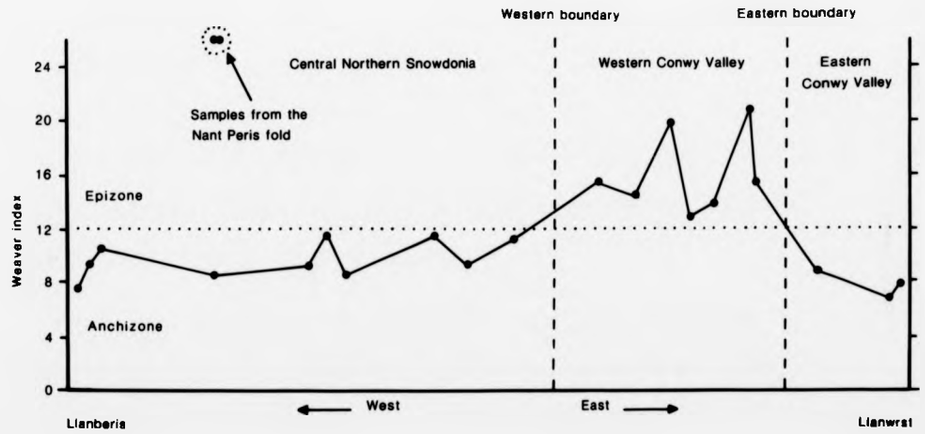

and Llanbedr-y-Cennin (SH 760695) the boundary is very sharp (Figure 5.13.2) and follows very closely the line of the Conwy valley fault (Howells et al.,1981). Comparison between the crystallinity maps (Figures 5.8. to 5.10) and the published maps (IGS Dolgarrog Special Sheet SH 76) indicates that the boundary in this area may be fault controlled. At Dolgarrog (SH 770675) the Conwy Valley fault splits into three branches with the main fault trending WNW towards Llanbedr-y-Cennin. At this point the trend of the crystallinity boundary also changes direction. In the north, around Tal-y-Fan (SH 735730) the boundary is most clearly defined and extremely sharp with the change from moderately high (>15.0 on the Weaver scale) to very low (<6.0 on the Weaver scale) crystallinity occurring between Tal-y-Fan and the hills above Penmaenmawr (SH 715765), a distance of less than 1.5 km (Figure 5.13.1.). The northern and northeastern part of the boundary corresponds very closely to Roberts'(1981) pumpellyite out/clinozoisite in isograd even, in detail, down to the kink in the isograd that Roberts' relates to the northwestern part of the Llanbedr fault in Bwylch-y-Ddeufaen (SH 715717). The northern part of the boundary is thus precisely defined over at least a part of its length utilising independent geological evidence. In at least two places the boundary closely follows or is affected by major faults. The critical factor is that the division between the two crystallinity zones is sharp and clearly defined rather than transitional.

South from Tal-y-Fan the change from typically epizone to typically anchizone crystallinity occurs along the eastern flank of the Carneddau mountain range and cannot be readily equated with any major geological features. From Capel Curig (SH 721581) southwards the boundary is less clearly defined, a reflection, in part, of a paucity of samples taken from this area.

Depending on the age relationships between illite crystallinity and deformation the boundary ought to be unaffected by major folds (post-deformation illite crystallinity) or folded by them (pre or syn-deformation illite crystallinity). In the vicinity of Capel Curig the boundary is sinuous and appears to be affected by the major large scale fold in the area, the Snowdonia syncline (Roberts, 1979). However, in order to conclusively prove whether or not the boundary is folded many more samples would be needed. This observation along with the clear association with the major faults might indicate that the areas of high and low illite crystallinity were established before the main Caledonian deformation.

5.8. The composite crystallinity index

The results obtained from the three crystallinity measurements can be amalgamated into a composite crystallinity index (CCI) for each sample. The CCI expresses the result of each crystallinity determination as a proportion of the total range in values observed in either the high or low crystallinity area and summates the values thus obtained. The values of 0.25^{o} 2θ, 12.0 and 185 for the Kubler, Weaver, Weber indices respectively, are used as a reference corresponding, approximately to the anchizone/epizone boundary (Section 5.6.1.) and are given values of zero. The maximum crystallinity value observed for each index is given a value of +100 whilst the minimum crystallinity value observed for each index is given a value of -100. The CCI is simply the increment of these values derived from the three crystallinity measurements.

The CCI can be calculated using the formula:

$$CCI = \left(\frac{Kref-Kobs}{KR(H)}\right) x100 + \left(\frac{Wobs-Wref}{WR(H)}\right) x100 + \left(\frac{Webref-Webobs}{Web\ R(H)}\right) x100$$

for samples where all three indices indicate epizone metamorphism, or

$$CCI = \frac{(Kobs-Kref)}{(KR(L))} \times 100 + \frac{(Wref-Wobs)}{(WR(L))} \times 100 + \frac{(Webobs-Webref)}{(WebR(L))} \times 100$$

for samples where all three indices indicate anchizone metamorphism:

Where;

Kobs/Wobs/Webobs = the observed crystallinity for each index.

Kref/Wref/Webref = the anchizone/epizone boundary values of 0.25^{o} 2θ, 12.0 and 185 respectively.

KR(H)/WR(H)/WebR(H) = the range of crystallinity values observed in the epizone, 0.075^{o} 2θ, 19.8 and 52 respectively

KR(L)/WR(L)/Web(L) = the range of crystallinity values observed in the anchzone, 0.41^{o} 2θ, 10.1 and 24.8 respectively.

For example, the CCI of sample R1 with crystallinity values of 0.2125^{o} 2θ, 19.7 and 158 for the Kubler, Weaver and Weber indices is calculated;

$$CCI = \frac{(0.25 - 0.2125)}{(0.075)} \times 100 + \frac{(19.7 - 12.0)}{(19.8)} \times 100 + \frac{(185 - 158)}{(52)} \times 100$$

$$CCI = 50.6 + 38.8 + 51.9 = 140.7$$

The calculated CCI for all samples are presented in Appendix 6 (iii) and the results are plotted on a map (Figure 5.14).

The main advantages in expressing the illite crystallinity results as a composite index are that data from three different determinations measured in two different ways are summarised as a single value and the data become amenable to parametric statistical testing,(see Section 5.6.2).

The expression of illite crystallinity as a proportion of the observed range in epizone or anchizone crystallinity is independent

FIGURE 5.14. A map showing the distribution of anchizone and epizone composite crystallinity index results in northern Snowdonia.

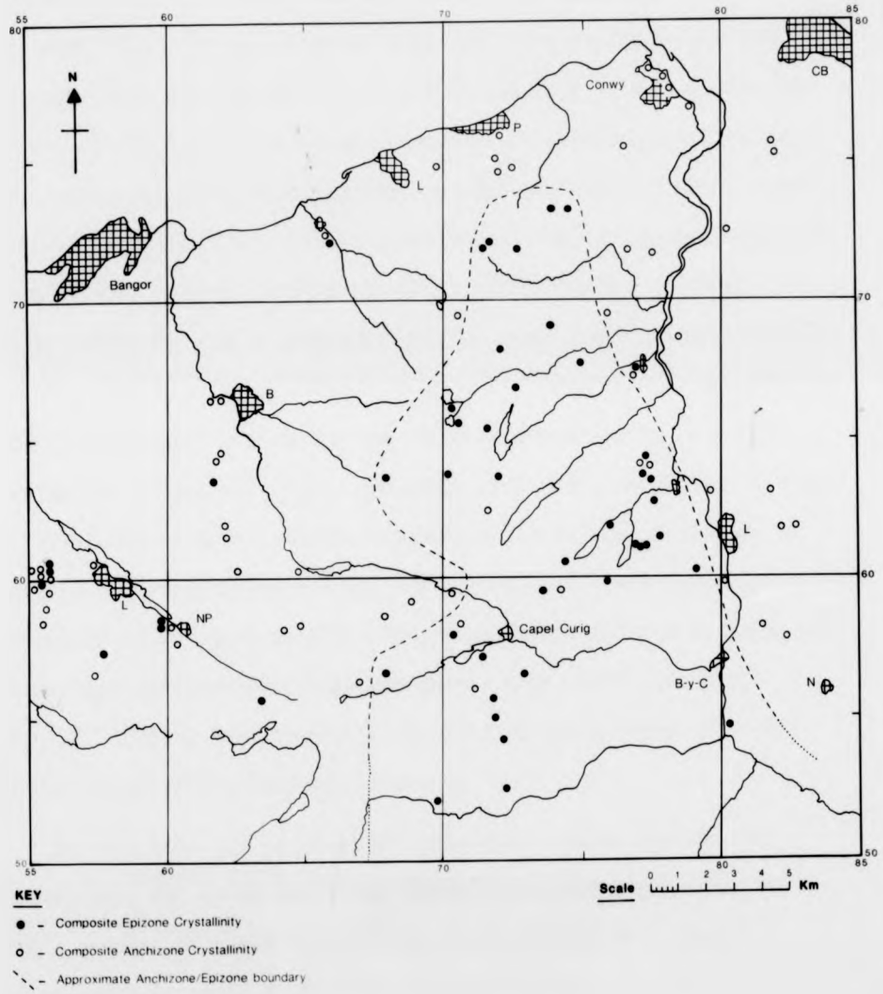

of the absolute values within the range and has the effect of "normalising" the data and reducing the variance between the two populations (areas A and B). An F-test was performed on 105 CCI results to test the H_o "that there is no significant difference in variance between populations taken from areas A and B". A value of F = 1.47 was obtained. The critical value of F is 1.61 (Davies and Goldsmith, 1976, Appendix Table D). As the calculated F statistic is lower than the critical F value H_o is accepted. The data, therefore, are suitable for statistical analysis using the powerful parametric T-test in order to test the H_o..... "that there is no significant difference in illite crystallinity between areas A and B", against the H_1 ...."that crystallinity in area A is significantly higher than crystallinity in area B". The calculated value of T is 11.01, the critical value of T, with 60 degrees of freedom at the 95% confidence limit, is ± 2.00 (Davies and Goldsmith, 1976, Appendix, Table C). Therefore, as the calculated value of T is higher than the critical value of T, H_o is rejected in favour of H_1 and the conclusion that there is a significant difference in illite crystallinity between areas A and B is supported. Hence, both parametric and non-parametric statistics uphold the emirical evidence that there are significant differences in illite crystallinity within northern Snowdonia.

The CCI does not provide any additional information to that derived from the three individual crystallinity measurements, it simply summarises these results and presents them as a single convenient bulk measure of illite crystallinity.

5.9. An example of the effect of folding on illite crystallinity

During the course of the illite crystallinity analysis it was found that several rather localised results within the area of generally anchizone illite crystallinity were much higher than the

majority of the crystallinity results in that area, in particular the results obtained from samples 40, 210, 212, 219, 279, 314 and 315. In the field it could be demonstrated that several of these samples were taken from the vicinity of anticlinal folds (samples 40, 279, 314 and 315).

As a result of an apparent correlation between high crystallinity and local folding it was decided to examine the relationship more closely. A particularly well exposed anticlinal fold was chosen for this purpose, exposed on the south side of the A4086 about 600m west of Nant Peris (SH 599587) in which slates, siltstones and sandstones of the Marchlyn Formation and slates of Llanvirn age are folded. The fold trends approximately north-south and plunges northwards at about 30^{o}, the wavelength is estimated to be about 300 - 400m and the amplitude about 100 - 150m. Ten samples were taken from the finer-grained horizons within the fold for illite crystallinity determination (Figure 5.15). The results obtained from these samples are presented in Table 5.E. and demonstrate that illite crystallinity rapidly increases towards the core of the fold. The crystallinity values obtained from the two samples taken closest to the core of the fold are some of the highest crystallinity values obtained in northern Snowdonia (samples 341 and 342), with Kubler values of $< 0.21^{o}$ 2θ, Weaver values of > 25.0; and Weber values < 150. The regional illite crystallinity determined in samples on the limbs of the fold is much lower with Kubler values of $> 0.25^{o}$ 2θ, Weaver values of < 10.0, and Weber values of > 185.

The three samples taken from the slate quarries (Figure 5.15) all exhibit low crystallinity. These results are thought to reflect the regional crystallinity of the area. The relationship between the Llanvirn slates and the main body of the fold is not clear in the field because of the presence of quarry spoil tips.Roberts (1979) observes that there is no obvious faulting and it was confirmed that the dips in the Llanvirn

FIGURE 5.15. Sketch of the Nant Peris anticline (SH 599587) showing sample locations and general geological characteristics.

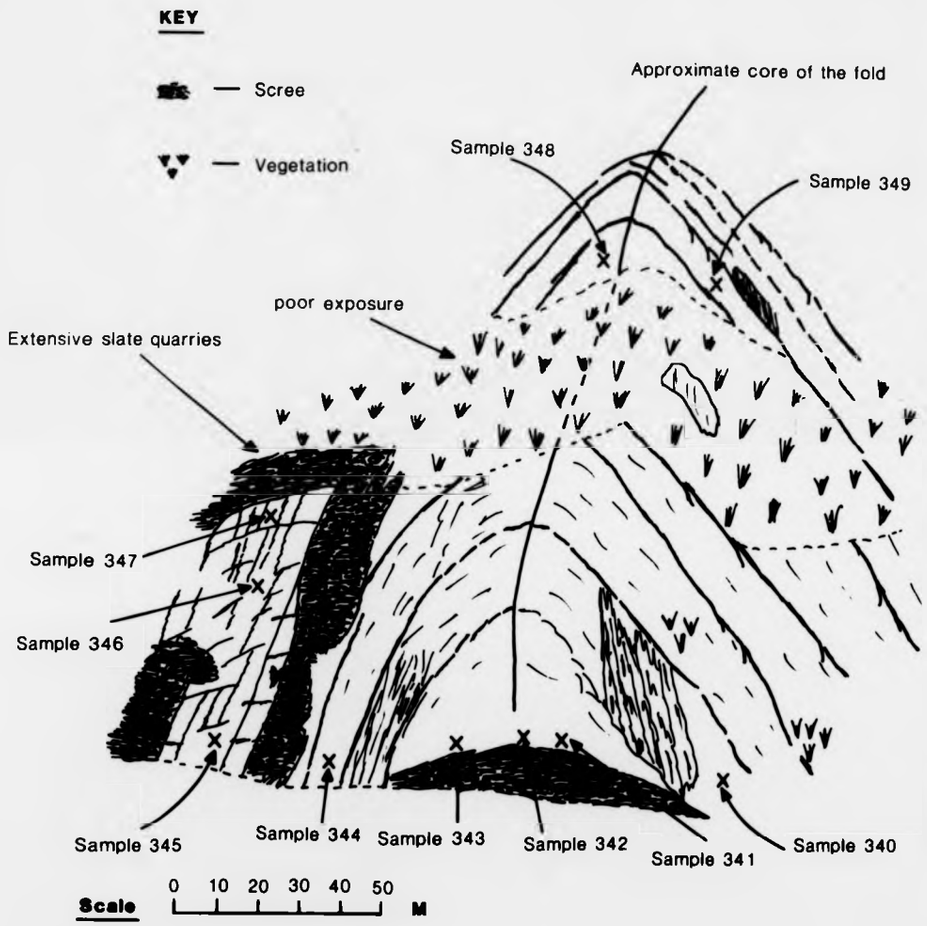

Sample Number	Kubler index	Weaver index	Weber index
340	$0.244^{o}2\theta$	13.2	183
341	$0.175^{o}2\theta$	31.2	147
342	$0.206^{o}2\theta$	25.4	150
343	$0.250^{o}2\theta$	10.5	192
344	$0.325^{o}2\theta$	7.7	225
345	$0.400^{o}2\theta$	6.9	300
346	$0.388^{o}2\theta$	5.8	292
347	$0.363^{o}2\theta$	7.8	258
348	$0.206^{o}2\theta$	14.4	166
349	$0.225^{o}2\theta$	16.2	183

TABLE 5.E. Illite crystallinity results for ten samples taken from an anticlinal fold near Nant Peris (SH. 599587).

slates were similar in direction and amount to those on the eastern limb of the anticline. The illite crystallinity determined on the two samples taken from around the axial zone of the fold on the hillside (samples 348 and 349, Figure 5.15) yield values significantly higher than those determined in the peripheral parts of the fold. The exact position of these samples in relation to the core of the fold was not clear because of large gaps in exposure on the hillside.

The evidence presented above clearly supports the conclusion that the local illite crystallinity can be markedly higher than the regional illite crystallinity in the axial zone of anticlinal folds, in the most extreme example in the Nant Peris fold by as much as 300% (samples 341 and 342). This fact could also account for the high crystallinity determined in sample 40 and the moderately high crystallinity determined in sample 39, both taken from the northeastern closure of the Arfon anticline (Roberts, 1979) exposed in mainly Upper Cambrian (Marchlyn Formation) slates near Aber (SH 656723). Similarly, sample 279 is taken from a small anticline developed within Caradoc sediments on the eastern side of Foel Goch (SH 578563). It is also possible that some of the higher crystallinity values observed in the slate belt samples around Llanberis could be related to the extensive small scale folding observed in many of the slate quarries.

The relationship between synclinal folds and illite crystallinity was not examined in as much detail, due in part to the lack of a suitable example of a well exposed synclinal fold. Crystallinity results from the vicinity of synclinal folds developed at Dolwyddelan (SH 700515), Grinwllm (SH 775625), Castell-y-Gwynt (SH 770610) and north of Trefriw (SH 775635), appear to reflect the regional crystallinity (samples 207, 201, 158, 151A, B and C, 127A, 128B and 129 respectively). However, all these folds are developed in the area of

typically epizone crystallinity where the effects of any crystallinity enhancement through folding might not be obvious. Also these samples are only taken from the general vicinity of synclinal folds and not necessarily from the actual cores.

From the investigation of the Nant Peris fold it is evident that local structure plays a potentially important part in determining local illite crystallinity. This example demonstrates that the enhancement of crystallinity in folds is confined to a relatively narrow belt within the axial zone. The possible causes of the higher crystallinity in folds are discussed in Section 5.10.2. It is felt, however, that structural control of illite crystallinity might account for some of the considerable local variation in crystallinity apparent within relatively small areas and as such constitutes an important consideration when interpreting regional illite crystallinity results.

5.10. The controls on illite crystallinity in northern Snowdonia

5.10.1. Compositional control

It has been shown that illite crystallinity determinations can be seriously affected by: i) major chemical variation between samples or groups of samples (Kubler, 1968), ii) the presence of significant amounts of paragonite (Frey, 1970; Dunoyer de Segonzac, 1970), and iii) the presence of mixed illite/swelling clay layers (Kubler, 1968). Approximate chemical and mineralogical homogeneity is essential otherwise apparent variation in crystallinity between samples, or groups of samples, might simply reflect original compositional differences rather than differences in metamorphic environment. Hence, if samples yielding epizone crystallinity (area A) are chemically and mineralogically different to those yielding anchizone crystallinity (area B) then the difference might reflect the compositional control rather than any metamorphic differences.

In order to quantify any variation in illite crystallinity related to mineralogical and chemical differences a number of bulk rock XRD scans were performed. Approximate chemical similarity between samples was assumed on the large scale due to the similar lithological and mineralogical characteristics of the samples. Broad mineralogical similarity was confirmed by undertaking 50 XRD bulk rock scans on pack mounted, crushed powders in the range 3 - 40^{o} 2θ (see Appendix 1(ii) for the machine conditions employed). The results are presented in Appendix 6 (iv) and show that the slates, shales and mudstones of northern Snowdonia consist largely of quartz + chlorite + mica (illite) ± albite in varying proportions. In addition several samples contained significant amounts of ore (pyrite or hematite) and one sample contained traces of calcite.

Over 70 samples were analysed for paragonite by scanning the critical range of 45 - 48^{o} 2θ (Frey, 1978). The results reveal that only 5 samples contain detectable quantities of paragonite (samples 209, 211, 237, 254 and 271), all from the Cambrian slate belt. The occurrence of paragonite indicates slightly higher Na_2O in some of the slate belt samples compared with samples from the rest of northern Snowdonia (Frey, 1978). The presence of paragonite can cause an underestimation of illite crystallinity when measured on the basis of half peak height width. Several samples revealed poor correlation between different pairs of indices (Figures 5.4. to 5.6) in particular samples 254, 237 and 211, all of which contain significant amounts of paragonite. The paragonite causes an effective broadening of the illite (001) peak due to the superimposition of the illite 10Å peak at 8.84^{o} 2θ and the paragonite 9.6Å peak at 9.20^{o} 2θ (Dunoyer de Segonzac, 1970). Hence poor correlation exists between indices that measure half peak height width (the Kubler and Weber indices) and are affected

by the paragonite 9.6$\mathring{A}$ peak and an index that ratios the intensity at a position on the high "d" spacing side of the illite 10$\mathring{A}$ peak (approximately 8.42^{o} 2θ) to the intensity of the 10$\mathring{A}$ peak itself (Weaver index) and is thus unaffected by the paragonite 9.6$\mathring{A}$ peak.

The absence of expanding clay layers within the illite was established by glycolation and subsequent heating to 550^{o}C. The presence of mixed swelling clay/illite layers would effectively broaden the illite 10$\mathring{A}$ peak. Interlayering of expanding clay and illite rapidly diminishes as pressures and temperatures increase (Dunoyer de Segonzac, 1970) so that if interlayering occurs it should be apparent in the lowest crystallinity (lowest grade) samples. The presence of mixed layers would result in peak shift after glycolation and partial peak collapse (due to dehydration) after heating to 550^{o}C. None of the samples treated displayed any peak shift or collapse leading to the conclusion that no expanding clay/illite mixed layers occur.

As a result of the above analyses it can be concluded that the differences in illite crystallinity observed in northern Snowdonia are not the result of additional mineral phases between samples or groups of samples but reflect genuine differences in the metamorphic environment.

5.10.2. Metamorphic control

The progessive sequence of changes leading to an increase in crystallinity with progressive burial were outlined in Section 5.2. Kubler (1968) and Padan et al. (1982) argue that increase in illite crystallinity is largely a function of increasing temperature. Dunoyer de Segonzac (1970) states that illite crystallinity is a function of temperature, pressure, fluid conditions and,possibly, local stress conditions.

If these conclusions are applied to the samples from northern Snowdonia it would follow that the area immediately west of the river Conwy (area A) was subjected to significantly higher grade metamorphism, in particular higher temperatures, than the rest of northern Snowdonia (area B). In the area of typically anchizone crystallinity (area B) a trend from low to intermediate crystallinity occurs from north to south and this is again thought to reflect significant differences in metamorphic grade. It thus seems likely that the major controlling factors on regional illite crystallinity are a combination of temperature and pressure which in turn reflect the depth to which the area has been buried. If temperature and pressure (burial) are the main controls on illite crystallinity it is evident from the presence of sometimes extreme local variation in crystallinity, particularly in the cores of folds, that other factors are of local importance as changes in temperatures and pressure cannot be invoked to account for such marked variation in so small an area. As a result it is felt that local conditions, in particular local stress and the passage of fluid through the system are major influences in producing the locally very high illite crystallinity developed in folds. Fracturing and small scale dislocations within the axial zones of folds would effectively open the system to the passage of fluids which would then in turn act as catalysts and markedly increase the amount of mineral recrystallisation (Dunoyer de Segonzac, 1970).

Knipe and White (1979) and Knipe (1981) examined the interaction of deformation (folding and cleavage development) and metamorphism in Ordovician slates and sandstones from Rhosneigr (Anglesey) that are of comparable lithology and have suffered similar metamorphism and deformation to the rocks of the present study. They conclude that deformation changes the composition of the illite/mica and argue that deformation will localise and enhance the transformation of illite into

phengitic mica (Knipe, 1981), which will lead to an increase in the illite crystallinity. Thus illite crystallinity is shown to be closely related to deformation with different intensity or style of folding and cleavage development leading, potentially, to differences in illite crystallinity.

The analysis of illite crystallinity is a bulk rock technique whereby the mean crystallinity of all the minerals present within the sample with a peak at about 10Å is determined (illite, muscovite, paragonite, biotite, and so on). The technique does not differentiate between different minerals and different phases of mineral growth. Maltman (1981) described primary bedding fabrics developed parallel to bedding in the Aberystwyth Grits in western central Wales. He argues that this is a reflection of compaction during burial prior to the Caledonian deformation during which a second fabric (cleavage) was produced. In northern Snowdonia it proved difficult to distinguish between early and late fabrics because of difficulty in recognising an early fabric due to the superimposed later cleavage. Maltmans conclusions could be interpreted to indicate that two generations of phyllosilicates exist. If the two generations of phyllosilicate have markedly different crystallinities, as seems likely from the work of Knipe (1980) then the mean crystallinity measured on the whole sample might simply reflect different proportions of each generation of phyllosilicate present within that sample. Hence it might be possible that the difference in regional crystallinity between areas A and B simply reflect more intense deformation in area A thus contributing a greater proportion of high crystallinity white mica to the bulk illite crystallinity figure. However, in the field this possibility was rigorously examined with respect to folding and cleavage development. In the field no difference in the intensity of cleavage or the intensity or style of folding could be distinguished between the areas of high and low crystallinity. This

observation was further supported by microscopic examination of the argillaceous rocks from both areas, again no systematic differences could be discerned.

As a result of these observations, it is felt that in the samples from northern Snowdonia the regional crystallinity reflects the temperatures and pressures associated with maximum burial, local departures from the regional crystallinity, particularly the high crystallinity observed in folds, reflects the development of high crystallinity white micas preferentially recrystallised in the axial zones of folds, largely as a result of local stresses and the passage of fluid through the system (Hobbs et al.,1976) and is clearly related to Caledonian deformation.

From the above discussion of the factors that control illite crystallinity and the application of these to the slates, shales and mudstones of northern Snowdonia, it would appear that the areas of high and low crystallinity (areas A and B respectively) reflect genuine differences in metamorphic temperatures and pressures with area A having experienced generally higher temperatures and pressure then area B. Robinson et al. (1980) suggest that in South Wales, low anchizone crystallinities indicate temperatures of about 200^{o}C. Frey et al.(1980) compared illite crystallinity with fluid inclusion homogenisation temperatures to correlate the base of the anchizone with temperatures of about 220^{o}C and the transition from low to high anchizone crystallinity with temperatures of about 270^{o}C. Schiffman and Liou (1980) suggest that the boundary between the prehnite/pumpellyite and greenschist facies occurs at between 325^{o}C at 2Kb and 375^{o}C at 5Kb. If these figures are applied to the illite crystallinity data from northern Snowdonia it would appear that metamorphic temperatures along the northern coast (area B_1) were between 220 - 270^{o}C; east of the river

Conwy and west of the Carneddau Glyders and Snowdon mountain ranges (area B_2) between 270°C and approximately 325°C; and immediately west of the river Conwy (area A) > 325°C. The implications of these findings along with information derived from other metamorphic indicators are discussed in Chapter 8.

5.11. The relationship between stratigraphy and illite crystallinity in northern Snowdonia

It is well established that illite crystallinity increases progressively with burial from low-grade diagenesis at shallow depths to epizone metamorphism at greater depths as pressure and temperature increases (Weaver, 1960; Dunoyer de Segonzac, 1970; Frey, 1970 and Kisch, 1980).

In northern Snowdonia illite crystallinity was determined on samples ranging in age from lower Cambrian to Silurian. No correlation was found to exist between illite crystallinity and the age of the sample as might be expected if a simple model is envisaged involving the burial of older (Cambrian) strata under progressively younger (Ordovician and Silurian) strata of uniform thickness. However, the Lower Palaeozoic geology of North Wales was influenced by numerous phases of uplift and erosion (Roberts, 1979) for example, at the base of the Arenig, at the base of the Caradoc and (locally) at the base of the Snowdon Volcanic Formation (Beavon, 1963).

An example of the importance of these unconformities in the geology of North Wales is provided by the Tremadoc-Arenig unconformity which increases in magnitude to the north and west. In Llyn over 5000m of Cambrian strata is thought to have been removed during uplift and erosion whilst to the south, around the Harlech Dome, very little material was removed (George, 1961). This marked variation in the effects of the lower Palaeozoic unconformities in North Wales is

thought to reflect relative movement on several large NE-SW and N-S trending, basement controlled faults that were operative during the Lower Palaeozoic (Kokelaar et al. in press). Deposition and preservation of both sedimentary and volcanic material has been strongly influenced by these vertical faults, examples of which include the Dinorwic fault, the Aber Dinlle fault, the Bangor fault, the Llanbedr fault and the Conwy valley fault, all of which can be shown to have influenced local palaeogeography during the Lower Palaeozoic. As a result of movement on these large faults large scale variation in stratigraphic thickness occur over very short distances with the ponding of sediments and volcanics in subsiding grabens and against scarps formed by vertical movement on the faults (Kokelaar et al., in press)and the removal of locally very great thicknesses of strata on the upthrown horst blocks (for example, the Padarn and Bangor ridges).

From the above discussion it is clear that by the end of the Silurian marked variation would have existed in the nature and thickness of Lower Palaeozoic material in North Wales. The complexity in Lower Palaeozoic deposition and preservation could account for some of the regional variation in illite crystallinity. It is, perhaps, not surprising that a simple stratigraphic age-illite crystallinity correlation is not found because samples were taken across the major structures. These structures would have played a significant role in the burial of material with greater thicknesses of material deposited on downthrown blocks, leading to higher temperatures and pressure, with thinner deposits on upthrown blocks leading to relatively lower temperatures and pressures.

In Section 5.7. it was seen that the boundary between areas displaying typically anchizone and areas displaying typically epizone crystallinity is very sharp and in several places is related to, or coincident with, major faults such as the Conwy Valley fault, the

Llanbedr fault and the fault in Bwlch-y-Ddeufon. As a result of this relationship and the influence of the faults on local stratigraphy and palaeogeography it would appear that metamorphism was also influenced by major faults operative during the Lower Palaeozoic. The effect of penecontemporaneous faulting would be to control the thickness of cover (burial) which in turn governs pressure and temperature. As the major faults operative during the Lower Palaeozoic are crossed there is likely to be a change in illite crystallinity as the stratigraphic control of temperature and pressure changes. This relationship can be seen in northern Snowdonia. To the west of the Conwy Valley fault higher crystallinity is developed (reflecting deeper burial) and to the east of the fault lower crystallinity is developed (reflecting shallower burial). Also, around Tal-y-Fan (SH 729727) the same pattern is observed with low crystallinities developed west of the fault in Bwylch-y-Ddeufan and high crystallinities to the east of the fault.

5.12. Concluding remarks

The analysis of illite crystallinity in northern Snowdonia has provided much valuable information concerning the metamorphism of the area. Utilising these results it is possible to define an area of typically epizone metamorphism (low greenschist facies) surrounded by an area of typically anchizone metamorphism (sub-greenschist facies) separated by a sharply defined break in illite crystallinity. In addition, a clear relationship between deformation and illite crystallinity has been demonstrated.

Analysis of the crystallinity of illite has led to the conclusion that regional variation is largely controlled by pressure and temperature and is thought to reflect burial under a stratigraphic pile of varying thickness. Local variation from the regional pattern is thought to

reflect the impact of local stress and fluid action during the Caledonian deformation which led to the localised re-crystallisation of generally high crystallinity white micas, particularly in the cores of folds.

Any model invoked to explain the pattern of metamorphism observed in northern Snowdonia must take account of:

i) the presence of a zone of typically epizone crystallinity surrounded on three sides by a zone of typically anchizone crystallinity,

ii) the very sharp nature of the boundary between these two zones, particularly in the north around Tal-y-Fan, and,

iii) the similar crystallinity of samples taken from different stratigraphic horizons in different areas, for example, the similar illite crystallinity values in the Cambrian slates around Llanberis and the Silurian shales and mudstones east of the river Conwy.

These observations, and the intimate relationship between illite crystallinity,major block faulting in the Lower Palaeozoic and local stratigraphy lead to the conclusion that the pattern of illite crystallinity (metamorphism) observed in northern Snowdonia has been markedly influenced by the operation of major Lower Palaeozoic block faults that are known to have influenced local deposition and preservation in North Wales (Kokelaar et al.,in press).

CHAPTER 6

WHITE MICA GEOBAROMETRY

6.1. Introduction

The composition of rock forming minerals has long been used to obtain information concerning the physical conditions prevalent during metamorphic events. Particularly useful in this context are minerals such as feldspars, micas, garnets and epidotes, all of which are characterised by being members of solid solution series. By considering the chemical composition of these minerals, either individually or as coexisting pairs, much valuable information concerning pressure, temperature, composition of the fluid phase and the attainment of equilibrium can be deduced.

In the context of this study structural data on the dioctahedral white micas is used to determine precise chemical compositions of the micas (Radoslovich and Norrish, 1962). For white mica geobarometry the critical compositional trend is that of increasing "celadonite" content within the white micas with increasing pressure (Sassi and Scolari, 1974, Guidotti and Sassi, 1976). Guidotti and Sassi (1976) define "celadonitic muscovites" as those containing "significant octahedral Fe^{2+} and Mg and represent partial solid solution towards celadonite, the dioctahedral, tetrasilicic mica". The approximate "celadonite" content of the white micas contained within an individual sample can be determined by means of X-ray diffractometry (XRD), specifically through the measurement of the b_o lattice parameter which has been shown to reflect the ionic substitution of Fe and Mg for Al and to progressively increase as pressure increases (Sassi and Scolari, 1974, Guidotti and Sassi, 1976). Hence b_o can be used to establish the approximate baric environment for the slates, shales and mudstones of northern Snowdonia. Subsequent utilisation of this technique

includes work by Fettes et al. (1976), Robinson (1981) and Padan et al. (1982). XRD was preferred to microprobe analysis of the white micas contained within the slates, shales and mudstones of northern Snowdonia due to the difficulty in obtaining reliable microprobe results for hydrous minerals in fine-grained rocks.

The aims of the white mica XRD analyses undertaken in northern Snowdonia include:

i) Establishing the approximate baric environment prevalent during low-grade metamorphism by determining the mean regional b_o of the white micas.

ii) The examination of any systematic variation in b_o on the regional and local scale.

iii) A critical assessment of the intensity ratio, I_{002}/I_{001} (Esqevin, 1969) as a geobarometer.

iv) The correlation and comparison of the white mica XRD results with other indicators of metamorphic conditions.

6.2. The principle of white mica geobarometry

6.2.1. The use of XRD to determine the composition of white mica.

The (060) peak can be conveniently used to distinguish between dioctahedral and trioctahedral micas (Brindley and Brown, 1980). Radoslovich and Norrish (1962) show that the lattice parameters (particularly the b direction) of micas are controlled by compositional variation in the octahedral layer. They found that as Fe and Mg replace Al in the octahedral sites the b dimension systematically increases, hence b_o can be used as a measure of the substitution of Fe and Mg for Al. Ernst (1963) found that low temperatures and high pressures favour higher octahedral Fe + Mg contents, a conclusion supported by the experimental work of Velde (1965). It thus follows that b_o is affected

by pressure as b_o changes with Fe and Mg substitution for Al which is directly related to pressure.

XRD has been used for the purpose of determining the "celadonite" content of white micas for the purpose of geobarometry by Esquevin (1969), Cipriani et al. (1971), Sassi and Scolari (1974), Guidotti and Sassi (1976) and Padan et al. (1982). White mica composition can be estimated from XRD data by determination of the lattice parameters b and c which are influenced by phengitic substitution in muscovite (Fe + Mg replace Al in the octahedral sites) and paragonitic substitution in muscovite (Na replaces K in the interlayer sites), respectively b and c (or more precisely c sin β) can be calculated from the d_{060} and d_{001} (where 1 is dependent on the structural type) reflections respectively.

Guidotti and Sassi (1976) suggest that:

i) With increase in Na/Na + K (reflecting the substitution of paragonite for muscovite) the "d" spacing of (001) will increase

ii) With increase in octahedral substitution of Fe and Mg for Al (reflecting the substitution of phengite for muscovite) the "d" spacing of (001) will decrease and the "d" spacing of (060) will increase.

In addition Esquevin (1969) suggests that as Fe and Mg replace Al in the octahedral sites the intensity ratio I_{002}/I_{001} will increase.

As it is the substitution of Fe and Mg for Al in the octahedral sites that is of interest in geobarometry, d_{060} and the intensity ratio are the most potentially useful diffractometric measurements. Since Esquevin (1969) first proposed the intensity ratio as a measure of octahedral Al/(Fe+Mg) several authors (for example, Kisch, 1980 and Padan et al., 1982) have cast doubt on the reliability of this factor as

a geobarometer. The reliability of the intensity ratio will be examined relative to the samples from northern Snowdonia in section 6.7.

Recently doubt has been expressed concerning the use of XRD to determine the precise phengite and paragonite contents of white micas (Naef and Stern,1982). It would appear that single sample diffractometric measurements may be potentially unreliable as large discrepancies can occur between the chemistry predicted from XRD and that determined by electron microprobe. However, the problem of large errors on XRD measurements on single samples is largely overcome by employing the method of Sassi and Scolari (1974) and Padan et al. (1982) whereby compositional data from a large number of samples is plotted on a b_o cumulative frequency diagram and the statistical characteristics of the population as a whole is then considered.

Alternative methods of determining white mica compositions include conventional wet chemical analysis and electron microprobe analysis, however, both alternative techniques are problematic. Because of the difficulty in separating white mica from other minerals (particularly chlorite) in low-grade metamorphic rocks wet chemical analysis tends not to be used as an alternative to XRD. Electron microprobe analysis is not always suitable because of the problem of fine grain size and dehydration due to the use of a finely focused beam on hydrous minerals. It would appear, therefore, that XRD is the most suitable method of determining the degree of substitution of Fe and Mg for Al in white micas. Compositions determined from XRD data for individual samples may be unreliable and thus of limited value, cumulative compositional data based on a large number of samples may, however, provide useful geobarometric information.

6.2.2. The effect of composition, temperature and pressure on b_o

It is evident that the three major controls on white mica octahedral chemistry and hence b_o are bulk rock composition, temperature and pressure (Guidotti and Sassi, 1976). Obviously any reliable use of b_o as a geobarometer must take into account any possible effect of factors such as temperature and host rock compositional control.

i) Composition. The white micas recommended for b_o analysis are those taken from assemblages where any change in mineral chemistry is independent of bulk rock chemistry (Guidotti, 1973). In practice compositional control is usually less rigorous. Sassi and Scolari (1974) and Guidotti and Sassi (1976) recommend that samples containing paragonite, K-feldspar, abundant quartz, abundant chlorite, carbonate minerals and significant hematite or magnetite should be avoided. They found that b_o is significantly increased in samples bearing K-feldspar and large amounts of chlorite or quartz, but significantly decreased in samples containing paragonite or carbonate minerals. The presence of significant amounts of hematite or magnetite would imply a high host rock Fe^3/Fe^{2+} ratio which would lead to a high white mica b_o.

ii) Temperature. In rocks that have suffered diagenetic change or anchizone metamorphism it would appear that increasing temperature results in a slight increase in b_o (Padan et al., 1982). In epizone rocks increase in temperature results in a progressive decrease in b_o reflecting a progressive increase in the muscovite content of the white micas (Velde, 1965; Guidotti and Sassi, 1976). The implication of these findings is that maximum b_o is developed in samples from the upper

anchizone or lower epizone of the facies series being examined.

iii) Pressure. As pressure increases there is also a progressive increase in Fe and Mg substitution for Al in the octahedral sites reflected by an increase in b_o. The increase in mean b_o from a low pressure facies series metamorphism to a high pressure facies series metamorphism is approximately from 8.990 (Bosost type) to 9.055 (Sanbagawa type), (Sassi and Scolari, (1974).

The relationship of b_o to temperature and pressure is shown in Figure 6.1.

For the white mica geobarometry undertaken on the samples from northern Snowdonia the effects of host composition and temperature on the b_o results are discussed in more detail in sections 6.3 and 6.6.2 respectively.

6.3. Problems of b_o analysis in the low-grade rocks of northern Snowdonia.

Although b_o analysis is a relatively rapid technique it can yield useful data concerning the baric environment prevalent during the formation of the white micas. However, several problems arise when attempting to use the technique on low or very low-grade rocks. Three major problems can be recognised i) the measurement of the exact position of(060)from a broad peak of low intensity, ii) mineralogical and chemical inhomogeneity potentially significantly influencing the octahedral chemistry of the white micas (Guidotti and Sassi, 1976), and iii) difficulty in assessing the potential role of temperature as a control on white mica octahedral chemistry.

The problems of measurement reflect the nature of the technique and

FIGURE 6.1. The influence of pressure and temperature on white mica b_o, from Guidotti and Sassi (1976).

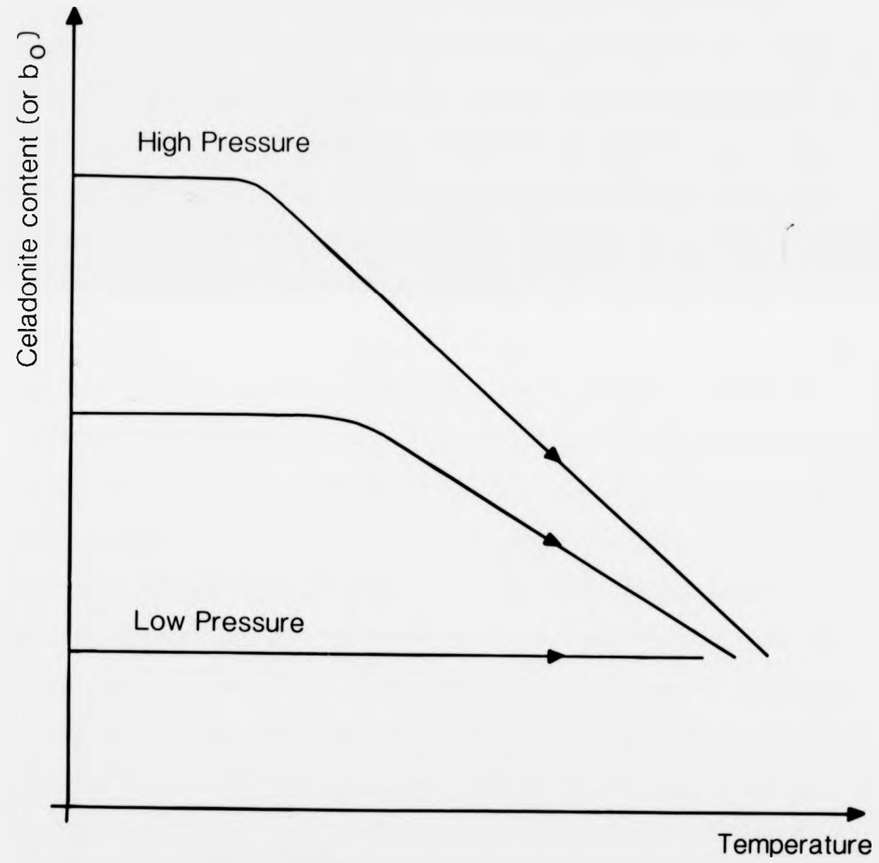

can be alleviated by careful sample preparation and statistical consideration of the results. The influence of host rock chemical control and the effects of temperature need careful consideration as they may influence the geological interpretation of the results.

Chemical and mineralogical inhomogeneity between samples could potentially diminish the value of the b_0 analyses. The effect of gross chemical and mineralogical differences between samples was outlined in section 6.2.2. In order to minimize large scale inter-sample compositional differences only slates, shales and mudstones of approximately similar mineralogical composition were utilized. This assertion was confirmed by a series of bulk rock XRD scans over the range 3 - 40° 2θ the results of which are presented in Appendix 6 (IV). Guidotti and Sassi (1976) recommend that quartz and chlorite rich samples be avoided for b_0 analysis as they found that white micas from these samples tend to yield anomalously high b_0 values. Clearly all the samples from northern Snowdonia contain significant amounts of both quartz and chlorite, however,none of the samples utilized contain a disproportionately large amount of either quartz or chlorite. The presence or absence of mixed layer clays was investigated by glycolation and heat treatment of the clay fraction and is discussed in Chapter 5 where it was concluded that mixed layer clays are generally absent in the samples from northern Snowdonia. The presence of significant amounts of paragonitic mica (mica in which Na has replaced K in the interlayer sites) was clearly demonstrated by scanning the critical 2θ range of 45 - 48°. Guidotti and Sassi (1976) and Robinson (1981) found that mean b_0 in paragonite-rich samples is significantly lowered. However, Padan et al. (1982) found that white micas from paragonite-rich assemblages need not necessarily contain significantly less octahedral Fe + Mg than those from paragonite-free samples from the same area. Although samples 209, 211 and 254 were found to contain

significant paragonite, the b_o of white micas from these samples does not appear to be any lower than the regional b_o. In the case of sample 211 the b_o is in fact rather higher than that determined on the surrounding paragonite-free samples.

The general affect of temperature on b_o was briefly outlined in section 6.2.2. This particular aspect of white mica geobarometry is criticaly important when interpreting b_o data obtained from rocks of very low metamorphic grade (Padan et al., 1982). The influence of metamorphic temperatures on b_o in the white micas from northern Snowdonia is discussed in some detail in section 6.6.2 where the correlation between illite crystallinity (reflecting metamorphic grade) and b_o (reflecting the relative pressure and temperature conditions) is critically examined.

6.4. Sample preparation and analysis.

White mica geobarometry was undertaken on 50 slates, shales and mudstones from northern Snowdonia. Samples were chosen to provide an even distribution of analyses over the area and to represent as wide a stratigraphic range as possible. The samples used for the b_o analyses were selected from those used for the illite crystallinity survey. Sample locations are listed in Appendix 2 (ii).

The "celadonite" content of white mica is estimated by precise measurement of the position of the (060) peak which is then used to calculate b_o. The quartz (211) peak at 1.541$\mathring{A}$ is used as an internal standard throughout. It was found that the smear mounts used for the illite crystallinity analyses were not suitable for b_o determination because during the preparation of the smear mounts most of the quartz had been removed, resulting in low intensity of the quartz (211) peak, and phyllosilicate orientation parallel to (001) occurred resulting in

very low (060) peak intensities. Therefore, cavity mounts of powdered bulk rock samples were prepared for the b_o determinations. Bulk rock powders were produced by ball milling a small amount of sample for about 15 minutes. The powder was then packed tightly into a modified cavity mount so that orientation of the phyllosilicate sheets was parallel to,rather than normal to,the X-ray beam (Robinson, 1981).

Despite using these cavity mounts the intensity of the white mica (060) peak was often very low and definition poor. As a result the potential error in measurement for a single b_o determination may be relatively large. In order to overcome this problem several determinations of the exact peak position of (060) were undertaken on each sample and the mean b_o value for these measurements utilized. The machine conditions employed for the b_o determinations are listed in Appendix I (ii).

6.5.1. The results.

The results of the b_o determinations performed on the samples from northern Snowdonia are tabulated in Appendix 6(v) and presented on a map of the area (Figure 6.2), they are also plotted as a histogram to which reference will be made later (Figure 6.3).

6.5.2. Reliability of the results.

White mica geobaraometry relies on the measurement of the exact position of the (060) diffraction peak and from this,calculation of the lattice parameter b_o. Three potential sources of error were considered, i) machine errors, ii) sample preparation errors,and,iii) measurement errors.

The reliability of the equipment was rigorously tested using pack and smear mounts containing mixtures of known standards CaF_2 (fluorite) $KBrO_3$ (potassium bromate) and SiO_2 (quartz). Numerous scans were

FIGURE 6.2. A map showing the distribution of relatively higher (> 9.000) and lower (< 9.000) white mica b_o results in northern Snowdonia.

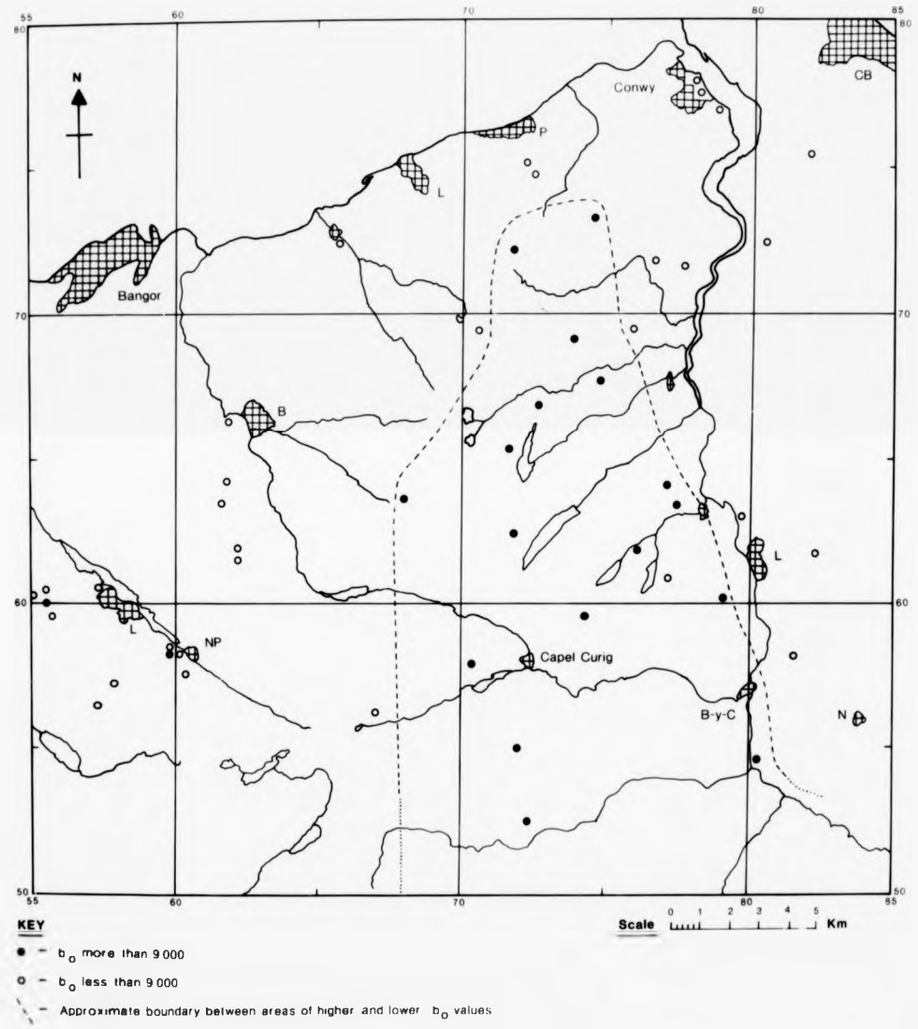

FIGURE 6.3. Histograms showing the distribution of white mica b_o results in (i) the western Conwy Valley, and (ii) the rest of northern Snowdonia.

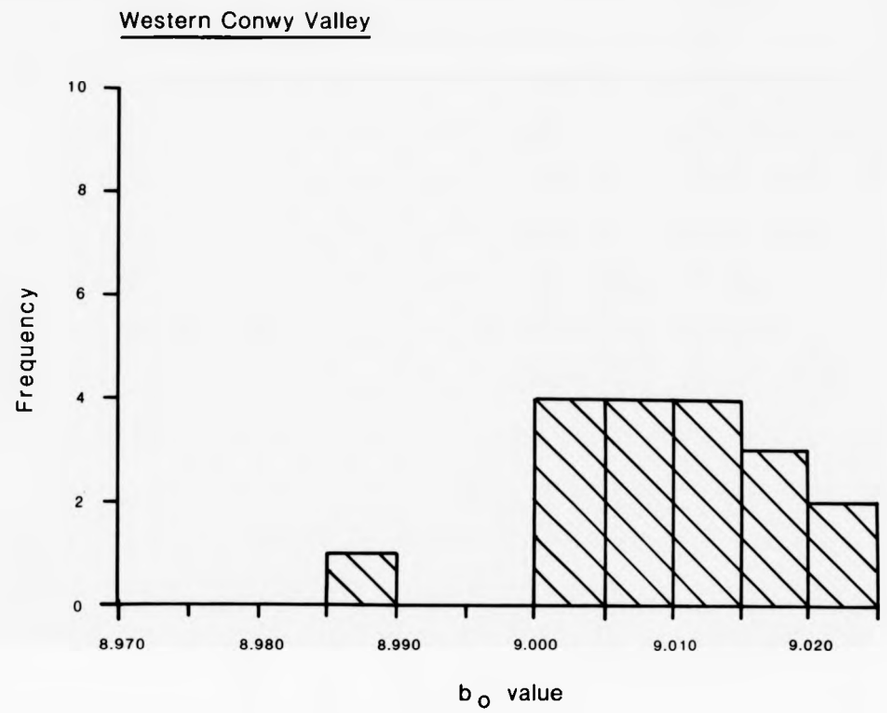

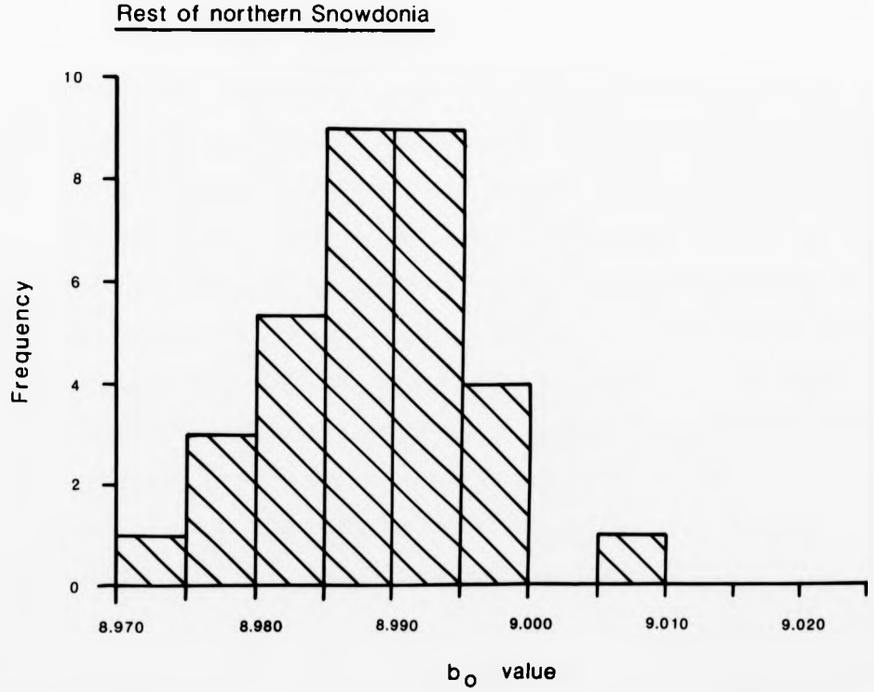

FIGURE 6.2. A map showing the distribution of relatively higher (> 9.000) and lower (< 9.000) white mica b_o results in northern Snowdonia.

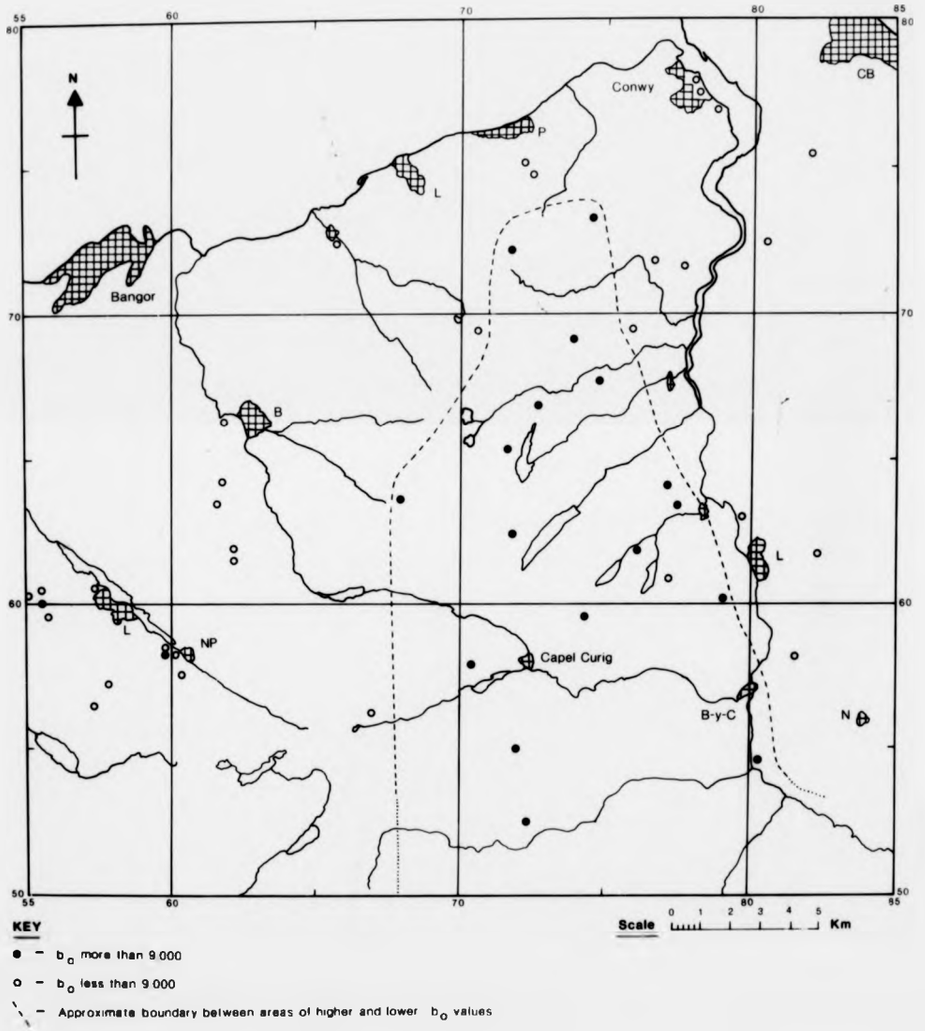

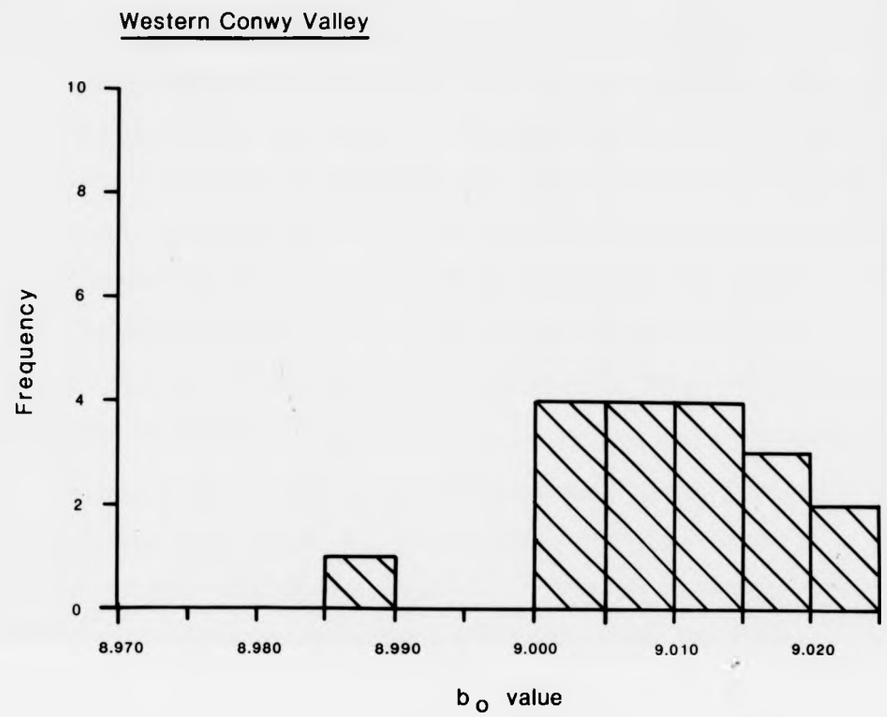

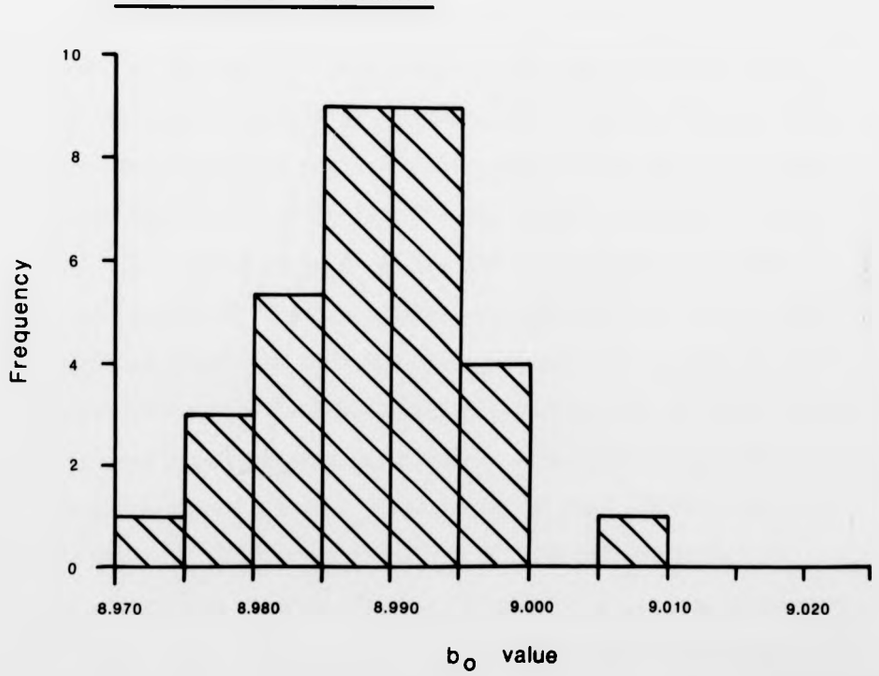

FIGURE 6.3. Histograms showing the distribution of white mica b_o results in (i) the western Conwy Valley, and (ii) the rest of northern Snowdonia.

undertaken between different peaks, utilizing a range of machine conditions, and the precise inter-peak distances were measured. This observed distance was then compared to the actual distance calculated from the known positions of the diffraction peaks of the three standards. In all cases the difference between the expected and observed figures was less then 0.5mm on the chart. This would indicate that errors related to machine factors are very low for the machine conditions employed in the calculation of b_o (less than 0.7% of the actual distance measured on the chart).

Errors related to sample preparation were not rigorously investigated, although about 20% of the samples had more than one mount prepared. It was found that no significant difference in the position of (060) occurred between different preparations of the same sample. The major difference between different mounts of the same sample occurred in peak intensity and definition and is thought to reflect the quality of the mount produced.

The third potential source of error results from the precise measurement of the position of poorly defined, low intensity peaks. The intensity and definition of (060) depends on the quality of the mount and the quantity of phyllosilicate minerals present within the sample and, therefore, varies considerably between samples. In order to quantify the variation in b_o determined on a single sample each sample was scanned at least five times. In several cases individual scans produced peaks that were too poorly defined to measure, in other cases scans produced several small peaks corresponding to (060), thereby rendering precise measurement impossible. In such cases each small peak was measured and a mean b_o calculated for that sample. The apparent multiple (060) reflections are not thought to reflect the presence of white micas with different octahedral Fe and Mg contents as usually only one, or occasionally two scans, out of five showed this

effect and the exact position of the peaks varied between runs. The standard deviation was calculated for all the measured (060) peaks for each sample and ranged from 0.0008 to 0.0116. This figure reflects the amount of variation between different scans on the same sample so that a higher standard deviation reflects greater variation between individual scans. In addition the pooled variance was calculated on all the measured scans and a mean one standard deviation pooled variance of 0.0058 produced.

Because of the potential errors outlined above, and the doubts expressed by Naef and Stern (1982) concerning the reliability of XRD as a method of determining the precise "celadonite" substitution in white mica, only the statistical characteristics of a group of samples can be considered with any confidence. By adopting this approach it was hoped to minimize the problems caused by the relatively low intensity and poor definition of the white mica (060) peak, chemical and mineralogical inhomogeneity between individual samples and the uncertainty of using XRD to measure the octahedral substitution of Fe and Mg for Al.

6.6. Discussion of the results.

6.6.1. Regional variation in b_o

From the results of the b_o determinations (Appendix 6(v) and Figures 6.2. and 6.3) it is evident that marked variation exists in white mica b_o values both on the large, regional, scale (between different parts of northern Snowdonia), and on the small, local, scale (between samples taken from a small area within northern Snowdonia).

In general higher b_o appears to be consistently displayed by samples from the western part of the Conwy Valley and lower b_o by samples from the rest of northern Snowdonia (Figure 6.2). The boundary of this zone of characteristically higher b_o appears to correspond to

the boundary between anchizone and epizone illite crystallinities described in Chapter 5. The correlation between illite crystallinity and white mica b_o is examined in detail in section 6.6.2. From the histogram (Figure 6.3) it would appear that the boundary between the zones of higher and lower b_o occurs at a b_o value of approximately 9.000. Although the absolute change in b_o between the two zones is very small, the break does appear to be sharp as only one sample with a mean b_o less than 9.000 occurs in the higher b_o zone (values > 9.000), and only one sample with a mean b_o greater than 9.000 occurs in the lower b_o zone (values < 9.000).

As well as the broad regional variation in b_o significant local variation in b_o occurs. Sassi and Scolari (1974) also describe similar variation in white mica b_o between samples of similar lithology and metamorphic grade and taken from a small area. Some small scale variation in b_o might reflect slight compositional differences between samples, however, this possibility was not rigorously examined as only gross compositional differences were investigated through the bulk rock XRD scans. The presence of significant inter-sample variation in b_o, even where samples are closely spaced, again indicates the need for caution when interpreting b_o results and is further justification for utilisation of the b_o - cumulative frequency approach of Sassi and Scolari (1974).

In addition to the regional and local variation in white mica b_o outlined above, the possible influence of stratigraphical control was also considered. However, it appears that variation in b_o is not related to stratigraphic control with low b_o values occurring throughout the stratigraphic column.

The empirical evidence would, therefore, indicate that two b_o groups can be distinguished in northern Snowdonia. It must be

emphasised that the difference between the two populations in absolute terms is not very great although the distinction is significant and the boundary does appear to be sharp.

Statistical examination of the white mica b_o results supports the empirical evidence above. Treatment of the results as a single population produces a mean b_o of 8.995 with a standard deviation of 0.012 (calculated on all 50 samples). This is higher than most of the standard deviations obtained by Sassi and Scolari (1974), Robinson (1981) and Padan et al. (1982) on b_o results obtained from similar populations of low-grade samples comparable with the samples from northern Snowdonia. Treatment of the b_o results as two sub-populations, as indicated by the empirical evidence, produces a mean b_o of 8.988 with a standard deviation of 0.006 for the area of lower b_o values (calculated on 32 samples) and a mean value of 9.008 with a standard deviation of 0.009 for the area of higher b_o values (calculated on 18 samples). These standard deviations are closely comparable to the figures obtained by Sassi and Scolari (1974).

The significance of the difference in b_o between the two apparent groups was tested using the T-test the suitability of which was examined by means of a standard F-test where,

$$F = \frac{\text{greater estimate of population variance}^2}{\text{lesser estimate of population variance}^2}$$

(Hammond and McCullugh, 1974). Using this equation a value of F = 1.29 was derived compared to a critical value of F = 2.01 (Davies and Goldsmith, 1976, Appendix D), hence the data are suitable for testing by the T-test statistic. The H_o tested by the T-test is that..... "no significant difference in b_o exists between samples taken from the western Conwy Valley and from the rest of northern Snowdonia". The H_1 against which H_o is tested is that....."the b_o obtained from samples taken from the western Conwy Valley is significantly higher than the

b_o obtained from samples taken elsewhere in northern Snowdonia". A value of T = 8.26 was obtained compared to a critical value of T = 2.02 (Davies and Goldsmith, 1976, Appendix C), therefore H_0 is rejected in favour of H_1.

It would, therefore, appear that both the empirical and statistical evidence supports the conclusion that two distinct zones representing white micas with relatively higher and lower "celadonite" contents occur within northern Snowdonia. The difference in b_o between the two groups of samples is not great but would appear to be consistent and significant.

6.6.2. Correlation between b_o and illite crystallinity.

In section 6.6.1 is was shown that the zone of higher b_o values corresponds closely to the higher illite crystallinity area. It might appear that the two measurements are causally inter-related with changes in b_o simply reflecting changes in metamorphic grade as mirrored in the illite crystallinity, thus having no independent geological significance. This factor is of critical importance if the crystallinity and b_o results are to be used as independent indicators of metamorphic conditions and must, therefore, be investigated rigorously.

It has been consistently shown that the grade of metamorphism influences octahedral substitution of Fe and Mg for Al in white micas (Cipriani et al., 1971; Sassi and Scolari, 1974 and Guidotti and Sassi, 1976). However, these studies investigated greenschist facies rocks and led to the conclusion that with increasing metamorphic temperatures b_o progressively falls. Padan et al. (1982) investigated the use of white mica geobarometry in sub-greenschist facies rocks and discovered that in diagenetic samples a significantly lower b_o is recorded than in

high anchizone and low epizone rocks from the same area. Hence the maximum b_o of white micas from a particular facies series will be developed in high anchizone or low epizone samples. Illite crystallinity has been used as a measure of grade by Padan et al. (1982) on samples from the Swedish Caledonides and the Andes and in the present study on samples from northern Snowdonia. Padan et al. (1982) show that as illite crystallinity increases, b_o progressively increases. In the transition from diagenesis to low epizone, for example in the Swedish Caledonides, the increase in mean b_o is 0.015. The increase in b_o is not marked where change in metamorphic grade is only from upper anchizone to low epizone, for example in the Andes, where the increase in mean b_o is only 0.008. Thus it would appear that there is a relationship between b_o and metamorphic temperatures. The change in b_o as metamorphic grade increases is clearly shown in figure 6.4. which is taken from Padan et al. (1982). In the samples from northern Snowdonia the same relationship is observed with middle anchizone samples yielding consistently lower b_o than epizone samples (figure 6.5). This relationship raises the critical question of whether the two b_o zones distinguished in section 6.6.1. merely reflect a difference in metamorphic temperatures. The difference in metamorphic grade observed in northern Snowdonia is from middle achizone to low epizone with a narrow band of low anchizone crystallinity occurring along the north coast (for a full description see Chapter 5).

The difference in mean b_o between the two zones is 0.020,rather greater than the difference in mean b_o observed between diagenetic and epizone samples in the Swedish Caledonides and much greater than the difference in mean b_o observed between the upper anchizone and low epizone samples in the Andes. The change in crystallinity in northern Snowdonia is significantly less than in the Swedish Caledonides being more typical of that observed in the Andes so that a small change in

FIGURE 6.4. The influence of metamorphic grade on white mica b_o in the Andes and the Swedish Caledonides, from Padan et al. (1982). Cumulative b_o curves 1 - 3 in the Andes reflect an increase in illite crystallinity from middle anchizone to epizone. Cumulative b_o curves 1 - 4 in the Swedish Caledonides reflect an increase in illite crystallinity from diagenesis to epizone.

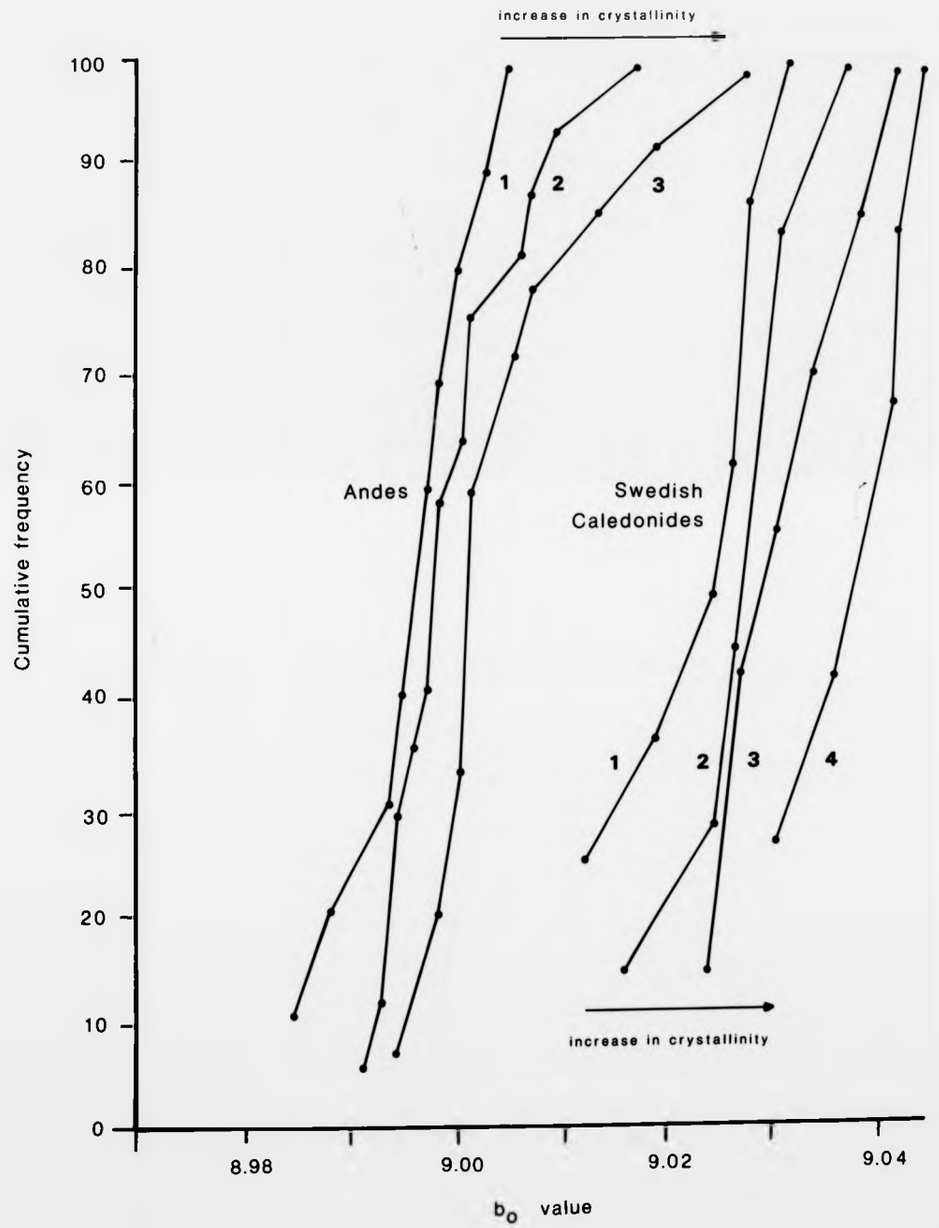

Sample Number	Position of the mica (060) peak ($^{o}2\theta$)	"d"spacing	Calculated mica b_o
340	61.820	1.4996	8.9976
341	61.870	1.4986	8.9916
342	61.935	1.4973	8.9838
343	61.860	1.4988	8.9928
344	61.960	1.4968	8.9808
345	61.950	1.4970	8.9820
346	61.970	1.4966	8.9796
347	61.980	1.4964	8.9784
348	-	-	-
349	61.840	1.4992	8.9952

TABLE 6.A. b_o results for samples from the Nant Peris anticline.

b_o of up to a maximum of 0.010 might be accounted for by the increase in metamorphic grade between the two areas. The observed difference in mean b_o between the zones of higher and lower b_o is double this figure thus implying that a small but significant difference exists between the two groups of b_o analyses that cannot be accounted for simply by the change in metamorphic grade.

Despite the overall good correlation between illite crystallinity and b_o, one group of samples exhibit poor correlation. Illite crystallinity (Chapter 5) was shown to be markedly enhanced in the cores of folds. However, when the white mica b_o for samples taken from the Nant Peris anticline was calculated no similar enhancement was observed (Table 6.A). Samples from the Nant Peris anticline plot in the high crystallinity-low b_o field of Figure 6.5. This observation would indicate that although crystallinity may be enhanced during deformation the "celadonite" content of the white micas remains unaffected. The implication, therefore, is that overall baric conditions remained relatively constant during the enhancement of illite crystallinity, presumably during the Caledonian deformation. Also the area of high illite crystallinity developed in the western Conwy Valley does not simply reflect a greater intensity of deformation as the b_o of the white mica is also markedly higher. The implication of this observation coupled with the definition of two groups of white mica with different "celadonite" contents, even after the possible affects of metamorphic grade are accounted for, is that a genuine but slight difference in baric conditions existed within northern Snowdonia.

6.6.3. The determination of facies series.

The determination of white mica b_o as a measure of the octahedral substitution of Fe and Mg for Al and its subsequent use as a geobarometer is a relatively new geological technique. Several regional studies,

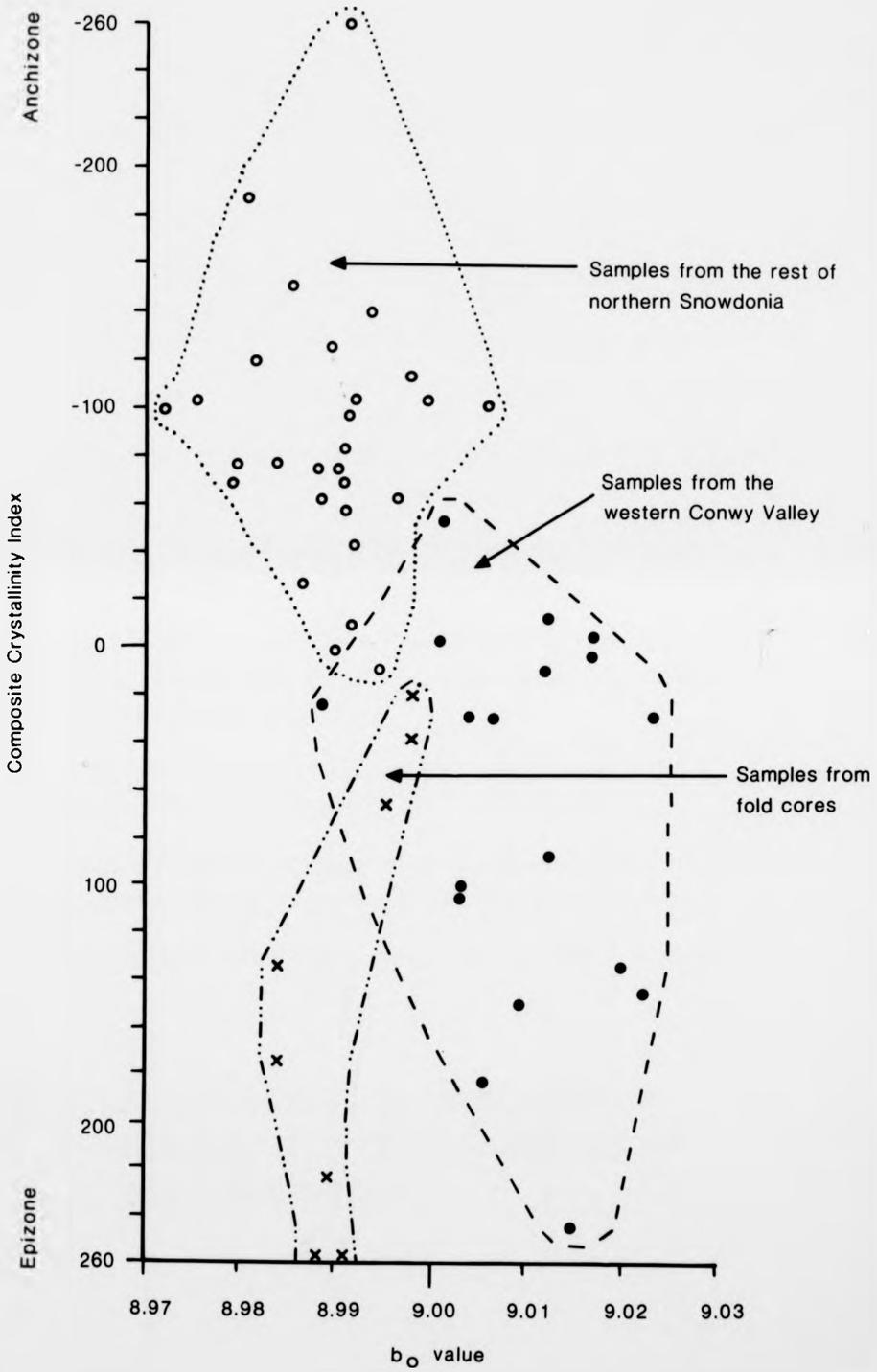

FIGURE 6.5. White mica b_o vs composite crystallinity index showing the fields of samples from the western Conwy Valley and the rest of northern Snowdonia. Also shown are samples taken from fold cores.

Facies Series	1	2	3	4	5	6
Mean b_o values	8.990	8.995	9.010	9.020 - 9.025	9.035	9.055

1 - Low-pressure metamorphism without chlorite zone (for example, Bosost).

2 - Low-pressure metamorphism with chlorite zone (for example, Hercynian metamorphism in the eastern Alps).

3 - Low-intermediate pressure metamorphism with the chlorite → biotite → almandine sequence in the greenschist facies (for example, New Hampshire).

4 - Typical Barrovian metamorphism (for example, Dalradian metamorphism in Scotland).

5 - Barrovian-type metamorphism with simultaneous first appearance of biotite and almandine (for example, Otago).

6 - Glaucophanitic greenschist facies (for example, Sanbagawa).

TABLE 6.B. Empirical scale of the b_o values in low-grade metamorphism of pelitic schists (from Sassi and Scolari, 1974, Table 2).

FIGURE 6.6. White mica b_o, cumulative frequency diagrams showing the cumulative curves for: (i) all samples from northern Snowdonia, (ii) samples from the western Conwy Valley, and (iii) samples from the rest of northern Snowdonia. Also shown are cumulative curves for Bosost and Northern New Hampshire (from Sassi and Scolari, 1974).

however, have utilised the method and Sassi and Scolari (1974) have proposed an empirical scale of b_o cumulative frequency curves as a function of pressure. Figure 6.6. plots the b_o data from northern Snowdonia and is compared with data from Bosost and northern New Hampshire (from Sassi and Scolari, 1974). Table 6.B. presents the empirical scale of mean b_o values (Sassi and Scolari, 1974).

From Figure 6.6. and Table 6.B. it can be seen that the mean b_o of 8.988 obtained for the lower b_o zone is very similar to the mean b_o of 8.990 typical of the "low-pressure" metamorphic facies series whilst the mean b_o of 9.008 obtained from the higher b_o zone is very similar to the mean b_o of 9.010 typical of the "low-intermediate pressure" facies series. From the b_o determinations it can be shown that northern Snowdonia has been metamorphosed in the low or low-intermediate pressure facies series of metamorphism as defined by Sassi and Scolari (1974).

6.7. Use of the intensity ratio (I_{002}/I_{001}) as a geobarometer

Esquevin (1969) proposed the use of the intensity ratio of the first and second order diffraction peaks of whitemicas as a measure of the Al/(Fe+Mg) ratio and as such might have potential geobarometric significance. However, several workers (referenced in Kisch, 1980), discovered very poor correlation between the actual Al/(Fe+Mg) ratio and the I_{002}/I_{001} ratio. Padan et al. (1982) observed poor correlation between b_o and the intensity ratio for rocks from different areas (the Andes and the Swedish Celdonides) where a significant difference in white mica "celadonite" content might be expected from the analyses of b_o which indicated significantly higher Fe and Mg contents in the white micas from Sweden relative to those from the Andes. Intensity ratio cumulative frequency curves, however, were found to be very similar for both areas.

FIGURE 6.7. White mica b_o vs the intensity ratio for samples from northern Snowdonia.

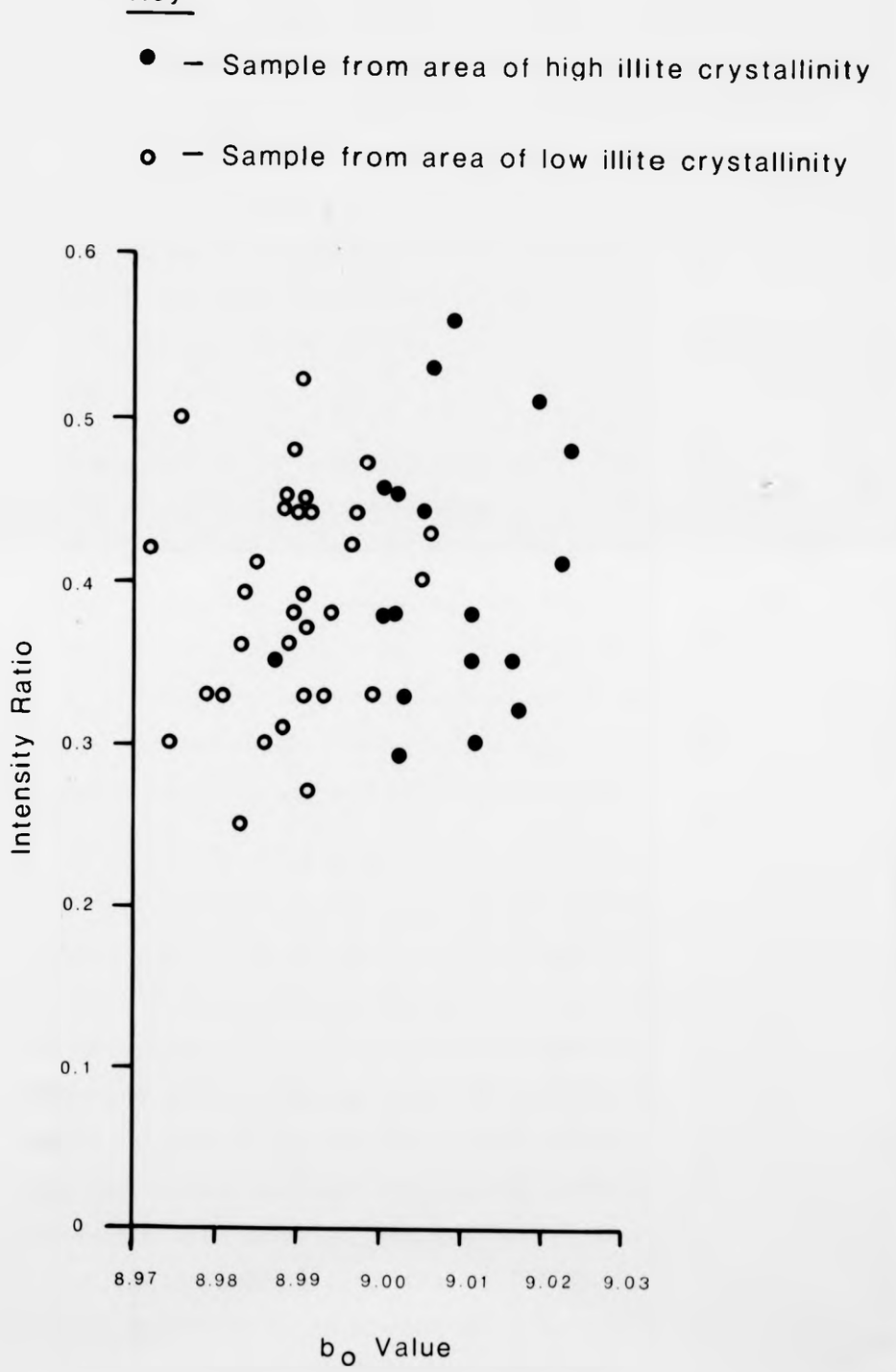

The intensity ratio was calculated for the 50 samples on which b_o was determined. The results are presented in Appendix 6 (vi). The range in intensity ratio is large, from 0.25 to 0.57. In Figure 6.7. the intensity ratio is plotted against b_o and there is clearly very little correlation between the two variables. In Figure 6.8. the intensity ratios are plotted as a cumulative frequency graph which demonstrates that there is no significant difference between the cumulative intensity ratios of samples taken from the higher and lower b_o zones.

A comparison of the Welsh data with those of Padan et al. (1982) for samples from the Swedish Caledonides and the Andes shows a significant difference in cumulative distribution. The mean intensity ratio of the Andean rocks is much lower than that of the rocks from northern Snowdonia (about 0.30 and 0.45 respectively), however, the mean b_o of the Andean rocks is very similar to that obtained in northern Snowdonia (between 8.996 - 9.004) implying that the "celadonite" content of the white micas from both areas is similar.

As a result of measuring the intensity ratio two points can be made: i) correlation between b_o and the intensity ratio is poor in northern Snowdonia, and ii) the cumulative intensity ratios for groups with very similar b_o values are markedly different. The conclusion that the intensity ratio is unreliable as a geobarometer due to the influence of factors other than octahedral chemistry (Padan et al., (1982) is supported by the data from northern Snowdonia. It would appear that factors other than the Al/(Fe+Mg) ratio play a potentially major role in determining the intensity ratio of the first and second order diffraction peaks in white mica. Differences in the intensity ratio are more likely to reflect chemical differences in the interlayer sites or in the interlayer structure than differences in octahedral site

FIGURE 6.8. Intensity ratio, cumulative frequency diagram for samples from the areas of high and low b_o. Also shown is the cumulative frequency, intensity ratio curve for samples from the Andes, (from Padan et al., 1982).

chemistry.

6.8. Concluding remarks.

White micas geobarometry utilising b_o has been undertaken on 50 slates, shales and mudstones from northern Snowdonia using the method recommended by Sassi and Scolari (1974). Several problems arise when attempting b_o determinations on very low-grade rocks although most can be alleviated by careful choice and preparation of samples, the statistical analysis of the results obtained from a group of samples and careful interpretation of the results.

The results of the b_o analyses would appear to indicate that:

i) two empirically and statistically distinct b_o groups (with means of 8.988 and 9.008) exist that closely correspond to the anchizone and epizone areas defined from the illite crystallinity, ii) the mean b_o of the anchizone samples is possibly lowered by as much as 0.010 as a result of the progressive increase in b_o as temperature increases in the lowest grades of metamorphism. This factor cannot, however, be invoked as a full explanation for the difference between the two groups of b_o values, iii) although good correlation exists between b_o and illite crystallinity poor correlation occurs in the cores of folds where, although crystallinity is often very high, the associated b_o is indistinguishable from the regional b_o, and, iv) the intensity ratio (I_{002}/I_{001}) of Esquevin (1969) would appear to be unreliable as a geobarameter.

Comparison of cumulate frequency curves constructed for the samples from northern Snowdonia with similar graphs for samples from other metamorphic terrains indicates that northern Snowdonia has been subjected to a "low pressure/low-intermediate pressure" facies series metamorphism as defined by Sassi and Scolari (1974).

Finally, it can be shown that in the western Conwy Valley there

is an area of higher mean crystallinity and slightly higher b_o compared with the rest of northern Snowdonia. This indicates that a definite metamorphic break in grade exists within northern Snowdonia. The implications of these conclusions along with the evidence derived from examination of the basic rocks and the fluid inclusions contained in vein quartz are discussed in Chapter 8.

CHAPTER 7

FLUID INCLUSION STUDY

7.1. Introduction

The systematic study of fluid inclusions on a large scale has only been undertaken in the last 20years. However, the existence of fluid inclusions had been known for many centuries (Roedder, 1972) and their significance and potential value as samples of fluid, trapped by crystal growth or recrystallisation, was largely realised by the mid-nineteenth century (Sorby, 1858).

Inclusions occur in many rock-forming minerals and the fluids they contain display a wide range of compositions (Roedder, 1972). By detailed observation and analysis of the inclusions contained within a sample, valuable information can be obtained concerning fluid composition, fluid evolution and the temperatures and pressures of host mineral crystallisation. If the precise timing of mineral growth can be established and the nature and age of the contained inclusions determined then fluid inclusions can provide a valuable insight into conditions prevalent during specific geological events. Fluid inclusions have recently been utilised in the study of hydrothermal ore deposits (Roedder, 1962; 1979), high-grade metamorphic belts (Hollister and Burruss; 1976, Touret, 1981), low-grade metamorphic belts (Tringham, 1979; Frey et al., 1980; Crawford, 1981) and igneous rocks (Roedder and Coombs, 1967).

In the present study about 650 inclusions were examined from 19 samples of vein quartz taken from representative locations throughout northern Snowdonia. The quartz veins are often found in close association with Si rich host rocks (sandstones, rhyolites, acid tuffs, etc.). This association probably indicates that Si has been only locally

mobilised as a result of Si release during low-grade metamorphic reactions and by Si solution in hot aqueous fluids (Fyfe et al., 1978). Determination of the age of quartz veining relative to mineral recrystallisation and end-Silurian Caledonian deformation is essential if the fluid inclusion data are to be interpreted, in conjunection with other geological data, to determine the conditions of metamorphism. Clearly, if data from a variety of contrasting sources are to be used it is essential that the data either reflect metamorphic conditions prevalent at the same time or that temporal relations between the different data sources are clearly defined. Veining appears to have occurred prior to deformation although in many specific cases the precise structural relationship of veins on field evidence alone is unclear. Evidence indicating that quartz veins were emplaced before deformation includes the folding of veins, the diffraction of cleavage against veins and the occasional presence of a weak, marginal fracture cleavage in some veins. Sample locations are listed in Appendix 2 (iii).

The aims of the fluid inclusion study were:-

i) detailed observation and description of inclusions to determine the relative proportions and distributions of primary (inclusions trapped at the time of host mineral crystallisation) and secondary (inclusions trapped at some time after host mineral crystallisation) fluid inclusions and to visually assess the degree of recrystallisation and internal deformation within the quartz veins.

ii) qualitative and semi-quantitative determination of fluid composition through careful petrographic observation, accurate measurement of the temperatures of critical phase changes and bulk chemical analysis.

iii) determination of fluid density as reflected by the filling temperatures, density being related to fluid composition and the

temperatures and pressures of trapping.

iv) determination of any variation in composition or characteristic filling temperatures between different 'suites' or types of inclusion present within a sample.

The ultimate aim of the fluid inclusion study was to combine the composition and filling temperature data with the geological information obtained in the previous chapters to derive the approximate temperatures and pressure of pre-deformation vein emplacement. In addition, any variation in filling temperature or composition between different types of inclusion (primary and secondary) might reflect fluid evolution over time.

7.2. The principle of fluid inclusion analysis.

7.2.1. Introduction

Two assumptions are critical in fluid inclusion analysis, these being:-

i) that there has been no leakage into or out of inclusions since the time of their formation, or if leakage has occurred that it can be recognised (Roedder, 1968, 1979), and ii) that the volume of the inclusion has remained constant, or that if any significant change in volume has occurred, it too can be recognised (Roedder, 1981). The validity of these assumptions has been seriously questioned in the past (Kennedy, 1950; Roedder, 1963) and it is important that they be considered when interpreting fluid inclusion results. In addition it is important that data from primary inclusions (formed during mineral growth) and secondary inclusions (formed at some time after mineral growth) should be distinguished. Independent geological data concerning either the temperature or pressure of trapping is necessary if a realistic interpretation of the results from simple fluid inclusions is

to be made (Roedder, 1979).

As the fluid inclusions from northern Snowdonia consist largely of water or dilute brine (see Sections 7.3. and 7.4.), only fluid inclusion analysis relating to simple aqueous inclusions will be examined.

7.2.2. Determination of fluid composition

Fluid composition can be qualitatively, semi-quantitatively and quantitatively determined in a variety of ways. The simplest method of determining approximate fluid composition is by careful petrographic observation. Information can be obtained concerning: i) the nature of the fluid based on the number and types of phases present within the inclusions. For example, in a mixed CO_2 - H_2O inclusion an immiscible relationship will exist between the two phases at a concentration greater than 2.1 Wt. % CO_2 when the CO_2 will appear as a distinctive rim around the H_2O vapour bubble (Alderton, 1976; Roedder, 1981) and, ii) the approximate salinity of the fluid based on the presence or absence of salt crystals within the inclusions (Roedder, 1972). For example, in mixed NaCl - H_2O inclusions cubes of halite will form at concentrations greater than about 25 Wt. % NaCl. These observations are obviously only qualitative but can yield valuable preliminary fluid composition data.

A more sophisticated method of determining fluid composition involves the careful observation of phase behaviour as inclusions are gradually heated from very low temperatures (< - 100^{o}C). At these temperatures most fluids should be frozen as ices, but as temperatures slowly increase melting will occur. The exact temperature of both the initial and final melting points are governed by fluid composition. For example, the initial melting temperature of NaCl + H_2O is - 20.8^{o}C, for $CaCl_2$ + H_2O - 49.8^{o}C and for KCl + H_2O - 10.6^{o}C (Crawford, 1981).

The depression of the final melting point below $0^{o}C$ (the final melting point of pure H_2O) reflects the total concentration of salts present so that measurement of the final melting point allows quantification of the salt concentration within the fluid.

Finally, fluid composition can be determined directly utilising a number of physical and chemical techniques such as the microchemical analysis of fluid contained within single inclusions, bulk chemical analysis of the fluids released upon crushing or digestion of a host mineral and microprobe analysis of daughter minerals (Roedder, 1972; Hollister and Crawford, 1981).

7.2.3. Determination of fluid density

The density of a fluid trapped in an inclusion can be established by the measurement of the homogenisation or filling temperatures. A simple aqueous fluid trapped at elevated temperatures will divide into a liquid phase, of relatively high density, and a vapour phase, of relatively low density, upon cooling. This behaviour is the result of differential contraction between the host mineral and the fluid as temperatures fall (Roedder, 1981). This process can be reversed by heating the sample thus causing fluid expansion. In complex fluid inclusions homogenisation temperatures are recorded whereby the inclusions are heated until all crystalline material has dissolved, solid solution between immiscible phases is achieved and the fluid expands to completely fill the inclusion. In simple inclusions (such as those of nothern Snowdonia) filling temperatures are recorded whereby the inclusion is heated until the vapour bubble is completely filled by the expanding liquid within the inclusion. Homogenisation and filling temperatures can be used directly to calculate fluid density from tables of published data (Fisher, 1976).

By heating an inclusion to its filling or homogenisation temperature

a minimum temperature of trapping can be determined. If the inclusion was trapped at elevated pressures, or the fluid is markedly saline, then the filling temperature will be significantly lower than the true trapping temperature. If composition can be measured and pressure determined from independent geological data, corrections may be made and the true temperature of trapping derived (Fisher, 1976; Potter, 1977).

7.3. Description of the fluid inclusions

All the vein quartz samples from northern Snowdonia contain some fluid inclusions, although the range in inclusion size, type and abudance is often very marked both between samples and between the different grains within a sample. Most of the samples contain some evidence of deformation with, for example, the development of widespread undulose extinction, the frequent occurrence of discrete fracture planes and recrystallisation. The effects of deformation are not uniform within a sample and it was often found that the least deformed grains contained many relatively large inclusions whilst the highly deformed, recrystallised grains contained relatively few, small inclusions. These observations are consistent with those of Kerrich (1976).

Two main morphological types of inclusion were recognised.

i) The majority of the fluid inclusions are relatively small(< 15μ in length) and rounded. They often occur on planes or form linear arrays (Figure 7.1.1.) and only rarely occur as isolated inclusions. The inclusion margins are often sharply defined and clear and the vapour bubble small. When these inclusions are heated the most obvious effects are slow shrinkage of the vapour bubble and, either, rapid movement of the vapour bubble, due to surface tension effects (Roedder, 1981) or, a smearing of the bubble against the inclusion walls. Occasionally these inclusions display the partial development

FIGURE 7.1.1. Linear array of small, rounded, secondary inclusions, sample 318. X 640.

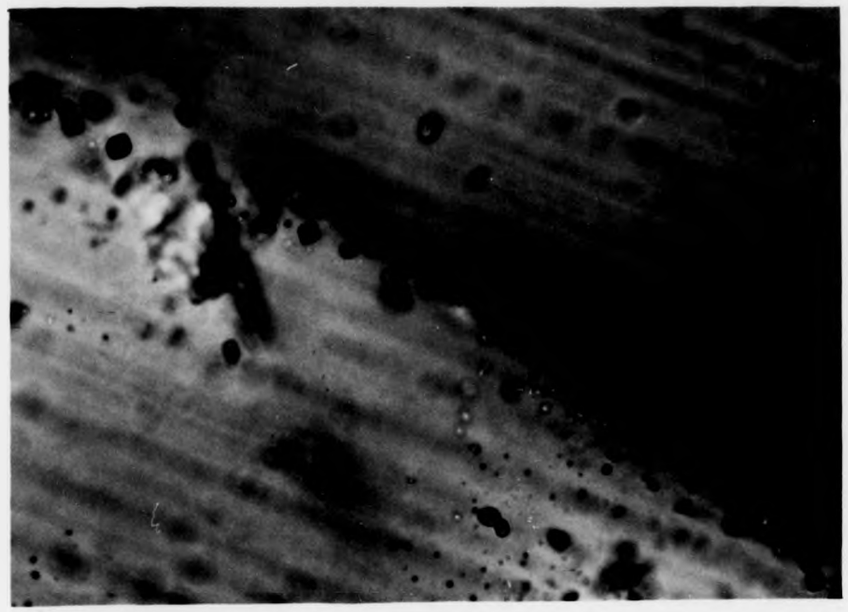

FIGURE 7.1.2. (i) Linear array of small, rounded, secondary inclusions and, ii) deformed inclusions, sample 225. X 250.

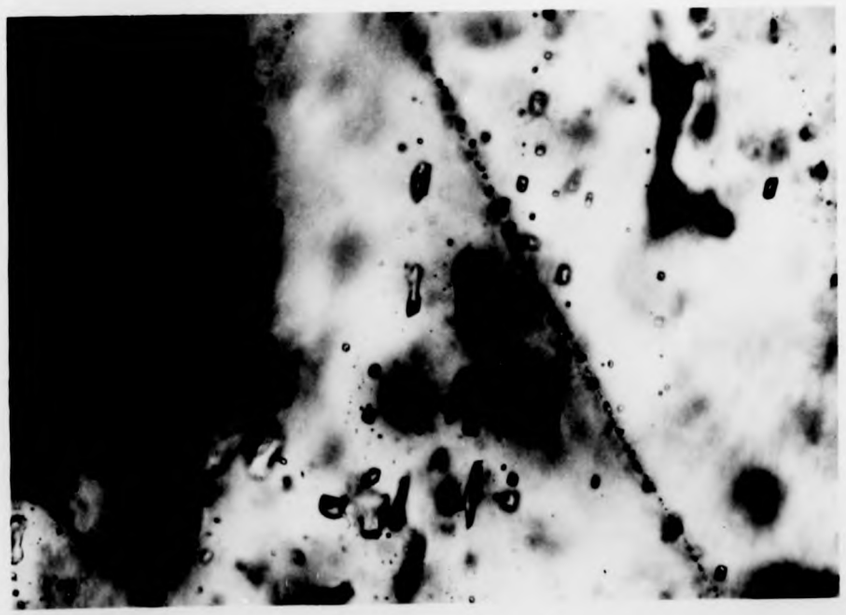

FIGURE 7.1.1. Linear array of small, rounded, secondary inclusions, sample 318. X 640.

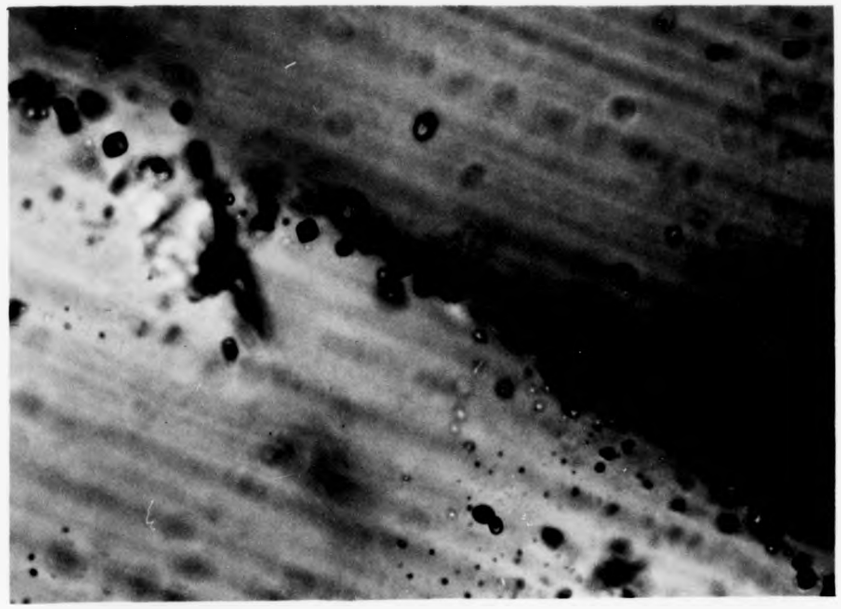

FIGURE 7.1.2. (i) Linear array of small, rounded, secondary inclusions and, ii) deformed inclusions, sample 225. X 250.

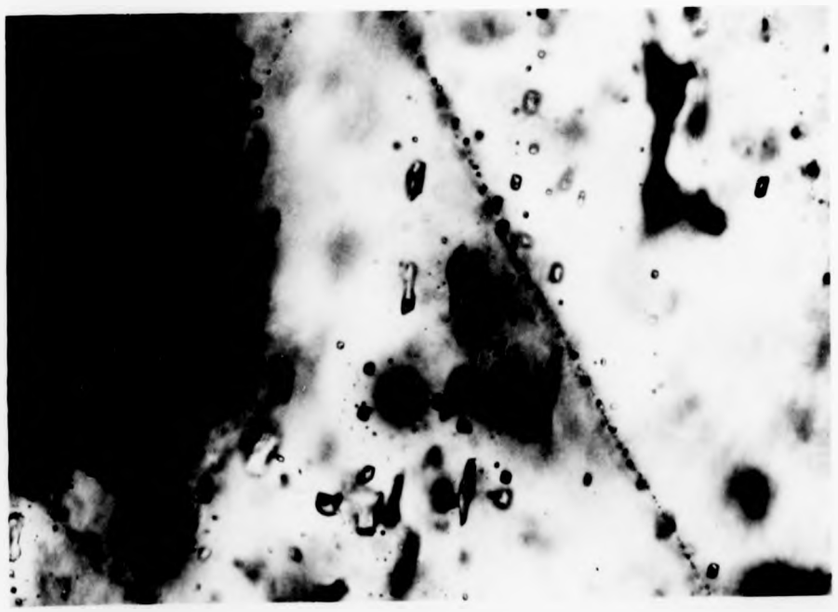

FIGURE 7.2.1. Irregular shaped, variably deformed primary inclusions, sample 225. X250.

FIGURE 7.2.2. Large (> 30 microns), isolated, primary inclusions showing the partial development of negative crystal faces, sample 225. X640.

FIGURE 7.2.1. Irregular shaped, variably deformed primary inclusions, sample 225. X250.

FIGURE 7.2.2. Large (> 30 microns), isolated, primary inclusions showing the partial development of negative crystal faces, sample 225. X640.

FIGURE 7.3. "Necking down" phenomena in fluid inclusions, sample 318. X800.

FIGURE 7.3. "Necking down" phenomena in fluid inclusions, sample 318. X800.

of negative crystal faces. In several samples they show some evidence of deformation such as stretching and flattening (Figure 7.1.2.). Many of these features are typical of 'secondary' inclusions formed after the host mineral crystallised (Roedder, 1979).

ii) The second, and less common, type of fluid inclusion is significantly larger (20 - 30μ in length), occurs in sub-rounded to sub-angular form and may often be very irregular in shape (Figure 7.2.1.). The walls of the inclusions are frequently diffuse and the vapour bubble large. Occasionally one or more negative crystal faces are developed (Figure 7.2.2.). These inclusions often occur in isolation or associated with several other large inclusions. The usual response to heating is rapid shrinkage of the vapour bubble which almost invariably remains stationary or slowly migrates to smear against the inclusion wall. Many of these features are typical of 'primary' or 'pseudo-secondary' inclusions formed during the crystallisation of the host mineral (Roedder, 1979).

In addition to these two main types of inclusion a number of inclusions were recognised displaying characteristics typical of 'necking-down' (Figure 7.3.) where deformation and recrystallisation has changed the inclusion volume and hence the fluid density (Roedder, 1981). 'Necked-down' inclusions are often difficult to petrographically detect and may only be obvious from their anomalously high or low filling temperatures.

In all the samples from northern Snowdonia inclusions consist of a relatively small vapour bubble contained within a liquid. No inclusions revealed the development of: i) daughter minerals (indicative of high salinities), ii) double vapour/liquid bubbles (indicative of complex inclusions containing immiscible CO_2 and H_2O fluids) or, iii) dominantly gas filled inclusions (indicative of low density fluids). The ratio of vapour to liquid is quite variable implying a range in fluid density,

however, this qualitative indication of fluid density is notoriously unreliable as inclusions are three dimensional but are only being examined in two dimensions on the microscope (Roedder, 1972).

Most observations and measurements were made on the larger inclusions as they are thought to most closely represent primary inclusions and thus the true composition and density of the vein forming fluid. Also, from the practical standpoint, observations and measurements were easier to make as a result of the greater inclusion size. In several cases numerous filling temperatures were obtained for both types of inclusion in order to examine any significant difference in properties between the primary and secondary inclusions within a sample (see Section 7.5.).

7.4. Fluid composition

Composition of the fluids within the inclusions was investigated both qualitatively and semi-quantitatively in three ways:

i) careful petrographic observations of numerous inclusions of different types. In Section 7.3. the inclusions were shown to be of relatively high density (mainly liquid) and free of daughter minerals and immiscible fluid phases. A number of conclusions can thus be drawn:

(a) the fluid is essentially aqueous in nature (b) the salinity is less than about 24 wt.% NaCl equivalent and (c) the fluid contains little or no CO_2.

ii) determination of the temperatures of critical phase changes can yield valuable information concerning the nature and concentration of salts contained within fluid inclusions (Crawford, 1981).

The heating and cooling work was undertaken on a Linkam Scientific Instruments TH600 Programmable Stage (Shepherd, 1981). Using pre-cooled nitrogen gas, temperatures as low as $-90^{o}C$ can be readily achieved and sustained. However, several problems arose during the cooling procedure,

including: a) metastable supercooling of liquid inclusions below their expected freezing temperatures. The problem of metastability in fluid inclusions is frequently observed and can preclude the determination of fluid compositions (Alderton, 1976; Roedder, 1979, 1981), b) extensive condensation within the equipment and on the sample; this was partly overcome by passing dry air through the stage but remained a serious problem, and, c) difficulty in controlling the temperature at these very low temperatures.

As a result of these difficulties no reliable data on low temperature phase changes was obtained, hence the exact nature of the fluid and the precise salt concentration could not be determined.

iii) bulk fluid chemical analysis can provide useful information concerning the relative proportions of ions within groups of inclusions. The bulk potassium/sodium (K/Na) ratio was determined for 5 samples. Two preparation techniques were employed: a) crushing and leaching of small amounts of fine, granular, vein quartz under distilled water (Alderton, 1976), and b) digestion of small amounts of vein quartz in hydrofluoric acid and solution of the residue in warm nitric acid. The leached solutions and salt residues from both techniques were then analysed for Na_2O and K_2O on an Atomic Absorption Spetrophotometer (Pye Unicam SP2900) in the flame emission mode. For the calculation of the K/Na ratio, K_2O and Na_2O were converted into elemental K and Na. As a check on sample reproducibility some analyses were undertaken on solutions derived from different quantities of a vein quartz sample. If the techniques are reliable different absolute amounts of Na_2O and K_2O should be obtained using different amounts of sample, however, the K/Na ratio should remain approximately constant for each sample. The results of the Na and K analyses and the calculated K/Na ratios are shown in Table 7.A. As the amount of fluid in the opened inclusions is unknown the absolute values of Na and K are of limited value and it is

TABLE 7.A. Results of the Na and K analyses (in ppm) and calculation of the K/Na ratio on crushed and digested vein quartz samples.

Sample number	Amount of sample (gms)	Crushed			Digested in acid		
		Na (ppm)	K (ppm)	K/Na ratio	Na (ppm)	K (ppm)	K/Na ratio
169X	5	5.5	1.7	0.31	6.8	1.2	0.18
	8	8.6	1.5	0.17	8.4	0.9	0.11
	10	4.4	2.7	0.61	4.9	1.5	0.31
	12	7.9	2.7	0.34	7.9	1.6	0.20
1B	4	13.3	1.0	0.08	12.8	13.0	1.02
	8	9.8	1.2	0.12	25.8	24.4	0.95
	12	12.8	3.8	0.30	44.3	35.5	0.80
71B	5	4.6	1.2	0.26	35.8	7.2	0.20
	8	8.2	0.5	0.06	53.8	10.1	0.19
	12	6.9	2.2	0.32	66.9	11.4	0.17
225	4	5.4	0.3	0.06	4.3	3.9	0.91
	8	5.2	0.6	0.12	8.7	7.3	0.84
	12	5.2	0.6	0.12	14.9	16.7	1.12
74	10	3.6	0.9	0.25	52.0	49.5	0.95

the K/Na ratio that is of most value.

The results show that more salts are liberated by acid digestion than by crushing and essentially reflects the relative efficiency of the two methods. The effects of alkali contamination by the hydrofluoric and nitric acids were quantified by running blank solutions, the data was corrected by subtracting the blank K_2O and Na_2O values from the sample runs. The absolute values of Na and K released during crushing varies widely and does not necessarily reflect the amount of sample crushed. In the digested samples the absolute amount of salts released correlates quite closely with the amount of sample treated. The acid treatment produces similar K/Na ratios for different analyses on a single sample although there is a broad range in the K/Na ration between different samples (1.12 in sample 225 to 0.11 in sample 169X).

The differences in K/Na ratio between crushed and digested samples may reflect enhancement of K_2O during acid digestion due to the possible breakdown of a small amount of a K-bearing mineral (clay, mica, feldspar, etc.). Petrographically there is evidence that this may have occurred with the occasional presence of small amounts of a fine-grained mineral along some quartz grain boundaries, only a small amount of a contaminant (< 0.5% of the total sample) need be digested to distort the results and produce misleading alkali results.

It is felt that although the crushed samples display variable K/Na ratios between different analyses on the same sample this is more likely to reflect the true K/Na ratio of the fluid because of the potential digestion of impurities when quartz is treated in acid. The results obtained from crushed samples, although individually variable, reveal no major differences in K/Na ratio between samples. The range in crushed sample mean K/Na ratio from 0.10 - 0.36 closely corresponds to

the typical K/Na ratio of about 0.2 determined on the fluid inclusions contained within quartzes from a broad range of low-grade metamorphic rocks (Crawford, 1981).

7.5. Fluid inclusion filling temperatures

Between 20 and 150 filling temperatures were determined for each of the 19 separate quartz samples. The measurement of filling temperatures aimed to: i) produce mean fluid inclusion filling temperatures for each sample in order to examine regional variation in filling temperatures within northern Snowdonia, ii) determine the characteristic filling temperatures for different types of inclusion within a sample, and, iii) determine the characteristic filling temperatures for the individual quartz grains within a sample. The filling temperatures can then be used, along with compositional data, to calculate fluid density which can then be used, in conjunction with independent geological data, to estimate either the temperature or pressure of trapping.

The heating stage was calibrated using standard substances with known melting points. A series of calibrations were undertaken at different heating rates ranging from $5^{o}C$ - $90^{o}C$ per minute. No significant difference in the recorded melting temperatures of the standards was observed at different heating rates suggesting that thermal equilibrium was attained between the stage and the standards, even at relatively rapid heating rates ($90^{o}C$ per minute). The results of the $90^{o}C$ per minute heating calibration (the heating rate employed throughout the measurements of filling temperatures) on 9 standards are shown in Figure 7.4.

The results of the bulk filling temperature measurements are presented as a series of histograms in Figure 7.5. and plotted on a map in Figure 7.6. A summary of the data are shown in Table 7.B. These diagrams and

FIGURE 7.4. Calibration of the Linkam TH 600 programmable stage.

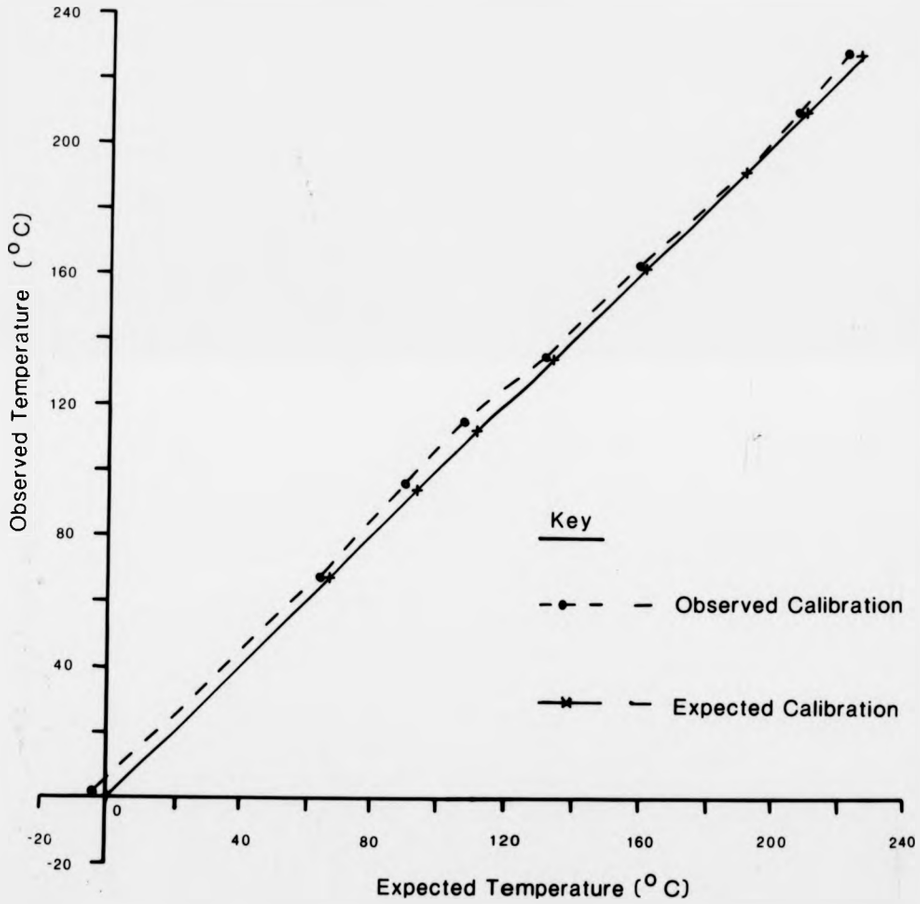

FIGURE 7.5. Fluid inclusion filling temperatures from the vein quartz samples from northern Snowdonia.

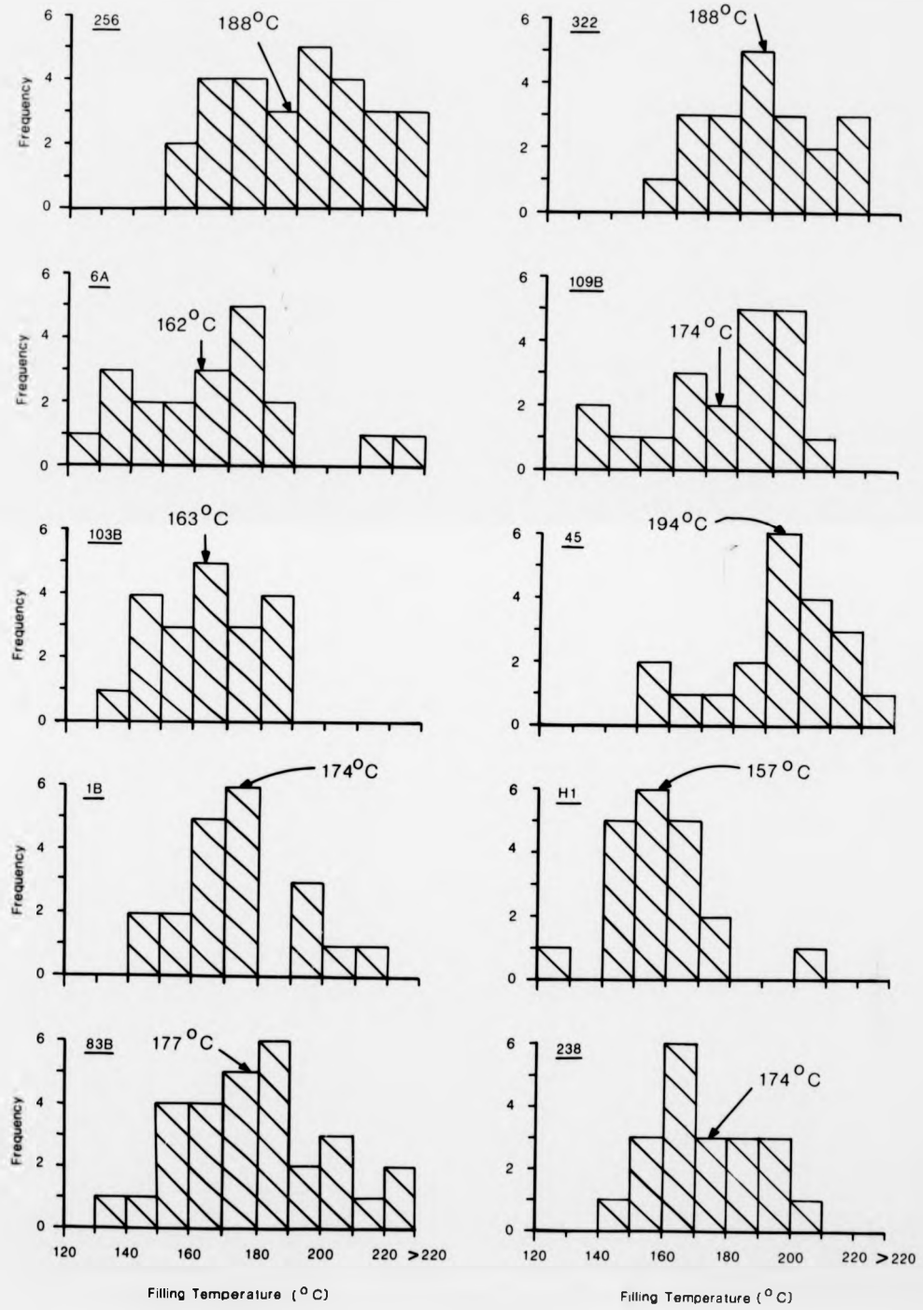

FIGURE 7.5. (continued) Fluid inclusion filling temperatures from the vein quartz samples from northern Snowdonia.

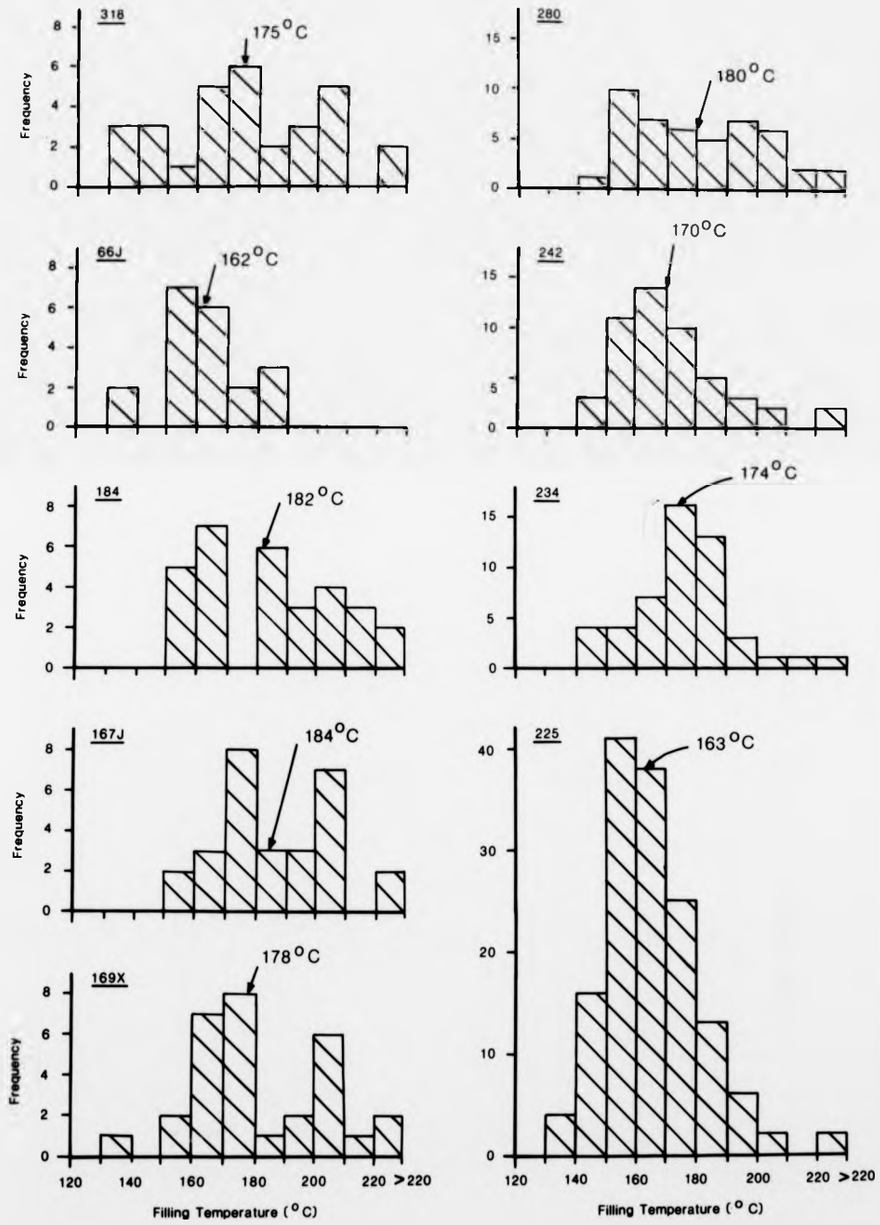

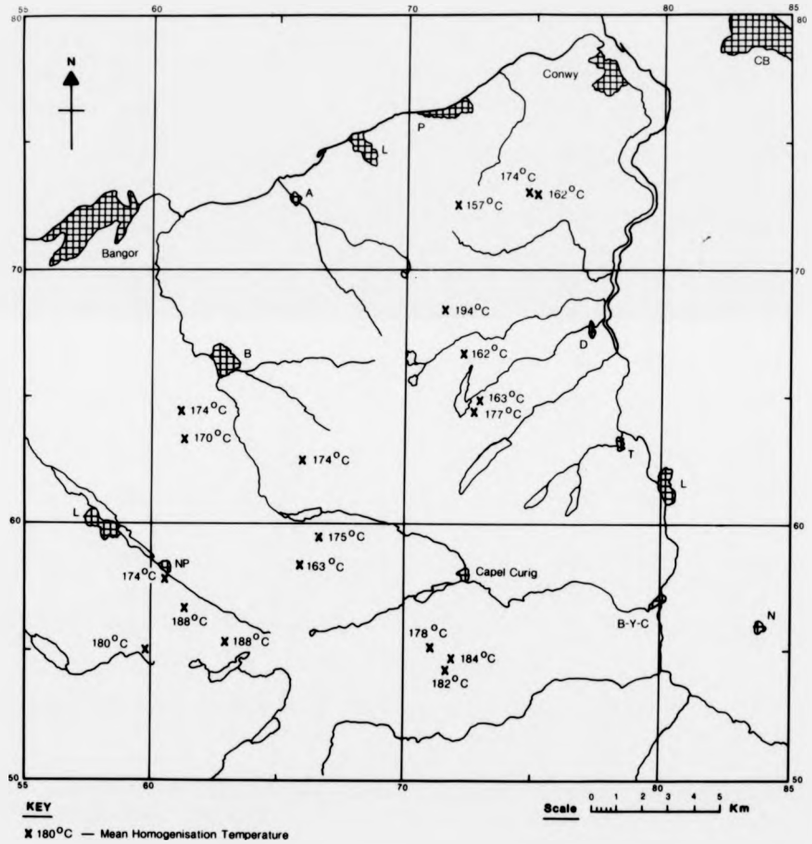

FIGURE 7.6. A map showing the mean fluid inclusion filling temperatures of the vein quartz samples from northern Snowdonia.

Area	Sample number	Number of measurements	Number of good[1] measurements	Mode (°C)	Mean[1] (°C)	Standard[1] deviation
	225*+	150	148	155	163	15.7
	318	30	29	175	174	24.0
	280*	50	49	155	180	20.1
Central	234*	50	49	175	175	14.7
northern	242*	50	49	165	170	16.9
Snowdonia	238	20	20	165	174	16.9
	109B	20	20	190	174	19.8
	322	30	27	195	188	20.2
	256	20	20	185	188	18.6
	83B	30	28	185	177	21.2
	66J	20	20	155	162	14.4
Northern	6A	20	19	175	162	22.2
Conwy	1B	20	20	175	174	19.2
Valley	H1	20	20	155	157	15.6
	103B	20	20	165	163	15.2
	45	20	20	195	194	20.3
Southern	169X	30	28	175	178	19.5
Conwy	167J	30	28	175	184	17.4
Valley	184	30	28	165	182	20.7

TABLE 7.B. Summary of the bulk filling temperature results

1 = anomalous filling temperatures from necked-down and fractured inclusions excluded.

\+ = sample in which the variation in filling temperatures between primary and secondary inclusions was examined (Figure 7.8).

* = sample in which the inter-grain variation in filling temperature was examined (Table 7.C).

tables show that no major differences in mean filling temperature occur throughout northern Snowdonia, although within the Conwy Valley there appears to be a slight overall increase in characteristic mean filling temperature from around 165^{o}C in the north to around 185^{o}C in the south. This increase in mean filling temperature southwards within the Conwy Valley is shown in Figure 7.7. These figures are of necessity based on relatively few samples. The regional difference in characteristic mean filling temperature between north and south is only slightly greater than the standard deviations calculated for some of the more variable samples (for example, samples 6A, 83B and 318), indicating that the regional variation is only just statistically significant in view of the degree of intra-sample variation in fluid inclusion filling temperatures. The mean filling temperature of samples from central northern Snowdonia is around 180^{o}C. Assuming a low salinity (1-10 wt.% NaCl equivalent) these results imply a fluid density of approximately 0.89g Cm^{-3} (Fisher, 1976).

The mean filling temperature determinations only reveal inter-sample variation, any systematic intra-sample difference in filling temperature would not be apparent. Sample 225 contains many fluid inclusions and as both major types of inclusion are well represented (Section 7.3.) a large number of filling temperatures were measured. From Figure 7.8. it is evident that no significant difference in characteristic filling temperature exists between the primary and secondary inclusions in this sample. The implication of this observation is that inter-sample variation in mean filling temperature does not reflect the relative abundance of primary and secondary inclusions yielding different characteristic filling temperatures.

Intra-sample variation in filling temperatures between different grains was examined in samples 225, 234, 242 and 280. The results of

FIGURE 7.7. A diagram showing the general increase in mean fluid inclusion filling temperatures southwards within the Conwy Valley.

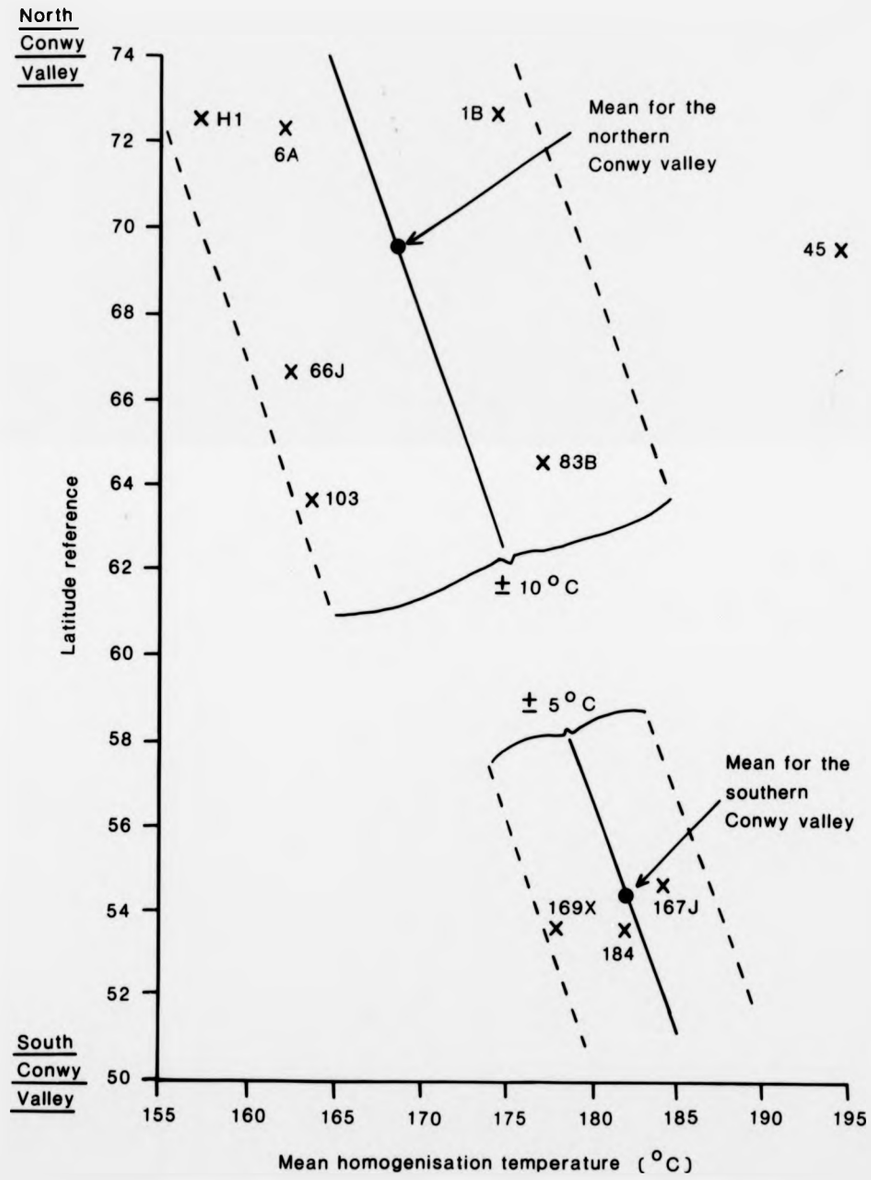

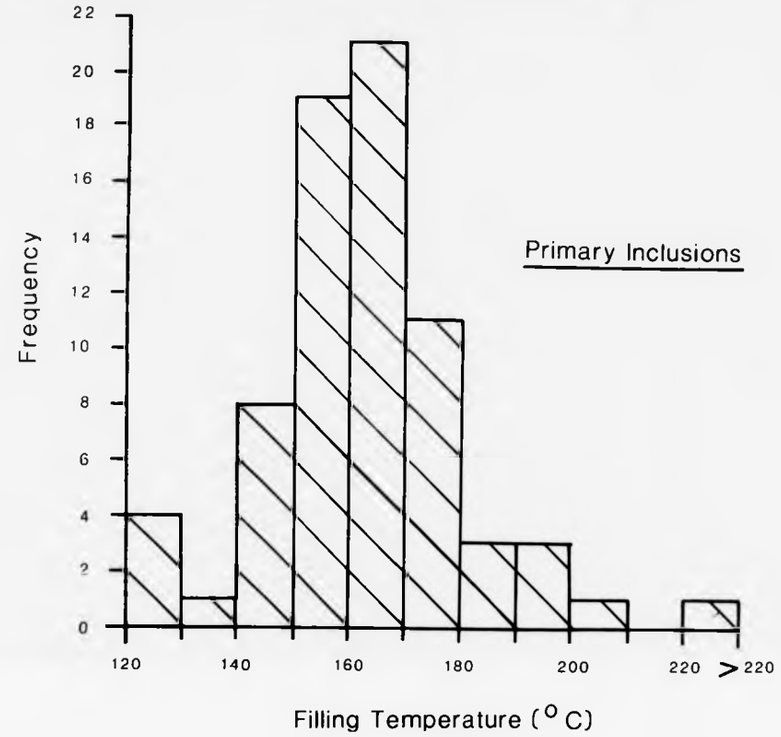

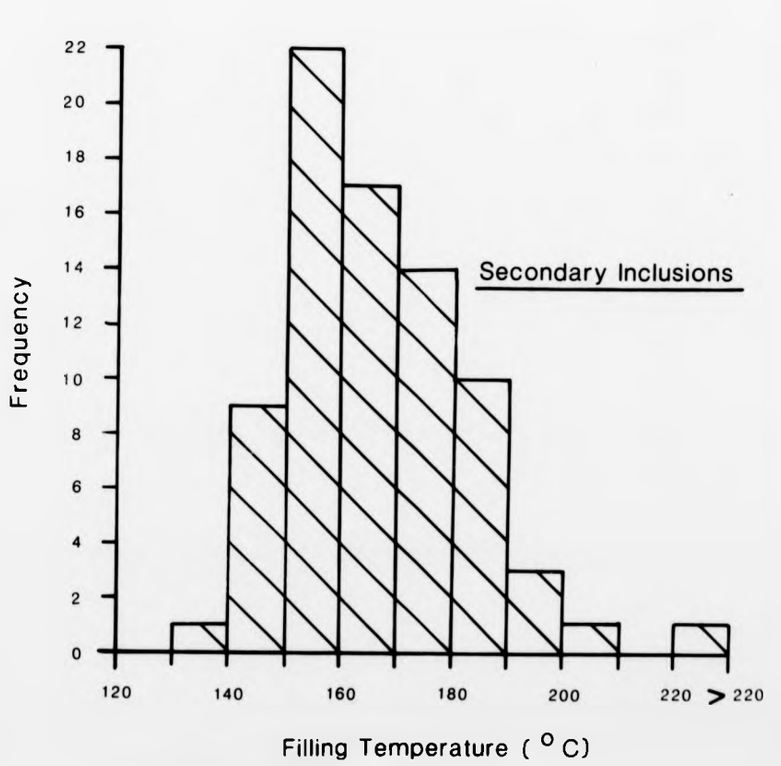

FIGURE 7.8. Fluid inclusion filling temperatures for the primary and secondary inclusions of sample 225.

Sample number	Mean bulk filling temperature (°C)	Grain	Number of measurements	Mean grain filling temperature (°C)
		1	27	168
		2	27	159
		3	5	155
		4	21	159
225	163	5	16	164
		6	16	153
		7	23	174
		8	5	160
		1	5	165
		2	5	192
		3	7	180
280	180	4	7	182
		5	6	176
		6	7	187
		7	5	153
		1	5	159
		2	7	185
234	175	3	5	171
		4	5	164
		5	7	179
		6	8	172
242		1	7	162
	170	2	7	176
		3	8	170

TABLE 7.C. Filling temperatures obtained from different grains within individual samples.

these determinations are shown in Table 7.C. and reveal that a significant range in filling temperatures exists between individual grains contained within the same sample, even though some grains contain relatively few inclusions. The intra-grain range in filling temperature is relatively high, from 15°C in sample 242 to 40°C in sample 280, this latter figure being significantly greater than the inter-sample variation in filling temperature observed within northern Snowdonia. However, in order to examine the effects of deformation on fluid inclusion filling temperatures, grains were chosen displaying a wide range and intensity of deformation characteristics (undulose extinction, recrystallisation, linear concentration of inclusions, fracturing, etc), whereas in the regional measurement of fluid inclusion temperature only primary inclusions from relatively undeformed quartz grains were used. Kerrich (1976) observed that filling temperatures obtained from inclusions in deformed quartz grains that had undergone grain size reduction and displayed undulose extinction were more variable,and often significantly higher, than those obtained from the adjacent, larger, undeformed quartz grains displaying normal extinction. It is possible, therefore, that some of the intra-sample variation in filling temperature is caused by differential deformation between quartz grains although in the absence of a precise method for measuring the degree of deformation within individual grains this could not be rigorously tested.

7.6. Corrections for pressure and fluid composition.

7.6.1. Introduction

From the filling temperature and compositional data some estimate of the geological conditions of vein emplacement can be made. The filling temperatures provide a minimum temperature for vein formation of between 157°C and 194°C. If veining occurred under elevated

pressures a correction to the filling temperatures must be made to account for the increase in density caused by the effects of pressure. In addition, consideration of fluid composition is necessary as this will also influence density. Fisher (1976) and Potter (1977) examined the effects of pressure on pure H_2O and mixed NaCl-H_2O systems respectively. In the current study the precise salinity of the fluid was not determined so corrections for composition can only be tentative.

In order to determine the physical conditions of vein formation from simple aqueous fluid inclusions, independent geological data concerning either pressure or temperature must be available. Two possible fluid compositions are considered: i) very low salinity - H_2O + 1% NaCl solution, chosen as representing the lowest probable salinity. The fluid cannot be pure water as significant amounts of Na_2O and K_2O were detected in the bulk inclusion chemical analyses (Section 7.4.) and, ii) intermediate salinity-H_2O + 10% NaCl solution, chosen because, in the absence of precise compositional data, this is least likely to cause significant errors when correcting the filling temperature data for the effects of pressure (Roedder, 1979). Both assumed fluid compositions allow use of the published corrections of Potter (1977).

With the data available in the present study two approaches to the determination of the true trapping temperatures or pressures from the fluid inclusion filling temperature data are considered.

7.6.2. Estimation of pressure and calculation of temperature

If the pressures of trapping can be independently determined a suitable pressure correction can be applied to the filling temperature data in order to obtain the true trapping temperature.

Relative pressures can be established from the b_o results (Chapter 6) which indicate that northern Snowdonia has undergone a low to low-

intermediate pressure facies series of metamorphism, with pressures being slightly higher in the western Conwy Valley. A maximum Lower Palaeozoic sedimentary and volcanic stratigraphic thickness of about 13km has been estimated for the central Welsh basin (Kelling, 1978) which corresponds to a pressure of just over 3kb (Bevins and Rowbotham, 1983). Northern Snowdonia is marginal to the main Welsh basin so that a maximum pressure of rather less than 3kb might be expected. However, detailed data on pressure is not available for northern Snowdonia and any estimate of stratigraphic thickness is complicated by the fact that the thickness of the Silurian overlying northern Snowdonia is unknown. All that can be said, therefore, is that pressures were probably less than 3kb generally, with slightly higher relative pressures in the western Conwy Valley. For the purpose of the fluid inclusion corrections pressures of 2.0 and 1.5 kb in the western Conwy Valley and central northern Snowdonia respectively, have been assumed.

Figures 7.9 and 7.10 are taken from Potter (1977) and illustrate the relevant pressure corrections at salinities of 1% and 10% respectively. From Figure 7.9 a pressure correction of 120^{o}C at 1.5kb for inclusions filling at 180^{o}C is calculated, such that trapping temperatures of about 300^{o}C in central northern Snowdonia are obtained. At 2.0kb a pressure correction of 160^{o}C is obtained for inclusions filling between 165^{o}C and 185^{o}C leading to trapping temperatures of about 325^{o}C in the northern Conway Valley and 345^{o}C in the southern Conwy Valley. From Figure 7.10 the corrections for estimated pressures of 1.5 and 2.0kb are 128^{o}C and 168^{o}C, yielding trapping temperatures of about 308^{o}C, 328^{o}C and 353^{o}C for central northern Snowdonia, the northern Conwy Valley and the southern Conwy Valley respectively. These results and calculations are summarised in Table 7.D. However, it must be stressed that the pressures used in these calculations are only assumed and are not based on reliable independent geological data, therefore, the trapping temperatures obtained

FIGURE 7.9. 0.25 - 2.0Kb pressure correction data for a 1% NaCl, aqueous fluid, from Potter, 1977.

FIGURE 7.10. 0.25 - 2.0Kb pressure correction data for a 10% NaCl, aqueous fluid, from Potter, 1977.

Area	Mean filling temperature (°C)	Salinity (Wt. % NaCl equivalent)	Estimated pressure (Kb)	Correction (°C) from figures 7.9 and 7.10	Calculated trapping temperature (°C)
Northern Conwy Valley	165	1	2	160	325
		10		168	333
Southern Conwy Valley	185	1	2	160	345
		10		168	353
Central northern Snowdonia	180	1	1.5	120	300
		10		128	308

TABLE 7.D. The estimation of pressure and the calculation of temperature from the fluid inclusions of northern Snowdonia.

must be viewed with extreme caution.

7.6.3. Estimation of temperature and calculation of pressure

Alderton (1976) and Fyfe et al. (1978) outline a geobarometer using fluid inclusion filling temperatures and oxygen isotope geothermometry. The oxygen isotope data provides the true trapping temperature. Fluid inclusions yield a filling temperature which is depressed by an amount that is directly proportional to the pressure of trapping, hence, from a combination of geological data, precise trapping pressures can be calculated. In the present study no oxygen isotope work was undertaken, however, approximate temperatures can be obtained from a combination of the illite crystallinity and meta-dolerite secondary assemblage data.

Robinson et al. (1980)and Frey et al. (1980) indicate that the base of the anchizone occurs at a temperature of about 220^{o}C. Frey et al. (1980) also indicate that the base of the "higher grade" part of the anchizone occurs at a temperature of about 270^{o}C based on the correlation between illite crystallinity, coal rank and fluid inclusion data. Schiffman and Liou (1980) demonstrate that at relatively low pressures (about 2.0kb) the transition from prehnite-pumpellyite to lower greenschist facies occurs at about 320^{o}C.

Illite crystallinity analyses indicates that the western Conwy Valley exhibits typical epizone crystallinity associated with prehnite-pumpellyite facies meta-dolerite assemblages in the north,and lower greenschist meta-dolerite assemblages in the south. The rest of northern Snowdonia exhibits typical middle-high anchizone crystallinity associated with a non-diagnostic pistacitic epidote and actinolite meta-dolerite assemblage. Temperatures of about 290^{o}C, 325^{o}C and 340^{o}C would, therefore, appear to be realistic estimates for central northern Snowdonia, the northern Conwy Valley and the southern Conwy Valley respectively, assuming that regional illite

crystallinity and meta-dolerite assemblages also reflect the temperatures prevalent during quartz vein formation. This assumption appears justified as there is good evidence indicating that regional illite and meta-dolerite recrystallisation and quartz vein emplacement are all pre-cleavage in northern Snowdonia.

From Figure 7.9. estimated trapping temperatures of 290°C, 325°C and 340°C indicate corrections of 110°C for central northern Snowdonia, 160°C for the northern Conwy Valley and 155°C for the southern Conwy Valley. These corrections correspond to pressures of approximately 1.4, 2,0 and 1.9kb respectively. From Figure 7.10 the corresponding derived pressures are 1.25, 1.90 and 1.85kb respectively. These results are summarised in Table 7.E.

Pressures of 1.4, 1.95 and 2.0kb indicate stratigraphic thicknesses of approximately 5.6, 7.8 and 8.0km respectively, assuming an average increase in pressure of 250 bars per km^{-1}.

Of the two approaches outlined above estimate of the trapping temperature and use of the fluid inclusion filling temperature data as a geobarometric tool seems most reliable as independent geological esimates of temperature are more precise than for pressure.

7.7. Calculation of the pre-deformation geothermal gradient

From a combination of derived and estimated data concerning the pressures and temperatures of vein formation (Table 7.E),it is possible to calculate approximate pre-deformation geothermal gradients for northern Snowdonia. From the data contained in Table 7.E. for low salinity fluids (1% NaCl equivalent), estimated temperatures of approximately 290°C in central northern Snowdonia are associated with a calculated pressure of 1.4kb, representing a geothermal gradient of

Area	Mean filling temperature (°C)	Salinity (Wt.% NaCl equivalent)	Estimated temperature (°C)	Temperature difference (°C)	Calculated trapping pressure (Kb)
Northern Conwy Valley	165	1	325	160	2.00
		10			1.90
Southern Conwy Valley	185	1	340	155	1.95
		10			1.85
Central northern Snowdonia	180	1	290	110	1.40
		10			1.25

TABLE 7.E. The estimation of temperature and the calculation of pressure from the fluid inclusions of northern Snowdonia.

about 53°C per km. In the northern Conwy Valley an estimated temperature of 325°C is associated with a calculated pressure of 2.0kb, reflecting a geothermal gradient of approximately 40°C per km. In the southern Conwy Valley an estimated temperature of 340°C is associated with a calculated pressure of 1.95kb, producing a geothermal gradient around 43°C per km.

If the fluid is markedly more saline (10% NaCl equivalent), the calculated pressures fall slightly (Table 7.E) resulting in a geothermal gradient approximately 3°C per km higher than that calculated using the 1% salinity fluid.

These pre-deformation geothermal gradients are clearly very high. The white mica b_0 data (Chapter 6) might support this conclusion, indicating a low-intermediate pressure facies series of metamorphism in the western Conwy Valley, corresponding to a calculated geothermal gradient of 40-43°C per km, and a low-pressure facies series of metamorphism in central northern Snowdonia, corresponding to a calculated geothermal gradient of 52°C per km. This inter-technique approach to calculating temperatures and pressures and the subsequent use of this data in turn to calculate past geothermal gradients depends on the compatibility of geological data obtained from a variety of techniques. This is discussed in some detail in the next chapter (Sections 8.2. and 8.3.). The significance of these results is also discussed in Chapter 8.

7.8. Discussion of the results

7.8.1. Problems of fluid inclusion analysis in northern Snowdonia

During the course of the fluid inclusion measurements several difficulties arose due to making precise observations on very small inclusions over a period of time, metastability in small inclusions and inclusion autodecrepitation.

i) Observational problems generally arose because of the small size of the inclusions and the necessity of monitoring precise changes. These observational problems were largely overcome by repeat measurements, relatively rapid heating (thus reducing the period of observation), careful choice of inclusions and observation of the temperature of reappearance of vapour bubble upon cooling. If the vapour bubble reappears after only slight cooling (< $10^{o}C$) total filling had probably not been achieved,if total filling had occurred undercooling of at least $15^{o}C$ was necessary before reappearance of the vapour bubble. This behaviour reflects surface tension on the inside walls of the inclusion (Roedder, 1972).

ii) Metastability was found to be a particularly serious problem in the current study and precluded detailed compositional analysis as most of the inclusions did not freeze upon cooling to very low temperatures (Section 7.4.) Roedder (1981) recognises this problem and observed that "inability to freeze small inclusions can actually preclude some investigations".

iii) Autodecrepitation can occur both naturally and experimentally when inclusions are heated beyond their filling temperature thus causing an increase in internal pressure. If internal pressure exceeds confining pressure fracturing will automatically occur resulting in an irreversible increase in inclusion volume. Autodecrepitation occurs frequently in soft, cleaved, host minerals (for example, fluorite and halite) containing large inclusions and less frequently in hard, cleavage free, host minerals (for example, quartz) containing small inclusions (Roedder, 1972, 1981; Crawford, 1981).

Several of the early measurements produced a number of very high filling temperatures. These were initially thought to be genuine high temperature inclusions as the measurements were repeatable and the

samples involved contained many large inclusions. Often a background filling temperature of around 180^{o}C was obtained from several inclusions before a high temperature inclusion (> 300^{o}C) was discovered, after this initial discovery, many other high filling temperatures were subsequently obtained. Originally it was thought that this pattern of filling temperature results reflected small pockets of high temperature inclusions. However, after a large number of repeat measurements on the samples concerned it was realised that autodecrepitation was occurring with fracturing of the inclusions during the heating of an original, presumably genuine, high temperature inclusion. These rare high temperature inclusions occasionally displayed some evidence of "necking-down", a feature frequently associated with anomalous filling temperatures (Roedder, 1979). The effects of autodecrepitation on samples 184, 234 and 280 are shown in Figure 7.11. Once autodecrepitation had been recognised it was resolved by discarding quartz grains after a temperature in excess of about 230^{o}C had been recorded for any inclusion within that grain. The problem of autodecrepitation is potentially very serious and difficult to visually detect and can result in misleading fluid inclusion filling temperatures. The problem of autodecreptiation can be simply overcome by fitting a microphone to the stage and monitoring the "explosions" as inclusions rupture (Roedder, 1979).

7.8.2. Reliability of the results

Three factors must be born in mind when assessing the reliability of the fluid inclusion results, these being: i) the reliability of the calibration and subsequent measurements of filling temperature, ii) inter- and intra-sample variation in characteristic filling temperature, and, iii) the accuracy of the assumptions made when calculating, either, the trapping temperatures, or pressures, from filling temperature data.

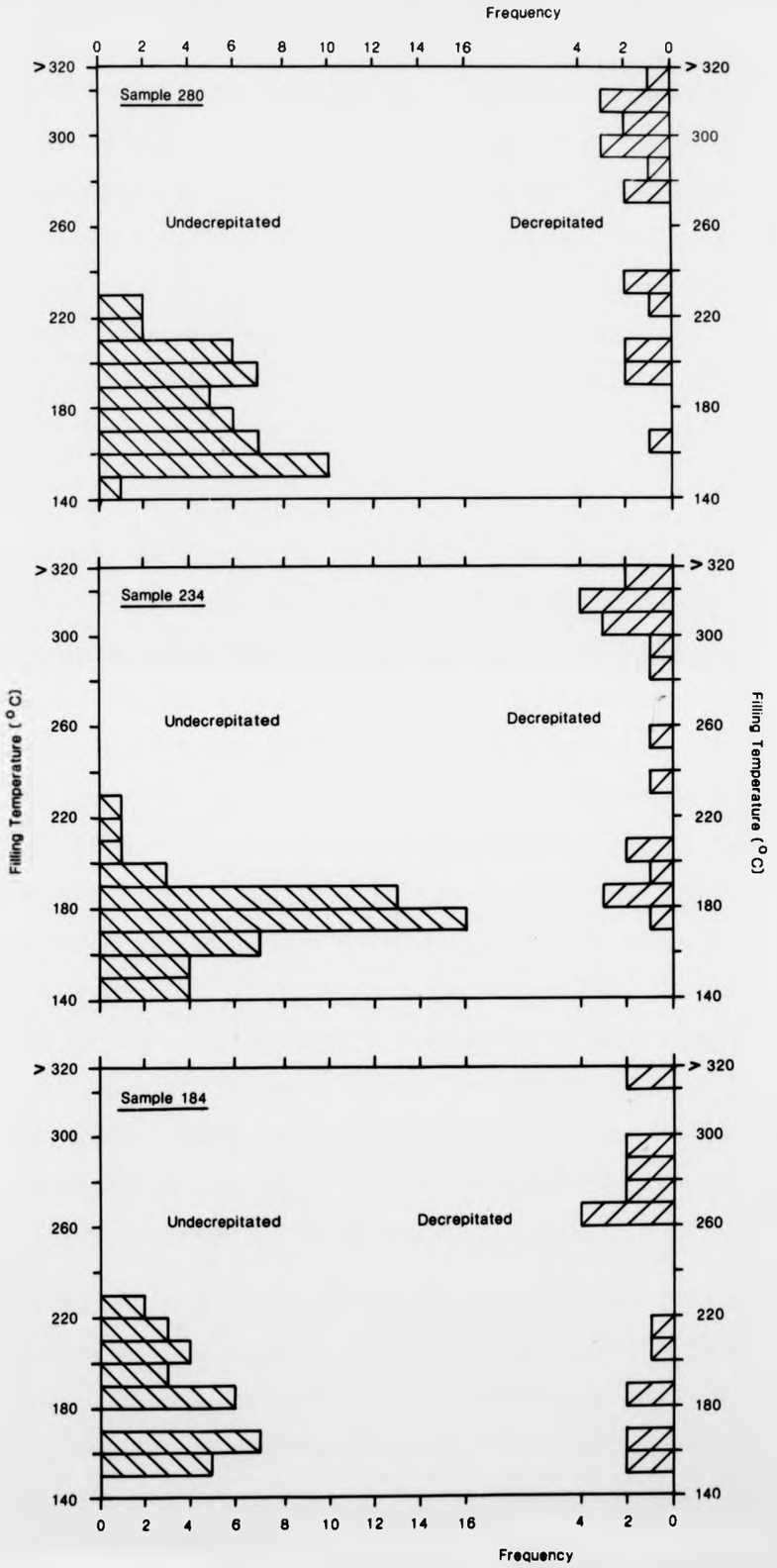

FIGURE 7.11. The effects of autodecrepitation on fluid inclusion filling temperatures in samples 280, 234 and 184.

i) The calibration of the heating stage is discussed in Section 7.5. and shown in Figure 7.4. In order to quantify the errors associated with the measurement of filling temperatures in small inclusions, repeat measurements were undertaken on the inclusions in Samples 66J and 6A and the pooled variance calculated. The standard deviation in Sample 66J, based on the triplicate measurement of filling temperatures on 20 inclusions, was found to be 3.2^{o}C. In sample 6A the standard deviation, based on the duplicate measurement of filling temperatures on 20 inclusions, was found to be 3.4^{o}C.

ii) In Section 7.5. approximate mean bulk filling temperatures of about 180^{o}C, 165^{o}C and 185^{o}C were determined for central northern Snowdonia, the northern Conwy Valley and the southern Conwy Valley respectively. However, it was also shown that significant variation in filling temperatures existed between samples within these areas and between the individual grains within a sample. This intra-sample variation was tentatively attributed to inhomogeneous deformation within the quartz grains. This is a potentially serious source of uncertainty in that inter-sample variation may simply reflect different intensities of quartz deformation, rather than true differences in the conditions of vein emplacement (pressure and temperature). This source of uncertainty was largely overcome by only measuring filling temperatures for the primary inclusions contained within the less deformed quartz grains displaying normal extinction, little recrystallisation, no fracturing and a general paucity of obviously secondary inclusions.

iii) From the preceding discussion it would appear that the individual filling temperature determinations and the mean regional bulk filling temperature determinations are relatively reliable in that there is a small total error between replicate measurements and there is broad similarity in filling temperatures for samples from a given area. In

extrapolating these results to derive either the true temperature or pressure of vein emplacement the major limitation lies in the reliability of the assumptions made.

In the present study, the precise composition of the fluid could not be determined. Differences in fluid composition have a small but significant effect on the calculations of trapping temperatures and pressures. For example, in northern Snowdonia differences of $8^{o}C$ and 0.1kb can occur between a 1% and a 10% salinity fluid (Tables 7.D. and 7.E). It was shown in Section 7.6. that the estimate of pressure, in particular, is poorly constrained and is subject to uncertainty of at least 0.5kb leading to errors of $\pm 40^{o}C$ in the calculation of trapping temperatures. The temperature estimates, from illite crystallinity and meta-dolerite assemblages, are rather more precise but uncertainties of as much as $\pm 20^{o}C$ are possible leading to errors of $\pm$ 0.25kb in the calculation of the trapping pressures.

In addition to the limitations imposed by the reliability of the assumptions used in the calculation of absolute trapping temperatures and pressures there is an additional uncertainty of $\pm 10^{o}C$ on the published pressure correction data for the H_2O - NaCl system (Potter, 1977).

It would appear, therefore, that whilst the relative temperatures and pressures in different areas of northern Snowdonia can be reasonably precisely determined, the calculations of absolute temperatures and pressures are, of necessity, less precise.

7.9. Concluding remarks

Examination of the aqueous inclusions contained within 19 quartz veins from northern Snowdonia has provided valuable information concerning

the approximate fluid composition and the pressures and temperatures of vein emplacement. Several problems were encountered that precluded full compositional analysis particularly the small inclusion size and the metastable persistence of super-cooled fluid.

The data obtained indicates that: i) there is no significant difference in fluid composition or filling temperatures between the primary and secondary fluid inclusions contained within a sample, ii) differential deformation within quartz veins has caused a significant amount of intra-sample variation in filling temperatures, and, iii) there is no major significant difference in characteristic filling temperature or fluid composition within northern Snowdonia although slight differences exist, with lower aggregate filling temperatures in the northern Conwy Valley and higher aggregate filling temperatures in the southern Conwy Valley. This trend is thought to reflect differences in the physical conditions prevalent during vein emplacement rather than differences in deformation as all the regional filling temperature measurements were made on the least deformed grains within a sample. In addition, no significant difference in the intensity or style of deformation is apparent within northern Snowdonia either in the field or in the vein quartz thin sections.

From a combination of the geological data obtained from the metadolerites and phyllosilicates and the fluid inclusion filling temperature data, estimates of the temperature and pressure of metamorphism have been obtained. Independent geological data is considered to be more reliable for the estimate of trapping temperatures thus allowing calculation of the associated pressures. Estimated temperatures are approximately 290^{o}C in central northern Snowdonia, 325^{o}C in the northern Conwy Valley and 340^{o}C in the southern Conwy Valley. Characteristic filling temperatures in these areas are 180^{o}C, 165^{o}C and 185^{o}C respectively.

These figures produce pressures of 1.4, 2.0 and 1.95kb assuming a low salinity fluid (1% NaCl equivalent). Calculation of the associated geothermal gradients indicate gradients of 40-43^{o}C per km in the western Conwy Valley and 52^{o}C per km in central northern Snowdonia.

The implications of the evidence derived from the fluid inclusions in the context of the metamorphic history of northern Snowdonia is discussed in detail in the next chapter. It would, however, appear that veining forms an integral part of the pre-deformation metamorphic history of the area. In this respect fluid inclusion compositions and the derived temperatures and pressures of vein emplacement probably closely reflect the actual fluid compositions, temperatures and pressures of pre-deformation metamorphism in northern Snowdonia.

CHAPTER 8

SUMMARY AND DISCUSSION

8.1. Summary of results

8.1.1. Meta-dolerites

The geochemistry, petrography and phase compositions of meta-dolerites from the western Conwy Valley were studied in detail. Meta-dolerites from central northern Snowdonia were also petrographically examined.

From the geochemical data it would appear that the meta-dolerites were originally tholeiitic intrusions displaying a range from primitive (for example, Cerrig Cochion, SH 727677) to relatively more differentiated compositions (for example, Moel Ddefaid, SH 730606). During low-grade metamorphism significant major element mobilisation appears to have occurred with only TiO_2, FeO* (total iron), Al_2O_3 and MnO showing consistent magmatic inter-element correlation as well as good correlation with "immobile" trace elements (particularly Zr and Y). CaO and Na_2O were mobile within intrusions with local relative enhancement and depletion of these oxides reflecting the importance of epidotisation and albitisation respectively. The geochemical analyses provide a data base from which the petrographic and mineral compositional data can be interpreted. Without the geochemical analyses it would be impossible to distinguish between effects related to metamorphism and host rock composition.

Petrographic observations have revealed significant regional and local variation in secondary mineral assemblages. In general, the regional variations are: i) lower grade prehnite- and pumpellyite-bearing assemblages, typical of the prehnite-pumpellite facies, in the

northern Conwy Valley, ii) higher grade actinolite- and clinozoisitic epidote-bearing assemblages, typical of the lower greenschist facies, in the central Conwy Valley, iii) intermediate grade pumpellyite-bearing, prehnite-free assemblages in the southern Conwy Valley, and iv) less diagnostic actinolite- and pistacitic epidote-bearing assemblages in central northern Snowdonia. This latter assemblage may reflect relatively low-grade with the critical index minerals prehnite and pumpellyite suppressed by slightly higher X_{CO_2} in the fluid. The effects of original differences in dolerite composition on secondary assemblages can be seen through the development of chlorite-rich and albite-rich meta-dolerites reflecting relatively less and more differentiated hosts respectively.

Petrographically there is evidence for disequilibrium on the thin section scale with most samples containing relict igneous phases, particularly pyroxene and plagioclase. Several mineral phases display clear reaction textures, particularly prehnite, pumpellyite and epidote. The phase rule was disobeyed by about 8% of the meta-dolerites sampled, particularly those from the lower grade area in the northern Conwy Valley where most of the mineral reaction was observed. In many cases the actinolite in these assemblages clearly overgrows relatively early formed phases such as epidote and chlorite.

Detailed microprobe analyses have enabled quantification of the compositional variation in secondary phases within the Conwy Valley. Comparison of the prehnite and pumpellyite compositions in the northern Conwy Valley with other areas of low-grade metamorphism indicates uppermost prehnite-pumpellyite facies metamorphism. The general compositional trends for epidote and pumpellyite in the central and southern Conwy Valley indicate a slight increase in grade southwards. Continuously zoned epidotes from relatively Fe-rich cores to Fe-poor rims indicate

progressive decrease in fO_2 together with increase in temperature throughout metamorphism. Crossing compositional tie lines indicate some chemical disequilibrium between co-existing metamorphic phases, particularly actinolite and chlorite.

The petrographic and microprobe data indicates that the grade of metamorphism in the northern Conwy Valley is uppermost prehnite-pumpellyite facies. Further south there is the development of diagnostic actinolite- and epidote-bearing, lowest greenschist facies assemblages, but still retaining small amounts of pumpellyite.

8.1.2. Phyllosilicates

Illite crystallinity and white mica b_0 values have been determined on phyllosilicates from the fine grained meta-sediments.

Significant variation in regional illite crystallinity occurs within northern Snowdonia with an epizonal area in the western Conwy Valley surrounded by an anchizone illite crystallinity region. The boundary between the two areas is sharp, and, over part of its length at least, related to major, deep rooted faults that are known to have influenced the deposition and preservation of Lower Palaeozoic sequences. Superimposed onto this pattern is a general trend towards slightly higher crystallinity southwards in both the areas of anchizone and epizone crystallinity. Local variation in illite crystallinity may be related to deformation with, for example, enhanced illite crystallinities in the core of the Nant Peris anticline (SH 599587).

White mica b_0 results reveal a bimodal distribution similar to that displayed by the illite crystallinity data. Two distinct geographical areas can be recognised with mean b_0 values of 8.988 and 9.008 indicating low and low-intermediate pressure facies series of metamorphism respectively. The boundary between the two areas appears to be coincident with

the boundary between the areas of typically epizone and anchizone illite crystallinities.

The significance of the results from the phyllosilicates is that they quantify aspects of metamorphism in areas where meta-dolerites do not occur. Both illite crystallinity and white mica b_o data indicate that an area of slightly higher grade (epizone), low-intermediate pressure facies series metamorphism surrounded by an area of slightly lower grade (anchizone), low-pressure facies series metamorphism can be distinguished within northern Snowdonia.

8.1.3. Fluid inclusions

Qualitative fluid compositions and quantitative filling temperatures have been obtained from vein quartz fluid inclusions.

Detailed observations show that inclusions contain two phase, vapour-liquid, aqueous inclusions. No immiscible relationships were observed indicating low CO_2 and CH_4 contents. No daughter salt crystals occur indicating a relatively low salinity fluid (< 22 wt% NaCl equivalent). Mean filling temperatures range from 157^oC - 194^oC with a trend towards slightly higher temperatures in the south. From a combination of fluid inclusion and independent geological data, pre-deformation temperatures and pressures ranging from approximately 290^oC and 1.4 kb in central northern Snowdonia to 340^oC and 2.0 kb in the western Conwy Valley have been calculated. These figures indicate very high pre-deformation geothermal gradients in northern Snowdonia (over 40^oC per km).

Table 8.A. is a summary of the results obtained from the meta-dolerites, phyllosilicates and fluid inclusions in the eastern, northern, central and southern Conwy Valley and central northern Snowdonia.

TABLE 8.A. Summary of results for different parts of northern Snowdonia.

Area/Method	Petrography	Phase compositions	Illite crystallinity	White Mica b_o	Fluid inclusions
Eastern Conwy Valley	———	———	Generally middle anchizone.	Low-pressure facies series.	Few quartz veins, often infill tension gashes. Very small inclusions. Possibly post deformation.
Northern Conwy Valley	Very variable, prehnite and pumpellyite bearing Fe-epidote, some actinolite, petrographic disequilibrium.	Fe-rich pumpellyite Fe-rich epidote Fe-poor prehnite	Low anchizone in the far north, low epizone further inland.	Low-pressure facies series in the north, Low-intermediate pressure facies series inland.	Small inclusions in the north, larger inclusions inland. TH 160°C-170°C pre-deformation.
Central Conwy Valley	Extensive actinolite and clinozoisitic-epidote. Rare pumpellyite no prehnite. More pervasive recrystallisation.	Fe-poor epidotes except in the more diffentiated intrusions. Fe-poor pumpellyites generally.	Generally epizone.	Low-intermediate pressure facies series.	Variable inclusions, TH generally 160°C-180°C but one of 194°C pre-deformation.
Southern Conwy Valley	Extensive actinolite continuously zoned epidotes. Some pumpellyite (particularly further south) little prehnite.	———	Generally epizone.	Low-intermediate pressure facies series.	Good inclusions, TH 180°C - 190°C pre-deformation.
Central Northern Snowdonia	Extensive actinolite and Fe-epidote, very rare pumpellyite, no prehnite.	———	Generally middle-upper anchizone. Some epizone values in fold cores.	Low-pressure facies series.	Abundant, good inclusions TH 170°C - 190°C. Slight increase southwards. Pre-deformation.

8.2. Inter-technique correlation

8.2.1. Good correlation between results

One of the clearest correlations is between the white mica b_0 and illite crystallinity results. Both sets of results display significant differences between the western Conwy Valley and the rest of northern Snowdonia. Both techniques are temperature sensitive indicators with higher crystallinity and b_0 values occurring at higher temperatures, in low-grade metamorphism, for a given pressure (Padan et al., 1982), hence correlation between illite crystallinity and b_0 might simply reflect this relationship. In Section 6.6.2. it was shown that the increase in temperature between middle-anchizone and low-epizone illite crystallinities is insufficient to account for the observed increase in b_0. In the Nant Peris anticline typically epizone crystallinities are developed, however, the associated b_0 values are indistinguishable from the regional, typically low, b_0 values. Individual anomalous illite crystallinity values do not correlate with individual anomalous b_0 values. This indicates that although good overall correlation exists between the statistical populations as a whole, individual results may show significant deviation from the general pattern. This supports the view that the relationship between crystallinity and b_0 reflects differences in the parameters of metamorphism and does not simply reflect autocorrelation, with variation in one causing the variation in the other.

Good correlation also exists between petrography and phase chemistry within the Conwy Valley. The petrographic study revealed that the lowest grade (prehnite-bearing) assemblages are developed in the northern Conwy Valley with higher grade (prehnite-free) assemblages developed in the central and southern Conwy Valley. Phase chemistry also indicated an increase in grade southwards within the Conwy Valley.

Phases whose compositions are sensitive to the grade of metamorphism include prehnite, pumpellyite and epidote. Host rock chemistry also effects the composition of these phases, however, by reference to the geochemical analyses it is possible to quantify this influence and assess any underlying compositional trends. Schiffman and Liou (1980) and Liou et al., (1983) show that as grade increases the Fe/Fe+Al content of prehnite, pumpellyite and epidote progressively falls. In the Conwy Valley there is a tendency for Fe/Fe+Al in pumpellyites to decrease southwards. Prehnite is typically Fe-poor. Epidote compositions are markedly influenced by host rock composition but there appears to be an underlying trend towards lower Fe/Fe+Al in the southern and, particularly, central Conwy Valley. Thus both the petrographic and phase chemistry results indicate upper prehnite-pumpellyite facies metamorphism in the northern Conwy Valley and lower greenschist facies metamorphism in the central and southern Conwy Valley.

Comparison of fluid inclusion filling temperatures with the meta-dolerite results in the Conwy Valley again reveals broad inter-technique agreement. The general increase in grade southwards, indicated by the meta-dolerite assemblages, is mirrored by a general trend towards higher homogonisation temperatures, from approximately 160^{o}C in the north (prehnite-pumpellyite facies assemblages) to 185^{o}C in the South (low greenschist facies assemblages). The major problem when comparing fluid inclusion data with other geological data is that only filling temperatures are measured which reflect both the temperature and pressure of trapping so that the filling temperatures are lower than the true trapping temperatures by an amount that is proportional to the pressure prevalent at the time of trapping.

8.2.2. Poor correlation between results

One of the clearest examples of disparity between techniques occurs

in the northern Conwy Valley, around Tal-y-Fan (SH 725725), where the illite crystallinity is typically low epizone but the meta-dolerite assemblages are typical of the prehnite-pumpellyite facies. It is possible that this discrepancy reflects imperfect correlation between low-grade metamorphic boundaries, defined in different lithologies, utilising different techniques. The exact position of the anchizone/epizone boundary has not been universally defined (Kisch, 1980). In the current study boundary values of 12.0, $0.25^{o}2\theta$ and 185 were chosen for the Weaver, Kubler and Weber indices, respectively. However, there is no reason why this boundary should correlate exactly with the prehnite-pumpellyite/greenschist facies boundary defined on meta-dolerite secondary assemblages (Kubler, 1968; Kisch, 1983a). In northern Snowdonia it would appear that low epizone illite crystallinities correlate with upper prehnite-pumpellyite facies meta-dolerite assemblages. Thus in the northern Conwy Valley the transition from uppermost prehnite-pumpellyite facies to lowest greenschist facies meta-dolerite assemblages is associated with a slight increase in mean, epizone, illite crystallinity. Bevins and Rowbotham (1983) observed some local discrepancy between phyllosilicate and meta-dolerite results concerning the exact position of the greenschist/sub-greenschist facies boundary within the Welsh basin. This they also thought reflected lack of direct correlation between the two techniques.

The evidence indicates that the prehnite-bearing meta-dolerites around Tal-y-Fan underwent progressive reaction with the breakdown of prehnite in particular. The compositional data supports the view that the Fe-poor prehnites around Tal-y-Fan are high-grade (Liou et al.,1983). The presence of typically low epizone illite crystallinities in this area is consistent with the observation that prehnite is at the upper limit of its stability. Further north, in the Penmaenmawr meta-diorite (SH 715755),clear fresh prehnite is associated with low-middle anchizone

crystallinities indicating that under these conditions of relatively lower grade metamorphism, prehnite is stable within the prehnite-pumpellyite facies.

In central northern Snowdonia there appears to be marked discrepancy between results obtained from different techniques. Illite crystallinity indicates relatively lower grade (anchizone). Whilst the meta-dolerites superficially indicate higher grade (low greenschist facies). However, in Chapter 4 it was argued that the prehnite- free assemblages of central northern Snowdonia may reflect slightly higher X_{CO_2} within the fluid causing the suppression of prehnite and pumpellyite relative to epidote and actinolite (Coombs et al., 1970; Brown, 1977). This conclusion is supported by the abundance of Fe-rich epidote and the rare occurrence of Fe-rich pumpellyite, both indicative of relatively low-grade (Schiffman and Liou, 1980; Liou et al., 1983). It thus appears that the poor inter-result correlation in central northern Snowdonia is only superficial with the apparently high-grade actinolite-epidote, meta-dolerite assemblages reflecting slight differences in fluid composition rather than higher pressures and temperatures of metamorphism.

The fluid inclusion filling temperatures from central northern Snowdonia are indistinguishable from those of the western Conwy Valley despite the fact that other techniques indicate that this is an area of relatively lower grade metamorphism. This might reflect the nature of the fluid inclusion technique with similar filling temperatures not necessarily reflecting similar trapping temperatures because of the influence of pressure. In Chapter 7 it was argued that the combined illite crystallinity and fluid inclusion data indicated significantly lower pressures in central northern Snowdonia (1.4 kb) than in the western Conwy Valley (2.0kb). The evidence indicates, therefore, that

the similar fluid inclusion filling temperatures disguise significant differences in metamorphic conditions within northern Snowdonia.

8.3. The timing of metamorphism

Data concerning the relative timing of burial, deformation, recrystallisation, etc., is essential if the results are to be meaningfully interpreted. Roberts (1981) argues that metamorphism is syn- to post-deformation and describes a relationship between metamorphic grade and the intensity of deformation. Coward and Siddons (1979) state that greenschist facies mineral assemblages in the pelitic rocks of the Welsh basin are syntectonic with the main cleavage and pre-date later crenulation cleavages. Lynas (1973), Maltman (1981) and Craig et al. (1982) all distinguish a phase of pre-deformation mineral growth within the meta-sediments producing chlorites and micas which are related within the first cleavage.

In North Wales the ages of deposition, dolerite intrusion and Caledonian deformation are known. Deposition ranged from late Pre-Cambrian to Llandovery times resulting in progressive burial throughout the Lower Palaeozoic. Many dolerites display characteristics consistent with their intrusion into wet sediments (Kokelaar et al., in press) indicating that they are probably of Caradoc age. The main deformation is end-Silurian with Llandovery sediments folded in the Llangollen syncline during Caledonian deformation and gently dipping lowermost Old Red Sandstone unconformably overlying Caledonian material on Anglesey (Roberts, 1979).

The relative age of meta-dolerite recrystallisation is difficult to determine. Much of the actinolite is demonstrably later than epidote, chlorite, albite, white mica and stilpnomelane all of which it is seen to overgrow. Occasionally, where recrystallisation is most pronounced,

actinolite needles display an oriented fabric along cleavage. Some actinolite growth, therefore, must have occurred during deformation. Epidote crystals are frequently continuously zoned with relatively Fe-rich cores and Fe-poor rims indicating a progressive fall in fO_2 as temperatures increased throughout their crystallisation (Liou et al., 1983). These epidotes are frequently found in textural equilibrium with chlorite and are occasionally found intergrown with pumpellyite or prehnite, indicating that these minerals crystallised at about the same time under similar P-T-X_{fluid} conditions. If the actinolite was produced under significantly different P-T-X_{fluid} conditions it is likely that some reaction would occur in the earlier formed minerals (prehnite, pumpellyite, epidote etc.). Evidence for this petrographic and chemical disequilibrium is found mainly in the northern Conwy Valley. Elsewhere reaction is limited to early formed Fe-rich epidotes. These features could be interpreted to indicate that there was a period of recrystallisation during which prehnite, pumpellyite, chlorite, epidote etc. were formed as temperatures progressively increased (zoned epidotes) which culminated in the crystallisation of actinolite during end-Silurian deformation. If this is so, recrystallisation in the meta-dolerites must have occurred before and during deformation although it is not possible to determine the exact period of time over which recrystallisation took place.

The presence of a widespread slaty cleavage and the high illite crystallinity values in fold cores clearly indicates a phase of syn-deformation phyllosilicate recrystallisation. However, the possible folding of the boundary between the areas of epizone and anchizone crystallinities by the Snowdonian Syncline, in the vicinity of Capel Curig, indicates that significant phyllosilicate crystallisation had occurred prior to deformation. Phyllosilicate crystallisation must

have occurred throughout the Lower Palaeozoic as older strata was progressively buried under a thickening cover, Lynas (1973), Maltman, (1981) and Craig et al. (1982) all describe fabrics parallel to the bedding in Wales thought to be caused by mineral growth under uniaxial, lithostatic stress during burial. No systematic relationship between regional illite crystallinity and deformation was observed in northern Snowdonia with the two crystallinity areas both displaying a similar style and intensity of deformation. As a result it is possible that regional illite crystallinity and b_0 could reflect pre-deformation phyllosilicate growth with the deformation controlled recrystallisation producing the regional slaty cleavage which in areas of high strain (fold cores),locally resulted in high illite crystallinity through enhanced phyllosilicate recrystallisation.

Much of the quartz veining in northern Snowdonia occurred before deformation. This is seen by folding of veins, diffraction of cleavage against veins and the occasional development of a weak fracture cleavage in the margins of veins. During deformation quartz veins were folded, fractured and partly recrystallised. It would appear that recrystallisation was not total so that fluid inclusions within the less deformed quartzes are generally larger, often isolated or in small groups and are probably primary. However, inclusions within the deformed quartzes are small, often occur in lines and planes and are probably secondary. Quartz veins are concentrated in the more siliceous lithologies and occur relatively frequently in strata up to the upper Caradoc, above this they are less frequently developed. It is possible that several generations of quartz vein exist with several of the rare veins in the Silurian sediments of the eastern Conwy Valley infilling tension gashes formed during deformation. Inclusions within these veins are very small and were not examined in detail. The evidence indicates that most veining in northern Snowdonia is pre-deformation. Primary

TABLE 8.B. Summary of data concerning the relative age of metamorphism in northern Snowdonia

Relative age	Basic assemblages	Phyllosilicates	Fluid inclusions
Post deformation			Some veining, possibly fracture and resealing.
Deformation	Growth of actinolite needles, occasionally in preferred orientation.	Folding with the production of an axial planar slaty cleavage or a fracture cleavage.	Some quartz recrystallisation, some possible opening and re-sealing of inclusions.
	Growth of chlorite and epidote, occasionally in association with prehnite and pumpellyite (pre-actinolite)	Recrystallisation of Phyllosilicates	
Pre-deformation	Zoned epidotes indicate increase in T and decrease in fO_2 throughout their growth.	Llandovery burial and diagenesis, recrystallisation of phyllosilicates along bedding	Vein emplacement generally pre-deformation. The precise date of veining is uncertain, definitely post-dolerite intrusion.
	Some disequilibrium between actinolite and the other minerals, the precise date of growth is unclear.	deposition	Possibly more than one phase of veining. Close association with Si-rich lithologies indicates equilibrium with host rock
Deposition and intrusion	Intrusion of dolerites (Probably Caradoc)	Lower Cambrian	

inclusions contained within these veins, therefore, were trapped at the temperatures and pressures prevalent at some time prior to end-Silurian deformation.

Table 8.B. is a summary of the relative ages of deposition, intrusion, periods of mineral crystallisation, vein emplacement and deformation. The evidence indicates that aspects of pre- and syn-deformation metamorphism can be recognised in northern Snowdonia possibly relating to Lower Palaeozoic burial and Caledonian deformation respectively.

8.4. The parameters of metamorphism

The use of a variety of techniques to study low-grade metamorphism in northern Snowdonia has enabled some quantification of the pressures, temperatures, fluid compositions and facies series of metamorphism.

Fluid inclusions and meta-dolerite assemblages indicate that the fluid associated with metamorphism was an essentially CO_2-free, low salinity, aqueous solution. With increasing X_{CO_2} prehnite, pumpellyite, epidote and actinolite become progressively suppressed (Coombs et al., 1970; Brown, 1977). All of these minerals are variably found within northern Snowdonia, although there is significant spatial variation in their development. This may partly reflect slight regional changes in in X_{CO_2}, with slightly higher X_{CO_2} in central northern Snowdonia possibly leading to the partial suppression of the expected (middle-anchizone illite crystallinity) prehnite-pumpellyite facies meta-dolerite assemblage. In addition, all the fluid inclusions are simple, single component, two phase (liquid-vapour), low salinity, aqueous inclusions displaying no immiscible relationships.

In Chapter 7 geological data from all the techniques utilised was used to establish the approximate pressures and temperatures of vein

emplacement. Independent geological data is considered most reliable for temperatures which enables the calculation of the pressure prevalent during veining. Estimates of temperatures are approximately 290^{o}C in central northern Snowdonia (middle-upper anchizone illite crystallinity), 320^{o}C in the northern Conwy Valley (low epizone illite crystallinity, prehnite-pumpellyite to lowest greenschist facies assemblages) and 340^{o}C in the southern Conwy Valley (epizone illite crystallinity, low greenschist facies assemblages). From these figures pressures of approximately 1.4kb and 2.0kb are calculated for central northern Snowdonia and the Conwy Valley respectively. These figures are thought to represent the temperatures and pressures of pre-deformation burial in northern Snowdonia.

Extrapolation of the derived data on pressures and temperatures to calculate a pre-deformation geothermal gradient produce figures of approximately 42^{o}C per km in the Conwy Valley and 52^{o}C per km in central northern Snowdonia. These geothermal gradients are clearly very high with the average regional metamorphism geothermal gradient being 25^{o}C per km (Miyashiro, 1979) and are similar to geothermal gradients calculated for the Buchan type of metamorphism in Scotland shown in Figure 8.1. (Turner, 1981). White mica b_0 supports the calculated high geothermal gradient indicating a low-to low-intermediate pressure facies series of metamorphism in northern Snowdonia.

Experimental studies on the stability of actinolite, prehnite and pumpellyite tend to confirm the relatively high temperature/low pressure nature of metamorphism in northern Snowdonia. Nitsch (1971) and Hinrichsen and Schurmann (1972) show that the breakdown of prehnite and pumpellyite is temperature dependent whilst the appearance of actinolite is pressure dependent. Work by Nitsch (1971), Zen (1974) and Schermerhorn (1975) reveals that the coexistence of pumpellyite and

FIGURE 8.1. The calculated pre-deformation pressure/temperature conditions of the western Conwy Valley and central northern Snowdonia. Also shown, for comparison, are the pressure/temperature conditions envisaged for blueschist, Barrovian and Buchan metamorphism, from Turner (1981).

actinolite occurs only at relatively high pressures (geothermal gradients less than $30^{o}C$ - $35^{o}C$ per km) and that the stability field of coexisting actinolite and pumpellyite increased rapidly with increase in relative pressure. From this it has been argued that the presence of pumpellyite and actinolite in a rock infers pressures of at least 2.5kb at temperatures of around $300^{o}C$. Although coexisting pumpellyite and actinolite were found in many of the meta-dolerites, it was shown in Chapters 3 and 4 that in many cases the chemical and petrographic evidence indicated that this is a disequilibrium assemblage with actinolite formed later. Where pumpellyite and actinolite coexist in the same thin section they usually occupy different alteration sites and never occur in intimate association, the essential criteria for the definition of the relatively high pressure pumpellyite-actinolite facies (Hashimoto, 1966).

Later deformation in northern Snowdonia resulted in vertical extension by as much as 150%(Coward and Siddans, 1979) which must have caused a significant increase in total pressure. This resulted in the production of an axial planar slaty cleavage and the growth of occasionally oriented actinolite needles. It is possible that the actinolite growth reflects the significant increase in total pressure during deformation.

From the above discussion it would appear that burial resulted in a low- to low-intermediate pressure facies series of metamorphism in northern Snowdonia with associated high geothermal gradients. End-Silurian deformation resulted in vertical extension with an associated significant increase in total pressure.

8.5. Geological interpretation

From the preceding discussion distinction between the metamorphic effects of deep burial and end-Silurian deformation is possible in

northern Snowdonia. These regionally developed effects reflect the influence of,i) progressive deposition throughout the Lower Palaeozoic with thicker deposits in the centre and thinner deposits towards the margins of the Welsh basin, and ii) the Caledonian orogeny. Much of the data obtained from the different techniques reflects conditions prevalent at some time before deformation, possibly the conditions of burial immediately prior to deformation. The current project has revealed significant variation in the effects of metamorphism within northern Snowdonia with a distinct, well defined area of relatively higher grade developed within the western Conwy Valley surrounded by an area of relatively lower grade.

Most of the meta-dolerites occur in the western Conwy Valley, the area of relatively higher grade. It could be, therefore, that the area of higher grade simply reflects the heating effects of the intrusive bodies. However, white mica b_0 indicates that the western Conwy Valley was metamorphosed under slightly higher relative pressures. If metamorphic grade was influenced by the high-level dolerite intrusions a lower relative pressure (higher temperature) would be expected compared to areas which had not suffered the heating effects to the same extent. Also, there is no difference in the fluid inclusion filling temperatures between the western Conwy Valley and central northern Snowdonia whereas if differences in metamorphism reflected the thermal effects of dolerite intrusions, significantly higher homogenisation temperatures might be expected in the western Conwy Valley.

If the observed pattern of metamorphism reflects the effects of both burial and deformation controlled metamorphism, it is possible that differences in the pattern simply reflect variation in the nature of burial and deformation metamorphic effects between different areas. It follows, therefore, that the western Conwy Valley might display more of

the effects of deformation controlled metamorphism whilst central northern Snowdonia retains many of the burial metamorphic characteristics. If this is so the differences between the western Conwy Valley and the rest of northern Snowdonia would reflect inhomogeneous deformation. The white mica b_0 data could be interpreted to support this argument with the white micas formed during burial being of a lower pressure facies series that those formed during deformation. However, in the field no systematic difference in the intensity and style of deformation could be discerned between the western Conwy Valley and the rest of northern Snowdonia. In Section 8.3. it was argued that the differences in metamorphic characteristics were largely established prior to deformation.

The boundary between the areas of typically anchizone and epizone illite crystallinity appears to correlate, at least along part of its length, with major basement controlled faults active throughout the Lower Palaeozoic. In the east the boundary closely follows the line of the Conwy Valley fault as far north as Dolgarrog (SH 770675) here it swings from N-S to NW-SE trending along the line of the Llanbedr fault. In the north of the area, around Tal-y-Fan (SH 730727), the precise nature of the boundary, although sharp, is unclear. The western part of the boundary is less clearly defined and does not immediately appear to relate to any obvious major faults in the field. However, recently Howells et al. (1983) and Kokelaar et al. (in press) have recognised a NE-SW trending 'hinge line' in the vicinity of Capel Curig which appears to have influenced deposition during the Ordovician. The nature of this active NE-SW trending flexure is unclear but is thought to possibly mark a concealed basement fracture with subsidence to the SE. Floyd et al. (1976) describe a 'fracture zone' in the vicinity of Cerrig Cochion (SH 723763) which they took to indicate a zone of incipient rifting during the Lower Palaeozoic. It is possible, therefore, that major Lower Palaeozoic structures may have influenced metamorphism within

northern Snowdonia. Bevins et al. (1981) observed marked changes in illite crystallinity across the Bala fault (to the south) with relatively lower grade, anchizone crystallinity, SE of the fault and higher grade, epizone crystallinity NW of the fault. Vertical tectonics are known to have played an important role in controlling the deposition and preservation of Lower Palazoic material throughout Wales (Coward and Siddans, 1979) with marked differences in local stratigraphy occurring across many of these major structures (Rast, 1969; Baker, 1971; Kokelaar, 1979).

Rast (1969) argued that the Lower Palaeozoic Welsh basin was divided into several large fault bounded blocks with the North Wales block being bounded by the Menai Straits and Church Stretton faults. Dunkley (1979) argued that the Welsh basin constituted a back arc basin with significant tensional stress reflected by the presence of large numbers of intra-basin normal faults (the Bala fault, Harlech Dome faults, Conwy Valley faults etc.). Many of the larger basement controlled structures take the form of high angled normal faults so that movement might result in a horst and graben system containing relatively upthrown and downthrown blocks. It is possible, therefore, that the differences in metamorphic characteristics observed within northern Snowdonia reflect metamorphism within a downthrown block (the western Conwy Valley) and on an upthrown block (the rest of northern Snowdonia), the blocks being separated by major tensional faults.

If the above model is accepted it is clear that differences in metamorphism reflect Lower Palaeozoic structure. In Section 8.3. it was argued that many of the metamorphic effects in northern Snowdonia reflect conditions prevalent at some time prior to end-Silurian deformation, possibly deep burial. If rifting occurred in northern Snowdonia it is probable that significant differences would exist between upthrown and downthrown blocks in terms of stratigraphic thickness, lithological

variation, heat flow, compaction, etc. In northern Snowdonia it appears that the downthrown block (western Conwy Valley) is characterised by relatively higher temperatures and pressures (> 320^{o}C and 2. Okb) but lower overall heat flow (40^{o}C - 43^{o}C per km), reflecting a greater depth of burial as sediments and volcanics collected in the downthrown graben. The upthrown block (the rest of northern Snowdonia) is characterised by lower temperatures and pressures (< 300^{o}C and 1.4kb) but higher overall heat flow (52^{o}C per km), reflecting shallow burial on the upthrown horst. The general slight increase in metamorphic grade southwards within northern Snowdonia may reflect a deepening of the Lower Palaeozoic basin southwards caused by south-easterly tilting of the fault bounded blocks (Ridgeway, 1976), resulting in greater aggregate depths of burial and hence slightly higher grades of pre-deformation metamorphism towards the south. The high geothermal gradients associated with the early metamorphism may reflect the effects of heating related to major plutonic activity with the relatively slow dispersal of heat from the major basic magmatic bodies known to underlie the area at depth (Rast, 1969).

Superimposed onto this pre-deformation metamorphic pattern are the effects of recrystallisation during Caledonian deformation. This is known to have caused significant crustal shortening/vertical extension in North Wales (Lynas, 1970; Coward and Siddans, 1979) resulting in an increase in total pressure, the production of a slaty cleavage and the growth of actinolite within the meta-dolerites.

The schematic representation of the metamorphic environment envisaged for northern Snowdonia during the Lower Palaeozoic is shown in Figure 8.2. where differences in the pre-deformation metamorphic characteristics are related to tensional, rift tectonics. The validity of this model depends on the recognition and distinction of pre- and

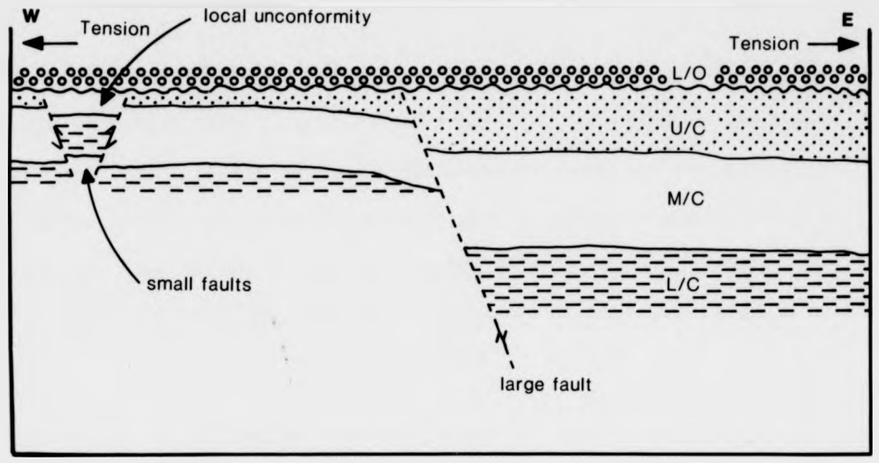

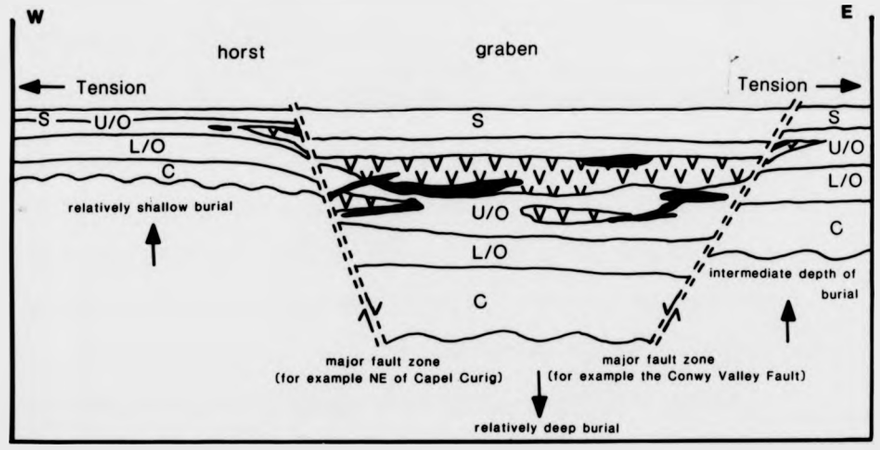

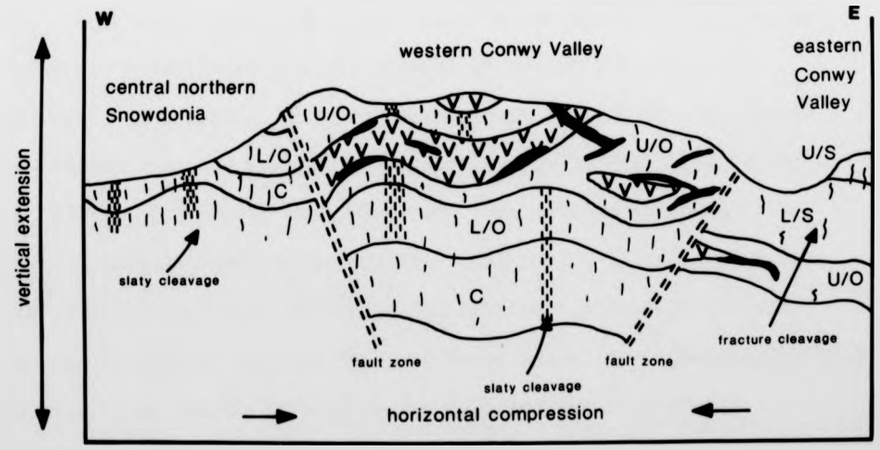

FIGURE 8.2. The Lower Palaeozoic metamorphic environment envisaged in northern Snowdonia. A Cambrian fault control on sedimentation resulting in lateral stratigraphic variation and unconformities. B Pre-Caledonian Major fault control on the deposition and preservation of Lower Palaeozoic volcanics and sediments in an ensialic back arc basin. Marked lateral variation in the relative depth of burial. Recrystallisation in the sediments and dolerites, emplacement of most of the quartz veins. C Caledonian Horizontal compression/vertical extension producing a cleavage in the sediments and volcanics and further re-crystallisation in the dolerites. Possibly minor quartz veining.

syn-deformation metamorphic effects. However, the model appears to fit the data available from a variety of contrasting techniques. The model also appears to be consistent with the known tectonic environment of North Wales during the Lower Palaeozoic with a period of extension during deposition within a back arc ensialic basin (Dunkley, 1979) and compression during end-Silurian deformation (Coward and Siddans, 1979).

8.6. Further research

The present study has highlighted several areas where further research could provide valuable information.

Probably the most serious problem in both the white mica b_o determinations and illite crystallinity measurements is that they are bulk techniques producing a mean b_o or illite crystallinity based on all the phyllosilicates present within a sample. No distinction is made between different generations or orientations of phyllosilicate so that the result obtained may simply be an average of the individual characteristics of several generations of phyllosilicate growth. Refinement of the technique is essential through the use of analytical scanning electron microscopy (SEM) and transmission electron microscopy (TEM). These techniques enable the compositions of individual crystals of different generations or orientations of phyllosilicate to be quantified. In addition potentially important changes in microfabric can be recognised utilising these techniques (White and Knipe, 1978; Knipe, 1981). Use of SEM and TEM on the fine-grained sediments of northern Snowdonia would allow detailed examination of the microfabric in the areas of typically anchizone and epizone illite crystallinity and across structures such as the Nant Peris anticline. These techniques would also allow quantification of the compositional differences

between phyllosilicates produced before and during deformation (Kisch, 1984, pers. comm.).

The use of other techniques to quantify low-grade metamorphism within the Welsh basin might also yield valuable information. Techniques such as conodont colour alteration, vitrinite reflectance and isotope geochemistry could all be usefully employed. Isotope geochemistry in particular appears promising with possibilities for oxygen isotope geothermometry using coexisting quartz-illite and quartz-chlorite mineral pairs in the meta-sediments and epidote-quartz mineral pairs in veins. Detailed microchemical isotope work on the fluid inclusions could provide information on the origin, nature and evolution of the fluid. Isotopic dating would allow the age of veining to be precisely determined.

Use of the techniques utilised in the project, along with those mentioned above, throughout the Welsh basin would provide detailed information over a much broader area which would increase understanding of the nature of low-grade metamorphism within the Lower Palaeozoic Welsh basin.

CHAPTER 9

CONCLUDING REMARKS

The current project has shown that northern Snowdonia has undergone low-grade metamorphism, probably within the prehnite-pumpellyite to lower greenschist facies. Diagnostic metamorphic assemblages and specific phase compositions, indicate that central northern Snowdonia and the northern and eastern Conwy Valley have undergone prehnite-pumpellyite facies metamorphism whilst much of the western Conwy Valley appears to have been metamorphosed in the lower greenschist facies. Illite crystallinity determinations tend to correlate well with the meta-dolerite observations with typically epizone illite crystallinity values being obtained from samples taken from the western Conwy Valley contrasting with typically anchizone illite crystallinity values obtained from samples taken elsewhere in northern Snowdonia. The boundary between the two areas is typically very sharp and corresponds to major faults over at least a part of its length. This distribution of results is mirrored by the b_0 white mica data with the occurrence of an area of higher b_0 in the western Conwy Valley (indicating slightly higher relative pressures) surrounded by an area of lower b_0 (indicating slightly lower relative pressures). Filling temperatures, determined on aqueous inclusions contained within extensively developed quartz veins throughout northern Snowdonia, are broadly similar throughout the area although there is a trend towards slightly higher filling temperatures southwards.

The available evidence indicates that many of the metamorphic characteristics observed within northern Snowdonia reflect conditions prevalent at some time prior to Caledonian deformation. The effects of deformation can be seen through the presence of relatively later

formed needles of actinolitic amphibole overgrowing the earlier epidote and chlorite within the meta-dolerites, and the local, occasionally extreme, increase in illite crystallinity in the cores of some of the well exposed Caledonian folds within the area. Much of the meta-dolerite and phyllosilicate reaction and recrystallisation and most of the quartz veining appears to be pre-tectonic. As a result, a combination of data obtained independently from a variety of techniques can be used to determine the approximate parameters of pre-deformation metamorphism. The evidence indicates that the metamorphic fluid was a relatively low salinity (< 20% NaCl equivalent), CO_2 poor (< 2%), aqueous solution. Estimates of the pre-deformation pressures and temperatures prevalent within northern Snowdonia vary from approximately 1.4 kb and 290^{o}C in central northern Snowdonia to 2.0 kb and 340^{o}C in the southern Conwy Valley reflecting the transition from prehnite-pumpellyite to lower greenschist facies conditions. From these estimates it would follow that the associated metamorphic geothermal gradient was relatively high (> 40^{o}C per km).

The geological interpretation of the above observations, in the context of the known Lower Palaeozoic geology, is that pre-deformation metamorphism was largely influenced by the activity of major basement controlled normal faults acting in a tensional environment within a back arc basin. Movement on these structures could have led to the development of a horst and graben topography which in turn would exert significant control on local stratigraphy. Hence significant differences in pre-deformation metamorphism could reflect movement along these major Lower Palaeozoic structures. Crustal thickening during subsequent deformation increased total pressure and produced a variable slaty or fracture cleavage and led to the growth of new amphibole needles within the basic intrusions of the area.

Extension of the area of study into other parts of the Welsh basin and the use of additional, relevant techniques would provide much valuable information on the development of low-grade metamorphic phenomena in this part of the Caledonides. Additional information would also enable further quantification of the parameters, effects and controls of low-grade metamorphism within the Lower Palaeozoic Welsh basin.

APPENDICES

APPENDIX 1 : MACHINE CONDITIONS EMPLOYED IN THE XRF ANALYSES AND XRD MEASUREMENTS.

1 (i) Bulk rock geochemical analyses (XRF).

1(ii) Illite crystallinity and white mica b_0 measurements (XRD).

APPENDIX 1 (i) Bulk rock geochemical analyses (XRF)

103 meta-dolerites were analysed for 10 major elements and 34 were analysed for both 10 major and 11 trace elements using x-ray fluorescence (XRF). The preparation techniques employed in this study were outlined in Section 2.2.

XRF analyses were performed on a Philips PW 1212 fully automatic sequential X-ray spectrometer in the department of Geology at the University of Keele, between January and June, 1982.

A full account of the XRF technique employed at Keele can be found in Bevins (1979) or Haselock (1982). A summary of the operating conditions employed in the course of the XRF analyses is presented in Table A. An indication of the precision of the technique, element detection limits and the coefficient of variation is presented for each element in Table B.

The precision is estimated using the formula:

$$\text{Precision} = \frac{\text{Standard deviation background(s)} + \text{Standard deviation peak}}{\text{Slope factor}}$$

The detection limits are calculated using the formula:

$$\text{Detection limit} = \frac{2 \times \text{Standard deviation background}}{\text{Slope factor}}$$

The coefficient of variation is calculated using the formula:

$$\text{Coefficient of variation} = \frac{\text{precision}}{\text{element mean}} \times 100$$

TABLE. A. XRF operating conditions

Tube	Cr									W	
Element	Na	Mg	Al	Si	P	K	Ca	Ti	Fe	Mn	Cr
Atomic No.	11	12	13	14	15	19	20	22	26	25	24
Peak	kα	kα	kα	kα	kα	kα	kα	kα	kα	kα	kα
Peak (2θ)	55.23	43.70	144.95	109.12	141.01	50.59	113.00	86.05	85.75	95.21	69.23
Background	+1.77	+2.80	-6.45	-4.12	+3.99	+2.91	+2.5	+2.46	+1.75	+1.89	+5.77
Volts (kv)	40	40	60	40	60	40	40	40	60	60	60
Current (mA)	32	32	24	16	24	8	8	8	8	28	28
Collimater	C	C	C	C	C	C	F	F	F	F	F
Counter	F	F	F	F	F	F	F	F	F	F	F
Crystal	TAP	KAP	PE	PE	GE	PE	LiF_{200}	LiF_{200}	LiF_{220}	LiF_{220}	LiF_{200}
Method	ABS	ABS	AR	AR	ABS	AR	AR	AR	AR	ABS	ABS
Time (secs)	40	100	FC	FC	40	FC	FC	FC	FC	40	40
Counts	FT	FT	10^4	10^4	FT	10^4	10^4	10^4	10^4	FT	FT
Cycles	4	3	3	3	3	3	3	3	3	3	4
Disc/P.P.	PP	D	D	D	D	D	D	D	D	D	PP

2 μ window used throughout.

TABLE A. (continued)

Tube	W						Mo			
Element	Ni	Nb	Ba	Ce	Nd	La	Rb	Sr	Y	Zr
Atomic No.	28	41	56	58	60	57	37	38	39	40
Peak	kα	kα	$L\beta_2$	$L\beta_1$	$L\beta l_1 4_1$	$L\alpha_1$	kα	kα	kα	kα
Peak (2θ)	71.24	30.29	115.24	111.68	99.13	138.95	37.85	35.71	33.74	31.95
Background	+2.26	+0.71 -0.39	+1.96 -1.24	+2.42	+1.37	-2.95	+0.75 -1.10	+1.04 -1.01	+0.96 -0.84	+0.95 -0.45
Volts (kv)	60	60	60	60	60	60	60	60	60	60
Current (mA)	28	28	32	32	32	32	28	28	28	28
Collimater	F	F	C	C	C	C	F	F	F	F
Counter	F	Scint	F	F	F	F	Scint	Scint	Scint	Scint
Crystal	LiF_{220}	LiF_{220}	LiF_{220}	LiF_{220}	LiF_{220}	LiF_{220}	LiF_{220}	LiF_{220}	LiF_{220}	LiF_{220}
Method	ABS	ABS	ABS	ABS	ABS	ABS	ABS	ABS	ABS	ABS
Time (secs)	40	40	40	40	40	40	40	40	40	40
Counts	FT	FT	FT	FT	FT	FT	FT	FT	FT	FT
Cycles	4	4	4	4	4	4	4	4	4	4
Disc/P.P.	PP	PP	PP	PP	PP	PP	PP	PP	PP	PP

TABLE B. Precision detection limits and coefficients of variation.

	Precision	Detection limit	Coefficient of variation
Wt%			
SiO_2	0.57	0.084	1.2%
TiO_2	0.04	0.003	2.0%
Al_2O_3	0.25	0.040	1.7%
Fe_2O_3	0.28	0.024	10.2%
FeO	0.17*	-	1.1%
MnO	0.001	0.0005	4.7%
MgO	0.32	0.280	4.1%
CaO	0.11	0.009	1.3%
Na_2O	0.08	0.050	3.1%
K_2O	0.01	0.002	2.0%
P_2O_5	0.012	0.009	4.5%
ppm			
Ba	61	39	49.0%
Ce	16	14	45.0%
Cr	3	1	1.3%
La	7	7	70.0%
Nb	3	2	38.0%
Nd	12	11	65.0%
Ni	5	3	4.5%
Rb	9	2	141.0%
Sr	10	2	3.6%
Y	8	2	28.0%
Zr	20	8	15.1%

* = from duplicate analyses.

APPENDIX 1 (ii) Illite crystallinity and white mica b_0 measurements (XRD)

X-ray diffraction (XRD) determinations of illite crystallinity and white mica b_0 were undertaken on 120 and 50 samples of fine grained meta-sediment respectively. In addition to these measurements, bulk rock compositional scans over the range 3 - 40^{o} 2θ were performed on the 50 samples for which b_0 was calculated.

The illite crystallinity determinations were made on < 2 μ clay fraction, sedimented smear mounts, whilst the b_0 measurements and bulk rock compositional scans were made on packed, crushed sample, cavity mounts. Detailed accounts of the sample preparation procedures for the production of both the smear mounts and packed cavity mounts are outlined in Sections 5.3.2. and 6.4. respectively.

The XRD work was performed on a Siemens diffractometer employing a Crystalloflex 4 generator, type F goniometer and Scintillation counter. The recording equipment consisted of a Kompensograph X - T chart recorder and NIM counting electronics.

The machine conditions employed during the measurement of illite crystallinity, determination of white mica b_0 and bulk rock compositional scans are outlined in Table C. From Table C it can be seen that machine conditions remained unchanged throughout both the bulk rock compositional scans and the determination of white mica b_0. Machine conditions (slits and rate meter setting) were, however, varied slightly during some of the illite crystallinity determinations. It was found that no single rate meter setting was suitable for all illite crystallinity measurements and was varied between 2×10^3 and 4×10^2 depending on the relative intensity of the illite (001) peak. In addition, the divergence slit was changed from $\frac{1}{2}^{o}$ to 1^{o} for the measurement of the Weber crystallinity index.

TABLE C. XRD operating conditions

	Radiation	Volts (kv)	Current (mA)	Divergence Slits	Receiving Slits	Scan Speed (per min)	Chart Speed (per min)	Rate Meter	Time Constant
Illite crystallinity determinations	Cukα (Ni filtered)	35	20	$\frac{1}{2}^{o}$ (Weaver and Kubler) 1^{o} (Weber)	0.1^{o}	$\frac{1}{2}^{o}$ 2θ	2 cm	*$2x10^3$ $1x10^3$ $4x10^2$	4
White mica b_o measurements	Cukα (Ni filtered)	35	20	1^{o}	0.1^{o}	$\frac{1}{4}^{o}$ 2θ	1 cm	$2x10^2$	4
Bulk rock compositional scans	Cukα (Ni filtered)	35	20	1^{o}	0.1^{o}	1^{o} 2θ	1 cm	$2x10^2$	4

* rate meter changed depending on illite (001) peak intensity.

APPENDIX 2 - SAMPLE LOCATIONS

2 (i) Location of meta-dolerites used in the petrographic descriptions, geochemical analyses and electron microprobe determinations. Pages 221 - 224.

2 (ii) Location of sediments used in the illite crystallinity and white mica b_o determinations. Pages 225-226.

2 (iii) Location of vein quartzes used in the fluid inclusion analyses. Page 227.

APPENDIX 2 (i) Location of meta-dolerites used in the petrographic descriptions, geochemical analyses and electron microprobe determinations.

Sample number	Grid Reference	Sample number	Grid Reference
A1	SH 72127162	T5*	SH 72927266
A2	SH 72157163	T6**	SH 72927265
A3	SH 72167163	T7*	SH 72967262
A4	SH 72187164	T8*	SH 72987260
A5	SH 72217165	T9*	SH 73007257
A6	SH 72287165	T10*	SH 73187235
A7	SH 72287169	T11*	SH 73287239
A8	SH 72307173	T12*	SH 73487229
A9	SH 72317175	T13**	SH 73627227
A10	SH 72327178	T14*	SH 73677217
D1	SH 72507204	TY*	SH 73147252
D12	SH 72507200	TZ*	SH 73157238
D13	SH 72517196	1A	SH 74937355
N1**	SH 72577388	2B	SH 74987362
N1A*	SH 72627389	2C	SH 74997362
N1C*	SH 72567385	4A	SH 74697325
N1D*	SH 72557390	4B	SH 74697325
N1E*	SH 72427380	5	SH 74747326
N1F*	SH 72577387	7	SH 74917336
N1G*	SH 72507380	8	SH 74857338
N1H**	SH 72637382	11	SH 74787340
N1J*	SH 72477384	15	SH 75377452
N1K**	SH 72457374	18A	SH 74437347
P1	SH 73837250	18B	SH 74457345
T1*	SH 72927268	18C	SH 74467341
T2*	SH 72927268	20	SH 74077347
T3*	SH 72927267	23	SH 74707295
T4*	SH 72927267	38A	SH 75397403

Sample number	Grid Reference	Sample number	Grid Reference
38B	SH 75407402	73D*	SH 71466562
38C	SH 75437402	73E*	SH 71416566
38D	SH 74467400	85A**	SH 71066287
38E	SH 74497399	85B*	SH 71086291
38F	SH 74557398	85C*	SH 71086298
38G	SH 74587397	85D*	SH 71066300
38H	SH 74627395	85E*	SH 71066302
47A*	SH 70656768	96A*	SH 70886274
47B*	SH 70686766	96B*	SH 70886268
47C*	SH 70706768	96C*	SH 70936268
47D*	SH 70716768	96D*	SH 70966270
47E*	SH 70736769	96E**	SH 70986275
47F*	SH 70756770	102A	SH 72206446
51E	SH 72356818	102B	SH 72286440
51F	SH 72396816	102C	SH 72426432
51G	SH 72456818	102D	SH 72486425
51H	SH 72476819	104A	SH 72596412
66A**	SH 72366745	104B	SH 72586406
66B*	SH 72376735	104C	SH 72606400
66C*	SH 72426723	104D	SH 72656398
66D*	SH 72356711	104E	SH 72686400
66E*	SH 72346704	104F	SH 72856403
66F**	SH 72346698	116	SH 66666095
66G*	SH 72286694	126A	SH 73266402
66H*	SH 72176676	126B	SH 73376399
66I**	SH 72136671	126C	SH 73416388
66K*	SH 73036700	126D	SH 73486381
66L*	SH 73106713	141A*	SH 73075915
73A*	SH 71616546	141B*	SH 73105915
73B*	SH 71566552	141C*	SH 73165914
73C*	SH 71516559	141D*	SH 73325913

Sample number	Grid Reference	Sample number	Grid Reference
141E*	SH 73405912	169R1*	SH 71195522
148A*	SH 72946060	169R2*	SH 71195522
148B*	SH 72976059	169R2**	SH 71195522
148C*	SH 73006058	169S*	SH 71155525
148D*	SH 73026058	169T*	SH 71135526
148E**	SH 73036058	169U*	SH 71125528
148F*	SH 73056058	169V*	SH 71105528
167A*	SH 71555477	169W*	SH 71095531
167B*	SH 71565477	177	SH 72105587
167C*	SH 71585475	179A*	SH 71905548
167D*	SH 71605474	179B*	SH 71965548
167E*	SH 71635472	179C*	SH 72005542
167F*	SH 71665468	185A	SH 72835842
167G*	SH 71705462	185B	SH 72925847
167H*	SH 71715459	197	SH 70915291
167K*	SH 71665468	198A	SH 70745247
168A*	SH 70575434	198B	SH 70705242
168B*	SH 70575437	198C	SH 70845237
168C*	SH 70585439	221	SH 64635800
168D*	SH 70595441	229	SH 69355865
168E**	SH 70595447	249A	SH 63085980
168F**	SH 70595451	249B	SH 63085980
168G*	SH 70585457	265A	SH 64085448
168H*	SH 70555460	265B	SH 64135448
168I*	SH 70555463	265C	SH 64185448
168J**	SH 70535464	265D	SH 64205450
168K*	SH 70495467	265E	SH 64235455
168L**	SH 70465466	265F	SH 64235458
168M*	SH 70445466	265G	SH 64205460
169P*	SH 71245520	265H	SH 64135458
169Q*	SH 71215521	283A	SH 60255575

Sample number	Grid Reference	Sample number	Grid Reference
283C	SH 60205580	307	SH 56256180
283D	SH 60255585	308	SH 56256178
283E	SH 60205593	310	SH 56606118
283F	SH 60205606	320	SH 60225835
283G	SH 60235616	324A	SH 62905635
304	SH 55756245	324B	SH 62915636
305	SH 55906200		

100 = Petrographic description only.
100* = Petrographic description and geochemical analysis.
100** = Petrographic description, geochemical analysis and microprobe determinations.

Note: Sample 35A is a meta-diorite from a vein in the Penmaenmawr intrusion (Grid Reference SH 71627509) for which microprobe data was obtained.

APPENDIX 2(ii) - Location of sediments used in the illite crystallinity and white mica b_0 determinations.

Sample number	Grid Reference	Sample number	Grid Reference
C1	SH 72597185	83C	SH 72006350
E1*	SH 71607204	88A*	SH 78776010
F1	SH 71557188	90	SH 70146353
R1	SH 73827326	97*	SH 71736236
V1	SH 72157508	107*	SH 68056362
V9	SH 72337469	127A*	SH 77106403
W1A*	SH 71817518	127B	SH 77286396
Y1	SH 69827495	128A	SH 77316372
13*	SH 74407323	128B*	SH 77516358
28	SH 76477568	129	SH 77406424
30B*	SH 78097819	137B*	SH 74285930
31*	SH 79007700	139A	SH 75855981
32	SH 78407748	150	SH 73685942
33*	SH 78747722	151A*	SH 77076098
36*	SH 77407182	151B	SH 76846100
37*	SH 76717174	151C	SH 76756103
39	SH 65807250	153*	SH 76006182
40*	SH 65907230	155	SH 77656126
52	SH 72126818	158	SH 77516263
55*	SH 70836960	159	SH 74286035
60	SH 76796769	160	SH 80175995
62	SH 76676762	162B*	SH 70455782
67*	SH 72586682	165	SH 70665820
69C	SH 70526541	167J*	SH 71725452
70	SH 70246615	170	SH 71255584
72*	SH 71766530	173	SH 71585696
75*	SH 74856780	176	SH 72905627
76*	SH 73866919	178	SH 71755553
82*	SH 75816953	186	SH 72235400

Sample number	Grid Reference	Sample number	Grid Reference
201	SH 69665113	272A	SH 55596003
207*	SH 72185212	273*	SH 55715978
209*	SH 55566040	275	SH 55705881
210	SH 55606021	276	SH 55635827
211*	SH 55706002	278*	SH 57515639
212	SH 55816021	279*	SH 58035701
213	SH 55936041	285*	SH 80097251
215	SH 65076012	287	SH 82017549
219	SH 64315800	288*	SH 82007551
223	SH 65055820	290	SH 78326869
227	SH 68015853	292*	SH 79516301
230	SH 69015903	293	SH 81756323
231	SH 70325929	294	SH 82786181
236*	SH 62036431	295*	SH 82656168
237	SH 62136438	297*	SH 81835813
241*	SH 61786351	298	SH 82495740
244*	SH 62416178	301*	SH 80135461
245*	SH 62436170	311*	SH 57456045
248	SH 62776021	314*	SH 59915851
254*	SH 61826615	315*	SH 59935853
255	SH 61906628	316*	SH 60005854
266*	SH 67015623	319*	SH 60515750
267	SH 68035641	326	SH 72137459
270*	SH 54886021	339	SH 63815550
271	SH 55516029		

100 = Illite crystallinity analysis only.

100* = Illite crystallinity and white mica b_0 determination.

APPENDIX 2 (iii) - Location of vein quartzes used in the fluid inclusion analyses

Sample number	Grid Reference	Sample number	Grid Reference
H1	SH 71957229	184	SH 72885864
1B	SH 74937355	225	SH 66105838
6A	SH 74747325	234	SH 66505930
45	SH 71556908	238	SH 62486433
66J	SH 72256709	242	SH 62706279
83B	SH 72006350	256	SH 64185543
103B	SH 72636426	280	SH 59005580
109B	SH 66606300	318	SH 60155810
167J	SH 71675463	322	SH 61255740
169X	SH 71245518		

APPENDIX 3 : RESULTS OF THE GEOCHEMICAL ANALYSES.

4 (i) Major element geochemical analyses of meta-dolerites from the Conwy Valley.

APPENDIX 3 (i) Major element geochemical analyses of meta-dolerites from the Conwy Valley.

Sample Number	N1	N1A	N1C	N1D	N1E	N1F	N1G	N1H
SiO_2	47.71	45.63	47.77	46.31	51.69	48.32	46.71	48.73
TiO_2	1.12	1.47	3.59	1.90	2.46	2.90	4.20	2.08
Al_2O_3	15.28	16.30	13.34	16.47	14.03	12.72	11.91	14.84
Fe_2O_3	0.56	1.20	4.40	2.85	4.06	4.26	6.86	2.39
FeO	9.51	8.59	10.42	7.82	3.81	11.03	9.93	7.78
MnO	0.20	0.18	0.29	0.20	0.19	0.28	0.31	0.21
MgO	6.66	10.59	4.44	7.54	4.81	4.34	4.47	6.88
CaO	10.00	9.20	6.25	9.43	13.55	6.52	7.62	9.38
Na_2O	2.66	1.27	3.57	2.25	4.54	3.57	3.27	3.14
K_2O	0.43	0.61	1.14	0.82	0.33	0.34	0.73	0.50
P_2O_5	0.33	0.21	0.67	0.31	0.38	1.04	0.70	0.35
Loss on Ignition	3.87	4.82	3.11	3.81	1.44	3.58	3.14	3.70
Total	98.33	100.07	98.99	99.71	101.29	98.90	99.85	99.98

Sample Number	N1J	N1K	T1	T2	T3	T4	T5	T6
SiO_2	45.81	44.55	45.78	45.31	45.46	45.90	48.18	43.81
TiO_2	1.94	5.61	2.57	2.64	2.48	2.37	1.91	1.62
Al_2O_3	13.21	9.43	14.97	15.41	15.21	15.04	15.99	15.73
Fe_2O_3	3.00	8.62	2.57	2.08	2.48	2.19	2.04	3.20
FeO	7.83	11.36	8.73	10.79	9.81	9.62	7.46	7.98
MnO	0.19	0.36	0.23	0.23	0.25	0.26	0.17	0.20
MgO	11.64	5.64	8.29	8.04	8.37	8.73	7.30	11.32
CaO	11.78	9.39	8.75	6.82	8.45	10.28	10.53	9.49
Na_2O	1.11	2.68	2.26	2.27	2.19	1.97	2.23	1.27
K_2O	0.25	0.56	0.76	0.97	0.75	0.53	1.34	0.42
P_2O_5	0.21	0.59	0.40	0.40	0.42	0.36	0.28	0.24
Loss on Ignition	4.50	2.82	4.63	4.57	4.69	4.06	3.21	5.05
Total	101.47	101.61	99.94	99.53	100.56	101.31	100.64	100.33

APPENDIX 3 (i) continued...

Sample Number	T7	T8	T9	T10	T11	T12	T13	T14
SiO_2	45.35	45.85	45.05	49.91	44.68	46.06	47.46	46.34
TiO_2	1.58	1.69	1.69	2.60	2.70	2.47	2.96	2.21
Al_2O_3	16.52	16.63	17.39	15.42	15.84	16.06	14.52	15.30
Fe_2O_3	1.80	2.10	1.16	3.07	1.76	2.11	2.19	1.91
FeO	7.89	7.53	8.20	7.41	10.42	9.97	9.68	9.22
MnO	0.20	0.17	0.17	0.18	0.21	0.20	0.24	0.20
MgO	10.01	8.79	8.33	4.31	7.45	7.49	6.95	7.60
CaO	9.74	9.88	10.54	6.90	8.71	8.84	7.46	8.08
Na_2O	1.34	1.62	1.52	4.03	2.45	2.12	2.47	1.76
K_2O	0.71	0.68	0.82	1.29	0.26	0.96	0.92	1.68
P_2O_5	0.30	0.23	0.27	0.52	0.43	0.35	0.48	0.30
Loss on Ignition	4.80	4.36	4.38	2.80	4.89	4.30	4.07	4.41
Total	100.24	99.53	99.52	98.44	99.80	100.93	99.40	99.01

Sample Number	TY	TZ	47A	47B	47C	47D	47E	47F
SiO_2	47.44	47.32	47.40	47.75	46.70	46.01	46.03	49.02
TiO_2	2.21	3.30	2.03	1.89	1.25	2.00	2.12	1.46
Al_2O_3	15.05	13.83	14.65	16.91	16.50	17.59	15.63	15.96
Fe_2O_3	2.24	2.64	2.58	3.07	2.52	2.87	3.44	2.82
FeO	7.98	11.61	8.08	7.23	7.43	7.35	8.34	5.51
MnO	0.20	0.21	0.22	0.19	0.16	0.22	0.20	0.17
MgO	6.86	4.40	7.74	7.35	9.10	6.68	7.89	7.94
CaO	12.76	7.52	10.37	8.70	10.39	9.86	10.46	11.39
Na_2O	2.26	3.52	2.43	3.04	2.04	2.77	2.36	2.52
K_2O	0.13	0.15	0.73	0.49	0.98	1.20	0.26	1.17
P_2O_5	0.28	1.46	0.23	0.26	0.09	0.25	0.27	0.13
Loss on Ignition	3.90	4.29	3.32	3.52	3.71	3.92	3.74	2.85
Total	101.31	100.25	99.78	100.40	100.87	100.72	100.74	100.94

APPENDIX 3 (i) continued...

Sample Number.	66A	66B	66C	66D	66E	66F	66G	66H
SiO_2	44.54	43.18	45.86	47.59	50.14	51.51	48.55	44.29
TiO_2	0.69	0.53	0.78	0.78	1.92	1.06	0.83	0.77
Al_2O_3	12.65	17.25	20.90	19.75	12.96	14.42	18.78	16.15
Fe_2O_3	2.58	2.77	2.05	2.05	1.58	1.54	1.91	3.01
FeO	6.14	4.72	3.39	4.52	7.80	5.56	4.41	5.40
MnO	0.16	0.14	0.12	0.14	0.18	0.15	0.12	0.14
MgO	18.07	15.31	9.03	7.81	7.40	8.59	9.43	14.71
CaO	9.22	9.37	9.82	8.03	9.45	10.97	9.23	9.87
Na_2O	0.27	0.87	2.39	2.99	3.18	3.55	2.42	0.69
K_2O	0.38	0.32	0.58	1.12	0.84	0.24	0.62	0.23
P_2O_5	0.02	0.06	0.10	0.08	0.13	0.09	0.08	0.08
Loss on Ignition	5.69	5.85	5.12	4.93	4.13	2.76	4.25	5.60
Total	100.41	100.37	100.14	99.79	99.71	100.44	100.63	100.94

Sample Number	66I	66K	66L	73A	73B	73C	73D	73E
SiO_2	44.62	45.85	45.87	44.79	44.90	49.96	46.51	44.15
TiO_2	0.71	0.86	1.07	1.75	3.86	2.03	2.06	1.09
Al_2O_3	16.49	17.58	16.44	15.16	12.20	16.00	9.84	14.90
Fe_2O_3	2.81	1.91	2.63	1.66	1.66	2.00	1.73	2.89
FeO	5.41	6.72	6.16	9.53	11.97	7.90	11.64	6.96
MnO	0.15	0.15	0.15	0.21	0.28	0.17	0.29	0.17
MgO	13.86	11.44	11.33	10.78	7.52	5.81	10.23	14.46
CaO	11.12	9.74	9.66	6.96	9.14	8.73	12.26	10.25
Na_2O	0.32	0.99	1.50	2.00	2.42	4.37	1.87	0.60
K_2O	0.30	0.98	0.38	0.12	0.18	0.54	0.16	0.36
P_2O_5	0.08	0.10	0.11	0.16	0.25	0.17	0.17	0.11
Loss on Ignition	5.12	4.95	4.57	5.61	5.18	3.09	3.96	5.25
Total	100.99	101.27	99.87	98.73	99.56	100.77	100.72	101.19

APPENDIX 3 (i) continued....

Sample Number.	85A	85B	85C	85D	85E	96A	96B	96C
SiO_2	45.76	41.11	46.01	49.14	47.04	48.44	47.33	48.14
TiO_2	3.46	3.08	1.97	1.79	1.62	1.78	1.90	2.06
Al_2O_3	12.65	13.36	15.52	14.25	17.58	17.23	15.77	14.92
Fe_2O_3	6.63	11.29	6.56	2.12	3.11	3.16	3.76	3.71
FeO	10.81	5.11	4.80	8.29	6.46	6.39	7.11	7.26
MnO	0.22	0.23	0.20	0.19	0.17	0.18	0.23	0.22
MgO	5.53	4.78	4.49	7.55	6.55	6.54	6.84	6.86
CaO	9.54	18.98	15.79	8.89	10.42	10.15	11.36	10.70
Na_2O	3.34	0.00	2.00	4.00	3.33	3.50	2.94	3.59
K_2O	0.19	0.28	0.12	0.14	0.18	0.60	0.57	0.24
P_2O_5	0.23	0.18	0.25	0.22	0.18	0.22	0.18	0.21
Loss on Ignition	3.40	3.04	3.38	3.32	3.81	2.97	3.03	2.93
Total	101.76	101.44	101.09	99.90	100.45	101.16	101.02	100.84

Sample Number.	96D	96E	141A	141B	141C	141D	141E	148A
SiO_2	48.26	48.21	45.09	44.69	51.42	50.65	45.09	46.43
TiO_2	2.07	1.99	2.84	3.13	2.47	3.00	5.96	1.79
Al_2O_3	14.11	14.41	15.18	14.18	13.90	13.11	11.69	15.67
Fe_2O_3	2.40	2.64	1.83	1.76	4.53	3.95	2.56	1.50
FeO	8.83	8.06	10.99	11.71	8.96	9.55	13.35	8.69
MnO	0.20	0.20	0.22	0.25	0.22	0.22	0.25	0.21
MgO	7.36	6.90	6.62	6.02	3.84	4.10	5.94	8.84
CaO	9.22	10.01	8.11	8.13	4.97	6.47	9.61	8.42
Na_2O	3.49	3.53	2.05	2.53	3.29	3.22	2.58	1.58
K_2O	0.42	0.57	1.00	0.69	0.97	0.90	0.41	0.70
P_2O_5	0.21	0.20	0.46	0.54	1.03	1.21	0.56	0.30
Loss on Ignition	3.32	2.94	4.49	5.83	3.35	3.31	3.78	4.63
Total	99.89	99.66	98.88	99.46	98.95	99.69	101.78	98.76

APPENDIX 3 (i) continued....

Sample Number	148B	148C	148D	148E	148F	167A	167B	167C
SiO_2	45.11	46.58	45.84	47.46	46.91	43.60	47.42	46.51
TiO_2	1.82	1.31	1.42	1.60	1.84	1.64	1.78	1.37
Al_2O_3	15.74	14.42	16.70	17.03	16.92	15.91	15.82	17.21
Fe_2O_3	3.33	3.50	2.09	1.99	2.14	1.48	2.20	2.62
FeO	7.78	4.49	7.91	7.58	7.73	8.51	8.52	6.42
MnO	0.22	0.16	0.18	0.19	0.17	0.22	0.20	0.17
MgO	10.24	7.18	8.83	7.83	7.27	9.78	8.40	8.80
CaO	10.02	19.31	9.67	8.58	9.48	6.28	8.71	11.32
Na_2O	2.33	0.00	1.94	2.65	2.61	1.62	3.15	2.37
K_2O	0.58	0.22	0.51	0.62	0.40	0.19	0.16	0.31
P_2O_5	0.28	0.19	0.22	0.22	0.25	0.17	0.15	0.12
Loss on Ignition	4.46	4.03	4.14	3.83	3.81	9.53	4.17	4.03
Total	101.91	101.39	99.45	99.58	99.53	98.93	100.68	101.25

Sample Number	167D	167E	167F	167G	167H	167K	168A	168B
SiO_2	44.81	48.56	49.13	49.88	48.70	47.70	41.62	48.41
TiO_2	1.49	1.57	1.92	1.88	1.85	2.24	1.76	1.80
Al_2O_3	17.82	16.06	16.17	14.09	19.01	16.10	14.83	15.66
Fe_2O_3	3.19	2.51	1.78	1.26	1.19	2.28	1.29	1.79
FeO	8.36	7.17	8.22	9.53	10.85	8.77	8.81	7.91
MnO	0.22	0.19	0.22	0.23	0.19	0.20	0.30	0.21
MgO	8.47	6.85	6.43	6.94	4.96	7.05	7.97	7.89
CaO	9.63	10.48	6.23	4.70	1.81	6.82	9.49	9.29
Na_2O	2.18	3.73	4.25	1.93	4.14	3.12	1.81	3.65
K_2O	0.22	0.19	0.66	0.16	0.17	0.98	0.20	0.22
P_2O_5	0.15	0.12	0.22	0.16	0.22	0.22	0.20	0.17
Loss on Ignition	4.80	3.33	4.10	7.82	5.23	4.21	10.87	3.84
Total	101.34	100.76	99.33	98.58	98.32	99.69	99.15	100.84

APPENDIX 3 (i) continued...

Sample Number	168C	168D	168E	168F	168G	168H	168I	168J
SiO_2	49.54	48.88	48.31	45.67	46.37	47.79	46.21	44.14
TiO_2	2.27	1.56	1.44	1.47	1.30	1.19	1.15	1.10
Al_2O_3	14.26	15.29	16.35	17.02	18.27	17.64	16.89	15.86
Fe_2O_3	1.58	1.74	2.77	2.51	2.61	2.21	2.60	2.76
FeO	8.21	7.00	5.90	8.18	5.58	5.98	6.78	6.71
MnO	0.22	0.18	0.17	0.19	0.16	0.16	0.18	0.18
MgO	8.55	8.48	8.95	9.31	8.54	9.00	11.27	11.95
CaO	9.76	9.60	10.57	9.72	11.48	10.09	9.76	12.06
Na_2O	3.69	3.58	3.15	2.79	2.85	2.73	1.85	0.34
K_2O	0.32	0.35	0.49	0.17	0.25	0.48	0.35	0.15
P_2O_5	0.23	0.10	0.14	0.12	0.15	0.13	0.12	0.12
Loss on Ignition	3.26	3.58	3.49	4.29	4.06	3.99	4.53	4.90
Total	101.89	100.34	101.73	101.44	101.62	101.39	101.69	100.27

Sample Number	168K	168L	168M	169P	169Q	169R(1)	169R(2)	169S
SiO_2	44.81	46.97	46.32	49.01	48.04	51.98	49.39	48.90
TiO_2	1.15	1.34	1.61	2.36	1.51	1.61	2.96	1.32
Al_2O_3	14.39	14.81	15.61	15.19	15.51	15.78	14.83	15.73
Fe_2O_3	2.06	1.63	1.63	1.53	1.77	8.05	3.57	2.21
FeO	8.08	8.15	8.35	10.69	8.50	3.24	10.04	6.96
MnO	0.18	0.20	0.20	0.26	0.21	0.18	0.29	0.18
MgO	14.35	11.34	9.49	7.93	8.97	1.45	4.19	8.24
CaO	9.36	7.76	8.29	5.21	8.53	13.43	7.12	10.39
Na_2O	0.83	2.58	2.74	3.23	3.13	1.48	3.36	3.53
K_2O	0.20	0.23	0.59	0.15	0.54	0.70	0.76	0.35
P_2O_5	0.12	0.12	0.16	0.24	0.14	0.56	0.54	0.10
Loss on Ignition	5.50	5.28	5.06	4.91	4.06	2.68	3.53	3.66
Total	101.30	100.41	100.05	100.71	100.91	101.14	100.58	101.57

APPENDIX 3 (i) continued....

Sample Number	169T	169U	169V	169W	179A	179B	179C
SiO_2	48.23	48.24	48.01	45.34	48.85	47.73	53.43
TiO_2	1.62	1.56	1.50	2.22	2.66	3.22	2.04
Al_2O_3	16.03	15.96	16.30	14.49	12.54	13.40	13.80
Fe_2O_3	3.62	2.88	2.78	2.29	1.79	1.87	7.58
FeO	6.69	6.91	7.23	10.15	10.51	11.06	6.20
MnO	0.18	0.18	0.19	0.39	0.28	0.27	0.25
MgO	7.59	8.04	7.92	9.99	6.74	6.75	3.41
CaO	10.96	10.89	10.22	7.14	8.38	7.09	3.02
Na_2O	3.14	2.94	2.76	2.40	3.76	3.81	4.41
K_2O	0.25	0.32	0.45	0.12	0.12	0.27	0.43
P_2O_5	0.14	0.14	0.13	0.21	0.35	0.33	0.66
Loss on Ignition	3.44	3.74	3.72	5.43	4.33	4.32	3.71
Total	101.89	101.80	101.21	100.17	100.31	100.12	98.94

APPENDIX 3 (ii) Trace element geochemical analyses of meta-dolerites from the Moel Siabod intrusion.

Sample Number	167A	167B	167C	167D	167E	167F	167G	167H	167K
Ba	83	110	135	47	74	280	49	59	268
Ce	36	30	22	32	29	33	22	28	35
Cr	346	219	254	58	199	186	258	370	370
La	8	6	4	9	8	8	7	7	11
Nb	7	7	5	6	5	9	9	9	8
Nd	18	17	9	15	11	28	22	18	16
Ni	169	132	159	95	64	26	80	136	55
Rb	5	3	6	5	4	14	3	2	14
Sr	275	228	277	366	237	227	176	104	226
Y	21	23	17	22	21	33	24	16	37
Zr	105	94	65	89	90	150	97	127	149

Sample Number	168A	168B	168C	168D	168E	168F	168G	168H	168I
Ba	43	158	171	164	344	76	92	148	166
Ce	28	28	29	9	17	24	20	19	14
Cr	233	234	250	250	330	242	212	248	382
La	8	9	11	4	5	5	4	5	3
Nb	7	6	7	7	8	8	7	6	6
Nd	20	18	18	14	11	16	16	13	20
Ni	76	64	34	121	139	134	144	255	307
Rb	3	5	7	8	9	2	2	7	6
Sr	320	523	270	292	363	307	255	312	401
Y	25	26	36	17	22	21	19	17	17
Zr	120	109	186	53	89	71	82	68	62

APPENDIX 3 (ii) continued...

Sample Number	168J	168K	168L	168M	169P	169Q	169R(1)	169R(2)	169S
Ba	41	49	96	224	67	274	105	120	175
Ce	23	19	17	21	55	25	96	88	21
Cr	495	596	304	242	184	289	16	23	262
La	8	7	8	4	15	8	38	32	3
Nb	6	7	7	7	10	7	15	14	7
Nd	12	15	14	17	17	9	37	35	7
Ni	377	394	221	136	34	65	0	0	74
Rb	2	4	3	17	2	12	9	10	6
Sr	119	152	176	341	108	440	768	224	441
Y	18	16	20	21	37	22	88	82	16
Zr	60	66	79	95	172	79	538	482	59

Sample Number	169T	169U	169V	169W	179A	179B	179C
Ba	43	73	205	19	29	41	231
Ce	20	28	22	47	47	61	108
Cr	283	314	268	157	75	62	18
La	7	7	7	7	14	17	37
Nb	7	8	7	7	10	11	14
Nd	16	15	14	24	22	28	49
Ni	73	74	75	49	10	6	0
Rb	3	5	7	1	2	4	26
Sr	419	235	289	112	127	92	280
Y	21	21	20	29	39	48	80
Zr	92	97	91	132	180	246	435

APPENDIX 4 - SECONDARY MINERAL ASSEMBLAGES FROM THE META-DOLERITES OF NORTHERN SNOWDONIA.

Sample Number	Chlorite	Albitised Plagioclase	Sphene	Epidote	Prehnite	Pump ellyite	Actin olite	Quartz	Calcite	White Mica	Stilp nomelane
A1	✓	✓	(✓)		✓	✓					
A2	✓	✓	(✓)	✓	✓ r	✓		(✓)			
A3	✓	✓	✓	✓	✓	✓	✓	✓		✓	
A4	✓	✓	✓	✓	✓		✓	✓		✓	
A5	✓	(✓)	(✓)	✓	(✓)	✓	✓	(✓)		✓	
A6	✓	(✓)	✓	✓	✓		✓			✓	
A7	✓	✓	✓	✓	✓	✓					
A8	✓	(✓)	(✓)	✓	✓		✓	(✓)		✓	
A9	✓	(✓)	(✓)		✓			✓		✓	
A10	✓	(✓)	✓	✓	✓	(✓)	✓	✓		✓	
D1	✓	✓	✓	✓		✓	✓				
D12	✓	✓	✓	✓		✓	✓				
D13	✓	✓	✓	✓		(✓)	✓				
N1	✓	✓	✓	(✓)	(✓)	✓	(✓)	(✓)			
N1A	✓	(✓)	(✓)	(✓)			✓	✓		✓	
N1C	✓	✓	(✓)	(✓)				(✓)		(✓)	✓
N1D	✓	(✓)	✓	✓			(✓)	(✓)	(✓)	✓	
N1E	(✓)	✓	✓	✓			(✓)				

(✓) = present in trace amount only.

r = reaction occurring.

Sample Number	Chlorite	Albitised Plagioclase	Sphene	Epidote	Prehnite	Pump ellyite	Actin olite	Quartz	Calcite	White Mica	Stilp nomelane
N1F	✓	✓	(✓)	✓			✓	✓	✓	✓	(✓)
N1G	✓	✓	✓	✓						(✓)	✓
N1H	✓	✓	(✓)	✓	✓	✓		(✓)			
N1J	✓	(✓)	✓	✓	✓	(✓)	✓	✓		(✓)	
N1K	✓	✓	✓	✓			(✓)			(✓)	✓
P1	✓	✓	✓			✓		✓	✓		
T1	✓	✓	(✓)		✓	✓	✓				
T2	✓	✓	✓		(✓)	✓	(✓)	(✓)			
T3	✓	✓	✓		✓		(✓)			(✓)	
T4	✓	✓	(✓)		✓	(✓)	(✓)				
T5	✓	✓	✓	✓	✓			✓	(✓)	(✓)	
T6	✓	(✓)*	(✓)	✓	✓	✓	✓	✓		✓	
T7	✓	(✓)*	✓	✓	✓	✓	✓	✓		✓	
T8	✓	(✓)*	(✓)		✓	(✓)	✓	✓		✓	
T9	✓	✓ *	✓		✓	(✓)	✓	(✓)		✓	
T10	✓	✓ *	(✓)		✓	✓				✓	
T11	✓	✓	✓	(✓)	✓	✓			(✓)	(✓)	
T12	✓	✓	✓	(✓)	(✓)			(✓)		✓	

(✓) = present in trace amount only.
r = reaction occurring.
* = relict calcic plagioclase.

Sample Number	Chlorite	Albitised Plagioclase	Sphene	Epidote	Prehnite	Pump ellyite	Actin olite	Quartz	Calcite	White Mica	Stilp nomelane
T13	✓	✓	✓	✓ r		✓					
T14	✓	✓	✓	(✓)	✓	✓ r	✓				
TY	✓	✓	✓	(✓)	✓	✓	(✓)	(✓)	(✓)		
TZ	✓	✓	✓	(✓)			(✓)	(✓)	✓	(✓)	(✓)
1A	✓	✓	(✓)								
2B	✓	(✓)	✓	✓	✓ r	(✓)	✓			(✓)	
2C	✓	✓	✓	(✓)	(✓)		✓	(✓)		✓	
4A	✓		✓				✓	✓	✓	✓	
4B	✓		✓		(✓)		✓	✓	(✓)	(✓)	
5	✓	(✓)	✓				✓			(✓)	
7	✓	✓	✓		✓		✓	(✓)	✓		
8	✓	✓	✓		✓	✓	(✓)			✓	
11	✓	✓	✓		✓	✓	✓	✓		✓	
15	✓	✓ *	✓		(✓)		✓	✓	✓	✓	
18A	✓	✓	(✓)			(✓)	(✓)		✓		
18B	✓	✓	(✓)	✓	✓	✓		(✓)			
18C	✓	✓	✓	✓		✓	(✓)				
20	✓		✓	✓	✓	✓	✓			✓	

(✓) = present in trace amount only.
r = reaction occurring
* = relict calcic plagioclase.

Sample Number	Chlorite	Albitised Plagioclase	Sphene	Epidote	Prehnite	Pump ellyite	Actin olite	Quartz	Calcite	White Mica	Stilp nomelane
23	✓	✓	✓		✓		✓			✓	
38A	✓	(✓)	(✓)		✓	✓	✓	✓		✓	
38B	✓	✓ *	✓		✓	(✓)	✓	✓	✓		
38C	✓	✓ *	✓		✓	(✓)	✓	✓	✓		
38D	✓	✓ *	✓		✓		✓	✓		✓	
38E	✓	(✓)	(✓)		✓	✓	✓	✓		(✓)	
38F	✓	✓ *	✓		(✓)		✓	(✓)	✓	✓	
38G	✓	✓ *	✓		✓	✓	✓	✓		✓	
38H	✓	(✓)*	(✓)		✓	✓ r	✓	✓	(✓)	✓	
47A	✓	✓	✓	✓			✓			(✓)	
47B	✓	✓	✓	✓			✓			✓	
47C	✓	✓	✓	✓			✓	✓		✓	
47D	✓	✓	✓	✓			(✓)		✓	✓	
47E	✓	✓	✓	✓	(✓)r			(✓)		(✓)	
47F	✓	✓	✓	✓			✓	✓		✓	
51E	✓	✓	(✓)	✓				✓	✓		
51F	✓	✓	✓	✓		(✓)	✓	✓			
51G	✓	(✓)	(✓)	✓			✓			✓	

(✓) = present in trace amount only.
r = reaction occurring.
* = relict calcic plagioclase

Sample Number	Chlorite	Albitised Plagioclase	Sphene	Epidote	Prehnite	Pumpellyite	Actinolite	Quartz	Calcite	White Mica	Stilpnomelane
51H	✓	✓	✓	✓			✓				
66A	✓	(✓)*	(✓)	✓		(✓)	✓			✓	
66B	✓	(✓)*	(✓)	✓		✓	✓	✓		✓	
66C	✓	✓	(✓)	✓	✓	(✓)	✓	✓	✓	✓	
66D	✓	✓	(✓)	(✓)			✓	(✓)	✓	✓	
66E	✓	✓ *	✓				✓	✓	✓	✓	
66F	✓	✓	✓	✓	✓	✓	✓			✓	
66G	✓	✓	✓	✓r	✓		✓	✓	✓	✓	
66H	✓	(✓)*		✓	✓r		✓	✓		✓	
66I	✓	(✓)*	(✓)	✓	✓r	✓	✓	✓		✓	
66K	✓	✓	✓	✓			✓	✓	(✓)	✓	
66L	✓	✓	(✓)	✓		✓	✓	✓	(✓)	✓	
73A	✓	✓	✓			(✓)	✓	✓	✓	✓	
73B	✓	✓	✓				✓		✓		
73C	✓	✓	✓	✓					✓	✓	
73D	✓	✓	✓	(✓)			✓	(✓)	✓		
73E	✓	(✓)	(✓)	✓			✓		✓	✓	
85A	✓	✓	✓	✓			✓				✓

(✓) = present in trace amount only.
r = reaction occurring.
* = relict calcic plagioclase.

Sample Number	Chlorite	Albitised Plagioclase	Sphene	Epidote	Prehnite	Pump ellyite	Actin olite	Quartz	Calcite	White Mica	Stilp nomelane
85B	(✓)		✓	✓			(✓)				✓
85C		✓	✓	✓			✓	✓	✓		
85D	✓	✓	✓	✓			✓	(✓)		(✓)	
85E	✓	✓	✓	✓			✓	✓	✓	✓	
96A	✓	✓	✓	✓			✓		✓	✓	
96B	✓	✓	✓	✓						✓	
96C	✓	✓	✓	✓			✓				
96D	✓	✓	✓	✓			✓			✓	
96E	✓	✓	✓	✓			✓			✓	
102A	✓	✓	✓				✓		✓		✓
102B	✓	✓	✓	✓	(✓)		✓			✓	
102C	✓	✓	✓	✓			(✓)				
102D	✓	✓		✓			✓	✓		✓	
104A	✓	✓	✓	✓			✓				
104B	✓	✓	✓	(✓)		(✓)	✓	✓		✓	
104C	✓	(✓)	✓	✓		✓	✓	✓	✓	✓	
104D	✓	✓	(✓)	✓			✓		(✓)	✓	
104E	✓	(✓)	(✓)	✓			✓	✓		✓	

(✓) = present in trace amount only.

Sample Number	Chlorite	Albitised Plagioclase	Sphene	Epidote	Prehnite	Pump ellyite	Actin olite	Quartz	Calcite	White Mica	Stilp nomelane
104F	✓	(✓)	(✓)	✓			✓			✓	
116	✓	✓	(✓)	✓			✓			✓	
126A	✓	✓	✓	✓		(✓)	(✓)			✓	
126B	✓	✓	✓	✓			✓	✓	✓	✓	
126C	✓	(✓)	✓	✓			✓			✓	
126D	✓		✓	(✓)			✓	✓	✓	✓	
141A	✓	✓	✓	(✓)			✓	(✓)	✓	(✓)	
141B	✓	✓	✓	(✓)			✓		✓		
141C	✓	✓	✓	(✓)	(✓)		✓			✓	✓
141D	✓	✓	✓				✓				✓
141E	✓	✓	✓	(✓)			✓		✓		(✓)
148A	✓	✓	✓	✓			✓	✓	✓		
148B	✓	(✓)	(✓)	✓		(✓)	✓	✓		✓	
148C	✓	(✓)	✓	✓		(✓)	✓	✓	✓	✓	
148D	✓	✓	✓	✓		✓r	✓	(✓)	(✓)	✓	
148E	✓	✓	✓	✓			✓			✓	
148F	✓	✓	✓	✓			✓				
167A	✓	✓	(✓)				(✓)	✓	✓		

(✓) = present in trace amount only.
r = reaction occurring.

Sample Number	Chlorite	Albitised Plagioclase	Sphene	Epidote	Prehnite	Pump ellyite	Actin olite	Quartz	Calcite	White Mica	Stilp nomelane
167B	✓	✓	✓	✓			✓		✓	✓	
167C	✓	✓	(✓)	✓		✓	✓				
167D	✓	✓	✓	✓			✓			✓	
167E	✓	✓	✓	✓			✓				
167F	✓	✓	✓	✓			(✓)		(✓)	✓	
167G	✓	✓	✓					✓	✓		
167H	✓	✓	✓					✓			
167K	✓	✓	✓	✓			(✓)			✓	
168A	✓	✓	✓					(✓)		(✓)	
168B	✓	✓	✓	✓r			✓		✓	✓	
168C	✓	✓	✓	✓			✓			✓	
168D	✓	✓	(✓)	✓		✓	✓			✓	
168E	✓	✓	✓	✓		✓	(✓)			✓	
168F	✓	✓	✓	✓	(✓)	✓	✓			(✓)	
168G	✓	✓	(✓)	✓	(✓)	✓	✓	(✓)		✓	
168H	✓	✓	(✓)	✓			✓	✓		✓	
168I	✓	✓	(✓)	✓			✓	✓		(✓)	
168J	✓		(✓)	✓			✓	✓		✓	

(✓) = present in trace amount only.
r = reaction occurring.

Sample Number	Chlorite	Albitised Plagioclase	Sphene	Epidote	Prehnite	Pump ellyite	Actin olite	Quartz	Calcite	White Mica	Stilp nomelane
168K	✓	(✓)	(✓)	✓			✓	✓		✓	
168L	✓	✓	(✓)	✓		✓	✓				
168M	✓	✓	✓	✓		(✓)	✓	✓	✓	✓	
169P	✓	✓	✓				✓	✓		(✓)	
169Q	✓	✓	✓	✓			✓	(✓)		✓	
169R1	(✓)	(✓)	✓	✓				✓	✓		✓
169R2	✓	✓	✓	✓			✓	(✓)			✓
169R3	✓	✓	✓	✓			✓	✓			✓
169S	✓	✓	✓	✓		✓	✓		✓	✓	
169T	✓	✓	✓	✓			✓				
169U	✓	✓	✓	✓			✓			✓	
169V	✓	✓	(✓)	✓			✓	✓			
169W	✓	✓	(✓)	✓			✓		✓		
177	✓	✓	✓	✓							
179A	✓	✓	✓	✓			✓				
179B	✓	✓	✓	✓			✓				
179C	✓	✓	✓	✓			✓	✓			✓
185A	✓	✓	✓	✓			✓			(✓)	

(✓) = present in trace amount only.

Sample Number	Chlorite	Albitised Plagioclase	Sphene	Epidote	Prehnite	Pump ellyite	Actin olite	Quartz	Calcite	White Mica	Stilp nomelane
185B	✓	✓	✓	✓		(✓)	✓			(✓)	
197	✓	✓	✓	✓		(✓)	✓		✓	✓	
198A	✓	✓	✓	✓			✓		✓	✓	
198B	✓	✓	✓	✓		✓	✓			(✓)	
198C	✓	✓	✓	✓		✓	✓	✓	✓	✓	
221	✓	✓	✓	✓			(✓)	✓	✓	✓	
229	✓	✓	✓	✓			✓				
249A	✓	✓	✓	✓			✓			✓	
249B	✓	✓	✓	✓			✓				
265A	✓	✓	✓	✓			✓			(✓)	(✓)
265B	(✓)	✓	✓	(✓)			✓	(✓)	✓	(✓)	(✓)
265C	✓	✓	✓	✓			✓	✓		(✓)	(✓)
265D	✓	✓	✓	(✓)			(✓)	✓		✓	✓
265E	✓	✓	✓				(✓)	✓			✓
265F	✓	✓	(✓)							✓	✓
265G	✓	✓	✓	✓			✓	✓	✓		
265H	✓	✓	✓	(✓)				✓		✓	✓
283A	✓	✓	✓	(✓)			✓			✓	(✓)

(✓) = present in trace amount only.

Sample Number	Chlorite	Albitised Plagioclase	Sphene	Epidote	Prehnite	Pumpellyite	Actinolite	Quartz	Calcite	White Mica	Stilpnomelane
283C	✓	✓	✓	✓			✓		✓	✓	
283D	✓	✓	✓	✓			✓		✓	(✓)	
283E	✓	✓	✓	✓			✓	✓	✓	(✓)	
283F	✓	✓	✓	✓			✓		✓	✓	
283G	✓	✓	✓	(✓)			✓	✓	✓	✓	
304	✓	✓	(✓)	✓			✓	✓	✓	✓	
305	✓	✓	(✓)	✓			✓		✓	✓	
307	✓	✓	(✓)	(✓)			(✓)		✓	✓	
308	✓	✓	(✓)	(✓)			✓	✓		✓	
310	✓	✓	✓	✓			✓		(✓)		
320	✓	✓	✓	✓			✓		(✓)		
324A	✓	✓	✓	✓		(✓)	✓			(✓)	
324B	✓	✓	✓	✓			✓	✓		(✓)	

(✓) = present in trace amount only.

APPENDIX 5 : ELECTRON MICROPROBE ANALYSES OF MINERAL CHEMISTRY

Index to phase chemistry analyses

WHITE MICA

Samples analysed - 66A, 66F, 66I, 96E, 148E, 168F.

Page number - 269-270.

PLAGIOCLASE FELDSPAR

Samples analysed - N1, N1K, T13, 66F, 66I, 85A, 96E, 148E, 168E, 168F, 169R3.

Page number - 271-272.

ALKALI FELDSPAR

Samples analysed - 168E.

Page number - 272.

CLINOPYROXENE ANALYSES (1)

Sample		N1H	N1H	T6	T6	66A	66A	66I	66I
SiO_2		50.57	49.93	50.05	49.87	49.30	49.88	50.71	48.75
TiO_2		1.31	1.64	1.48	2.00	2.88	2.27	1.20	2.62
Al_2O_3		2.75	3.55	2.64	3.41	4.34	3.54	3.91	3.90
FeO*		7.85	8.23	8.76	8.13	6.62	6.32	5.91	7.31
MnO		0.13	0.12	0.19	0.17	n.d.	0.29	0.29	n.d.
MgO		14.12	13.72	14.02	14.28	15.01	15.06	15.83	14.68
CaO		21.81	21.74	21.42	21.78	21.85	21.79	22.01	21.43
Na_2O		n.d.	n.d.	n.d.	n.d.	0.71	0.51	n.d.	n.d.
K_2O		n.d.	n.d.	n.d.	n.d.	n.d.	n.d.	n.d.	n.d.
Total		98.54	98.93	98.56	99.64	100.71	99.66	99.86	98.69

Recalculation on the basis of 6 oxygens

Si	z	1.90	1.88	1.90	1.86	1.82	1.86	1.87	1.83
Al^{iv}	z	0.10	0.12	0.10	0.14	0.18	0.14	0.13	0.17
Σ		2.00	2.00	2.00	2.00	2.00	2.00	2.00	2.00
Al^{vi}	y	0.02	0.04	0.02	0.01	0.01	0.02	0.04	0.00
Fe	y	0.25	0.26	0.28	0.25	0.20	0.20	0.18	0.23
Mg	y	0.79	0.77	0.79	0.80	0.83	0.84	0.87	0.82
Mn	y	0.00	0.00	0.01	0.01	-	0.01	0.01	-
Ti	y	0.04	0.05	0.04	0.06	0.08	0.06	0.03	0.07
Σ		1.10	1.12	1.14	1.13	1.12	1.11	1.13	1.12
Ca	x	0.88	0.88	0.87	0.87	0.86	0.87	0.87	0.86
Na	x	-	-	-	-	0.05	0.04	-	-
K	x	-	-	-	-	-	-	-	-
Σ		0.88	0.88	0.87	0.87	0.91	0.91	0.87	0.86
Total		3.98	4.00	4.01	4.00	4.03	4.02	4.00	3.98

* = Total iron as FeO

n.d. = Not detected

CLINOPYROXENE ANALYSES (2)

Sample	96E	96E	148E	148E	168E	168E	168J	168J
SiO_2	51.89	49.90	50.94	50.54	52.05	50.66	49.10	51.33
TiO_2	1.10	1.71	1.16	1.32	0.77	1.24	2.07	0.92
Al_2O_3	2.69	3.74	2.45	3.17	1.81	3.33	3.36	2.02
FeO*	8.06	9.75	9.64	9.65	6.51	6.82	7.92	6.18
MnO	0.40	0.30	0.31	0.45	0.40	0.44	0.26	0.48
MgO	15.01	14.19	14.26	14.78	15.60	14.99	14.48	16.02
CaO	21.20	20.18	21.31	20.79	21.24	21.67	21.22	21.75
Na_2O	0.60	n.d.	n.d.	0.61	n.d.	n.d.	n.d.	n.d.
K_2O	n.d.	n.d.	n.d.	n.d.	n.d.	n.d.	n.d.	n.d.
Total	100.95	99.77	100.07	101.31	98.38	99.15	98.41	98.70

Recalculation on the basis of 6 oxygens

Si	z	1.91	1.87	1.90	1.87	1.95	1.89	1.86	1.92
Al^{iv}	z	0.09	0.13	0.10	0.13	0.05	0.11	0.14	0.08
Σ		2.00	2.00	2.00	2.00	2.00	2.00	2.00	2.00
Al^{vi}	y	0.03	0.04	0.01	0.01	0.03	0.04	0.01	0.01
Fe	y	0.25	0.31	0.30	0.30	0.21	0.21	0.25	0.19
Mg	y	0.82	0.79	0.79	0.82	0.87	0.83	0.82	0.89
Mn	y	0.01	0.01	0.01	0.01	0.01	0.01	0.01	0.01
Ti	y	0.03	0.05	0.03	0.04	0.02	0.04	0.06	0.03
Σ		1.14	1.20	1.14	1.18	1.14	1.13	1.15	1.13
Ca	x	0.84	0.81	0.85	0.83	0.85	0.87	0.86	0.87
Na	x	0.04	-	-	0.04	-	-	-	-
K	x	-	-	-	-	-	-	-	-
Σ		0.88	0.81	0.85	0.87	0.85	0.87	0.86	0.87
Total		4.02	4.01	3.99	4.05	3.99	4.00	4.01	4.00

* = Total iron as FeO

n.d. = Not detected.

PUMPELLYITE ANALYSES (1)

Sample	35A	35A	N1	N1	N1H	N1H	T13	T13
SiO_2	36.83	37.61	36.58	36.89	36.38	36.79	36.96	36.53
TiO_2	n.d.	n.d.	n.d.	n.d.	n.d.	n.d.	n.d.	n.d.
Al_2O_3	20.09	21.07	24.25	23.83	22.34	23.88	23.38	23.64
FeO*	11.88	9.54	6.87	7.78	9.22	7.95	7.23	6.49
MnO	n.d.	n.d.	n.d.	0.12	0.16	n.d.	0.17	n.d.
MgO	1.49	2.13	1.17	1.16	1.31	1.08	1.68	1.88
CaO	22.78	22.63	22.76	22.76	22.70	22.94	22.62	22.44
Na_2O	n.d.	n.d.	n.d.	n.d.	n.d.	n.d.	n.d.	n.d.
K_2O	n.d.	n.d.	n.d.	n.d.	n.d.	n.d.	n.d.	n.d.
Total	93.07	92.98	91.63	92.54	91.95	92.64	91.87	90.98

Recalculation on the basis of 16 Cations

Si	z	6.07	6.15	6.03	6.04	6.02	6.02	6.09	6.05
Al^Z	z	-	-	-	-	-	-	-	-
Σ		6.07	6.15	6.03	6.04	6.02	6.02	6.09	6.05
Al^y	y	3.90	4.00	4.00	4.00	4.00	4.00	4.00	4.00
Fe^{3+}	y	0.10	-	-	-	-	-	-	-
Σ		4.00	4.00	4.00	4.00	4.00	4.00	4.00	4.00
Al^x	x	-	0.06	0.71	0.60	0.36	0.61	0.53	0.61
Fe	x	1.54	1.30	0.95	1.07	1.28	1.09	0.99	0.90
Mg	x	0.37	0.52	0.29	0.28	0.32	0.26	0.41	0.46
Mn	x	-	-	-	0.02	0.02	-	0.02	-
Σ		1.91	1.88	1.95	1.97	1.98	1.96	1.95	1.97
Ca	w	4.02	3.96	4.02	3.99	4.03	4.02	3.98	3.98

* = Total iron as FeO

n.d. = Not detected.

PUMPELLYITE ANALYSES (2)

Sample	T13	66A	66A	66F	66F	66F	66I	66I
SiO_2	36.62	35.86	36.47	37.57	38.28	38.29	36.84	37.13
TiO_2	n.d.	n.d.	n.d.	n.d.	n.d.	n.d.	n.d.	n.d.
Al_2O_3	24.10	24.68	24.88	23.75	24.84	23.19	26.05	25.15
FeO*	6.68	4.93	6.24	7.33	5.46	6.50	6.60	6.40
MnO	n.d.	n.d.	n.d.	n.d.	n.d.	n.d.	0.38	n.d.
MgO	1.47	3.35	3.07	2.74	2.58	2.68	1.09	1.62
CaO	22.68	21.82	21.48	23.06	23.40	23.01	23.50	23.48
Na_2O	n.d.	n.d.	n.d.	n.d.	n.d.	n.d.	n.d.	n.d.
K_2O	n.d.	n.d.	n.d.	n.d.	n.d.	n.d.	n.d.	n.d.
Total	91.55	90.64	92.14	94.45	94.56	93.67	94.46	93.78

Recalculation on the basis of 16 Cations

Si	z	6.03	5.89	5.92	5.98	6.06	6.15	6.01	5.96
Al^Z	z	-	0.11	0.08	0.02	-	-	-	0.04
Σ		6.03	6.00	6.00	6.00	6.06	6.15	6.01	6.00
Al^y	y	4.00	4.00	4.00	4.00	4.00	4.00	4.00	4.00
Fe^{3+}	y	-	-	-	-	-	-	-	-
Σ		4.00	4.00	4.00	4.00	4.00	4.00	4.00	4.00
Al^x	x	0.68	0.67	0.68	0.44	0.64	0.39	0.84	0.72
Fe	x	0.92	0.68	0.85	0.98	0.72	0.87	0.65	0.86
Mg	x	0.36	0.82	0.74	0.65	0.61	0.64	0.43	0.39
Mn	x	-	-	-	-	-	-	-	-
Σ		1.96	2.07	2.27	2.07	1.97	1.90	1.82	1.97
Ca	w	4.00	3.84	3.73	3.94	3.97	3.95	4.08	4.04

* = Total iron as FeO

n.d. = Not detected.

PUMPELLYITE ANALYSES (3)

Sample	148E	148E	148E	168E	168E	168F	168F	168F
SiO_2	37.05	36.36	36.13	38.62	37.53	37.38	37.62	36.38
TiO_2	n.d.	n.d.	n.d.	n.d.	n.d.	n.d.	n.d.	n.d.
Al_2O_3	23.56	21.91	22.85	25.27	24.65	24.77	25.14	23.85
FeO*	7.28	9.44	8.33	5.75	6.01	6.23	4.57	4.41
MnO	n.d.	n.d.	n.d.	0.15	n.d.	n.d.	n.d.	n.d.
MgO	1.95	2.14	1.91	1.64	1.79	1.57	3.06	2.90
CaO	23.14	22.93	23.01	23.20	23.39	23.00	23.05	23.09
Na_2O	n.d.	n.d.	n.d.	n.d.	n.d.	n.d.	n.d.	n.d.
K_2O	n.d.	n.d.	n.d.	n.d.	n.d.	n.d.	n.d.	n.d.
Total	92.98	92.78	92.23	94.63	93.37	92.95	93.44	90.63

Recalculation on the basis of 16 Cations

Si	z	6.01	5.95	5.93	6.15	6.04	6.05	6.00	5.99
Al^Z	z	-	0.05	0.07	-	-	-	-	0.01
Σ		6.01	6.00	6.00	6.15	6.04	6.05	6.00	6.00
Al^y	y	4.00	4.00	4.00	4.00	4.00	4.00	4.00	4.00
Fe^{3+}	y	-	-	-	-	-	-	-	-
Σ		4.00	4.00	4.00	4.00	4.00	4.00	4.00	4.00
Al^x	x	0.51	0.17	0.35	0.74	0.68	0.73	0.72	0.62
Fe	x	0.99	1.29	1.14	0.77	0.81	0.84	0.61	0.61
Mg	x	0.47	0.52	0.47	0.39	0.43	0.38	0.73	0.71
Mn	x	-	-	-	0.02	-	-	-	-
Σ		1.97	1.98	1.96	1.92	1.92	1.95	2.06	1.94
Ca	w	4.02	4.02	4.04	3.96	4.04	3.99	3.94	4.07

* = Total iron as FeO

n.d. = Not detected.

PREHNITE ANALYSES (1)

Sample	35A	35A	N1	N1	N1H	N1H	T6	T6
SiO_2	43.56	45.05	43.01	42.80	43.44	44.20	43.59	43.87
TiO_2	n.d.	n.d.	n.d.	n.d.	n.d.	n.d.	n.d.	n.d.
Al_2O_3	23.20	24.61	22.35	23.69	23.11	24.04	24.12	23.96
Fe_2O_3*	1.63	0.20	2.55	0.60	1.82	0.36	0.27	0.54
MnO	n.d.	n.d.	n.d.	n.d.	n.d.	n.d.	n.d.	n.d.
MgO	n.d.	n.d.	n.d.	n.d.	n.d.	n.d.	n.d.	n.d.
CaO	27.45	27.53	27.20	26.66	27.08	26.37	27.09	26.76
Na_2O	n.d.	n.d.	n.d.	n.d.	n.d.	n.d.	n.d.	n.d.
K_2O	n.d.	n.d.	n.d.	n.d.	n.d.	n.d.	n.d.	n.d.
Total	95.84	97.39	95.11	93.75	95.45	95.36	95.07	95.13

Recalculation on the basis of 22 oxygens

Si	6.01	6.07	6.01	6.01	6.02	6.07	6.02	6.05
Al	-	-	-	-	-	-	-	-
Σ	6.01	6.07	6.01	6.01	6.02	6.07	6.02	6.05
Al	3.77	3.91	3.68	3.92	3.77	3.89	3.93	3.90
Fe^{3+}	0.17	0.02	0.27	0.06	0.19	0.04	0.03	0.06
Mg	-	-	-	-	-	0.08	-	-
Ca	4.06	3.97	4.07	4.01	4.02	3.88	4.01	3.96
Σ	8.00	7.90	8.02	7.99	7.98	7.89	7.97	7.92

* = Total iron as Fe_2O_3

n.d. = Not detected

PREHNITE ANALYSES (2)

Sample	T13	T13	66F	66F	66I	66I	168F	168F
SiO_2	42.45	42.88	42.76	42.91	43.49	43.91	44.04	43.70
TiO_2	n.d.	n.d.	n.d.	n.d.	n.d.	n.d.	n.d.	n.d.
Al_2O_3	19.22	19.44	23.50	24.31	24.42	24.46	23.12	22.97
Fe_2O_3*	7.01	6.33	2.12	2.17	n.d.	n.d.	1.80	1.82
MnO	n.d.	n.d.	n.d.	n.d.	n.d.	n.d.	n.d.	n.d.
MgO	n.d.	n.d.	0.34	0.36	n.d.	n.d.	n.d.	n.d.
CaO	25.35	25.82	26.57	26.70	27.41	27.87	26.84	27.00
Na_2O	n.d.	n.d.	n.d.	n.d.	n.d.	n.d.	n.d.	n.d.
K_2O	n.d.	n.d.	n.d.	n.d.	n.d.	n.d.	n.d.	n.d.
Total	94.03	94.47	95.29	96.45	95.32	96.24	95.80	95.49

Recalculation on the basis of 22 oxygens

Si	6.07	6.09	5.94	5.88	6.00	6.00	6.06	6.05
Al	-	-	0.06	0.12	-	-	-	-
Σ	6.07	6.09	6.00	6.00	6.00	6.00	6.06	6.05
Al	3.24	3.25	3.79	3.81	3.97	3.94	3.75	3.75
Fe^{3+}	0.75	0.68	0.22	0.22	-	-	0.19	0.19
Mg	-	-	0.07	0.07	-	-	-	-
Ca	3.88	3.93	3.95	3.92	4.05	4.08	3.96	4.00
Σ	7.87	7.86	8.03	8.02	8.02	8.02	7.90	7.94

* = Total iron as Fe_2O_3

n.d. = Not detected

EPIDOTE ANALYSES (1)

Sample		35A	35A	N1	N1H	N1H	N1H	N1K	T6
					r		c		
SiO_2		38.03	39.35	37.74	38.29	38.35	38.05	37.50	38.84
TiO_2		n.d.	n.d.	n.d.	n.d.	n.d.	0.14	n.d.	n.d.
Al_2O_3		22.28	26.45	22.65	24.45	23.64	23.54	21.64	26.74
Fe_2O_3*		15.47	10.09	13.63	12.03	13.43	13.51	15.20	9.17
MnO		0.15	0.21	n.d.	n.d.	n.d.	0.14	0.13	n.d.
MgO		n.d.	n.d.	n.d.	n.d.	n.d.	n.d.	n.d.	n.d.
CaO		22.88	24.38	23.57	23.95	23.57	23.56	22.87	23.67
Na_2O		n.d.	n.d.	n.d.	n.d.	n.d.	n.d.	n.d.	n.d.
K_2O		n.d.	n.d.	n.d.	n.d.	n.d.	n.d.	n.d.	n.d.
Total		98.81	100.48	97.59	98.72	98.99	98.44	97.34	98.42

Recalculation on the basis of 12.5 oxygens

Si	z	3.02	3.01	3.02	3.01	3.02	3.00	3.02	3.02
Σ		3.02	3.01	3.02	3.01	3.02	3.00	3.02	3.02
Ti	y	-	-	-	-	-	0.00	-	-
Al	y	2.08	2.39	2.14	2.27	2.19	2.19	2.06	2.45
Fe^{3+}	y	0.92	0.58	0.82	0.71	0.79	0.80	0.92	0.54
Σ		3.00	2.97	2.96	2.98	2.98	2.99	2.98	2.99
Mn	w	0.01	0.01	-	-	-	0.00	0.00	-
Ca	w	1.94	2.00	2.02	2.02	1.99	1.99	1.98	1.97
Σ		1.95	2.01	2.02	2.02	1.99	1.99	1.98	1.97
Total		7.97	7.99	8.00	8.01	7.99	7.98	7.98	7.98

* = Total iron as Fe_2O_3

n.d. = Not detected

r——c = Rim to core of zoned epidote

EPIDOTE ANALYSES (2)

Sample	T13	T13	66A	66F	66F	66I	85A	96E
SiO_2	36.30	37.15	38.70	39.28	39.50	39.12	37.54	38.60
TiO_2	n.d.	n.d.	n.d.	n.d.	n.d.	n.d.	n.d.	n.d.
Al_2O_3	19.07	20.11	30.15	29.28	28.05	30.28	21.66	23.72
Fe_2O_3*	17.72	16.29	4.02	5.73	7.44	4.89	15.02	13.64
MnO	n.d.	n.d.	n.d.	n.d.	n.d.	n.d.	n.d.	0.39
MgO	n.d.	n.d.	n.d.	n.d.	n.d.	n.d.	n.d.	n.d.
CaO	22.76	22.34	25.00	24.78	24.15	24.64	23.98	23.22
Na_2O	n.d.	n.d.	n.d.	n.d.	n.d.	n.d.	n.d.	n.d.
K_2O	n.d.	n.d.	n.d.	n.d.	n.d.	n.d.	n.d.	n.d.
Total	95.85	95.89	97.87	99.07	99.14	98.93	98.20	99.57

Recalculation on the basis of 12.5 oxygens

Si	z	3.01	3.05	2.99	3.01	3.03	2.99	3.01	3.02
Σ		3.01	3.05	2.99	3.01	3.03	2.99	3.01	3.02
Ti	y	-	-	-	-	-	-	-	-
Al	y	1.86	1.95	2.74	2.64	2.54	2.73	2.05	2.19
Fe^{3+}	y	1.11	1.01	0.23	0.33	0.43	0.28	0.91	0.80
Σ		2.97	2.96	2.97	2.97	2.97	3.01	2.96	2.99
Mn	w	-	-	-	-	-	-	-	0.03
Ca	w	2.02	1.97	2.07	2.03	1.99	2.02	2.06	1.95
Σ		2.02	1.97	2.07	2.03	1.99	2.02	2.06	1.98
Total		8.00	7.89	8.03	8.01	7.99	8.02	8.03	7.99

* = Total iron as Fe_2O_3

n.d. = Not detected

EPIDOTE ANALYSES (3)

Sample	148E	148E	148E	148E	168E	168E	168E	168L
					r		c	
SiO_2	35.82	37.48	39.02	38.87	38.61	39.07	38.61	38.19
TiO_2	n.d.	n.d.	n.d.	n.d.	n.d.	n.d.	n.d.	n.d.
Al_2O_3	21.13	22.22	28.57	28.98	28.25	27.54	26.14	28.32
Fe_2O_3*	14.63	14.75	6.94	6.04	6.67	8.25	9.46	6.68
MnO	n.d.	n.d.	n.d.	n.d.	n.d.	n.d.	n.d.	n.d.
MgO	n.d.	n.d.	n.d.	n.d.	n.d.	n.d.	n.d.	n.d.
CaO	22.37	22.48	24.38	24.60	24.20	24.07	24.28	23.57
Na_2O	n.d.	n.d.	n.d.	n.d.	n.d.	n.d.	n.d.	n.d.
K_2O	n.d.	n.d.	n.d.	n.d.	n.d.	n.d.	n.d.	n.d.
Total	93.95	96.93	98.91	98.49	97.73	98.93	98.46	96.76

Recalculation on the basis of 12.5 oxygens

Si	z	3.00	3.02	3.00	3.00	3.00	3.02	3.01	3.01
Σ		3.00	3.02	3.00	3.00	3.00	3.02	3.01	3.01
Ti	y	-	-	-	-	-	-	-	-
Al		2.08	2.11	2.59	2.63	2.59	2.51	2.41	2.63
Fe^{3+}		0.92	0.90	0.40	0.35	0.39	0.48	0.56	0.34
Σ		3.00	3.01	2.99	2.98	2.98	2.99	2.97	2.97
Mn	w	-	-	-	-	-	-	-	-
Ca		2.00	1.94	2.01	2.03	2.02	1.99	2.03	1.99
Σ		2.00	1.94	2.01	2.03	2.02	1.99	2.03	1.99
Total		8.00	7.97	8.00	8.01	8.00	8.00	8.01	7.97

* = Total iron as Fe_2O_3

n.d. = Not detected

r____c = Rim to core of zoned epidote

EPIDOTE ANALYSES (4)

Sample	168F r	168F	168F	168F	168F c	168J r	168J	168J
SiO_2	39.37	38.59	38.56	38.59	37.98	38.95	39.12	38.75
TiO_2	n.d.	n.d.	n.d.	n.d.	n.d.	n.d.	n.d.	n.d.
Al_2O_3	28.41	26.78	23.73	22.86	22.20	29.45	29.05	28.13
Fe_2O_3*	7.26	8.80	12.37	14.46	14.24	5.52	5.67	7.24
MnO	n.d.	n.d.	n.d.	n.d.	n.d.	n.d.	n.d.	n.d.
MgO	n.d.	n.d.	n.d.	n.d.	n.d.	n.d.	n.d.	n.d.
CaO	24.29	23.83	23.84	23.87	23.42	24.33	24.47	24.45
Na_2O	n.d.	n.d.	n.d.	n.d.	n.d.	n.d.	n.d.	n.d.
K_2O	n.d.	n.d.	n.d.	n.d.	n.d.	n.d.	n.d.	n.d.
Total	99.33	98.00	98.50	99.78	97.84	98.25	98.31	98.57

Recalculation on the basis of 12.5 oxygens

Si	z(3.02	3.01	3.04	3.02	3.02	3.00	3.01	3.00
Σ	3.02	3.01	3.04	3.02	3.02	3.00	3.01	3.00
Ti	(-	-	-	-	-	-	-	-
Al	y(2.57	2.47	2.21	2.11	2.08	2.67	2.64	2.56
Fe^{3+}	(0.42	0.52	0.73	0.85	0.85	0.32	0.33	0.42
Σ	2.99	2.99	2.94	2.96	2.93	2.99	2.97	2.98
Mn	(-	-	-	-	-	-	-	-
Ca	w(1.99	1.99	2.01	2.00	2.07	2.01	2.02	2.03
Σ	1.99	1.99	2.01	2.00	2.07	2.01	2.02	2.03
Total	8.00	7.99	7.99	7.98	8.02	8.00	8.00	8.01

* = Total iron as Fe_2O_3

n.d. = Not detected

r_____c = Rim to core of zoned epidote.

EPIDOTE ANALYSES (5)

Sample	168J	168J	168J	168J	168J	168J	168J	169R[3]
	←———	c	r	———	———	———	———	c
SiO_2	39.05	38.97	36.00	37.43	38.46	38.62	38.87	38.10
TiO_2	n.d.	n.d.	n.d.	0.12	0.13	n.d.	n.d.	0.18
Al_2O_3	27.78	27.46	28.04	28.24	28.89	27.48	27.62	22.25
Fe_2O_3*	7.73	7.90	5.08	5.65	5.57	7.89	8.06	15.27
MnO	n.d.	n.d.	n.d.	n.d.	n.d.	n.d.	n.d.	n.d.
MgO	n.d.	n.d.	n.d.	n.d.	n.d.	n.d.	n.d.	n.d.
CaO	24.13	24.57	23.63	23.72	24.31	24.00	24.31	23.45
Na_2O	n.d.	n.d.	n.d.	n.d.	n.d.	n.d.	n.d.	n.d.
K_2O	n.d.	n.d.	n.d.	n.d.	n.d.	n.d.	n.d.	n.d.
Total	98.69	98.90	92.75	95.15	97.36	97.99	98.86	99.25

Recalculation on the basis of 12.5 oxygens

Si	z	3.02	3.01	2.95	2.98	2.99	3.01	3.00	3.01
Σ		3.02	3.01	2.95	2.98	2.99	3.01	3.00	3.01
Ti		-	-	-	0.01	0.01	-	-	0.01
Al	y	2.53	2.50	2.71	2.65	2.65	2.52	2.52	2.07
Fe^{3+}		0.45	0.46	0.31	0.34	0.33	0.46	0.47	0.91
Σ		2.98	2.96	3.02	3.00	2.99	2.98	2.99	2.99
Mn	w	-	-	-	-	-	-	-	-
Ca		2.00	2.03	2.07	2.03	2.03	2.00	2.01	1.99
Σ		2.00	2.03	2.07	2.03	2.03	2.00	2.01	1.99
Total		8.00	8.00	8.04	8.01	8.01	7.99	8.00	7.99

* = Total iron as Fe_2O_3

n.d. = Not detected

r——c = Rim to core of zoned epidote

CHLORITE ANALYSES (1)

Sample	N1	N1H	N1K	T6	T13	66A	66F	66I
SiO_2	28.23	28.23	25.47	28.62	26.47	31.36	29.38	29.20
TiO_2	n.d.	n.d.	n.d.	n.d.	n.d.	n.d.	n.d.	n.d.
Al_2O_3	18.13	17.34	18.02	18.41	19.34	18.20	20.73	19.45
FeO*	27.89	26.42	37.17	20.40	28.42	12.90	20.79	13.51
MnO	0.26	0.38	0.31	0.23	0.41	n.d.	n.d.	n.d.
MgO	14.13	16.19	8.36	19.73	12.61	25.31	19.54	23.96
CaO	0.24	0.16	0.18	0.21	0.10	0.54	n.d.	n.d.
Na_2O	n.d.	n.d.	n.d.	n.d.	n.d.	n.d.	n.d.	n.d.
K_2O	n.d.	n.d.	n.d.	n.d.	n.d.	n.d.	n.d.	n.d.
Total	88.88	88.72	89.51	87.60	87.35	88.31	90.44	86.12

Recalculation on the basis of 14 oxygens

Si	z	2.96	2.95	2.81	2.93	2.85	3.03	2.89	2.92
Al^{IV}	z	1.04	1.05	1.19	1.07	1.15	0.97	1.11	1.08
Σ		4.00	4.00	4.00	4.00	4.00	4.00	4.00	4.00
Al^{VI}	y	1.20	1.09	1.16	1.15	1.30	1.11	1.30	1.21
Fe^{2+}	y	2.45	2.31	3.43	1.75	2.56	1.04	1.71	1.13
Mn	y	0.02	0.03	0.03	0.02	0.04	-	-	-
Mg	y	2.21	2.52	1.38	3.01	2.02	3.65	2.87	3.57
Ca	y	0.03	0.02	0.02	0.02	0.01	0.11	-	-
Σ		5.91	5.97	6.02	5.95	5.93	5.91	5.88	5.91
Total		9.91	9.97	10.02	9.95	9.93	9.91	9.88	9.91

* = Total iron as FeO

n.d. = Not detected

CHLORITE ANALYSES (2)

Sample	85A	96E	148E	168E	168F	168J	168L	169R[3]
SiO_2	25.19	26.01	26.90	28.08	27.81	28.90	27.27	25.49
TiO_2	n.d.	n.d.	n.d.	n.d.	n.d.	n.d.	n.d.	n.d.
Al_2O_3	18.88	18.66	19.54	19.82	20.31	19.08	18.90	18.26
FeO*	32.78	29.99	23.70	19.87	22.12	16.19	18.57	31.66
MnO	0.40	0.43	0.39	0.29	0.54	0.32	0.27	0.37
MgO	10.65	12.72	16.15	19.32	17.82	22.73	20.01	10.63
CaO	n.d.	n.d.	0.28	0.23	n.d.	0.15	0.08	0.27
Na_2O	n.d.	n.d.	n.d.	n.d.	n.d.	n.d.	n.d.	n.d.
K_2O	n.d.	n.d.	n.d.	n.d.	n.d.	n.d.	n.d.	n.d.
Total	87.90	87.81	86.96	87.61	88.60	87.37	85.10	86.68

Recalculation on the basis of 14 oxygens

Si	2.75	2.81	2.83	2.87	2.83	2.90	2.85	2.83
Al^{IV}	1.25	1.19	1.17	1.13	1.17	1.10	1.15	1.17
Σ	4.00	4.00	4.00	4.00	4.00	4.00	4.00	4.00
Al^{VI}	1.18	1.18	1.25	1.26	1.27	1.16	1.18	1.22
Fe^{2+}	3.00	2.71	2.08	1.70	1.88	1.36	1.63	2.94
Mn	0.04	0.04	0.03	0.03	0.05	0.03	0.01	0.03
Mg	1.73	2.05	2.53	2.94	2.70	3.40	3.12	1.76
Ca	-	-	0.03	0.03	-	0.02	0.01	0.03
Σ	5.95	5.98	5.92	5.96	5.90	5.97	5.95	5.98
Total	9.95	9.98	9.92	9.96	9.90	9.97	9.95	9.98

* = Total iron as FeO

n.d. = Not detected

STILPNOMELANE ANALYSES

Sample	85A	169R3
SiO_2	45.12	45.42
TiO_2	n.d.	n.d.
Al_2O_3	5.97	5.83
Fe_2O_3*	33.14	32.00
MnO	1.09	1.18
MgO	4.86	5.58
CaO	0.19	0.14
Na_2O	n.d.	0.31
K_2O	5.08	1.77
Total	95.45	92.23

Recalculation on the basis of 8 Si cations

Si	z	8.00	8.00
Σ		8.00	8.00
Al	x,y	1.25	1.21
Ti	x,y	-	-
Fe^{3+}	x,y	4.42	4.24
Mn	x,y	0.16	0.18
Mg	x,y	1.28	1.47
Σ		7.11	7.10
Ca	w	0.04	0.03
Na	w	-	0.10
K	w	1.15	0.40
Σ		1.19	0.53

SPHENE ANALYSES

Sample	N1	85A	96E	169R3
SiO_2	31.16	30.87	30.68	30.55
TiO_2	33.49	34.70	37.06	37.25
Al_2O_3	3.24	2.98	1.73	1.74
Fe_2O_3*	2.70	1.81	1.92	0.97
MnO	n.d.	n.d.	n.d.	n.d.
MgO	n.d.	n.d.	n.d.	n.d.
CaO	27.43	29.33	28.57	28.78
Na_2O	n.d.	n.d.	n.d.	n.d.
K_2O	n.d.	n.d.	n.d.	n.d.
Total	98.02	99.69	99.96	99.29

Recalculation on the basis of 4 Si cations

Si	z	4.00	4.00	4.00	4.00
Σ		4.00	4.00	4.00	4.00
Al	y	0.49	0.40	0.27	0.27
Ti	y	3.23	3.38	3.63	3.67
Fe^{3+}	y	0.26	0.18	0.19	0.09
Σ		3.98	3.96	4.09	4.07
Ca	x	3.77	4.07	4.00	4.04
Σ		3.77	4.07	4.00	4.04

* = Total iron as Fe_2O_3

n.d. = Not detected

AMPHIBOLE ANALYSES (1)

Sample	T6	66A	66A	66I	66I	85A	96E	148E
	F	F	N	F	N	N	N	F
SiO_2	55.16	54.74	51.74	56.30	55.15	52.52	52.85	52.85
TiO_2	n.d.	n.d.	n.d.	n.d.	n.d.	n.d.	n.d.	n.d.
Al_2O_3	0.60	2.50	4.90	1.69	1.21	1.46	3.15	3.80
FeO*	12.85	8.95	8.89	10.31	9.16	19.22	19.07	13.25
MnO	0.12	n.d.	0.32	n.d.	n.d.	n.d.	n.d.	n.d.
MgO	15.56	17.69	19.57	18.15	18.23	11.64	11.31	14.63
CaO	13.01	12.91	10.86	12.73	13.23	12.27	12.43	12.90
Na_2O	n.d.	n.d.	0.53	n.d.	n.d.	n.d.	n.d.	0.74
K_2O	n.d.	n.d.	0.13	n.d.	n.d.	n.d.	n.d.	0.19
Total	97.30	96.79	96.94	99.18	96.98	97.11	98.81	98.36

Recalculation on the basis of 23 oxygens

Si	z	7.96	7.76	7.38	7.83	7.83	7.80	7.69	7.59
Al^{IV}	z	0.04	0.24	0.62	0.17	0.17	0.20	0.31	0.41
Σ		8.00	8.00	8.00	8.00	8.00	8.00	8.00	8.00
Al^{VI}	x,y	0.06	0.18	0.20	0.11	0.03	0.06	0.23	0.23
Ti	x,y	-	-	-	-	-	-	-	-
Fe^{2+}	x,y	1.55	1.06	1.06	1.20	1.09	2.39	2.32	1.59
Mn	x,y	0.02	-	0.04	-	-	-	-	-
Mg	x,y	3.35	3.74	4.16	3.76	3.86	2.58	2.46	3.13
Σ		4.98	4.98	5.46	5.07	4.95	5.03	5.01	4.95
Ca	w	2.01	1.96	1.66	1.90	2.01	1.95	1.94	1.99
Na	w	-	-	0.15	-	-	-	-	0.21
K	w	-	-	0.02	-	-	-	-	0.03
Σ		2.01	1.96	1.83	1.90	2.01	1.95	1.94	2.23
Total		14.99	14.94	15.29	14.97	14.96	14.98	14.95	15.18

* = Total iron as FeO
n.d. = Not detected

F = Amphibole fringing pyroxene
N = Needle of amphibole

AMPHIBOLE ANALYSES (2)

Sample	148E	168E	168F	168F	168J	168J	168L	169R[3]
	N	F	F	N	F	N	N	F
SiO_2	54.12	54.50	51.87	53.64	54.33	54.68	54.14	52.77
TiO_2	n.d.	n.d.	n.d.	n.d.	n.d.	n.d.	n.d.	n.d.
Al_2O_3	2.92	0.71	4.69	2.36	1.93	1.72	0.56	1.48
FeO*	12.88	11.37	12.72	11.83	10.46	9.60	11.37	19.94
MnO	n.d.	0.19	0.39	0.26	0.17	0.13	0.22	0.36
MgO	15.25	16.13	14.72	15.26	17.14	18.16	15.98	11.00
CaO	13.04	13.11	11.61	12.73	12.62	12.41	12.64	12.23
Na_2O	n.d.	n.d.	n.d.	n.d.	n.d.	n.d.	n.d.	0.49
K_2O	n.d.	n.d.	n.d.	n.d.	n.d.	n.d.	n.d.	n.d.
Total	98.21	96.01	96.00	96.08	96.65	96.70	94.91	98.27

Recalculation on the basis of 23 oxygens

Si	z	7.71	7.92	7.57	7.79	7.81	7.82	7.97	7.83
Al^{IV}	z	0.29	0.08	0.43	0.21	0.19	0.18	0.03	0.17
Σ		8.00	8.00	8.00	8.00	8.00	8.00	8.00	8.00
Al^{VI}	x,y	0.20	0.04	0.38	0.20	0.14	0.11	0.07	0.09
Ti	x,y	-	-	-	-	-	-	-	-
Fe^{2+}	x,y	1.53	1.38	1.55	1.44	1.26	1.15	1.40	2.47
Mn	x,y	-	0.02	0.05	0.03	0.02	0.02	0.03	0.05
Mg	x,y	3.24	3.49	3.20	3.31	3.67	3.87	3.51	2.43
Σ		4.97	4.93	5.18	4.98	5.09	5.15	5.01	5.04
Ca	w	1.99	2.04	1.82	1.98	1.94	1.90	1.99	1.94
Na	w	-	-	-	-	-	-	-	0.14
K	w	-	-	-	-	-	-	-	-
Σ		1.99	2.04	1.82	1.98	1.94	1.90	1.99	2.08
Total		14.96	14.97	15.00	14.96	15.03	15.05	15.00	15.12

* = Total iron as FeO

n.d. = Not detected

F = Amphibole fringing pyroxene

N = Needle of amphibole

WHITE MICA ANALYSES (1)

Sample	66A	66A	66A	66F	66F	66I	66I	66I
SiO_2	49.39	49.41	49.08	49.13	48.33	46.11	47.26	47.61
TiO_2	n.d.	n.d.	n.d.	n.d.	n.d.	n.d.	n.d.	n.d.
Al_2O_3	30.16	29.71	31.62	30.73	28.39	34.75	30.42	34.21
FeO*	1.35	1.35	1.20	1.23	2.03	1.41	1.41	1.72
MnO	n.d.	n.d.	n.d.	n.d.	n.d.	n.d.	n.d.	n.d.
MgO	3.42	3.80	3.01	2.92	4.47	0.48	2.41	1.59
CaO	n.d.	n.d.	0.18	0.30	0.20	n.d.	n.d.	n.d.
Na_2O	n.d.	n.d.	0.51	n.d.	n.d.	n.d.	n.d.	n.d.
K_2O	10.85	10.45	10.75	10.17	10.47	10.56	10.11	10.52
Total	95.17	94.72	96.35	94.48	93.89	93.31	91.61	95.65

Recalculation on the basis of 22 oxygens

Si	z	6.56	6.58	6.46	6.54	6.54	6.22	6.50	6.28
Al^{IV}	z	1.44	1.42	1.54	1.46	1.46	1.78	1.50	1.72
Σ		8.00	8.00	8.00	8.00	8.00	8.00	8.00	8.00
Al^{VI}	x,y	3.28	3.24	3.37	3.36	3.07	3.75	3.43	3.59
Fe^{2+}	x,y	0.15	0.15	0.13	0.13	0.23	0.16	0.16	0.19
Mg	x,y	0.68	0.75	0.59	0.58	0.90	0.10	0.49	0.31
Σ		4.11	4.14	4.09	4.07	4.10	4.01	4.08	4.09
Na	w	-	-	0.13	-	-	-	-	-
K	w	1.84	1.77	1.80	1.73	1.81	1.82	1.77	1.77
Ca	w	-	-	0.03	0.04	0.03	-	-	-
Σ		1.84	1.77	1.96	1.77	1.84	1.82	1.77	1.77
Total		13.95	13.91	14.05	13.84	13.94	13.83	13.85	13.86

* = Total iron as FeO

n.d. = Not detected

WHITE MICA ANALYSES (2)

Sample	96E	96E	148E	148E	148E	168F	168F	168F
SiO_2	50.08	49.65	50.00	47.76	46.92	50.27	48.96	49.67
TiO_2	n.d.	n.d.	n.d.	n.d.	n.d.	n.d.	n.d.	n.d.
Al_2O_3	31.38	33.19	29.77	32.45	32.26	27.42	29.03	28.90
FeO*	2.06	2.11	2.12	2.49	1.90	2.94	4.10	2.56
MnO	n.d.	n.d.	n.d.	n.d.	n.d.	n.d.	n.d.	n.d.
MgO	1.14	0.52	1.62	1.68	1.54	3.30	3.49	2.35
CaO	n.d.	n.d.	0.24	0.19	n.d.	0.26	n.d.	0.22
Na_2O	n.d.	n.d.	0.67	n.d.	n.d.	1.22	n.d.	0.66
K_2O	9.08	8.83	10.02	10.68	10.67	9.06	9.90	9.74
Total	93.74	94.30	94.44	95.25	93.29	94.47	95.48	94.10

Recalculation on the basis of 22 oxygens

Si	z	6.68	6.56	6.69	6.37	6.38	6.75	6.54	6.69
Al^{IV}	z	1.32	1.44	1.31	1.63	1.62	1.25	1.46	1.31
Σ		8.00	8.00	8.00	8.00	8.00	8.00	8.00	8.00
Al^{VI}		3.61	3.73	3.39	3.47	3.55	3.09	3.11	3.28
Fe^{2+}	x.y	0.23	0.23	0.24	0.28	0.22	0.33	0.46	0.29
Mg	x.y	0.23	0.10	0.32	0.33	0.31	0.66	0.69	0.47
Σ		4.07	4.06	3.95	4.08	4.08	4.08	4.26	4.04
Na	w	-	-	0.17	-	-	0.32	-	0.17
K	w	1.55	1.49	1.71	1.82	1.85	1.55	1.69	1.67
Ca	w	-	-	0.03	0.03	-	0.04	-	0.03
Σ		1.55	1.49	1.91	1.85	1.85	1.91	1.69	1.87
Total		13.62	13.55	13.86	13.93	13.93	13.99	13.95	13.91

* = Total iron as FeO

n.d. = Not detected

FELDSPAR ANALYSES (1)

Sample	N1	N1K	T13	66F	66I	66I	85A	96E
SiO_2	66.11	67.92	66.10	65.18	53.35	53.20	67.47	68.77
TiO_2	n.d.	n.d.	n.d.	n.d.	n.d.	n.d.	n.d.	n.d.
Al_2O_3	20.25	19.22	19.78	21.96	28.39	29.76	19.85	21.10
FeO*	0.16	0.33	1.61	n.d.	0.77	0.81	n.d.	n.d.
MnO	n.d.	n.d.	n.d.	n.d.	n.d.	n.d.	n.d.	n.d.
MgO	n.d.	n.d.	n.d.	n.d.	n.d.	n.d.	n.d.	n.d.
CaO	1.31	0.31	0.93	2.76	11.46	12.69	n.d.	1.16
Na_2O	10.93	11.24	10.09	9.86	5.02	4.64	11.79	9.86
K_2O	0.07	n.d.	0.13	n.d.	0.18	0.20	n.d.	n.d.
Total	98.83	99.02	98.64	99.76	99.17	101.30	99.11	100.89

Recalculation on the basis of 8 oxygens

Si	2.94	3.00	2.94	2.86	2.44	2.39	2.97	2.96
Al	1.06	1.00	1.04	1.14	1.53	1.57	1.03	1.07
Fe	0.01	0.01	0.06	-	0.03	0.03	-	-
Ca	0.06	0.01	0.04	0.13	0.56	0.61	-	0.05
Na	0.94	0.96	0.87	0.84	0.44	0.40	1.01	0.82
K	0.00	-	0.01	-	0.01	0.01	-	-
Σ	5.01	4.98	4.96	4.97	5.01	5.01	5.01	4.90
Ab	94	99	95	87	44	39	100	94
An	6	1	4	13	55	59	0	6
Or	0	0	1	0	1	2	0	0

* = Total iron as FeO

n.d. = Not detected

FELDSPAR ANALYSIS (2)

					Alkali Feldspar		
Sample	148E	168E	168F	169R3	168E	168E	168E
SiO_2	66.18	66.53	68.03	69.33	63.48	63.60	63.84
TiO_2	n.d.	n.d.	n.d.	n.d.	n.d.	n.d.	n.d.
Al_2O_3	22.37	20.44	20.45	19.25	18.60	18.60	18.44
FeO*	n.d.	0.35	n.d.	0.48	0.27	0.42	0.15
MnO	n.d.	n.d.	n.d.	n.d.	n.d.	n.d.	n.d.
MgO	n.d.	n.d.	n.d.	n.d.	n.d.	n.d.	n.d.
CaO	2.05	1.34	1.02	0.32	0.34	0.97	0.22
Na_2O	10.78	10.56	10.85	11.53	0.33	n.d.	n.d.
K_2O	0.12	0.09	n.d.	n.d.	15.65	15.41	15.79
Total	101.5	99.31	100.35	100.91	98.34	99.00	98.44

Recalculation on the basis of 8 oxygens

Si	2.86	2.94	2.96	3.00	2.96	2.96	2.98
Al	1.14	1.06	1.05	0.98	1.02	1.02	1.01
Fe	-	0.01	-	0.02	0.01	0.02	0.01
Ca	0.09	0.06	0.05	0.01	0.02	0.05	0.01
Na	0.90	0.90	0.91	0.97	0.03	-	-
K	0.01	0.00	-	-	0.94	0.91	0.94
Σ	5.01	4.97	4.97	4.98	4.98	4.96	4.95
Ab	90	92	95	99	3	0	0
An	9	7	5	1	2	5	1
Or	1	1	0	0	95	95	99

* = Total iron as FeO

n.d. = Not detected

APPENDIX 6 : X-RAY DIFFRACTION RESULTS

APPENDIX 6 (i) Results of the illite crystallinity analyses.

Sample Number	Mean Kubler Index	Weaver Index	Weber Index
C1	0.238	14.3	166
E1A	0.267	11.2	188
E1B (1)	0.231	15.5	183
E1B (2)	0.243	14.3	183
E1B (3)	0.245	14.3	174
F1	0.225	17.9	166
R1	0.213	19.7	158
V1	0.450	3.1	308
V9	0.365	4.7	266
W1A	0.350	5.5	258
Y1	0.350	5.2	233
13	0.256	11.7	179
28	0.355	4.8	233
30B	0.660	1.9	433
31A	0.408	4.3	275
31c	0.340	5.3	255
32	0.493	2.6	350
33A (1)	0.405	3.9	286
33A (2)	0.425	4.5	283
33A (3)	0.357	4.9	258
33B	0.500	3.1	250
36	0.305	8.6	233
37	0.330	6.2	233
39	0.270	10.3	200
40	0.216	17.3	150
52	0.195	21.8	150
55	0.250	10.7	183
60	0.250	12.5	183
62	0.250	11.6	200
67	0.175	24.0	142
69C	0.213	13.2	167
70	0.195	20.3	150
72	0.200	16.3	166
75	0.225	11.3	183
76	0.188	23.5	183
82	0.320	8.6	233

Appendix 6 (i) ... continued...

Sample Number	Mean Kubler Index	Weaver Index	Weber Index
83C	0.230	12.4	150
88A	0.230	17.7	167
90	0.250	13.9	183
97	0.263	11.7	183
107	0.230	16.4	167
127A (1)	0.250	10.0	200
127A (2)	0.313	7.1	233
127B	0.257	9.6	183
128A	0.238	14.7	167
128B	0.225	18.7	167
129	0.230	13.3	175
137B (1)	0.250	10.1	175
137B (2)	0.250	7.1	167
139A	0.188	15.5	138
150	0.203	13.1	162
151A	0.250	14.4	175
151B	0.250	12.9	200
151C	0.238	19.8	150
153	0.207	14.6	150
155A	0.245	12.5	154
155B	0.218	25.3	133
158	0.230	20.9	166
159	0.200	15.3	154
160	0.275	8.8	175
162B	0.250	10.4	183
165	0.250	15.0	154
167J	0.200	22.4	150
170	0.280	8.9	200
173	0.194	31.8	137
176	0.275	19.6	177
178	0.190	13.0	133
186	0.210	23.5	137
201	0.200	21.5	154
207	0.210	17.6	146
209 (1)	0.289	9.7	217
209 (2)	0.294	8.3	250

Appendix 6 (i)... continued...

Sample Number	Mean Kubler Index	Weaver Index	Weber Index
209 (3)	0.300	8.2	217
210	0.240	11.3	166
211	0.310	7.6	283
212	0.225	14.2	166
213	0.240	14.7	166
215	0.319	7.2	217
219	0.238	11.3	166
223	0.275	9.3	183
227	0.280	11.35	187
230	0.288	9.2	217
231	0.268	11.6	208
236	0.330	6.8	230
237	0.425	9.5	208
241	0.238	10.9	183
244	0.344	6.8	250
245	0.313	8.8	229
248	0.350	9.3	250
254	0.419	8.5	300
255 (1)	0.256	12.2	200
255 (2)	0.300	8.4	208
266	0.288	7.7	208
267	0.231	14.2	175
270	0.300	10.2	217
271	0.319	8.1	233
272 (A)	0.275	11.5	200
273	0.268	10.5	200
275	0.322	9.0	225
276	0.331	7.7	267
278	0.344	7.2	250
279	0.231	15.1	192
285	0.325	9.0	233
287	0.338	5.4	250
288	0.365	3.7	258
290	0.315	8.6	221
292	0.313	8.7	208

Appendix 6 (i)... continued...

Sample Number	Mean Kubler Index	Weaver Index	Weber Index
293	0.313	7.5	250
294	0.300	7.9	225
295	0.331	5.8	250
297	0.365	6.1	258
298	0.250	11.3	192
301	0.238	13.5	183
311	0.338	8.3	246
314	0.188	27.7	150
315	0.194	29.0	133
316	0.337	8.6	241
319	0.275	15.0	200
326	0.463	4.4	283
339	0.238	10.9	183

APPENDIX 6 (ii) Repeat analyses of illite crystallinity.

Sample Number	Mean Kubler Index	Weaver Index	Weber Index
E1A	0.256	11.6	183
E1A (rerun)	0.288	10.8	192
E1B (3)	0.250	13.6	166
E1B (3) (rerun)	0.243	15.1	183
13	0.250	10.4	183
13 (rerun)	0.263	13.0	175
31A	0.400	4.3	266
31A (rerun)	0.413	4.3	283
32	0.500	2.7	350
32 (rerun)	0.488	2.4	350
33A (1)	0.413	4.0	282
33A (1) (rerun)	0.393	3.8	291
40	0.218	18.6	150
40 (rerun)	0.213	15.9	150
137B (1)	0.250	9.7	183
137B (1) (rerun)	0.263	10.6	167
155A	0.250	11.7	150
155A (rerun)	0.250	14.2	150
155A (rerun)	0.200	12.1	166
155A (rerun)	0.275	13.0	150
173	0.188	32.0	133
173 (rerun)	0.200	31.6	142
186	0.218	23.1	145
186 (rerun)	0.200	23.9	133
207	0.200	16.8	150
207 (rerun)	0.213	18.4	142
209	0.300	8.0	217
209 (rerun)	0.300	8.3	217
227	0.281	11.4	192
227 (rerun)	0.250	11.3	183
236	0.319	6.5	217
236 (rerun)	0.350	7.0	242
245	0.313	8.9	233
245 (rerun)	0.313	8.8	225
248	0.350	10.0	250

APPENDIX 6 (ii) ... continued...

Sample Number	Mean Kubler Index	Weaver Index	Weber Index
248 (rerun)	0.350	8.5	250
255 (1)	0.256	11.9	200
255 (1) (rerun)	0.256	12.4	200
266	0.288	8.0	217
266 (rerun)	0.288	7.4	200
275	0.331	9.6	233
275 (rerun)	0.313	8.4	216
290	0.325	8.0	225
290 (rerun)	0.306	9.3	217
297	0.350	6.0	266
297 (rerun)	0.375	6.1	250
311	0.300	8.2	225
311 (rerun)	0.375	8.3	267
316	0.387	6.8	283
316 (rerun)	0.288	10.4	200

APPENDIX 6 (iii) Calculation of the composite crystallinity index

Sample Number	Kubler Component	Weaver Component	Weber Component	Composite Index
C1	+17	+12	+37	+ 66
E1A	- 4	- 8	- 1	- 13
E1B	+14	+14	+10	+ 38
F1	+33	+30	+37	+100
R1	+50	+39	+52	+141
V1	-49	-88	-50	-187
V9	-28	-72	-33	-133
W1A	-24	-64	-29	-117
Y1	-24	-67	-19	-110
13	0	- 3	+12	+ 9
28	-26	-71	-19	-116
30B	-100	-100	-100	-300
31A	-38	-76	-36	-150
31C	-22	-66	-28	-116
32	-59	-93	-67	-219
33A	-35	-75	-37	-147
33B	-61	-88	-26	-175
36	-13	-34	-19	- 66
37	-20	-57	-19	- 96
39	- 5	-17	- 6	- 28
40	+45	+27	+67	+139
52	+73	+49	+67	+189
55	0	-12	+ 4	- 9
60	0	+ 3	+ 4	+ 7
62	0	- 4	- 6	- 10
67	+100	+61	+83	+244
69C	+50	+ 6	+35	+ 91
70	+73	+42	+67	+182
72	+67	+22	+37	+126
75	+33	- 7	+ 4	+ 30
76	+83	+58	+ 4	+145
82	-17	-34	-19	- 70
83C	+27	+ 2	+67	+ 94
88A	+27	+29	+35	+ 91
90	0	+10	+ 4	+ 14
97	- 3	- 3	+ 4	- 2

APPENDIX 6 (iii).... continued....

Sample Number	Kubler Component	Weaver Component	Weber Component	Composite Index
107	+ 33	+ 22	+ 35	+ 90
127A	- 8	- 35	- 13	- 56
127B	- 2	- 24	+ 4	- 22
128A	+ 17	+ 14	+ 35	+ 66
128B	+ 33	+ 34	+ 35	+102
129	+ 27	+ 7	+ 19	+ 53
137B	0	- 34	+ 19	- 15
139A	+ 83	+ 18	+ 35	+136
150	+ 63	+ 6	+ 44	+113
151A	0	+ 12	+ 19	+ 31
151B	0	+ 5	- 6	- 1
151C	+ 17	+ 39	+ 67	+123
153	+ 57	+ 13	+ 67	+137
155A	+ 7	+ 3	+ 60	+ 70
155B	+ 43	+ 67	+100	+210
158	+ 27	+ 45	+ 37	+109
159	+ 67	+ 17	+ 60	+144
160	- 6	- 32	+ 19	- 19
162B	0	- 16	+ 4	- 12
165	0	+ 15	+ 60	+ 75
167J	+ 67	+ 53	+ 67	+187
170	- 7	- 31	- 6	- 44
173	+ 75	+100	+ 92	+267
176	- 6	+ 38	+ 15	+ 47
178	+ 80	+ 5	+100	+185
186	+ 53	+ 58	+ 92	+203
201	+ 67	+ 48	+ 60	+175
207	+ 53	+ 28	+ 75	+156
209	- 11	- 33	- 17	- 61
210	+ 13	- 7	+ 37	+ 43
211	- 15	- 44	- 40	- 99
212	+ 33	+ 11	+ 37	+ 81
213	+ 13	+ 14	+ 37	+ 64
215	- 17	- 48	- 13	- 78
219	+ 16	- 7	+ 37	+ 46
223	- 6	- 27	+ 4	- 29

APPENDIX 6 (iii) ... continued...

Sample Number	Kubler Component	Weaver Component	Weber Component	Composite Index
227	- 7	- 6	- 1	- 14
230	- 9	- 28	- 13	- 50
231	- 4	- 4	- 9	- 17
236	- 20	- 51	- 18	- 89
237	- 43	- 25	- 9	- 77
241	+ 16	- 11	+ 4	+ 9
244	- 23	- 51	- 26	-100
245	- 15	- 32	- 18	- 65
248	- 24	- 27	- 26	- 77
254	- 41	- 35	- 46	-113
255	- 7	- 17	- 8	- 32
266	- 9	- 43	- 9	- 61
267	+ 25	+ 11	+ 19	+ 55
270	- 12	- 18	- 13	- 43
271	- 17	- 39	- 19	- 75
272(A)	- 6	- 5	- 6	- 17
273	- 4	- 15	- 6	- 25
275	- 18	- 30	- 16	- 64
276	- 20	- 43	- 33	- 96
278	- 23	- 48	- 26	- 97
279	+ 25	+ 16	- 3	+ 38
285	- 18	- 30	- 19	- 67
287	- 21	- 65	- 26	-112
288	- 61	- 82	- 29	-172
290	- 16	- 34	- 15	- 65
292	- 15	- 33	- 9	- 57
293	- 15	- 45	- 26	- 86
294	- 12	- 41	- 16	- 69
295	- 20	- 61	- 26	-107
297	- 61	- 59	- 29	-149
298	0	- 7	- 3	- 10
301	+ 16	+ 8	+ 4	+ 28
311	- 21	- 37	- 25	- 83
314	+ 83	+ 79	+ 67	+229
315	+ 75	+ 86	+100	+261

APPENDIX 6 (iii) .... continued...

Sample Number	Kubler Component	Weaver Component	Weber Component	Composite Index
316	- 21	- 34	- 23	- 78
319	- 6	+ 15	- 6	+ 3
326	- 52	- 75	- 40	-167
339	+ 16	- 11	+ 4	+ 9

APPENDIX 6 (IV) Mineral assemblages of slates and shales from northern Snowdonia from bulk rock scans.

Sample Number.	Mineral assemblage determined by X-ray diffraction
E1A	Chlorite + muscovite + quartz + (tr) albite + (tr) hematite
V9	Chlorite + muscovite + quartz + calcite
W1A	Chlorite + muscovite + quartz + (tr) pyrite
13	Chlorite + muscovite + quartz + (tr) albite
30B	Muscovite + quartz
31A	Chlorite + muscovite + quartz
33B	Chlorite + muscovite + quartz
36	Chlorite + muscovite + quartz + (tr) albite
37	Chlorite + muscovite + quartz
40	Chlorite + muscovite + quartz
55	Chlorite + muscovite + quartz + (tr) albite
67	Chlorite + muscovite + quartz + (tr) hematite
72	Chlorite + muscovite + quartz
75	Muscovite + quartz + (tr) albite
76	Chlorite + muscovite + quartz
82	Chlorite + muscovite + quartz
88A	Muscovite + quartz + albite
97	Chlorite + muscovite + quartz + (tr) albite
107	Chlorite + muscovite + (tr) quartz
127A	(tr) chlorite + muscovite + quartz + albite
128A	Chlorite + muscovite + quartz + albite
137B	Muscovite + quartz
151A	Chlorite + muscovite + quartz + albite
153	(tr) chlorite + muscovite + quartz + albite
162B	Chlorite + muscovite + quartz
167J	Chlorite + muscovite + quartz + albite
207	Muscovite + quartz + hematite + (tr) chlorite
209	Chlorite + muscovite + quartz + paragonite
211	(tr) chlorite + muscovite + quartz + hematite + paragonite
236	Chlorite + muscovite + quartz + (tr) albite + (tr) hematite
241	Chlorite + muscovite + quartz
244	Chlorite + muscovite + quartz
245	Chlorite + muscovite + quartz + (tr) pyrite
254	Chlorite + muscovite + quartz + (tr) hematite + paragonite
266	Chlorite + muscovite + quartz + (tr) hematite + (tr) albite

APPENDIX 6 (IV) ... continued...

Sample Number.	Mineral assemblage determined by X-ray diffraction
270	Chlorite + muscovite + quartz + (tr) albite + (tr) hematite
273	Chlorite + muscovite + quartz
278	Chlorite + muscovite + quartz
279	Chlorite + muscovite + quartz + (tr) albite
285	Chlorite + muscovite + quartz
288	Chlorite + muscovite + quartz
292	Chlorite + muscovite + quartz
295	Chlorite + muscovite + quartz + (tr) albite + (tr) pyrite
297	Chlorite + muscovite + quartz + (tr) hematite
301	Chlorite + muscovite + quartz
311	(tr) chlorite + muscovite + quartz + hematite
314	Chlorite + muscovite + quartz + (tr) albite + (tr) pyrite
315	Chlorite + muscovite + quartz + (tr) albite + (tr) hematite
316	Chlorite + muscovite + quartz + (tr) albite
319	Chlorite + muscovite + quartz

APPENDIX 6 (V) Calculation of b_o values.

Sample Number.	Number of Peaks.	Position illite (060) Peak ($^o2\theta$).	"d" spacing.	Calculated b_o value.	One Standard Deviation error.
E1A	6	61.6688	1.5026	9.0155	0.0022
V9	6	61.9417	1.4967	8.9801	0.0070
W1A	6	61.9375	1.4969	8.9813	0.0086
13	6	61.7063	1.5018	9.0107	0.0039
30B	6	61.8750	1.4985	8.9908	0.0038
31A	6	61.9169	1.4973	8.9836	0.0108
33B	4	61.9500	1.4966	8.9793	0.0069
36	5	61.8775	1.4984	8.9901	0.0080
37	4	61.8813	1.4983	8.9899	0.0051
40	5	61.9275	1.4972	8.9829	0.0056
55	5	61.7050	1.4985	8.9907	0.0043
67	6	61.6875	1.5023	9.0135	0.0027
72	8	61.7469	1.5011	9.0064	0.0066
75	7	61.6140	1.5038	9.0225	0.0062
76	7	61.6147	1.5034	9.0204	0.0059
82	5	61.9028	1.4978	8.9869	0.0059
88A	5	61.7050	1.5019	9.0114	0.0061
97	6	61.8000	1.5000	9.0000	0.0070
107	4	61.6878	1.5003	9.0015	0.0030
127A	6	61.7938	1.5001	9.0008	0.0035
128B	5	61.7800	1.5004	9.0024	0.0040
137B	3	61.6583	1.5028	9.0170	0.0017
151A	6	61.9100	1.4977	8.9862	0.0073
153	6	61.6396	1.5032	9.0193	0.0049
162B	6	61.7063	1.5019	9.0113	0.0036
167J	6	61.7583	1.5008	9.0048	0.0116
207	5	61.7300	1.5014	9.0084	0.0008
209	6	61.9300	1.4978	8.9870	0.0062
211	5	61.7575	1.5009	9.0051	0.0029
236	5	61.8813	1.4983	8.9899	0.0088
241	5	61.8500	1.4990	8.9940	0.0057
244	3	61.8750	1.4985	8.9910	0.0075
245	5	61.9700	1.4959	8.9754	0.0052
254	4	61.8969	1.4981	8.9886	0.0072
266	5	61.8300	1.4994	8.9964	0.0047

APPENDIX 6 (V) ... continued...

Sample Number.	Number of peaks.	Position illite (060)Peak ($^{o}2\theta$).	"d" spacing.	Calculated b_o value.	One Standard Deviation error.
270	4	61.8775	1.4985	8.9906	0.0092
273	5	61.9100	1.4977	8.9862	0.0060
278	5	61.9849	1.4955	8.9727	0.0094
279	5	61.8175	1.4997	8.9979	0.0039
285	6	61.9479	1.4966	8.9794	0.0076
288	4	61.8512	1.4990	8.9942	0.0097
292	5	61.8775	1.4984	8.9902	0.0057
295	4	61.8063	1.4999	8.9993	0.0063
297	6	61.8353	1.4993	8.9960	0.0084
301	5	61.7725	1.5006	9.0033	0.0027
311	4	61.8775	1.4984	8.9903	0.0029
314	4	61.8900	1.4979	8.9876	0.0063
315	5	61.8900	1.4979	8.9876	0.0059
316	4	61.9275	1.4972	8.9831	0.0077
319	6	61.8889	1.4981	8.9886	0.0099

APPENDIX 6 (V1) Results of the intensity ratio (I_{002}/I_{001}) measurements.

Sample Number.	Intensity Ratio (I_{002}/I_{001})	Sample Number	Intensity Ratio (I002/I001)
E1A	0.35	167J	0.44
V9	0.33	207	0.57
W1A	0.39	209	0.31
13	0.35	211	0.40
30B	0.44	236	0.37
31A	0.41	241	0.38
33B	0.33	244	0.33
36	0.37	245	0.50
37	0.52	254	0.38
40	0.36	266	0.42
55	0.39	270	0.44
67	0.38	273	0.30
72	0.53	278	0.42
75	0.41	279	0.47
76	0.48	285	0.30
82	0.45	288	0.33
88A	0.30	292	0.45
97	0.46	295	0.33
107	0.46	297	0.44
127A	0.38	301	0.33
128B	0.36	311	0.44
137B	0.32	314	0.36
151A	0.35	315	0.43
153	0.51	316	0.25
162B	0.38	319	0.48

REFERENCES

ALDERTON, D.H.M., 1976. The geochemistry of mineralisation at Pendarves, and other Cornish areas. Ph.D. thesis (unpublished), Kings College, University of London.

BAKER, J.W., 1971. Intra-Lower Palaeozoic faults in the southern Irish Sea area. Geol. Mag., 108. pp. 501-509.

BEAVON, R.V., 1963. The succession and structure east of the Glaslyn river, North Wales. Q. Jl. geol. Soc. Lond., 119. pp. 479-512.

BEVINS, R.E., 1978. Pumpellyite-bearing basic igneous rocks from the Lower Ordovician of North Pembrokeshire. Mineral. Mag., 42. pp. 81-83.

BEVINS, R.E., 1979. The Geology of the Strumble Head-Fishguard region, Dyfed, Wales. Ph.D. thesis (unpublished), University of Keele.

BEVINS, R.E., ROBINSON, D., ROWBOTHAM, G. and DUNKELY, P.N., 1981. Low grade metamorphism in the Welsh Caledonides. J. geol. Soc. Lond., 138. p. 634.

BEVINS, R.E., and ROWBOTHAM, G., 1983. Low-grade metamorphism within the Welsh sector of the paratectonic Caledonides. Geol. J., 18. pp.141-167.

BEVINS, R.E., and ROWBOTHAM, G., (In Press). Greenschist facies metabasites from the Hellefiskefjord - G.B.Schley Fjord area, eastern Peary Land, North Greenland.

BIRD, D.K. and HELGESON, H.C., 1981. Chemical interaction of aqueous solutions with epidote-feldspar mineral assemblages in geologic systems. II. Equilibrium constraints in metamorphic/geothermal processes. Am. J. Sci., 281. pp.576-614.

BISHOP, D.G., 1972. Progressive metamorphism from prehnite-pumpellyite facies to greenschist facies in the Dansey Pass area, Otago, New Zealand. Geol. Soc. Am. Bull., 83. pp.3177-3198.

BOLES, J.R. and COOMBS, D.S., 1977. Zeolite facies alteration of sandstones in the Southland Syncline, New Zealand. Am. J. Sci., 277. pp.982-1012.

BORG, I.Y., 1967. Optical properties and cell parameters in the Glaucophane -Riebeckite Series. Contrib. Mineral. Petrol., 15. pp.67-92.

BRINDLEY, G.W. and BROWN, G., 1980. Crystal structures of clay minerals and their X-ray identification. Mineralogical Society Monograph No. 5.

BROMLEY, A.V., 1969. Acid plutonic igneous activity in the Ordovician of North Wales. In : Wood, A. (Ed), The Pre-Cambrian and Lower Palaeozoic Rocks of Wales. University of Wales Press, Cardiff, pp. 409-433.

BROWN, E.H., 1967. The greenschist facies in part of Eastern Otago, New Zealand. Contrib. Mineral. Petrol., 14. pp.259-292.

BROWN, E.H., 1977. Phase equilibria among pumpellyite, lawsonite, epidote and associated minerals in low-grade metamorphic rocks. Contrib. Mineral. Petrol., 64. pp. 123-136.

CANN, J.R., 1969. Spilites from the Carlsberg Ridge, Indian Ocean. J. Petrol., 10. pp. 1-19.

CANN, J.R., 1970. Rb, Sr, Y, Zr and Nb in some ocean floor basaltic rocks. Earth Planet. Sci. Lett., 19. pp. 7-11.

CIPRIANI, C., SASSI, F.P. and SCOLARI, A., 1971. Metamorphic white micas : definition of paragenetic fields. Schweiz. Mineral. Petrog. Mitt., 51. pp.259-302.

COOMBS, D.S., 1953. The pumpellyite mineral series. Mineral. Mag., 30. pp. 113-135.

COOMBS, D.S., 1960. Lower grade mineral facies in New Zealand. Rep. Int. geol. Conr. 21st Session, Norden, 1960. 13. pp.339-351.

COOMBS, D.S., HORODYSKI, R.J. and NAYLOR, R.S., 1970. Occurrence of prehnite-pumpellyite facies metamorphism in Northern Maine. Am. J. Sci., 268. pp.142-156.

COOMBS, D.S., NAKAMURA, Y. and VUAGNAT, M., 1976. Pumpellyite-actinolite facies schists of the Taveyanne Formation, near Loeche, Valais, Switzerland. J. Petrol. 17. pp.440-471.

COWARD, M.P. and SIDDANS, A.W.B., 1979. The tectonic evolution of the Welsh Caledonides. In : HARRIS, A.L., HOLLAND, C.H. and LEAKE, B.E. (Eds). The Caledonides of the British Isles-reviewed. Spec. Publ. geol. Soc. Lond., 8. pp.187-198.

COX, K.G., BELL, J.D. and PANKHURST, R.J., 1979. The Interpretation of Igneous Rocks. George,Allen and Unwin, London.

CRAIG, J., FITCHES, W.R. and MALTMAN, A.J., 1982. Chlorite-mica stacks in low-strain rocks from Central Wales. Geol. Mag., 119. pp.243-256.

CRAWFORD, M.L., 1981. Phase equilibria in aqueous fluid inclusions. In : HOLLISTER, L.S., and CRAWFORD, M.L. (Eds). Short course in fluid inclusions : Applications to Petrology. Mineral. Assoc. Canada, Short Course 6, Calgary, pp.75-101.

CRAWFORD, M.L., 1981. Fluid inclusions in metamorphic rocks - low and medium grades. In : HOLLISTER, L.S. and CRAWFORD, M.L. (Eds). Short course in fluid inclusions : Applications to Petrology. Mineral. Assoc. Canada, Short Course 6, Calgary, pp. 157-182.

CRIMES, T.P., 1971. A facies analysis of the Cambrian of Wales. Palaeogeogr. Palaeoclimatol. Palaeoecol., 7. pp.113-170.

DALY, J.S., 1978. Geochemical and Geochronological studies in the Stora Le - Marstrand Belt of Orust, S.W.Sweden. Ph.D. Thesis (unpublished), University of Keele.

DAVIES, D.L. and GOLDSMITH, P.L., 1976. Statistical methods in research and production. Longmans, London.

DEER, W.A., HOWIE, R.A. and ZUSSMAN, J., 1962. Rock-forming minerals. (5 volumes). Longmans, London.

DUNKLEY, P.N., 1979. Ordovician volcanicity of the SE Harlech Dome. In : HARRIS, A.L., HOLLAND, C.H. and LEAKE, B.E. (Eds). The Caledonides of the British Isles - reviewed. Spec. Publ. geol. Soc. Lond., 8. pp. 597-601.

DUNOYER DE SEGONZAC, G., 1970. The transformation of clay minerals during diagenesis and low-grade metamorphism : a review. Sedimentology, 15. pp. 281-346.

ERNST, W.G., 1963. Significance of phengitic micas from low-grade schists. Am. Min., 48. pp. 1357-1373.

ESQUEVIN, J., 1969. Influence de la composition des illites sur leur cristallite. Bull. Cent. Rech. Pau-SNPA, 3. pp.147-153.

EVANS, C.D.R., 1968. Geological succession and structure of the area east of Bethesda. Ph.D. thesis (unpublished) University of Wales, Aberystwyth.

FETTES, D.J., GRAHAM, C.M., SASSI, F.P. and SCOLARI, A., 1976. The basal spacing of potassic white micas and facies series variation across the Caledonides. Scott. J. Geol.,12, pp. 227-236.

FISHER, J.R., 1976. The volumetric properties of H_2O - A graphical portrayal. U.S. Geol. Surv. Jour. Res., 4(2). pp.189-144.

FITCHES, W.R., 1972. Polyphase deformation structures in the Welsh Caledonides near Aberystwyth. Geol. Mag., 109. pp.149-155.

FLOYD, P.A., 1983. Composition and petrogenesis of the Lizard Complex and pre-orogenic basaltic rocks in Southwest England. In : HANCOCK, P.L. (Ed)., The Variscan Fold Belt in the British Isles. Hilger, Bristol. pp. 130-153.

FLOYD, P.A., LEES, G.J. and ROACH, R.A., 1976. Basic intrusions in the Ordovician of North Wales - geochemical data and tectonic setting. Proc. Geol. Assoc., 87. pp. 389-400.

FLOYD, P.A., and TARNEY, J., 1979. First order alteration chemistry of Leg 49 basement rocks. Initial Reports Deep Sea Drilling Project, 49. pp. 683-708.

FLOYD, P.A., and WINCHESTER, J.A., 1975. Magma type and tectonic setting discrimination using immobile elements. Earth Planet. Sci. Lett., 27. pp. 211-218.

FRANCIS, E.H. and HOWELLS, M.F., 1973. Transgressive welded ash-flow tuffs among the Ordovician sediments of NE Snowdonia, N. Wales, J. geol. Soc. Lond.. 129. pp. 621-641.

FREY, M., 1970. The step from diagenesis to metamorphism in pelitic rocks during Alpine orogenesis. Sedimentology, 15. pp. 261-279.

FREY, M., 1978. Progressive low-grade metamorphism of a black shale formation, Central Swiss Alps, with special reference to pyrophyllite and margarite bearing assemblages. J. Petrol. 19. pp. 95-135.

FREY, M., TEICHMÜLLER, M., TEICHMÜLLER, R., MULLIS, J., KÜNZI, B., BREITSCHMID, A., GRUNER, U. and SCHWIZER, B., 1980. Very low-grade metamorphism in external parts of the Central Alps : Illite crystallinity, coal rank and fluid inclusion data. Eclogae geol. Helv., 73. pp.173-203.

FYFE, W.S., PRICE, N.J. and THOMPSON, A.B., 1978. Developments in Geochemistry 1. Fluids in the Earth's Crust. Elsevier, Amsterdam.

GEORGE, T.N., 1961. British Regional Geology : North Wales. Third Edition. Inst. Geol. Sci., H.M.S.O., London.

GLASSLEY, W.E., 1974. A model for phase equilibria in the prehnite-pumpellyite facies. Contrib. Mineral. Petrol., 43. pp.317-332.

GRAHAM, C.M., 1974. Metabasite amphiboles of the Scottish Daldradian. Contrib. Mineral. Petrol., 47. pp. 165-185.

GUIDOTTI, C.V., 1973. Compositional variation of muscovite as a function of metamorphic grade and assemblage in meta-pelites from N.W. Maine. Contrib. Mineral. Petrol., 42. pp. 23-42.

GUIDOTTI, C.V., and SASSI, F.P., 1976. Muscovite as a petrogenetic indicator mineral in pelitic schists. Neues Jahrb. Mineral. Abh., 127. pp.97-142.

HAMMOND, R. and MCCULLUGH, P.S., 1978. Quantitative Techniques in Geography, an Introduction. Clarendon Press, Oxford.

HART, S.R., 1969. K, Rb, Cs contents and K/Rb, K/Cs ratio of fresh and altered submarine basalts. Earth Planet. Sci. Lett., 6. pp. 295-303.

HART, S.R. and NALWALK, A.J., 1970. K, Rb, Cs and Sr relationships in submarine basalts from the Puerto Rico Trench. Geochim. Cosmochim. Acta, 34. pp. 145-156.

HASELOCK, P.J., 1982. The Geology of the Corrieyairack Pass area, Inverness-shire. Ph.D. thesis (Unpublished), University of Keele.

HASHIMOTO, M., 1966. On the prehnite-pumpellyite-metagreywacke facies. J. geol. Soc. Japan, 72. pp.253-265.

HASHIMOTO, M., 1972. Reactions producing actinolite in basic metamorphic rocks. Lithos, 5. pp. 19-31.

HATHAWAY, J.C., 1956. Procedure for clay mineral analysis used in the Sedimentary Petrology Laboratory of the U.S.Geological Survey. Clay Min. Bull., 3. pp.8-13.

HAWKINS, J.W., 1967. Prehnite-pumpellyite facies metamorphism of a greywacke-shale series, Mount Olympus, Washington. Am. J. Sci., 265. pp. 798-818.

HELM, D.G., ROBERTS, B. and SIMPSON, A., 1963. Polyphase folding in the Caledonides south of the Scottish Highlands. Nature, 200. pp. 1060-1062.

HEY, M.H., 1954. A new review of the chlorites. Mineral. Mag., 30. pp. 277-292.

HINRICHSEN, T. and SCHÜRMANN, K., 1972. Mineral reactions in burial metamorphism. Neues Jahrb. Mineral. Monat., 1972. pp. 35-48.

HOBBS, B.E., MEANS, W.D. and WILLIAMS, P.F., 1976. An outline of Structural Geology. Wiley, New York.

HOLDAWAY, M.J., 1972. Thermal stability of Al-Fe epidotes as a function of fO_2 and Fe content. Contrib. Mineral. Petrol., 37. pp. 307-340.

HOLLISTER, L.S. and BURRUSS, R.C., 1976. Phase equilibria in fluid inclusions from the Khatada Lake metamorphic complex. Geochim. Cosmochim. Acta, 40. pp. 163-175.

HOLLISTER, L.S. and CRAWFORD, M.L., 1981. Short course in fluid inclusions : Applications to petrology. Mineral Assoc. Canada, Short Course 6, Calgary.

HOWELLS, M.F., FRANCIS, E.H., LEVERIDGE, B.E. and EVANS, C.D.R., 1978. Capel Curig and Betws-y-Coed : Description of 1 : 25000 Geological Sheet SH 75, Classical Areas of British Geology. Institute of Geological Sciences, H.M.S.O., London.

HOWELLS, M.F., LEVERIDGE, B.E., EVANS, C.D.R. and NUTT, M.J.C., 1981a. Dolgarrog : Description of 1 : 25000 Geological Sheet SH 76, Classical Areas of British Geology. Institute of Geological Sciences, H.M.S.O. London.

HOWELLS, M.F., LEVERIDGE, B.E., EVANS, C.D.R., REEDMAN, A.J. and ADDISON, R., 1983. The Lithostratigraphical subdivision of the Ordovician underlying the Snowdon and Crafnant Volcanic Groups, North Wales. Rep. Inst. geol. Sci. Lond., 83, pp. 11-15.

HOWELLS, M.F., LEVERIDGE, B.E. and REEDMAN, A.J., 1981b. Snowdonia. Unwin, London.

HUMPHRIS, S.E. and THOMPSON, G., 1978. Hydrothermal alteration of oceanic basalts by seawater. Geochim. Cosmochim. Acta, 42, pp. 107-125.

JENKINS, D.A. and BALL, D.F., 1964. Pumpellyite in Snowdonian soils and rocks. Mineral. Mag., 33, pp. 1093-1096.

JOLLY, W.T., 1970. Zeolite and prehnite-pumpellyite facies in south central Puerto Rico. Contrib. Mineral Petrol., 27, pp. 204-224.

KAWACHI, Y., 1975. Pumpellyite-actinolite and contiguous facies metamorphism in part of the Upper Wakatipu district, South Island, New Zealand. N.Z. Jl. Geol. Geophys., 18, pp.401-441.

KELLING, G., 1978. The paratectonic Caledonides of mainland Britain. In : IGCP Project 27, Caledonian-Appalachian Orogen of the North Atlantic Region. Geol. Surv. Pap. Can., 78-13, pp. 89-95.

KENNEDY, G.C., 1950. Pressure-volume-temperature relations in water at elevated temperatures and pressures. Am. J. Sci., 248, pp. 540-564.

KERRICH, R., 1976. Some effects of tectonic recrystallisation on fluid inclusions in vein quartz. Contrib. Mineral. Petrol., 59. pp. 195-202.

KISCH, H.J., 1980. Incipient metamorphism of Cambro-Silurian clastic rocks from the Jamtland Supergroup, central Scandinavian Caledonides, western Sweden : illite crystallinity and "vitrinite" reflectance. J. geol. Soc. Lond., 137, pp. 271-288.

KISCH, H.J., 1983a, Mineralogy and petrology of burial diagenesis (burial metamorphism) and incipient metamorphism in clastic rocks. In : LARSEN, G. and CHILINGAR, G.V. (Eds).

Developments in Sedimentology 25B, Diagenesis in Sediments and Sedimentary Rocks,2, Elsevier, Amsterdam, pp.289-495.

KISCH, H.J., 1983b. Appendix B. Mineralogy and petrology of burial diagenesis (burial metamorphism) and incipient metamorphism in clastic rocks. In : LARSEN, G. and CHILINGAR, G.V. (Eds)., Developments in Sedimentology 25B, Diagenesis in Sediments and Sedimentary Rocks, 2, Elsevier, Amsterdam, pp. 513-543.

KNIPE, R.J., 1981. The interaction of deformation and metamorphism in slates. Tectonophys., 78. pp. 249-272.

KNIPE, R.J. and WHITE, S.H., 1977. Microstructural variation of an axial plane cleavage around a fold - a H.V.W.M. Study. Tectonophys., 39. pp. 355-380.

KOKELAAR, B.P., 1979. Tremadoc to Llanvirn volcanism on the southeast side of the Harlech Dome (Rhobell Fawr), N.Wales. In : HARRIS, A.L., HOLLAND, C.H. and LEAKE, B.E. (Eds), The Caledonides of the British Isles - reviewed. Spec. Publ. geol. Soc. Lond., 8, pp. 591-596.

KOKELAAR, B.P., HOWELLS, M.F., BEVINS, R.E., ROACH, R.A. and DUNKLEY, P. N., (In Press). The Ordovician marginal basin of Wales.

KUBLER, B., 1967. Anchimetamorphisme et schistosite. Bull. Cent. Rech. Pau - SNPA, 1, pp.259-278.

KUBLER, B., 1968. Evaluation quantitative du metamorphisme par la cristallinite de l'illite. Bull. Cent. Rech. Pau - SNPA. 2, pp. 753-777.

LEBAS, M.J., 1962. The role of aluminium in igneous clinopyroxenes with relation to their parentage. Am. J. Sci., 260, pp.267-288.

LIOU, J.G., 1971a. P - T stabilities of laumontite, wairakite, lawsonite and related minerals in the system Ca Al_2 Si_2O_8 - SiO_2 - H_2O. J. Petrol., 12. pp. 379-411.

LIOU, J.G., 1971b. Synthesis and stability relations of prehnite, Ca_3 Al_2 Si_3 O_{10} $(OH)_2$. Am. Min.,56, pp. 507-531.

LIOU, J.G., 1973. Synthesis and stability relations of epidote, Ca_2 Al_2 Fe Si_3 O_{12} (OH). J. Petrol., 14, pp. 381-413.

LIOU, J.G., KIM, H.S., and MARUYAMA, S., 1983. Prehnite-epidote equilibria and their petrologic applications. J. Petrol.,

24, pp. 321-342.

LYNAS, B.D.T., 1970. Clarification of the polyphase deformations of North Wales Palaeozoic rocks. Geol. Mag., 107, pp.505-510.

LYNAS, B.D.T., 1973. The Cambrian and Ordovician rocks of the Migneint area, North Wales. J. geol. Soc. Lond., 129. pp. 481-503.

MALTMAN, A.J., 1981. Primary bedding-parallel fabrics in structural geology. J. geol. Soc. Lond., 138. pp. 475-483.

MANSON, V., 1968. Geochemistry of basaltic rocks : Major elements. In: HESS, H.H. and POLDERVAART, A. (Eds), Basalts - the Poldervaart treatise of rocks of basaltic composition. Interscience, New York, 1. pp. 215-269.

MAXWELL, D.T. and HOWER, J., 1967. High-grade diagenesis and low-grade metamorphism of illite in the Pre Cambrian Belt Series. Am. Min., 52. pp. 843-857.

MIYASHIRO, A., 1974. Volcanic rock series in island arcs and active continental margins. Am. J. Sci., 274. pp. 321-355.

MIYASHIRO, A., 1979. Metamorphism and Metamorphic Belts. George, Allen and Unwin, London.

MIYASHIRO, A, and SEKI, Y., 1958. Enlargement of the compositional field of epidote and piedmontite with rising temperatures. Am. J. Sci., 256, pp. 423-430.

MIYASHIRO, A., SHIDO, F. and EWING, M., 1971. Metamorphism in the mid-Atlantic Ridge near 24^{o} and 30^{o}N. Phil. Trans. R. Soc. Lond. Ser. A, 268, pp. 589-603.

NAEF, U. and STERN, W.B. 1982. Some critial remarks on the analysis of phengitic and paragonitic components in muscovite by X-ray diffractometry. Contrib. Mineral. Petrol., 79, pp. 355-360.

NAKAJIMA, T., BANNO, S, and SUKUSI, T., 1977. Reactions leading to the disappearance of pumpellyite in low-grade metamorphic rocks of the Sanbagawa Metamorphic belt in Central Shikoku, Japan. J. Petrol., 18. pp. 263-284.

NICHOLLS, G.D., 1959. Autometasomatism in the lower spilites of the Builth Volcanic Series. Q. Jl. geol. Soc. Lond., 114, pp. 137-162.

NITSCH, K.H., 1971. Stabalitätsbeziehungen von prehnit und pumpellyit-

haltigen paragenesen. Contrib. Mineral. Petrol., 30, pp. 240 - 260.

NYSTROM, J.O., 1983. Pumpellyite-bearing rocks in Central Sweden and extent of host rock alteration as a control of pumpellyite composition. Contrib. Mineral. Petrol., 83. pp. 159-168.

OFFLER, R., BAKER, C.K. and GAMBLE, J., 1981. Pumpellyites in two low grade metamorphic terranes north of Newcastle, N.S.W. Australia. Contrib. Mineral. Petrol., 76, pp. 171-176.

OLIVER, G.J.H. and LEGGETT, J.K., 1980. Metamorphism in an accretionary prism : prehnite-pumpellyite facies metamorphism of the Southern Uplands of Scotland. Trans. R. Soc. Edinb., Earth Sci., 71. pp. 235-246.

PADAN, A., KISCH, H.J. and SHAGRAM, R., 1982. Use of the lattice parameter b_0 of dioctahedral illite/muscovite for the characterisation of P/T gradients of incipient metamorphism. Contrib. Mineral. Petrol., 79, pp. 85-95.

PASSAGLIA, E. and GOTTARDI, G., 1973. Crystal chemistry and nomenclature of pumpellyites and julgodites. Can. Miner., 12, pp. 219-223.

PEARCE, J.A., 1975. Basalt geochemistry used to investigate past tectonic environments on Cyprus. Tectonophys., 25. pp.41-68.

PEARCE, J.A., 1976. Statistical analysis of major element patterns in basalts. J. Petrol., 17. pp. 15-43.

PEARCE, J.A. and CANN, J.R., 1973. Tectonic setting of basic volcanic rocks determined using trace element analyses. Earth Planet. Sci. Lett., 19. pp. 290-300.

PEARCE, J.A. and NORRY, M.J., 1979. Petrogenetic implications of Ti, Zr, Y and Nb variations in volcanic rocks. Contrib. Mineral. Petrol., 69. pp. 33-47.

POLDERVAART, A. and HESS, H.H., 1951. Pyroxenes in the crystallisation of basaltic magma. J. Geol., 59. pp.472-490.

POTTER, R.W., 1977. Pressure corrections for fluid-inclusion homogenisation temperatures based on the volumetric properties of the system $NaCl-H_2O$. U.S. Geol. Surv. Jour. Res., 5 (5), pp. 603-607.

RADOSLOVICH, E.W. and NORRISH, K., 1962. The cell dimensions and symmetry of layer lattice silicates : 1 Some structural considerations. Am. Min., 47. pp.599-617.

RAST, N.J., 1969. The relationship between Ordovician structure and volcanicity in Wales. In : WOOD, A. (Ed). The Pre-Cambrian and Lcwer Palaeozoic Rocks of Wales. University of Wales Press, Cardiff, pp. 305-335.

REEDMAN, A.J., WEBB, B.C., ADDISON, R., LYNAS, B.D.T., LEVERIDGE, B.E. and HOWELLS, M.F., 1983. The Cambrian-Ordovician boundary at Aber and Betws Garmon, Gwynedd, North Wales. Rep. Inst. geol. Sci. Lond., 83. pp. 7-10.

RIDGEWAY, J., 1971. The stratigraphy and petrology of Ordovician volcanic rocks adjacent to the Bala Fault in Merioneth-shire, North Wales. Ph.D. Thesis (unpublished) University of Liverpool.

RIDGEWAY, J., 1976. Ordovician palaeogeography of the southern and eastern flanks of the Harlech Dome, Merionethshire, North Wales. Geol. J., 11, pp. 121-136.

ROBERTS, B., 1967. Succession and structure in the Llwyd Mawr syncline, Caernarvonshire, North Wales. Geol. J., 5, pp. 369-390.

ROBERTS, B., 1979. The geology of Snowdonia and Llyn : an outline and field guide. Hilger, Bristol.

ROBERTS, B., 1981. Low grade and very low grade regional metabasic Ordovician rocks of Llyn and Snowdonia, Gwynedd, North Wales. Geol. Mag., 118, pp. 189-200.

ROBINSON, D., 1981. Metamorphic rocks of an intermediate facies series juxtaposed at the Start boundary, southwest England. Geol. Mag., 118, pp. 297-301.

ROBINSON, D., NICHOLLS, R.A. and THOMAS, L.J., 1980. Clay mineral evidence for low-grade Caledonian and Variscan metamor-phism in south-western Dyfed, South Wales. Mineral. Mag., 43, pp. 857-863.

ROEDDER, E., 1962. Ancient fluids in crystals. Sci. Am., 207. pp. 38-47.

ROEDDER, E., 1963. Studies of field inclusions II : Freezing data and their interpretation. Econ. Geol., 58. pp. 167-211.

ROEDDER, E., 1968. Temperature, salinity and origin of the ore-forming fluids at Pine Point, Northwest Territories, Canada, from fluid inclusion studies. Econ. Geol., 63, pp. 439-450.

ROEDDER, E., 1972. Composition of fluid inclusions. In : Data of Geochemistry, Chapter JJ. U.S. Geol. Surv. Prof. Pap., 440 - JJ, pp. 1-164.

ROEDDER, E., 1979. Fluid inclusions as samples of ore fluids. In : BARNES, H.L. (Ed), Geochemistry of hydrothermal ore deposits. Wiley - Interscience, New York, pp. 684-737.

ROEDDER, E., 1981. Origin of fluid inclusions and changes that occur after trapping. In : HOLLISTER, L.S. and CRAWFORD, M. L. (Eds), Short course in fluid inclusions : Applications to petrology. Mineral. Assoc. Canada, Short Course 6, Calgary, pp. 101-138.

ROEDDER, E. and COOMBS, D.S., 1967. Immiscibility in granitic melts, indicated by fluid inclusions in ejected granitic blocks from Ascension Island. J. Petrol.,8, pp. 417-451.

SASSI, F.P. and SCOLARI, A., 1974. The b_o value of potassic white micas as a barometric indicator in low-grade metamorphism of pelitic schists. Contrib. Mineral. Petrol., 45, pp. 143-152.

SCHERMERHORN, L.J.G., 1975. Pumpellyite-facies metamorphism in the Spanish pyrite belt. Petrologie, 1, pp. 71-86.

SCHIFFMAN, P., ELDERS, W.A. and BIRD, D.K., (In Press). Calc-silicate paragenesis in the Cerro Prieto Geothermal System, Baja California, Mexico.

SCHIFFMAN, P. and LIOU, J.G., 1980. Synthesis and stability relations of Mg - Al pumpellyite, $Ca_4\ Al_5\ Mg\ Si_6\ O_{21}\ (OH)_7$. J. Petrol., 21, pp. 441-474.

SHACKLETON, R.M., 1954. The structure and succession of Anglesey and the Lleyn Peninsula. Adv. Sci. Lond., XI (41), pp.106-108.

SHEPHERD, T.J., 1981. Temperature-programmable, heating-freezing stage for microthermometric analysis of fluid inclusions. Econ. Geol., 76, pp. 1244-1247.

SIEGEL, S., 1956. Nonparametric Statistics. McGraw-Hill, New York.

SIGVALDSASON, G.E., 1962. Epidote and related minerals in two deep geothermal drillholes, Reykjavik and Hveragerdi, Iceland. U.S. Geol. Surv. Prof. Pap., 450-E, pp. 77-79.

SMITH, R.E., 1968. Redistribution of major elements in the alteration of some basic lavas during burial metamorphism. J. Petrol., 9, pp. 191-219.

SORBY, H.C., 1858. On the microscopic structure of crystals indicating the origin of minerals and rocks. Q. Jl. geol. Soc. Lond., 14, pp. 453-500.

SURDAM, R.C., 1969. Electron microprobe study of prehnite and pumpellyite from the Karmutsen Group, Vancouver Island, British Columbia. Am. Min., 54, pp. 256-266.

TOURET, J., 1981. Fluid inclusions in high grade metamorphic rocks. In : HOLLISTER, L.S. and CRAWFORD, M.L. (Eds). Short course in fluid inclusions : Applications to petrology. Mineral. Assoc. Canada, Short Course 6, Calgary, pp. 182-210.

TRINGHAM, M.E., 1979. Structures in Upper Carboniferous rocks in the Pembrokeshire coalfield, Dyfed, Wales. Ph.D. thesis (unpublished) University of Bristol.

TURNER, F.J., 1981. Metamorphic Petrology : Mineralogical,Field and Tectonic Aspects. McGraw-Hill, New York.

VALLANCE, T.G., 1965. On the chemistry of pillow lavas and the origin of spilites. Mineral. Mag., 34, pp. 471-481.

VALLANCE, T.G., 1969. Spilites again. Some consequences of the degradation of basalts. Proc. Linn. Soc. N.S.W., 94, pp.8-51.

VALLANCE, T.G., 1974. Spilitic degradation of a tholeiitic basalt. J. Petrol., 15, pp. 79-96.

VELDE, B., 1965. Phengitic micas : synthesis, stability and natural occurrence. Am. J. Sci., 263, pp. 886-913.

WEAVER, C.E., 1960. Possible use of clay minerals in search for oil. Bull. Am. Assoc. Petrol. Geol., 44, pp. 1505-1518.

WEBB, B.C., 1983. Early Caledonian structures in the Cambrian Slate Belt, Gwynedd, North Wales. Rep. Inst. geol. Sci. Lond., 83, pp. 1-6.

WEBER, K.L. 1972. Notes on the determination of illite crystallinity. Neues Jahrb. Mineral. Monat., 6, pp. 267-276.

WHITE, S.H. and KNIPE, R.J., 1978. Microstructure and cleavage development in selected slates. Contrib. Mineral. Petrol., 66, pp. 165-174.

WILLIAMS, H., 1927. The geology of Snowdon (North Wales). Q. Jl. geol. Soc. Lond., 83, pp. 346-431.

WINCHESTER, J.A. and FLOYD, P.A., 1976. Geochemical magma type discrimination : application to altered and metamorphosed basic igneous rocks. Earth Planet. Sci. Lett., 28, pp. 459-469.

WOOD, D.S., 1969. The base and correlation of the Cambrian rocks of North Wales. In : WOOD, A. (Ed), The Pre-Cambrian and Lower Palaeozoic Rocks of Wales. University of Wales Press, Cardiff. pp. 47-66.

WOOD, D.S., 1974. Ophiolites, melanges, blueschists and ignimbrites : early Caledonian subduction in Wales? In : DOTT, R.H. and SHAVER, R.H. (Eds), Modern and Ancient Geosynclinal Sedimentation. Soc. Econ. Palaeontol. Mineral. Spec. Publ., 19, pp. 334-344.

WOODLAND, A.W., 1938. Petrological studies in the Harlech Grit Series of Merionethshire. I. Metamorphic changes in the mud-stones of the Manganese Shale Group. Geol. Mag., 75, pp. 366-382.

ZEN, E-AN., 1974. Prehnite- and pumpellyite-bearing assemblages, west side of the Appalachian metamorphic belt, Pennsylvania to Newfoundland. J. Petrol., 15, pp. 197-242.

A1

55
60
70
80
70

N

Llanfairfechan

Penmaenmawr

NORTHERN CONWY
VALLEY

Aber

Bangor

Bethesda

A2

70

80

85

80

Colwyn Bay

Conwy

Llanfairfechan

Penmaenmawr

NORTHERN CONWY
VALLEY

Aber

Bethesda

Dolgarrog

CONWY VALLEY

CONWY VALLEY

70

B1

Bethesda

LLANBERIS AREA

60

Llanberis

Nant Peris

Capel

SOUTHERN CO

SNOWDON AREA

B2

Bethesda

Dolgarrog

CENTRAL CONWY VALLEY

CONWY VA

Trefriw

Llanrwst

60

Capel Curig

SOUTHERN CONWY VALLEY

Betws-y-Coed

Nebo

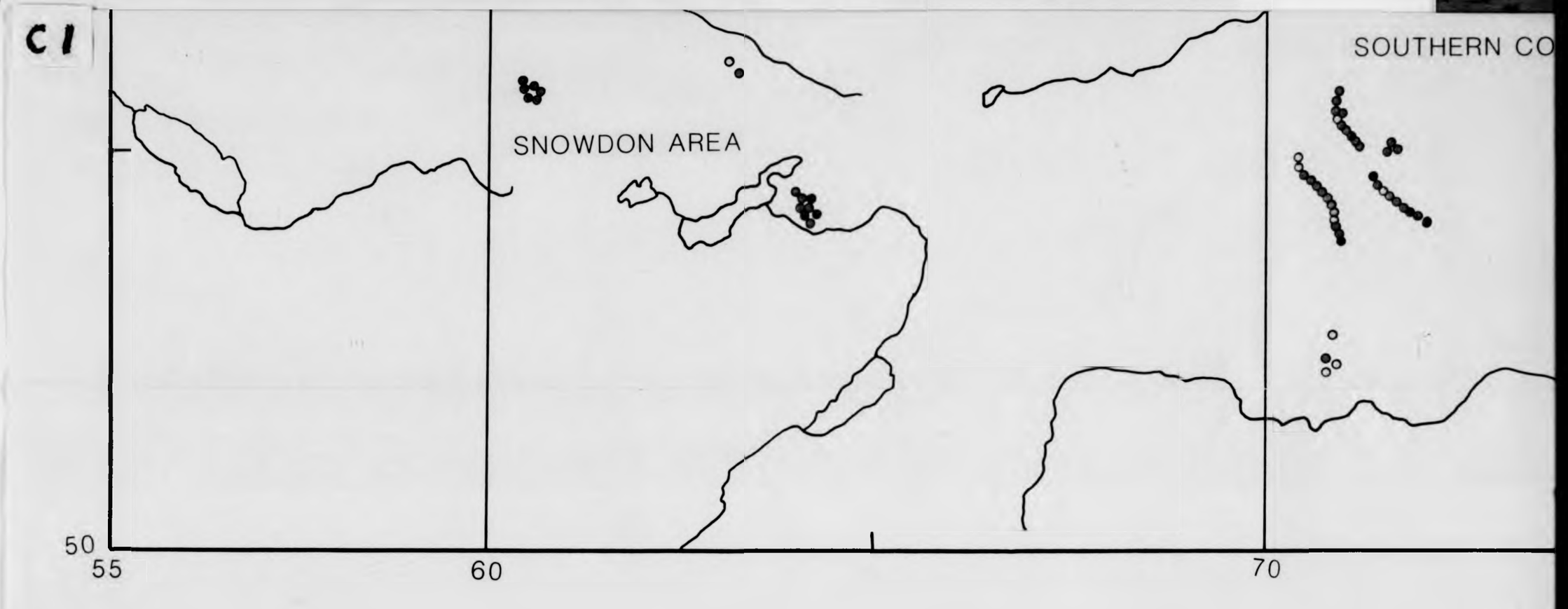

Key

- ○ — Prehnite ± Pumpellyite (no Actinolite)
- ◦ — Prehnite + Pumpellyite + Actinolite
- • — Prehnite + Actinolite (no Pumpellyite)
- ○ — Pumpellyite (no Prehnite or Actinolite)
- ◦ — Pumpellyite + Actinolite (no Prehnite)
- • — Actinolite (no Prehnite or Pumpellyite)
- • — Non-diagnostic assemblage

FIGURE 3.2 A map showing the distribution in northern Snowdonia.

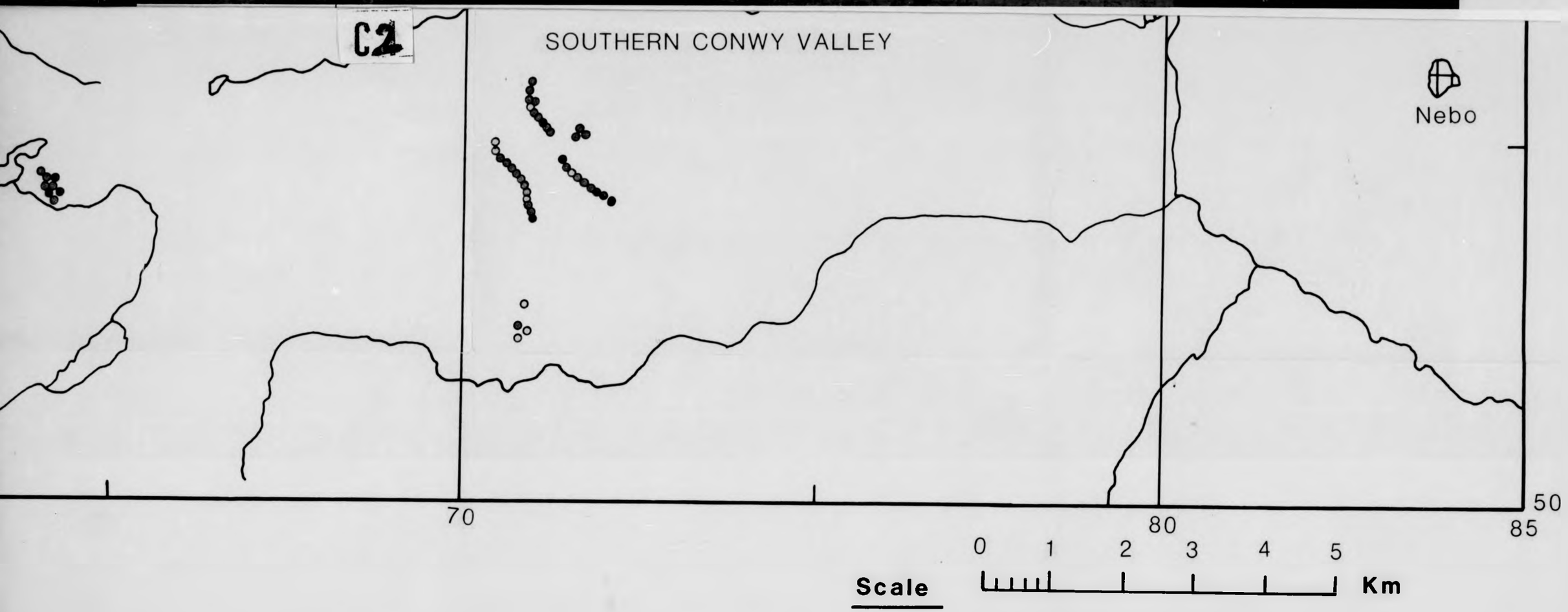

FIGURE 3.2 A map showing the distribution of prehnite, pumpellyite and actinolite in northern Snowdonia.

A 1

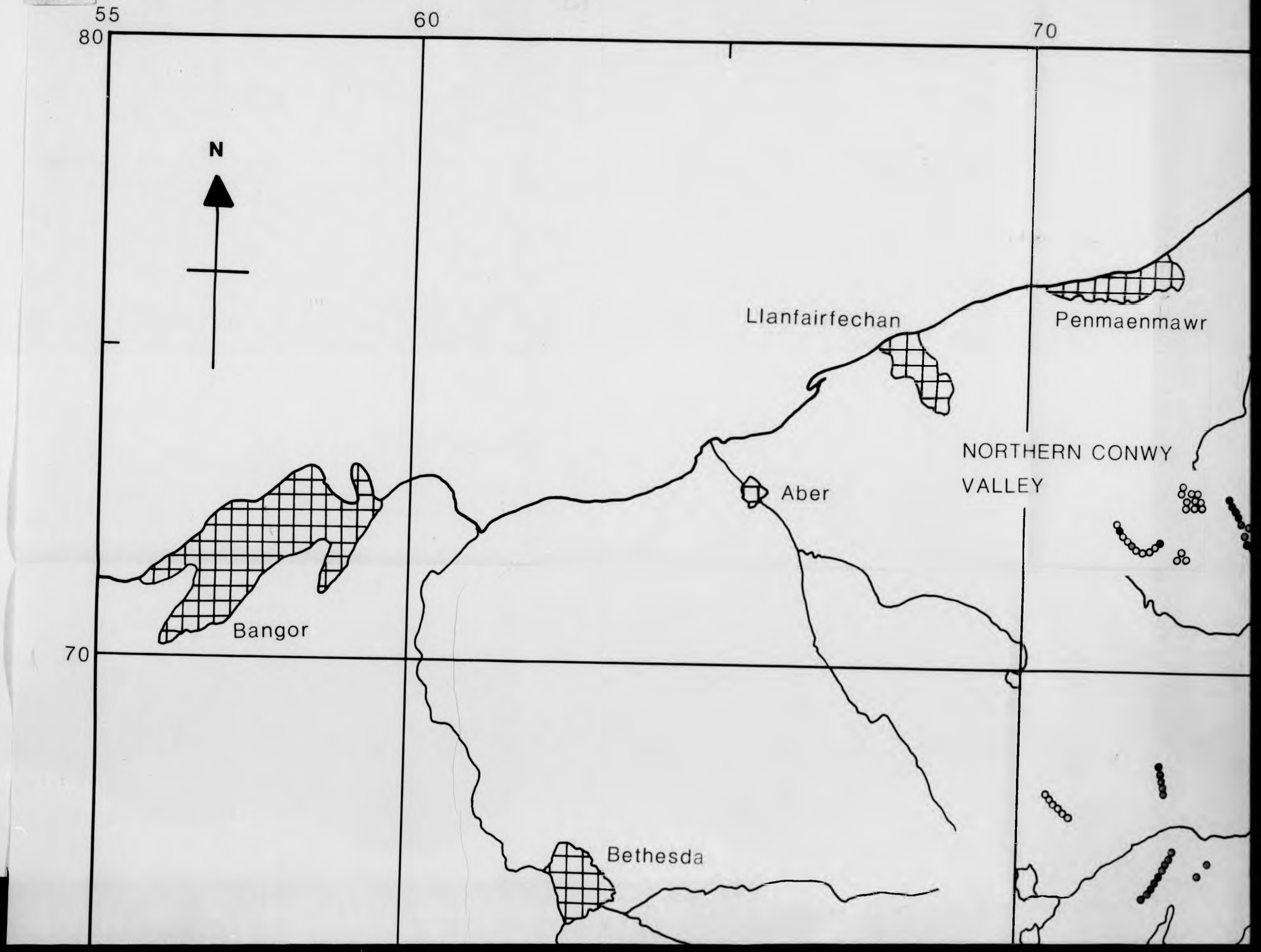
55
80
60
70
N
Llanfairfechan
Penmaenmawr
NORTHERN CONWY
VALLEY
Aber
Bangor
70
Bethesda

A2

70

80

85

80

Colwyn Bay

Conwy

Llanfairfechan

Penmaenmawr

NORTHERN CONWY
VALLEY

Aber

70

Bethesda

Dolgarrog

CONWY VALLEY

CONWY VALLEY

B1

LLANBERIS AREA

Bethesda

60

Llanberis

Nant Peris

SNOWDON AREA

Capel C

SOUTHERN CON

B2

Bethesda

Dolgarrog

CENTRAL CONWY VALLEY

CONWY VALLEY

Trefriw

Llanrwst

60

Capel Curig

SOUTHERN CONWY VALLEY

Betws-y-Coed

Nebo

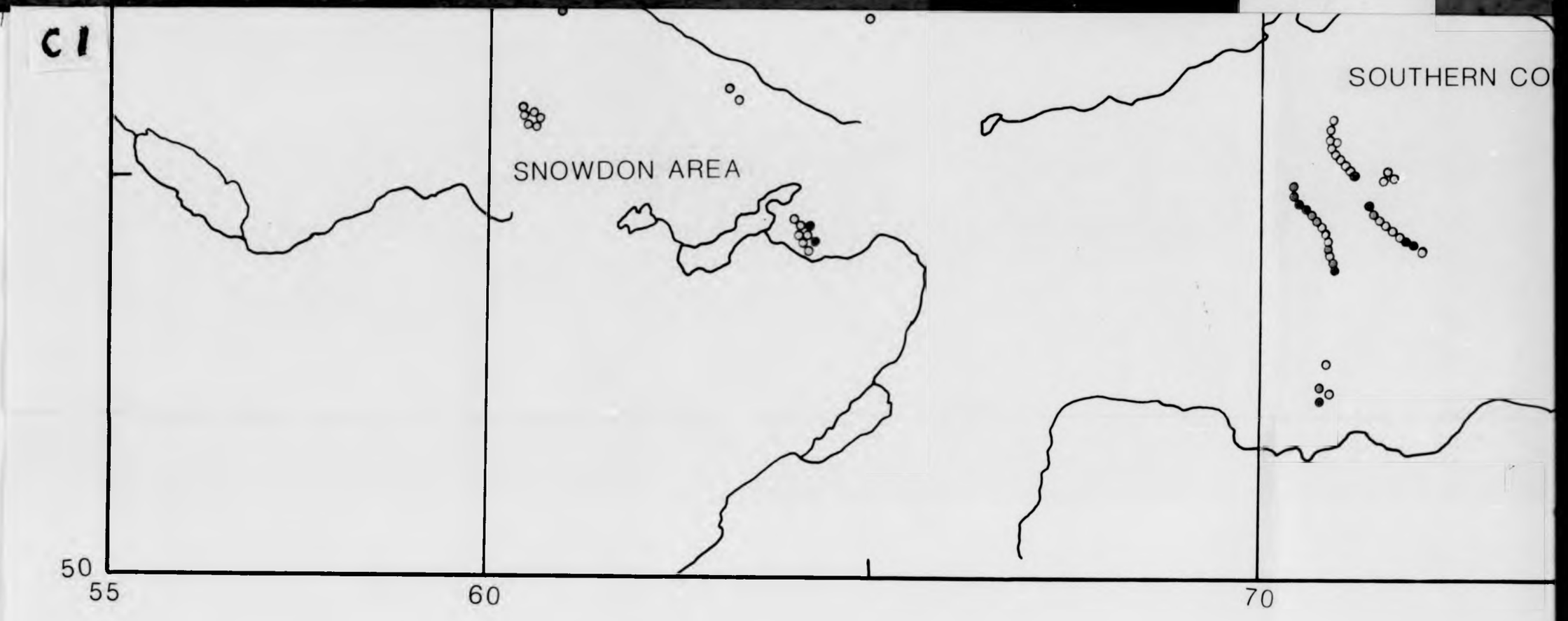

Key

- ○ — Pistacitic Epidote
- ● — Clinozoisitic Epidote
- ◉ — Zoned Epidote
- ● — Epidote Free Sample

FIGURE 3.3 A map showing the distribution of epid

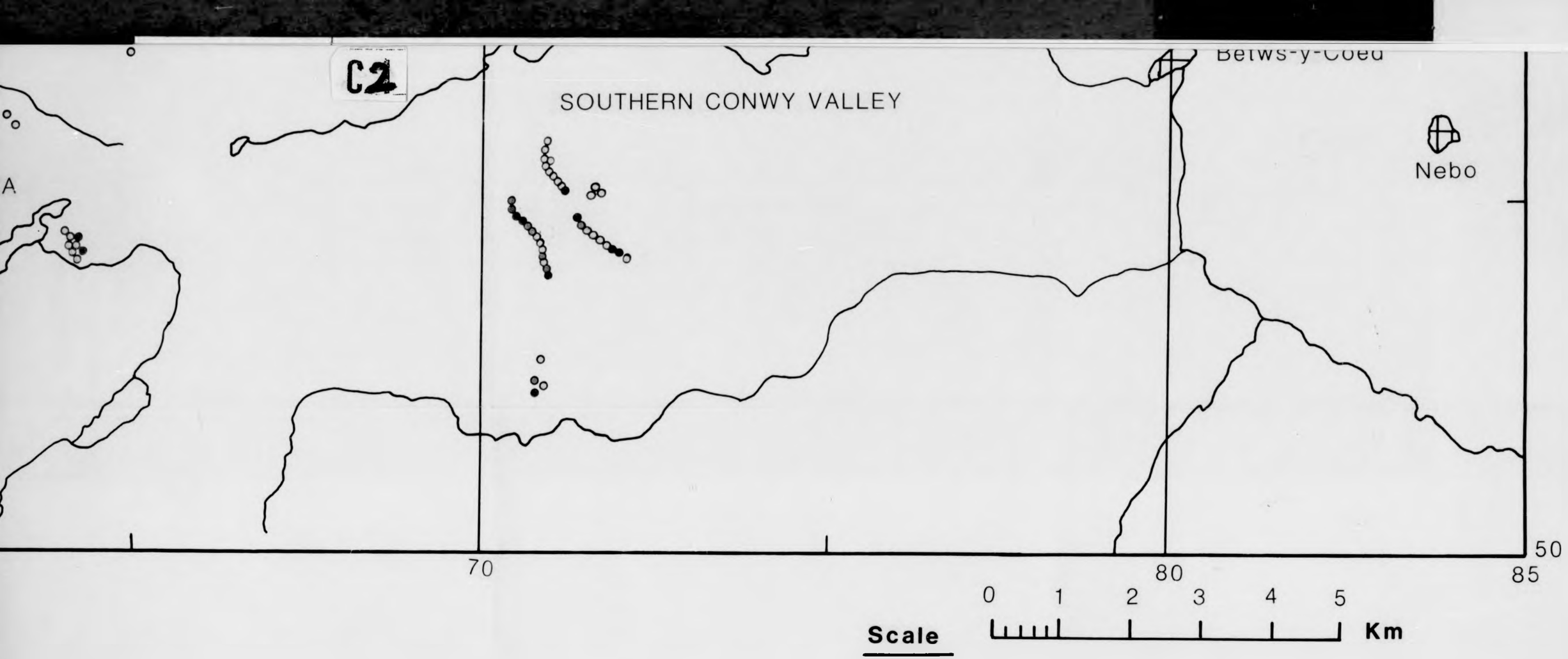

FIGURE 3.3 A map showing the distribution of epidotes in northern Snowdonia.